



2016 | Faculty of Sciences

DOCTORAL DISSERTATION

Towards a circular economy – Development, characterisation, techno-economic analysis and applications of activated carbons from industrial rest streams

Doctoral dissertation submitted to obtain the degree of
Doctor of Science: Chemistry, to be defended by

Kenny Vanreppelen

Promoter: Prof. Dr Robert Carleer

Co-promoters: Prof. Dr Jan Yperman
Prof. Dr Sonja Schreurs



D/2016/2451/32

Dankwoord

September 2008, Project Ingenieur bij Deme dredging International, een super toffe job, fijne collega's, enz. maar toch knaagde het: "Waarom ben ik niet ingegaan op de vraag van mijn docenten om te doctoreren". De vraag was me regelmatig gesteld. Er was namelijk een doctoraatsassistentenschap vrij en toch ging ik er niet op in. De reden is tot op vandaag nog altijd niet duidelijk... De laatste weken van september, de roep om aan een doctoraat te starten klonk luider en luider. Een telefoontje later vernam ik dat de positie ingevuld was, hij of zij startte 1 oktober. Maar het tij keerde, een week later, een oproep van Gerard Peeters departementshoofd XIOS Hogeschool Limburg met de vraag: "Kenny ben je nog steeds geïnteresseerd om te doctoreren gecombineerd met een assistentschap? En wanneer zou je kunnen beginnen?" (Mijn voorganger heeft het voor bekeken gehouden). Hier moest ik niet meer over nadenken: "Ja dat wil ik, ik vraag het onmiddellijk na!" Tijdens een gesprek met het management van Deme zag men snel dat een doctoraat halen echt mijn grote liefde was. Na een week opzeg, kreeg ik nog een hoop goede raad mee, een stevige handdruk met de melding: "Na je doctoraat kunnen we je terug gebruiken". Als ik er nu op terugkijk, kan ik alleen maar bedenken hoe dankbaar ik ben voor de industriële ervaring, het projectmatig werken, ... dat ik bij Deme heb kunnen leren. Zonder deze "academische pauze" zou mijn doctoraat nooit gelopen zijn zoals ze hier nu voor U ligt.

21 oktober 2008, de deuren van de universiteit Hasselt en de toenmalige XIOS Hogeschool Limburg openden zich opnieuw. Vanaf dag 1 stond ik voor groepen studenten uit diverse ingenieursrichtingen. Verder stond ook nog een vergadering gepland voor het uitstippelen van het doctoraatsonderzoek. Mijn promotoren hadden er alle vertrouwen in en gaven mij de vrijheid om zelf het onderwerp uit te werken op één voorwaarde na: "alles mag/kan voorgesteld worden zolang het met pyrolyse verband houdt". Door het combineren van de industriële ervaring met actieve kool zuiveringsinstallaties (Deme), de academische ervaring met pyrolyse en mijn motivatie om mijn steentje bij te dragen aan duurzame ontwikkeling, werd de richting al zeer snel duidelijk. *Pyrolyse technologie gebruiken voor het economisch rendabel produceren van actieve kool uit afval of reststromen voor het zuiveren van vervuild water.*

Uit mijn 7 jarige doctoraatscarrière kan ik besluiten dat een doctoraat bestaat uit hard werken, s 'nachts wakker worden met ideeën om uit te werken, mislukkingen, vertragingen en zo nu en dan een eureka moment. Ik heb echt genoten van mijn doctoraatsjaren, maar het halen was niet mogelijk geweest zonder de hulp van velen.

Eerst en vooral gaat mijn dank uit naar mijn promotoren, Robert, Jan en Sonja, die mij de gedurende vele jaren hebben begeleid tijdens dit doctoraat. Graag wil ik jullie bedanken voor de vrijheid die ik gekregen heb om mijn eigen weg te zoeken. Jullie stonden altijd klaar om mijn vragen met veel enthousiasme te beantwoorden, mijn teksten te verbeteren, ... Bij mislukkingen gaven jullie mij steeds opnieuw vertrouwen en moed om er eens zo hard tegenaan te gaan. Ik ben ook dankbaar voor de fijne gesprekken die we samen hadden en in de toekomst ongetwijfeld nog zullen hebben!

Daarnaast wil ik ook alle collega's van TANC bedanken. Dank jullie allemaal voor alle hulp tijdens mijn doctoraat, de fijne etentjes en feestjes met of zonder bowling ;o). Ik vond het altijd fijn om met jullie samen te werken, te praten, te klagen over van alles en nog wat, ... Ivo, altijd vrolijk en manusje van al. Dank je wel om altijd klaar te staan met raad en daad. We stonden zeker op plaats 1 & 2 (maak zelf maar uit wie eerst stond ;o)) bij de eigenschap "plagen en steuken". Onze voornaamste slachtoffers Elsy en Greet, dank jullie wel voor de vele babbels. Samen stonden jullie steeds klaar om stalen te analyseren met de ICP-AES en om mijn studenten op te vangen als ik weer eens op de XIOS moest zijn. Guy onze TGA koning, dank je wel voor alle hulp tijdens het opnemen van TGA's. Op een of andere manier kan je TGA 5 steeds met veel liefde opnieuw aan de praat te krijgen als deze weer eens moeilijk doen. Martine, altijd geïnteresseerd in mijn bouwplannen. Infrarood analyse heeft geen enkel geheim meer voor jou. Ondanks de moeilijkheden en de vele pogingen om mijn "vuile" zwarte stalen te analyseren, bleef je dit proberen. Jan en Linda, jullie zijn echte experts in GC-MS. Dank jullie wel om me steeds bij te staan in de analyses en het analyseren van de mogelijkheden om stalen zo goed mogelijk te karakteriseren. Linda, de maand november blijft voor altijd verbonden met de lekkere speculaas. Ik durf niet tellen hoeveel kg ik op al die jaren heb opgegeten... Jenny, dank je wel voor de hulp met de HPLC, IC, GPC. Je stond altijd klaar om nieuwe methodes te ontwikkelen en te helpen. Koen en Johan, dank jullie wel voor alle hulp met apparatuur en het ontwikkelen van nieuwe pyrolyse reactoren, adsorptieapparatuur, ... Huegette, Christel, Wanda en Peter, dank jullie wel voor de fijne gesprekken.

Ook een welgemeende dank je wel aan alle college-doctoraatstudenten (Jens V., Jens M., Sara, Marco, Niels V., Tom C., Mark, Eva, Koen, Tom, Niels) voor de vele fijne momenten (etentjes, congressen) discussies, tips, aangename werksfeer, ... Ik vond het zeer fijn om met jullie samen te werken. Sara, Niels V en Robin, ik ben heel dankbaar dat ik zulke toffe studenten heb mogen begeleiden tijdens jullie respectievelijke bachelor- en

masterthesis. Jullie hebben allen bijgedragen tot het uiteindelijke doctoraatsonderzoek. Mijn Cubaanse collega's Harold en Monica: Thank you for the interesting discussions and talks. I will plan a trip to Cuba!

Iedereen van NuTec en de opleiding NT, ik ben heel blij dat ik zolang heb deel mogen uitmaken van deze onderzoeksgroep. Ik heb het altijd fijn gevonden om samen met jullie de opleiding Nucleaire Technologie te vertegenwoordigen. Dank jullie wel voor alle fijne momenten, de adviezen en de feestjes.

De collega's van economie specifiek, dank jullie wel voor jullie raad en daad bij het economische deel van mijn thesis. Het congres in Dubrovnik zal me altijd bijblijven. Tom, het was zeer fijn om met je samen te werken. Je stond altijd klaar om mijn economische vragen te beantwoorden. Deze samenwerking moeten we zeker verderzetten!!

Daarnaast wil ik de collega's van het oude XIOS en PXL-Bio bedanken voor de aangename momenten tijdens het middageten, de raad, de hulp, ... en de fijne werksfeer. Ik zou hier iedereen persoonlijk willen bedanken maar dat is spijtig genoeg niet mogelijk in dit dankwoord. Voor enkele personen wil ik graag een uitzondering maken. Ida, dank je wel voor alle hulp tijdens de labo's en de uren babbelle plezier! Els en Nadia, ik vond het super om in mijn eerste jaren samen een bureau te delen. We zaten daar goed! Roger, dank je wel om alle problemen zo snel mogelijk op te lossen en de dames van het secretariaat voor de fijne samenwerking.

Vera (Universiteit Antwerpen), dank je wel om de stalen op porositeit te analyseren. Grazyna (Wrocław University of Technology), thank you for analysing the samples with XPS.

En zo neig ik langzaam naar het einde van mijn dankwoord, maar toch moeten er nog enkele belangrijke mensen de revue passeren. Zoals mijn broer, zusje, (schoon)familie en vrienden. Hoewel jullie nog altijd niet echt weten wat ik nu juist gedaan heb de afgelopen jaren, waren jullie altijd geïnteresseerd in het onderzoek. Dank jullie wel om er voor mij te zijn! Zonder jullie steun weet ik niet of ik ondanks alle tegenslagen in de verbouwing, tijdens het bouwen en het verlies van mijn schoonpapa* en papa* erin geslaagd zou zijn om het doctoraat af te ronden.

Mama, dank je wel om er steeds voor mij te zijn! Ongeacht wat, je stond/staat altijd voor mij klaar. Jij en papa hebben me vele levenslessen bijgebracht die ervoor gezorgd hebben dat ik dit doctoraat tot een goed einde heb kunnen brengen! Papa, je kan niet geloven hoe moeilijk ik dit nog steeds vind om te schrijven. Je was/bent mijn rots in de branding! Je stond

er altijd met raad en daad, altijd geïnteresseerd, ... Zelfs toen je al zeer ziek was, bleef je me motiveren en helpen! Je bent mijn GROTE voorbeeld!

Sarah, ja het moment is nu echt daar, het doctoraat is af!! Dank je wel!! Jouw steun en onvoorwaardelijke liefde zijn onbetaalbaar. Als ik druk in de weer was met het doctoraat, de verbouwingen, het bouwen stond jij er om al de rest te runnen en twee mooie kindjes op de wereld te zetten. Jij verdient een standbeeld!!! Jasper en Fiene, mijn lieve kindjes, als ik moe of geambeteerd van een of ander mislukt experiment thuiskwam, toverden jullie onmiddellijk een smile op mijn gezicht!

Dank U Wel!!!!

Kenny

Table of contents

1	Introduction	25
1.1	Particle Board	27
1.2	Brewer's spent grain.....	29
1.3	Activated Carbon	30
1.3.1	Production of activated carbon (based on Menéndez-Días & Martín-Gullón (2006)).....	32
1.3.1.1	Thermal activation	35
1.3.1.2	Chemical activation	36
1.3.2	Porous texture	38
1.3.3	Surface functional groups	39
1.3.3.1	Oxygen-containing functionalities	40
1.3.3.2	Nitrogen-containing functionalities	41
1.3.3.3	Other heteroatoms.....	42
1.3.4	Adsorption theoretical background.....	42
1.3.4.1	Adsorption equilibrium.....	44
1.3.4.3	Adsorption kinetics.....	46
1.3.4.4	Adsorption dynamics	47
1.4	Techno-economic assessment.....	49
1.5	Research questions	51
2	Material and methods	55
2.1	Waste Materials	57
2.1.1	Brewer's spent grain	57
2.1.2	Particle board samples	57
2.1.3	Melamine formaldehyde glue.....	57
2.2	Waste characterisation	57
2.2.1	Moisture and ash content.....	58
2.2.2	Thermogravimetric analysis	58
2.2.3	Ultimate analysis	58
2.2.4	Component analysis.....	59

2.3	Char and Activated carbon Production	59
2.4	Activated carbon characterization.....	61
2.4.1	Ash content	61
2.4.2	Point of zero charge	61
2.4.3	Acid-basic groups	61
2.4.4	Ultimate analysis	61
2.4.5	X-ray photoelectron spectroscopy	61
2.5	Adsorption experiments	62
2.5.1	Nitrogen adsorption studies (porosity characteristics).....	62
2.5.2	Liquid phase adsorption studies of phenol.....	62
2.5.2.1	Adsorption isotherm studies	62
2.5.2.2	Adsorption kinetic studies	63
2.5.2.3	Effect of initial pH, ionic strength and standard water	63
2.5.2.4	Dynamic phenol adsorption and effect of temperature	64
2.5.2.5	Column adsorption experiments.....	65
2.5.3	Liquid phase adsorption studies of pharmaceutically active compounds (PhAC's)	66
2.5.3.1	Screening assay	66
2.5.3.2	Equilibrium assay.....	67
2.5.3.3	Kinetic assay	67
2.6	Techno-economic assessment.....	67
3	Development of the pyrolysis/activation reactor	71
4	Preliminary techno-economic analysis.....	77
4.1	Introduction	77
4.2	Process design.....	79
4.3	Economic feasibility model	82
4.4	Model assumptions.....	83
4.4.1	Total capital investment	86
4.4.2	Expenditure	89
4.4.3	Revenues	92
4.5	Results and Discussion	93

4.5.1	Economic evaluation of the base case	93
4.5.2	Economic impact of the nitrogen content of the activated carbon 97	
4.5.3	Economies of scale	98
4.5.4	Share of expenditure items in total expenditure.....	99
4.5.5	Monte Carlo Sensitivity analysis.....	100
4.5.6	Identification of the key variables	106
4.6	Conclusion	107
5	Screening of activated carbon produced by co-pyrolysis and steam activation from particle board and melamine formaldehyde resin.....	111
5.1	Abstract.....	111
5.2	Introduction	112
5.3	Methodology.....	114
5.3.1	Economic feasibility model.....	114
5.3.2	Sample preparation	115
5.3.3	Characterisation of the input materials	116
5.3.4	Preparation of the activated carbon.....	116
5.3.5	Batch adsorption experiments	117
5.4	Results and discussion.....	117
5.4.1	Characterisation of the input material	117
5.4.2	Pyrolysis and activation experiments.....	119
5.4.3	Low concentration phenol adsorption	121
5.4.4	Economic evaluation base case.....	122
5.4.5	Economic impact of the gate fee for MF	126
5.4.6	Economic impact of the nitrogen content	126
5.4.7	Economies of scale	127
5.4.8	Monte Carlo Sensitivity analysis.....	127
5.5	Conclusion	130
6	Waste particle board as a renewable source for the production of activated carbon.....	133
6.1	Abstract.....	133
6.2	Introduction	134

6.3	Methods and materials.....	135
6.4	Results and discussion.....	140
6.4.1	Characterisation of the particle board samples	140
6.4.2	Activated carbon yield	143
6.4.3	Activated carbon screening for phenol adsorption	144
6.4.4	Correction factor	144
6.4.5	Activated carbon characterisation	146
6.4.5.1	Nitrogen adsorption isotherm	146
6.4.5.2	Surface functionalities	150
6.4.6	Liquid phase adsorption studies of phenol.....	159
6.4.6.1	Kinetics of adsorption.....	159
6.4.6.2	Dynamic adsorption experiments	162
6.4.6.3	Adsorption equilibria	164
6.4.6.4	Effect of ionic strength and pH.....	167
6.5	Conclusion	172
7	Activated carbon from pyrolysis of brewer's spent grain: Production and Adsorption properties.....	175
7.1	Abstract.....	175
7.2	Introduction	176
7.3	Methods and materials.....	177
7.4	Results and discussion.....	182
7.4.1	Characterisation of the input material	182
7.4.2	Activated carbon yield and characterization.....	183
7.4.3	Phenol adsorption.....	186
7.4.4	Porosity.....	189
7.4.5	Surface functionalities	193
7.4.6	Effect of contact time	197
7.4.7	Effect of pH, ionic strength and standard water	199
7.4.8	Economic evaluation	201
7.5	Conclusion	205
8	Adsorption screening of pharmaceutically active compounds	209

8.1	Abstract.....	209
8.2	Introduction	209
8.3	Methods and materials.....	211
8.4	Results and discussion.....	213
8.4.1	Screening assay	213
8.4.2	Equilibrium assay	214
8.4.3	Kinetic assay.....	219
8.5	Conclusion	224
9	Summary and general conclusions	227
10	Samenvatting en algemeen besluit.....	233

List of tables

Table 1-1: General features distinguishing physical adsorption from chemisorption (Ruthven 1984)	43
Table 4-1: Multiplying factor for the Delivered-equipment cost	85
Table 4-2: Major equipment cost and their scaling factors used	86
Table 4-3: Summary of the fixed annual operating factors	90
Table 4-4: Estimated yields of the input feed	92
Table 4-5: Summary of costs for the production of Activated Carbon by this model	95
Table 4-6: IRR for the 1 t/h feed input factory	96
Table 4-7: Variables with their profitability distribution.....	101
Table 4-8: Percentage of Monte Carlo Simulation Runs that gain a positive NPV	103
Table 4-9: Minimal selling price at which the activated carbon should be sold to guarantee a 95% chance on a positive NPV.....	104
Table 5-1: Ultimate analysis	119
Table 5-2: AC yield and ultimate analysis	120
Table 5-3: Guideline for calculating the annual operating costs (from ref (Vanreppelen et al. 2011) and Chapter 4).....	123
Table 5-4: Total capital investment, annual expenditure and minimum selling price for the production of AC.....	124
Table 6-1: Elemental analysis particle board samples.....	142
Table 6-2: Activated carbon yields from particle board samples.....	143
Table 6-3: Activated carbon phenol adsorption screening assay.....	144
Table 6-4: Porosity characteristics: BET analysis (S_{BET}), t-plot analysis for micropore (S_{micro}) and external surface (S_{ext}) based on De Boer, and micropore characterization based on the Dubinin-Radushkevich method (V_T , V_{DR} , V_{Meso} , L_0 and E_0).....	150
Table 6-5. pH_{PZC} and amount of acid / basic groups mounted on the activated carbon surfaces	151
Table 6-6: Carbon, Oxygen and Nitrogen atomic concentration and the surface functionalities distribution derived from the C1s, O1s and N1s spectra.....	154
Table 6-7. Ultimate analysis (on dry base).....	158
Table 6-8. Comparison of the pseudo-first-order and pseudo-second-order model by non-linear regression analysis	159
Table 6-9. Comparison of the kinetic constants obtained by non-linear regression analysis of the pseudo-first-order and pseudo-second-order model	164
Table 6-10. Isotherm parameters + R_L	166
Table 6-11. Equilibrium phenol removal at different pH values	170

Table 6-12. Effect of standard water on the removal efficiency of phenol .	171
Table 7-1. Chemical composition and EA of BSG	183
Table 7-2. Ultimate analysis.....	185
Table 7-3. Isotherm constants.....	188
Table 7-4: Porosity characteristics: BET analysis (S_{BET}), t-plot analysis for micropore (S_{micro}) and external surface (S_{ext}) based on De Boer, and micropore characterization based on the Dubinin-Radushkevich method (V_T , V_{DR} , V_{Mesor} , L_0 and E_0).....	191
Table 7-5. pH_{pZC} and amount of acid and basic group mounted on the surface.....	193
Table 7-6. XPS analysis of selected ACBSGs: Carbon, Oxygen and Nitrogen atomic concentration and the surface functionalities distribution derived from the C1s, O1s and N1s spectra	195
Table 7-7. Comparison of the pseudo-first-order and pseudo-second-order model by non-linear regression analysis	197
Table 7-8: Total capital investment, annual expenditure and minimum selling price for the production of AC onsite	203
Table 7-9: Total capital investment, annual expenditure and minimum selling price for the production of AC offsite	205
Table 8-1: Molecular structure, solubility and pK_a values of the PhACs (Jung et al. 2013a).....	213
Table 8-2: Langmuir and Freundlich constants based on nonlinear modelling of the experimental equilibrium data points	216
Table 8-3. Comparison of the kinetic constants obtained by non-linear regression analysis of the pseudo- n^{th} -order model	220

List of figures

Figure 1-1: Circular economy conceptual diagram (European Commission 2014).....	26
Figure 1-2: Schematic representation of the major allotropic form of carbon and examples of the possible derived structures (Menéndez-Días & Martín-Gullón 2006).....	31
Figure 1-3: Schematic overview of activated carbon production (Menéndez-Días & Martín-Gullón 2006).....	34
Figure 1-4: Char formation reaction scheme (Menéndez-Días & Martín-Gullón 2006).....	35
Figure 1-5: Oxygen-containing functionalities: (a) carboxyl groups, (b), lactone, (c) hydroxyl, (d) carbonyl, (e) quinone, (f) ether, (g) pyrone, (h) carboxylic anhydride, (i) chromene, (j) lactol, and (k) n electron density on carbon basal planes (Bandosz 2009)	41
Figure 1-6: Nitrogen-containing functionalities: (a) pyrrole- like group, (b) nitrile, (c) secondary amine, (d) nitroso group, (e) nitro group, (f) tertiary amine, (g) primary amine, (h) pyridine-like group, (i) imine, (j) amide, (k) lactam, (l) pyridone, (m) quaternary amine (Bandosz 2009).....	42
Figure 1-7: Practice-oriented adsorption theory (Worch 2012)	44
Figure 1-8: The mass transfer-adsorption process (Le Cloirec 2002)	46
Figure 1-9: Unsteady-state fixed bed adsorber concentration profile (Chowdhury et al. 2013)	48
Figure 2-1: Schematic overview of the experimental approach	56
Figure 2-2: Pyrolysis and activation routes	60
Figure 2-3: Set-up dynamic adsorption	65
Figure 2-4: Column adsorption set-up.....	66
Figure 3-1: Horizontal tubular pyrolysis reactor set-up.	71
Figure 3-2: Steam activation setup	71
Figure 3-3: 3-D model pyrolysis and activation reactor (above), manufactured reactor in comparison with the quartz reactors (below).....	73
Figure 3-4: Home-built pyrolysis / activation set-up.....	74
Figure 4-1: Process flow	81
Figure 4-2: Net Present value for a 1 t/h processing facility	94
Figure 4-3: Net Present value for a 2 t/h processing facility	99
Figure 4-4: Importance of the distinct expenditure items.....	100
Figure 4-5: Mean NPV Output after Monte Carlo analysis	102
Figure 4-6: Average sensitivity of the crucial variables on the NPV for a 1 t/h facility.....	107
Figure 5-1: Economical strategy	116
Figure 5-2: TGA of PB (a) and MF (b).....	118

Figure 5-3: Effect of adsorbent dosage (1 mg/l, 5 mg/l, 10 mg/l, 30 mg/l, 50 mg/l, 80 mg/l and 100 mg/l activated carbon; 50 ml of a 100 mg/l unbuffered phenol solution)	121
Figure 5-4: NPV for a 1 t/h production facility	125
Figure 5-5: Payback time for a 1 t/h production facility at a selling price of 2.5 kEUR/t.....	125
Figure 5-6: NPV for a 2 t/h waste processing facility	126
Figure 5-7: NPV distribution.....	128
Figure 5-8: Average sensitivity for a 1 t/h processing facility	129
Figure 6-1: Experimental approach and strategy for the production and characterization of activated carbons from particle board.....	136
Figure 6-2: Thermo-gravimetric analysis a) particle board glued with melamine formaldehyde (PBMUF) and b) particle board glued with urea formaldehyde PBUF.....	141
Figure 6-3: Correction factor phenol determination in function of the solutions pH	145
Figure 6-4: Nitrogen adsorption-desorption isotherms at 77 K for the selected activated carbons from particle board	147
Figure 6-5: Pore size distribution of the activated carbons determined by DFT method for a, b) PBMUF (a: micropores, b: mesopores) ; c, d) PBUF (c: micropores, d: mesopores)	148
Figure 6-6: C1s, N1s and O1s XPS spectra of ACPBUF06	153
Figure 6-7. Effect of contact time on the phenol removal (Filled and dashed lines refer to the pseudo-second-order model)	160
Figure 6-8. Deviation between calculated (pseudo-second-order) and experimental adsorption capacities	161
Figure 6-9: Kinetic evolution of the phenol and phenolate concentration with a) activated carbon from particle board (ACPBMUF07) and b) reference activated carbons (Norit GAC 1240)	163
Figure 6-10: Adsorption equilibrium isotherm of phenol.....	165
Figure 6-11: Effect of the ionic strength on the removal of phenol	168
Figure 7-1: Experimental approach and strategy for the production and characterization of activated carbons from particle board.....	178
Figure 7-2: TGA/DTG curves of BSG	182
Figure 7-3. Pyrolysis and ACBSG yield.....	183
Figure 7-4. Comparison of adsorption isotherms of phenol onto different BSG activated carbons	186
Figure 7-5. Effect of AC dosage on phenol removal	188
Figure 7-6: N ₂ adsorption-desorption isotherms at 77K	189
Figure 7-7: Pore size distribution of the activated carbons determined by DFT method for a) micropores; b) mesopores (2.5 – 8.5 nm)	192
Figure 7-8: C1s, N1s and O1s XPS spectra of ACBSG07.....	196

Figure 7-9. Effect of contact time on the phenol removal: pseudo-second-order model fitted to the experimental data points.....	198
Figure 7-10. Deviation between the calculated by the pseudosecond-order model and the experimental adsorption capacity (Q_t).....	199
Figure 7-11. Effect of initial pH on the phenol removal	200
Figure 7-12: Effect of ionic strength and standard water on the phenol adsorption capacity.....	200
Figure 7-13: NPV for a 1 t/h and 2 t/h onsite production facility	202
Figure 7-14: NPV for a 1 t/h and 2 t/h offsite production facility	204
Figure 8-1: Screening assay for the adsorption of IBP, SMX and DCF on activated carbons produced from brewer's spent grain ACBSF) and particle board glued with melamine urea formaldehyde (ACPBMUF) and urea formaldehyde (ACPBUF)	214
Figure 8-2: Equilibrium assay.....	217
Figure 8-3: Final pH pharmaceutical active compounds solution in function of activated carbon dosage.....	218
Figure 8-4: intraparticle diffusion for the adsorption of DCF on ACPBUF06	221
Figure 8-5: Residual concentration of PhACs in function of contact time for the different adsorbents	223

Outline

In order to cope with the increasing global population, increasing environmental pressure and depletion of natural resources, a rapid and radically change to a circular bioeconomy will be key to secure growth and jobs. A circular economy is designed to keep added value in products for as long as possible. Transition to a circular economy will require changes throughout the entire value chain. One part in the transition to a more circular economy is turning today's waste into resources. Development of new recycling and reengineering methods will thus be key for future waste stream valorisation keeping value in the products. Interesting renewable resources for further valorisation are industrial organic waste streams. Despite their potential (high volume, known composition, ...) as valuable and renewable resources for industrial exploitation, they have received little attention as a marketable product.

Another problem arising from the production of goods and the increasing population that needs to be tackled is the contamination of water supplies e.g., groundwater, surface water, ...

As part of the transition to a more circular economy, addressing the remediation of water supplies, is the development of high value activated carbon from industrial organic waste streams replacing virgin resources.

In this study, three industrial organic residues (brewer's spent grain, particle board [glued with urea formaldehyde and glued with melamine urea formaldehyde] and melamine formaldehyde) are selected as precursors for the production of high value activated carbon for the remediation of contaminated water. The main objective is to answer the question whether industrial organic waste streams (i.e., brewer's spent grain, melamine formaldehyde and particle board) are interesting renewable resources for the profitable production of activated carbons.

In chapter 1, an introduction about the circular economy and the investigated industrial waste streams is presented. In addition, an overview of the production of activated carbon, its characteristics and the adsorption theory is discussed. The general framework for techno-economic assessment is provided. The research question and subquestions are formulated at the end of this chapter.

The experimental approach and the methodology used for the characterisation of the waste streams and the production, characterisation and performance of activated carbons produced from the waste stream are described in Chapter 2.

The development of a new laboratory pyrolysis/activation reactor which is suitable to produce sufficient amounts of activated carbon resembling industrial plants is discussed in Chapter 3.

In Chapter 4, a preliminary techno-economic assessment is carried out for the production of activated carbon from particle board and melamine formaldehyde. First a process diagram of an activated carbon production technique (co-pyrolysis combined with physical activation) is developed and a discounted cash flow model is made. Based on this model, the net present value of the cash flows generated by an investment in co-pyrolysis and char activation is calculated. Because a number of values that have been assumed in the cash flow model are uncertain, Monte Carlo Sensitivity analysis is performed to identify the key variables for the profitability of the production of activated carbon from particle board and melamine formaldehyde waste. Before up scaling the research, the profitability of activated carbon production from blends of particle board and melamine waste is further evaluated based on preliminary research results and the discounted cash flow model (developed in Chapter 4) in Chapter 5.

The valorisation of activated carbon from brewer's spent grain and particle board for the remediation of phenol contaminated water is investigated in Chapter 6 and 7. First the characteristics of the waste materials are investigated followed by the effect of the temperature and time of steam activation on the yield and characteristics of the produced carbons. The performance of the activated carbons is evaluated by batch adsorption experiments in function of different parameters like time, temperature, ionic strength and pH using phenol as target compound.

In Chapter 8 the performance of the produced carbons is evaluated for the remediation of water contaminated with pharmaceutical active compounds (ibuprofen, diclofenac and sulfamethoxazole) in three sequential types of assays e.g.: Screening assay, Equilibrium assay and Kinetic assay.

1 Introduction

Nowadays our economy is based on the linear “take-make-consume-dispose” model which relies on large quantities of easily accessible resources. In fact the global economy and our quality of life is underpinned by natural resources, which include raw materials such as fuels, minerals, food, biomass, air, water and ecosystems. If current trends continue, the global population is expected to grow by 30 % to around 9 billion people by 2050 (European Commission 2011). Even the most conservative projections for global economic growth for the next decade suggest that the demand for coal, oil, iron ore and other natural resources will rise by at least a third (Ellen MacArthur Foundation 2013). In order to cope with the resulting increasing environmental pressure and rapid depletion of resources, resource efficiency and a shift to a circular economy will be the keys to secure growth and jobs.

A circular economy is designed to keep added value in products as long as possible, to eliminate waste and to run on renewable energy. At the end of a product’s life, its resources are recycled again and again, creating further value, reducing raw materials input. It thus requires changes and innovation throughout the entire value chain, rather than solely on end of life solutions (European Commission 2011). The European Commission published a conceptual diagram to illustrate the main phases of a circular economy model (Figure 1-1). As shown, the different phases are interlinked, illustrating the cascade resource usage, minimizing resource leakage from the economy.

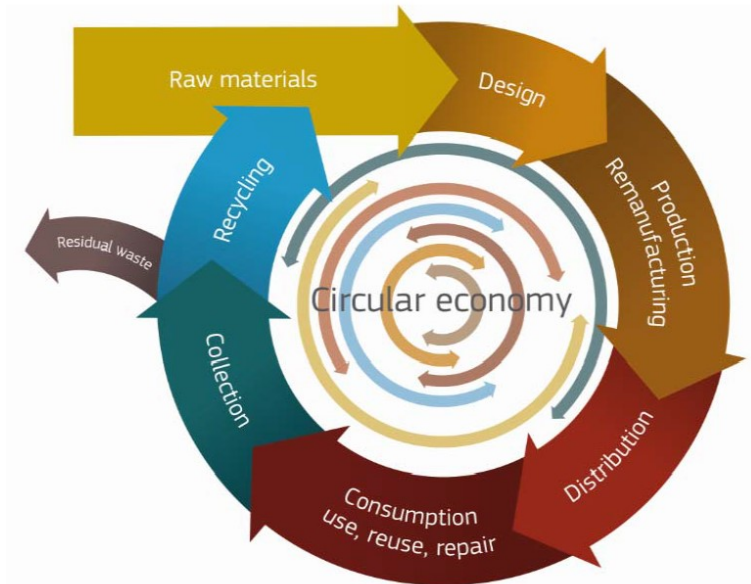


Figure 1-1: Circular economy conceptual diagram (European Commission 2014)

One part of the transition to a more circular economy is turning today's waste into a resource. Despite the active European waste management legislation, which stimulates innovation in recycling and reuse, limits landfilling, reduces losses of resources and creates incentives for behavioural change, still little more than a third (40 %) of the waste generated in the EU (2,7 billion tonnes of waste in 2010 ~ 5 tonnes of waste per person per year) is recycled, reused, composted or digested (Ellen MacArthur Foundation 2013, European Commission 2014). It is thus necessary to search for new recycling/reengineering methods for waste products that are still landfilled or burned.

Another problem arising from the production of goods and the increasing population is the contamination of water supplies e.g., groundwater, surface water, ... These contaminants pose a serious obstacle in delivering good quality and high quantity of water to the public. Furthermore, the development of more environmentally responsible water resources, that do not rely on large water projects in pristine environments, are threatened by the emerging contaminants (Crittenden et al. 2005).

1.1 Particle Board

Forests provide a long range of wood and non-wood products, they offer habitats for animals, play an important role in climate change mitigation, ... However over the last years, threats to forests and forestry are increasing due to growing demand for wood and bioenergy. In Europe, forests and other wooded land cover over 40% of the EU's land area from which 57 % of the total EU forest area is designated primarily for timber production (Ciccarese et al. 2014, European Commission 2013). Several actions like afforestation and natural succession have increased the EU's forest area by around 0.4% per year over recent decades in contrary to the global decrease (European Commission 2013). Currently (2013) 60-70 % of the yearly increment in wood is being cut (European Commission 2013). However, harvest rates are expected to increase by around 30% by 2020 as compared to 2010 (European Commission 2013). As example, forest biomass now accounts for around half of the EU's total renewable energy consumption (European Commission 2013). To fulfil the 2020 renewable target the amount of wood used for energy purposes in the EU would be equivalent to the total wood harvest in 2013 according to the National Renewable Energy Plans (European Commission 2013). Sustainable forest management is thus necessary to deliver and provide enough wood in Europe on a balanced way. During the Ministerial Conference on the Protection of Forests in Europe, Helsinki, 1993 sustainable forest management is defined as (Europe 1993):

"Sustainable forest management means using forests and forest land in a way, and at a rate, that maintains their biodiversity, productivity, regeneration capacity, vitality and their potential to fulfil, now and in the future, relevant ecological, economic and social functions, at local, national, and global levels, and that does not cause damage to other ecosystems."

The European Commission (2013) suggests to build a new framework to fulfil the growing demand for raw materials ensuring a sustainable and balanced management of our forests by adopting a "cascade" principle. This principle implies prioritizing forest outputs / resources that have higher added-value, to create more jobs and to contribute to a rural development and a better carbon balance (Ciccarese et al. 2014, European Commission 2013).

Today, wood is already a good example of intense reuse and recycling operations (cascades). Mantau (2012) described and calculated a cascade factor for wood resources in Europe (EU27). The cascade factor calculates the relation between the total wood resources from trees and other wood resources on basis of the total wood resources from trees. He found that wood resources from trees have been used 1.57 times (so they are used one and a half time). The biggest waste wood user (six million tonnes dry wood

Chapter: 1

waste per year in 2012) is the particle board production industry (Knauf 2014). On average the current level of recycled wood for particle board is 33% (typically between 25 – 95 %) (Harwell 2010, Knauf 2014). However, it is technically possible to use up to 100% of waste wood (Knauf 2014). In addition for its production low grade logs such as thinnings, twisted/bowed logs, knots, branches, stumps, ... can be used (Thoemen et al. 2010).

The first step in particle board production is mechanically reducing the wood input materials into small particles which have a high degree of slenderness (long, thin particles, no dust, no splinters and no oversized particles) (Forest Products Laboratory 2010). Once they have been cut their moisture content is reduced to 2 – 8 % (Thoemen et al. 2010). Next, thermosetting adhesives are applied and the particles are distributed in several layers (typically three). Core particles are long and thin, surface particles are shorter, thinner and smaller for a smoother surface (Forest Products Laboratory 2010). The most commonly used adhesive is urea formaldehyde (UF), followed by melamine formaldehyde (MF), followed by phenol formaldehyde (PF) blended with some additives e.g., hardeners, pigments, fire retardants, preservatives, etc. (Thoemen et al. 2010). MF resins are often used in combination with UF as melamine urea formaldehyde to reduce cost. The amount of resin used depends on the desired product characteristics. The overall resin content usually ranges between 4 – 10 % based on the dry resin and particle weight. The next step in the panel production is the pre-pressing (cold pressing to reduce the height by 50 – 70 %) and hot-pressing (plates have a temperature of 200 – 220 °C, pressure 2 – 4 MPa) of the mat to form panels followed by trimming, sanding and packaging of the panels (Thoemen et al. 2010).

The world production of particle board in 2013 was 99.28 Mm³, with Europe (47.7 %) as major producer followed by America (34.6 %) and Asia (15.5 %) (FAOStat 2015). As every product, particle board has a limited service life. Garcia & Freire (2014) estimated the average service life is around 10 years for wood-based panels. Reuse of this material is often limited due to the harsh environments where particle boards have been used (BFM 2004, Harwell 2010). Also recycling of the panels is difficult as the size of the wood particles is often reduced (Harwell 2010). For example, the use of reject panels and off-cuts for the production of new particle board panels is usually less than 5 % because of the desired chip geometry and the final panel properties (Wrap 2007). Besides the (partly) recycling of particle board, classical thermo-chemical conversion (e.g., combustion) is performed of the generated waste containing aminoplasts resins might cause pollution because it results in the production of toxic gases like ammonia, isocyanic acid and hydrocyanic acid and nitrous oxides (Girods et al. 2008a, Girods et al. 2009b, Girods et al. 2008b). The disposal and environmental problems

associated with particle board require a processing technique which results in products of added value and which meets both ecological and economical needs. In addition, during the production of particle board a considerable amount of waste resin is produced that cannot be re-used or recycled at this moment.

A sustainable solution is therefore more and more required to avoid environmental problems and landfilling costs, and to turn these waste streams in a rather profitable material resource.

1.2 Brewer's spent grain

To meet the Europe 2020 Strategy Calls for a bio economy and a resource efficient Europe agro-industrial by-products (lignocellulosic biomass waste) are seen as promising sources of carbon and energy (European Commission 2012). A large producer of these by-products (spent yeast, brewer's spent grain) is the brewing industry. Brewer's spent grain (BSG) represents around 85% of the total by-products generated by the brewing industry (Aliyu & Bala 2011, Cook 2011, Gupta et al. 2010, Mussatto 2013, Mussatto et al. 2006). In the brewery, the milled malted barley (and some possible additives) is mixed with water and slowly heated from 37 °C to 78 °C (Gupta et al. 2010). This starts an enzymatic hydrolysis which converts the malt starch into fermentable (mainly maltose and maltotriose) and non-fermentable sugars (dextrins) (Mussatto 2013). During this stage, proteins of the malted barley are also partly degraded into polypeptides and amino acids as well as solubilizing many low molecular weight compounds and soluble gums (Cook 2011, Mussatto 2013). At the end of the process, a mixture of sweet liquid (wort) and insoluble, undegraded part of the malted barley grain (known as brewer's spent grain) is obtained. The wort is filtered through the brewer's spent grain and transferred to the next step of the brewing process (boiling, clarification, fermentation, ...). Brewer's spent grain are thus the remains (husk, pericarp-seed coat layers) from the barley malt after the mashing process combined with the insoluble part of the adjuncts (other cereal grains). It is a lignocellulosic material rich in fibres (60 - 70 wt. % dry matter; cellulose, hemicellulose and lignin) and proteins (20 wt. % dry matter; from which app. 30 % essential amino acids) (Gupta et al. 2010, Mussatto 2013, Mussatto et al. 2006). On average its weight accounts for 31% of the original malt. 14 - 20 kg of wet BSG (20 - 25 wt. % dry matter) is produced per 100 l beer (Cook 2011, Deconinck et al. 2001, Gupta et al. 2010, Mussatto et al. 2006). For Europe (EU27 in 2011) with a total beer production of 38400 Ml (Eurostat 2011) the average production capacity was around 5.38 - 7.68 Mt of wet BSG. The worldwide annual brewer's spent grain production is estimated to be approximately 38,6 Mtonnes.

Traditionally this material has been landfilled or sold as animal feed mostly for ruminants which can cope with the high fibre content (Cook 2011, Gupta et al. 2010). However, brewer's spent grain is difficult to store because of the rapid deterioration due to microbial activity and therefore it is not always suitable for food applications. In warm climates for example spoilage due to mould growth can occur within five to seven days (Cook 2011). Furthermore, the environmental implications of increased methane emission due to this hard to digest material are gaining attention (Cook 2011). Additionally, the number of agricultural businesses is decreasing, resulting in a considerable decline in prices for brewer's spent grain.

Despite its potential as a valuable and renewable resource for industrial exploitation, it has received little attention as a marketable product yet.

1.3 Activated Carbon

Activated carbon is a part of the carbon materials family. The element carbon with its atomic structure ($1s^2, 2s^2, 2p^2$) has unique bonding possibilities with other elements or with itself. When carbon atoms bond with each other three major allotropic forms of carbon materials can be formed (depending on the hybridisation type) (Menéndez-Días & Martín-Gullón 2006, Radovic et al. 2009) as schematically depicted in Figure 1-2. All carbon materials are formed in either the gas, fluid or solid phase; and this phase and the conditions dictate in large extent the variability in their physicochemical properties (Radovic et al. 2009).

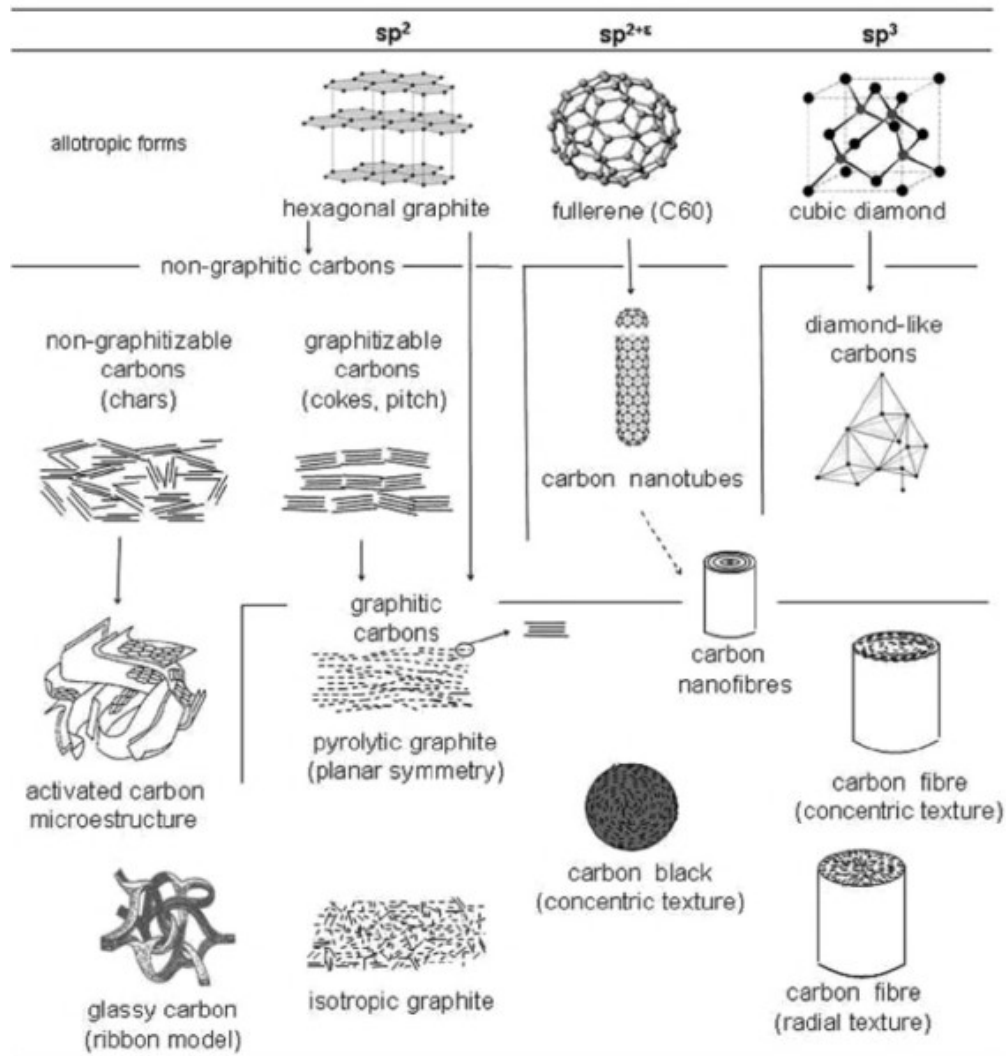


Figure 1-2: Schematic representation of the major allotropic form of carbon and examples of the possible derived structures (Menéndez-Días & Martín-Gullón 2006)

Most of the carbon materials exhibit the allotropic form of graphite (sp^2), and depending on the degree of crystallographic order in the c -direction they can be classified into graphitic and non-graphitic carbons (Menéndez-Días & Martín-Gullón 2006). The non-graphitic form can further be divided in graphitizable (conversion by heat treatment at high temperature up to 3300 K under atmospheric pressure or at lower pressure) and non-graphitizable (Bansal & Goyal 2005, Menéndez-Días & Martín-Gullón 2006). Activated

carbon can be formed out of the non-graphitizable non-graphitic carbons which are produced in the solid phase out of thermosetting carbons such as thermosetting polymers, wood, peroxidised bituminous coal (Radovic et al. 2009). The absence of a plastic phase during the devolatilisation process gives rise to a strong developed cross-linking (promoted by the presence of associated oxygen or insufficient hydrogen amount in the original material) between neighbouring randomly oriented elementary crystallites, resulting in a rigid immobile mass and extensive development of porosity in the resulting chars (Bansal & Goyal 2005, Radovic et al. 2009). The graphene layers are thus piled up on top of each other by Van der Waals interactions to form a turbostatic structure (Bandosz & Ania 2006). Selective gasification or chemical activation can further tailor the porosity to produce activated carbons.

Activated carbons are able to adsorb a multiplicity of organic molecules, mainly by weak intermolecular interactions, which can be superimposed by π - π interactions in the case of aromatic adsorbates or by electrostatic interactions (Worch 2012). Their high adsorption capacities make them a preferred adsorbent in all water treatment processes where organic impurities should be removed (Worch 2012). Yearly around 80 % of the total activated carbon is consumed for liquid-phase applications (Bansal & Goyal 2005).

88 % C, 0.5 % H, 0.5 % N, 1 % S, 6 – 7 % O and 3 - 4 % ash is the standard composition of an activated carbon (Menéndez-Días & Martín-Gullón 2006). These values can shift depending on the precursor and its production process.

1.3.1 Production of activated carbon (based on Menéndez-Días & Martín-Gullón (2006))

Almost any carbonaceous solid material with a high carbon and a low inorganic content, which does not pass through a fluid or pseudo-fluid phase, can be converted into an activated carbon. However, the selection of the precursor (in combination with the thermal treatment and activation) influences to a great extent the final properties of the resulting activated carbon (Menéndez-Días & Martín-Gullón 2006). A good precursor for the production of activated carbon is selected on the following criteria (Marsh & Rodríguez-Reinoso 2006a, Menéndez-Días & Martín-Gullón 2006):

- low ash content
- low cost and high availability
- low degradation during storage

- ease of activation
- possibility of high activated carbon yield with high density, hardness and highly developed pore structure

After selection of a good precursor a series of steps are performed to produce activated carbon. A schematic overview of the activated carbon production is shown in Figure 1-3.

First some **pre-treatments** could be necessary like crushing, sieving, coagulating, washing, mixing, etc. to prepare the input material for the carbonisation and activation step. For example, it could be that for a specific activated carbon with a well-defined granular form, several different kinds of coals need to be crushed, washed, mixed and finally coagulated before thermal treatment to obtain specific properties. After the pretreatments, a **carbonisation** step (also called pyrolysis) is carried out. This very important step lays the foundation of the microporous structure of the resulting char. The precursor is heated in an inert atmosphere resulting in a decomposition of the macromolecular structure yielding a gaseous fraction (hydrogen, light hydrocarbons and tar) and a solid fraction namely char (Menéndez-Días & Martín-Gullón 2006). Figure 1-4 depicts a typical reaction scheme of the char formation during carbonisation. When heating a raw material in an inert atmosphere, gasses and vapours (primary products) devolatilize (raw material decomposes in gasses and vapours). These primary products may react with each other to form secondary cracking products depending on the residence time and treatment temperature (Menéndez-Días & Martín-Gullón 2006). At temperatures around 500 °C the gas phase consists out of mainly stabilized primary products (Menéndez-Días & Martín-Gullón 2006). With increasing temperature the secondary cracking reactions become more important. At temperatures between 800 – 900 °C, olefins, methane, hydrogen, water and carbon oxides together with stabilized polyaromatics (polycyclic aromatic hydrocarbons; intermediates of soot) can be formed which can be deposited over the char particles, especially at high heating rates. At temperatures above 1000 °C, the secondary reactions are more important with the formation of methane, hydrogen and soot at these extreme conditions (Menéndez-Días & Martín-Gullón 2006). During the carbonisation a large part of the initial raw material is devolatilized, increasing the carbon content and aromaticity of the char, accompanied by an increase of incipient microporosity (Menéndez-Días & Martín-Gullón 2006). The resulting char is made out of groups of small disordered graphitic crystals with void spaces, which are often not accessible from the external surface due to soot deposition in the meso- and macropore structures (Menéndez-Días & Martín-Gullón 2006). The resulting structure of the char varies with the pyrolysis temperature. During the devolatilisation, the resulting skeletal structure becomes extremely unstable and carbons within

this structure will combine with other carbon atoms creating arrangements of maximum stability (Marsh & Rodríguez-Reinoso 2006b). An increase of the pyrolysis temperature moves the structure to greater stability (Marsh & Rodríguez-Reinoso 2006b). The heating rate is also an important factor influencing the final properties of the char. A low heating rate induces a slow release of volatiles, resulting in a well-developed microporosity, a good hardness and density. A high heating rate results in a quick release of volatiles, promoting a large meso and macro structure with a lower density and hardness (Menéndez-Días & Martín-Gullón 2006). The microporosity developed with a low or a high heating rate is similar. Therefore, a moderate temperature with a low heating rate and long soaking times gives the best conditions.

The next step is the **activation** of the char to enhance the incipient porous structure. The activation production methods can be grouped into two defined groups: thermal (physical) activation and chemical activation.

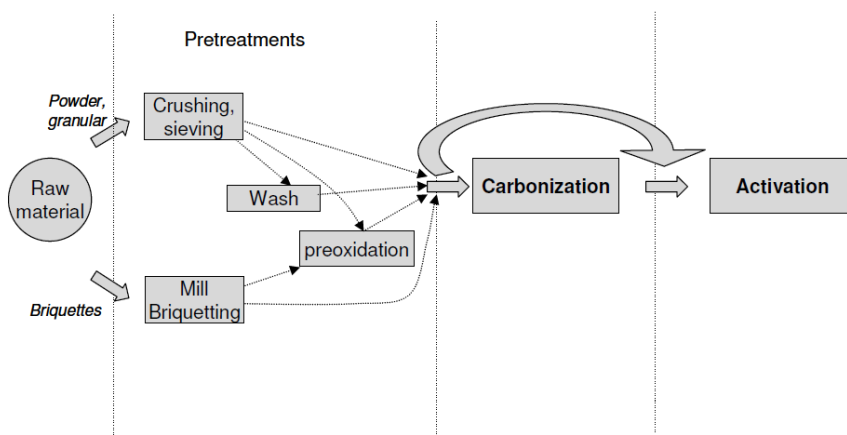


Figure 1-3: Schematic overview of activated carbon production (Menéndez-Días & Martín-Gullón 2006)

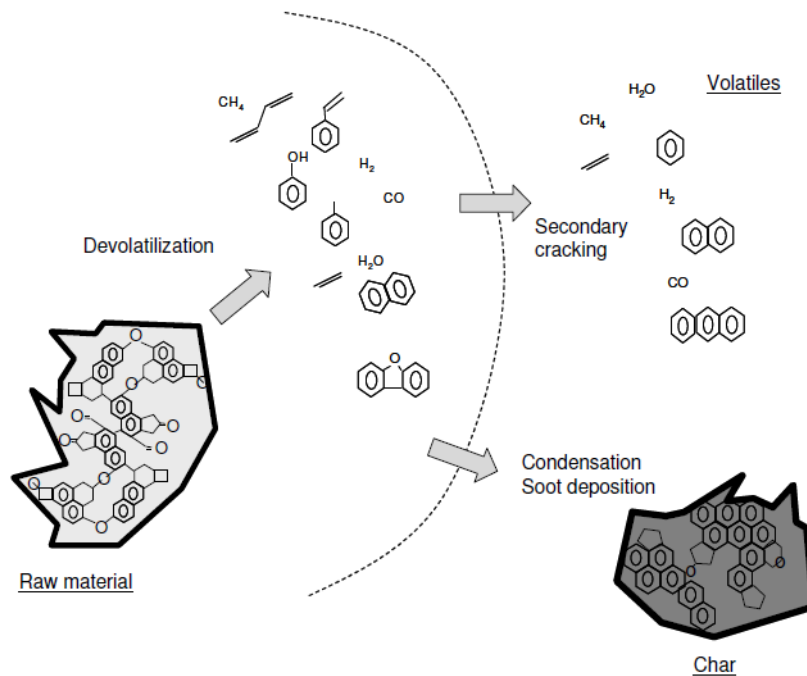
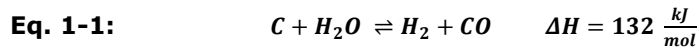


Figure 1-4: Char formation reaction scheme (Menéndez-Días & Martín-Gullón 2006)

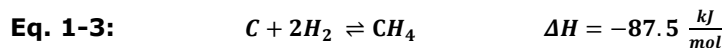
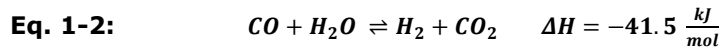
1.3.1.1 Thermal activation

During the thermal activation, the char is partially gasified with an oxidizing agent (oxygen, steam, carbon dioxide) at temperatures between 800 – 1000 °C. The gas reacts with carbon atoms removing some internal mass of the char, creating a well-developed microporous structure. To produce an activated carbon, it is necessary that gasification progress is under chemical control instead of diffusion control (Menéndez-Días & Martín-Gullón 2006). Under chemical control the reaction obeys the uniform conversion model, the oxidizing reagent first diffuses through the pore network and then reacts with the internal active sites (Menéndez-Días & Martín-Gullón 2006). Under diffusion control the reaction occurs on the external particle surface which is burned off (Menéndez-Días & Martín-Gullón 2006).

Due to the high exothermic and difficult to control reaction of oxygen with carbon material at high temperature it is only scarcely applied (Marsh & Rodríguez-Reinoso 2006a, Menéndez-Días & Martín-Gullón 2006). In contrast to oxygen activation both steam and carbon dioxide activation follow an endothermic pattern (Eq. 1-1) and are thus controllable.

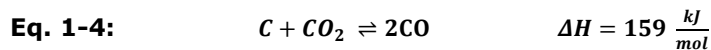


The reaction products could also react with each other, but this takes hardly place due to the very slow kinetics.



Steam activation has the advantage of achieving chemical control up to temperatures of 1000 °C and is therefore the most widely used method in industry (Menéndez-Días & Martín-Gullón 2006). Activation by steam is taking place throughout the whole char and is similar for all chars. Differences are due to active sites because of differences in chemical structure of the precursor and mineral content. The obtained activated carbons are microporous, with increasing micropore size as activation proceeds, but with no development of mesopores (Menéndez-Días & Martín-Gullón 2006). Steam activation easily reaches surface areas of 1000 m²/g at activation conversion degrees (burn-off) of 50% regardless of the carbonization yield with an initial ash content of the precursor below 10% (Menéndez-Días & Martín-Gullón 2006).

Carbon dioxide activation is similar to steam activation an endothermic reaction (See Eq. 1-4) but its reaction rate is somewhat slower (Menéndez-Días & Martín-Gullón 2006).



Under chemical control the porosity development is as high as with steam activation. However in industrial applications carbon dioxide tends to react under diffusion control limiting its use.

1.3.1.2 Chemical activation

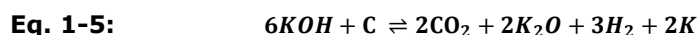
Chemical activation is mostly carried out in a one step process, i.e., simultaneously with the carbonization step. The raw materials are impregnated with chemicals, followed by heating in an inert atmosphere. Final temperatures for chemical activation are lower than required for thermal activation. The most commonly used chemicals in industry are zinc chloride, phosphoric acid and potassium hydroxide (Marsh & Rodríguez-Reinoso 2006a, Menéndez-Días & Martín-Gullón 2006)

An aqueous zinc chloride paste is used to impregnate preferably precursors with a high volatile content (lignocellulosic materials) (Menéndez-Días &

Martín-Gullón 2006). After impregnation, the residual water is evaporated which causes hydrolysis reaction (which are dependent on the ZnCl_2 amount) within the lignocellulosic structure increasing both elasticity and swelling of the particles (Menéndez-Días & Martín-Gullón 2006). Finally the impregnated raw material is heated in an inert atmosphere at temperatures between 500 – 800 °C. The chemical activation with zinc chloride produces an activated carbon with a wide (wider than thermal activation) and open microporosity. This is due to the restriction of tar formation and the prevention of particle contraction by zinc chloride (Menéndez-Días & Martín-Gullón 2006). In comparison to thermal activation, higher yields, lower particle density and lower abrasion/hardness values are obtained by zinc chloride activation (Menéndez-Días & Martín-Gullón 2006). However, due to low recovery efficiencies, corrosion problems, presence of residual zinc in the particles and the emissions from the production plant, zinc chloride is more and more replaced by phosphoric acid. As with zinc chloride this activation agent also needs a precursor with a high volatile content. In addition to the structure of the starting material, the impregnation ratio (acid/precursor ratio mostly ~ 1.5) and heat treatment profiles have an impact on the activation (Menéndez-Días & Martín-Gullón 2006). The carbonization is usually carried out in two consecutive steps. First, the material is slowly heated to a temperature of 150 – 200 °C and held isothermally for an hour, followed by a slow heating to 400 – 500 °C with an isothermal period of around one hour (Menéndez-Días & Martín-Gullón 2006). During the low temperature segment, the acid catalyses the hemicellulose and lignin hydrolysing the glycosidic linkage of the hemicellulose and cleaving the aryl ether bonds of lignin accompanied by secondary degradation and condensation reactions (Menéndez-Días & Martín-Gullón 2006). In the higher temperature segment, crosslinking reactions promoted by phosphate esters among the cellulose fibres, are predominantly developing porosity (Menéndez-Días & Martín-Gullón 2006). The resulting activated carbons have, like activation with zinc chloride, a lower abrasion/hardness value and a higher yield than thermal activation. A wider micropore size distribution but a higher adsorption capacity than thermal activation is also obtained (Menéndez-Días & Martín-Gullón 2006). In addition, a more developed mesopore structure is obtained (Menéndez-Días & Martín-Gullón 2006).

In contrast with the other two discussed chemical activation agents, potassium hydroxide activation needs a precursor with a low volatile content rich in carbon (Menéndez-Días & Martín-Gullón 2006). The first step of the activation process is the impregnation which can be performed with an aqueous solution or with solid potassium hydroxide in a ratio between 2 and 4 (Menéndez-Días & Martín-Gullón 2006). The heat treatment is carried out at 700 – 900 °C with a soaking time of around one hour if the agent is physically mixed with the raw material (Menéndez-Días & Martín-Gullón 2006).

2006). For the impregnation method, first a drying step at 100 °C is applied. The activation with potassium hydroxide works different from both zinc chloride and phosphoric acid. Potassium hydroxide attacks the carbon skeleton, producing solid and gaseous products, which results in carbon burn-off developing porosity (Menéndez-Días & Martín-Gullón 2006) with the following reaction proposed by Lillo-Ródenas et al. (2003):



This reaction is thermodynamically favourable above 600°C (Lillo-Ródenas et al. 2003). An extreme narrow microporous structure with no mesopores is formed by the potassium hydroxide activation (Menéndez-Días & Martín-Gullón 2006).

After activation the produced activated carbons are subsequently washed removing the remaining activation agents and the produced salts and metals. The recovery yield strongly influences the feasibility of the chemical activation process (Menéndez-Días & Martín-Gullón 2006).

1.3.2 Porous texture

In all adsorptions (in gaseous and fluid phase), molecules or atoms (adsorbable) are adsorbed on the surface of the adsorbent by physical interactions (electrostatic and dispersive forces) and/or chemical bonds (Menéndez-Días & Martín-Gullón 2006). Therefore the resulting porous structure of the activated carbon is an important parameter for its physical adsorption properties. In addition, the porous structure is also important if chemical adsorption would occur. The internal surface area of an activated carbon usually exceeds the external surface area many times. The total amount of pores, their size and shape determine to a large extent the adsorption capacity and even the rate of adsorption. The International Union for Pure and Applied Chemistry (IUPAC) proposed a classification based on their width (distance between the walls of a slit-shaped pore or the radius of a cylindrical pore) into three categories: micropores (<2 nm), mesopores (2 – 50 nm) and macropores (> 50 nm) (Sing et al. 1985). In the micropores the adsorption is taking place by volume filling without capillary condensation (Bansal & Goyal 2005). Due to the overlapping of adsorption forces from the opposite walls, the adsorption energy is much larger than in the meso- and macropores (Bansal & Goyal 2005). The micropores make 90 – 95 % of the surface area of an activated carbon with pore volumes of 0.15-0.70 cm³/g (Bansal & Goyal 2005, Menéndez-Días & Martín-Gullón 2006). Mesopores serve as a passages to the micropores. They are characterized by capillary condensation (with the formation of a meniscus), a surface area of < 5 % of the total surface area and a volume of 0.2 – 0.65

cm³/g (Bansal & Goyal 2005, Menéndez-Días & Martín-Gullón 2006). The macropores serve also as a passage to mesopores and micropores. However, for adsorption capacity they are not of importance. They have a surface smaller than 0.5 m², large pores usually in the range of 500 – 2000 nm and a pore volume of 0.2 – 0.4 cm³/g (Menéndez-Días & Martín-Gullón 2006). However, the adsorption capacity is not always proportional with the surface area, the pore shape and size is also important for the adsorption process. For instance, a large circular molecule could be blocked to enter a slit shaped pore of a small pore. For large molecules, the mesopore and macropore content can become more important.

The pore structure of activated carbon is usually characterized by using physical adsorption of gasses. Nitrogen gas at 77 K is used most often (Inagaki & Tascón 2006). Recently (after the experiments and writing of this thesis), new IUPAC Technical Report is released on analysing microporous materials (Thommes et al. 2015). For many years, nitrogen adsorption at 77 K has been generally accepted as the standard method for micropore and mesopore size analysis. However, it becomes evident that nitrogen is not entirely satisfactory for assessing micropore size distribution. The quadrupolar nature of nitrogen molecule is largely responsible for specific interactions with a variety of surface functional groups and exposed ions affecting the orientation of the adsorbed nitrogen molecule on the surface. The molecular cross-sectional area can be affected to a degree of 20% for some surfaces. Furthermore, the micropore filling pressure can be strongly affected. Additional problems are associated with pre-adsorbed N₂ molecules, which can block the entrances of narrow micropores, and specific interactions with surface functional groups so that the pore filling pressure is not clearly correlated with the pore size/structure. Argon at 87 K, which has no specific interaction with surface functional groups, is an alternative. However, due to the kinetic restrictions it is of limited value for very narrow micropores (<1 nm) where CO₂ at 273 K performs very good if no polare surface groups are present.

1.3.3 Surface functional groups

Although a good porous structure and pore size distribution are required, the chemical structure of the activated carbon strongly influences the adsorption properties. The edges of the carbon layers and the large number of imperfections and defects (e.g., structural carbon vacancies, non-aromatic rings) which are present in the disordered fraction of the carbon materials are the active sites (Bandosz & Ania 2006). These sites have a high density of unpaired electrons, which can chemisorb heteroatoms leading to stable surface compounds (Bandosz & Ania 2006). A part from the chemisorption, heteroatoms and surface groups are also present from the precursor. The

presence of surface functionalities is thus carbon dependent. The production technique plays therefore an important role. The resulting carbon surface induces a very complex interaction of different surface groups influencing each other by the so-called inductive effect (Bandosz & Ania 2006). The presence of surface functionalities can have an important effect on the interaction with an adsorbate by influencing the hydrophobic/hydrophilic and the acidic/basic character of the activated carbon (Bandosz & Ania 2006).

1.3.3.1 Oxygen-containing functionalities

Oxygen-functionalities are the most common functionalities on an activated carbon surface. Oxygen is adsorbed even at low temperatures. A part of this adsorbed oxygen is irreversibly adsorbed. At room temperature the amount of chemisorbed oxygen is very low. By increasing the temperature the amount of chemisorbed oxygen increases until a maximum at 400 - 500 °C (Bandosz & Ania 2006). However, oxygen functionalities are usually obtained by oxidation. An overview of the different oxygen surface groups is shown in Figure 1-5. Acidic surface groups are formed by oxidizing the carbon at high temperatures or by using oxidizing agents in solution (Bandosz & Ania 2006). Basic oxygen surface groups are formed when an oxidized surface is reduced at high temperatures in inert atmosphere (Bandosz & Ania 2006). The active sites resulting from the decomposition of acidic sites (e.g., carboxylic acid, lactone, phenol groups) attract oxygen-forming basic functional groups like chromene, quinones and pyrone when re-exposure to air occurs after cooling down in an inert atmosphere (Bandosz & Ania 2006). In addition, non-heteroatomic Lewis base sites (regions of π electron density) on the basal planes are also contributing to the basicity (Bandosz & Ania 2006). However, the oxygen functionalities which determine the basic sites of the activated carbon surfaces are still under discussion (Bandosz & Ania 2006).

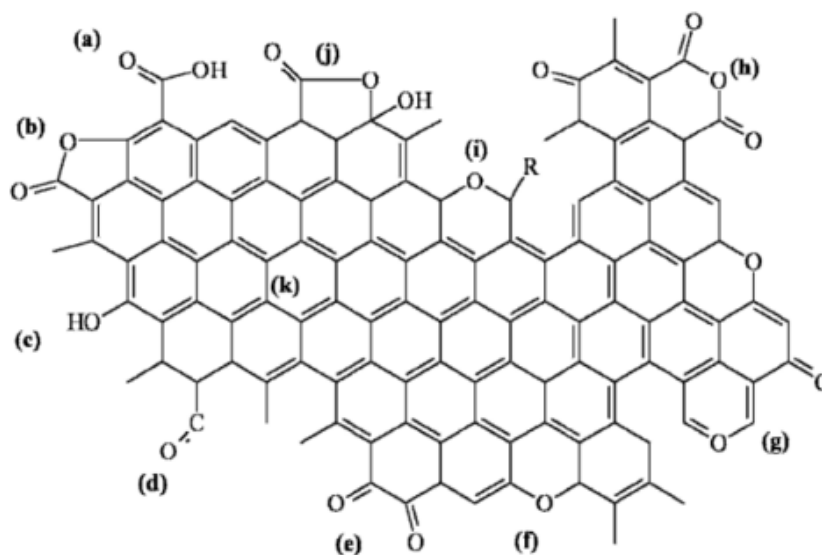


Figure 1-5: Oxygen-containing functionalities: (a) carboxyl groups, (b), lactone, (c) hydroxyl, (d) carbonyl, (e) quinone, (f) ether, (g) pyrone, (h) carboxylic anhydride, (i) chromene, (j) lactol, and (k) π electron density on carbon basal planes (Bandosz 2009)

1.3.3.2 Nitrogen-containing functionalities

Nitrogen surface groups are not formed spontaneously on the surface by contact with air and under normal conditions the amount of nitrogen in the AC is negligible. However, results have demonstrated that nitrogen incorporation improves the adsorptive properties of activated carbon (Bandosz 2009, Bandosz & Ania 2006, Rivera-Utrilla et al. 2011). It can be performed in two ways. The first way is nitrogenation (nitrogen modification) by treating the activated carbon with gaseous nitrogen containing reagents (i.e., ammonia, hydrogen cyanide, amines) or liquid state (i.e., nitric acid, urea amines, ammonia) followed by or during a heat treatment. Another approach for introducing nitrogen is using a nitrogen-containing precursor. The different types of nitrogen functionalities that can be formed are displayed in Figure 1-6. The occurrence of a particular type is function of the nitrogen-containing precursor, heat treatment and activity of the carbon surface. The heat treatment especially plays an important role because of the thermal stability of the different nitrogen surface functionalities (Bandosz & Ania 2006). Generally the treatment with nitrogenation reagents at low temperature (< 527 °C) leads to the formation of slightly acidic surface groups like lactams, imides and amines (Bandosz & Ania 2006). At high

temperatures the formation of quaternary nitrogen, pyridine and pyrrole groups increases (the latter two are basic in nature) (Bandosz & Ania 2006).

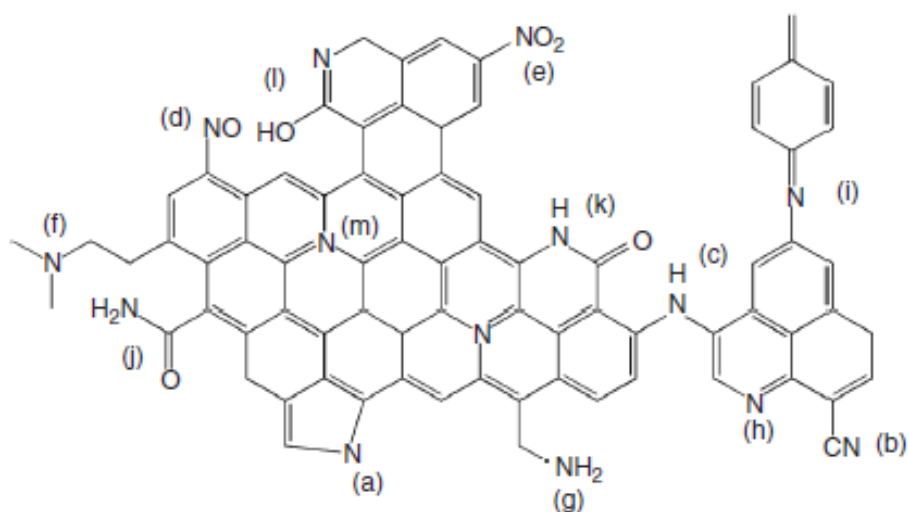


Figure 1-6: Nitrogen-containing functionalities: (a) pyrrole- like group, (b) nitrile, (c) secondary amine, (d) nitroso group, (e) nitro group, (f) tertiary amine, (g) primary amine, (h) pyridine-like group, (i) imine, (j) amide, (k) lactam, (l) pyridone, (m) quaternary amine (Bandosz 2009).

1.3.3.3 Other heteroatoms

In addition to nitrogen and oxygen, also other heteroatoms can be introduced into the activated carbon. Since, this is not in the scope of this dissertation it will not be further discussed here. More information is found in the following references: Bandosz (2009), Bandosz & Ania (2006)

1.3.4 Adsorption theoretical background

Adsorption is defined as an enrichment of chemical species from a fluid (liquid / gaseous) phase on the surface of a liquid or a solid (Worch 2012). The adsorption process is an exothermic ($\Delta H < 0$) and thus a spontaneous process as a decrease of entropy is established during adsorption. The entropy decreases as a result of a decrease of disorder in the adsorbate/adsorbent system. In addition, the adsorbate species have less degrees of freedom if they are adsorbed (Worch 2012).

Eq. 1-6:
$$\Delta G = \Delta H - T\Delta S$$

Depending upon the nature of the forces involved, two types of adsorption can be distinguished namely physical adsorption and chemisorption. In the case of physical adsorption, relatively weak intermolecular Van Der Waals forces are involved, including:

- London forces [dispersion-repulsion]
- Electrostatic interaction [polarization, dipole and quadrupole] (Keesom and Debye forces)

are involved. Chemisorption involves the formation of a chemical bond (exchange or sharing of electrons between adsorbate and adsorbent) (Bansal & Goyal 2005, Ruthven 1984). The general difference between physical adsorption and chemisorption is summarized in Table 1-1:

Table 1-1: General features distinguishing physical adsorption from chemisorption (Ruthven 1984)

Physical adsorption	Chemisorption
Low heat of adsorption ($\sim 10 - 20$ KJ/mol; $-\Delta H$)	High heat of adsorption ($\sim 40 - 400$ KJ/mol, $-\Delta H$)
Nonspecific interaction	Specific interaction
Monolayer or multilayer No dissociation of adsorbate	Monolayer May involve dissociation of adsorbate
Only significant at relative low temperatures	Possible over a wide temperature range
Rapid, no activation energy and reversible	Activation energy, maybe slow and irreversible
No electron transfer, polarization may occur	Electron transfer, leading to a bond formation

For practical applications of adsorption, it is important to study the dependency of the adsorbed amount on the key process parameters and to describe these on a theoretical basis (Worch 2012). This practice-oriented adsorption theory consists out of three constituents: the adsorption equilibrium, the adsorption kinetics and the adsorption dynamics. The relation between the three parts is shown in Figure 1-7.

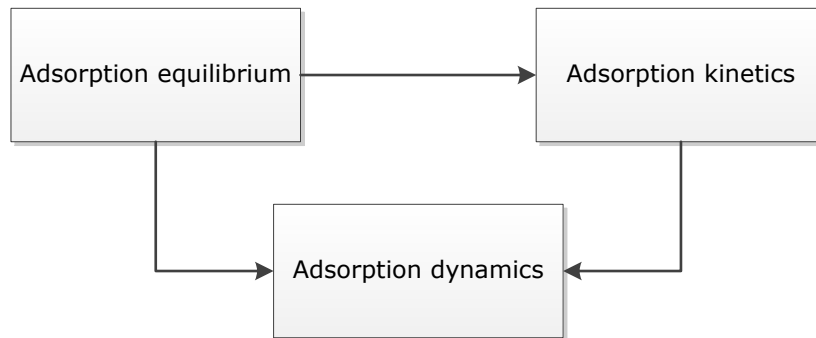


Figure 1-7: Practice-oriented adsorption theory (Worch 2012)

1.3.4.1 Adsorption equilibrium

The adsorption equilibrium (adsorption isotherm) is the most extensively employed method for representing the equilibrium states of an adsorption system. The isotherm reflects the relationship between the amount of a solute adsorbed at constant temperature and its equilibrium concentration in the solution providing essential physicochemical data for assessing the applicability of the adsorption process (Hamdaoui & Naffrechoux 2007, Worch 2012, Yousef et al. 2011). It is the basis of all adsorption models and is a precondition for the application of both kinetic and dynamic adsorption models (see Figure 1-7). In addition the isotherm test is a convenient method for comparing different carbons and for the investigation of the effects of temperature, pH, background matrix, ... The determination of adsorption isotherms is usually determined with the bottle-point method at constant temperature. In this method, a set of bottles is filled with the adsorbate solution of know volume (V_L) and initial concentration (C_i) and different amounts of adsorbent (mass adsorbent = m_{AC}). This mixture is shaken until equilibrium is reached typically less than 24h, but sometimes much longer or also shorter times are needed. The residual concentration (C_e) is determined and the adsorbed amount (Q_e) is calculated by Eq. 1-7.

Eq. 1-7:

$$Q_e = \frac{(C_0 - C_e)V}{m_{AC}}$$

Several isotherm models are available for analysing experimental adsorption data. In this work the equilibrium data are fitted by two two-parameter models: the Langmuir and the Freundlich model.

The Langmuir model (Eq. 1-8) assumes uniform energies of adsorption (and thus uniform energy of the active sites) onto the surface, no transmigration of adsorbate in the plane of the surface and monolayer adsorption (Hamdaoui & Naffrechoux 2007, Yousef et al. 2011).

Eq. 1-8:
$$Q_e = \frac{Q_m K_L C_e}{1 + K_L C_e}$$

where Q_e (mg/g) is the amount of solute (phenol in this work) adsorbed per unit weight of adsorbent at equilibrium, C_e (mg/l) the equilibrium concentration of the solute in the bulk solution, Q_m (mg/g) the maximum adsorption capacity and K_L ($l\ mg^{-1}$) the constant related to the free energy of adsorption or net enthalpy of adsorption.

The favourable nature of adsorption can be expressed in terms of a dimensionless parameter, the separation factor R_L which is defined by Eq. 1-9 (Hamdaoui & Naffrechoux 2007):

Eq. 1-9:
$$R_L = \frac{1}{1 + K_L C_i}$$

where C_i (mg/l) is the initial concentration of the adsorbate. R_L indicates whether the adsorption is irreversible ($R_L = 0$), favourable ($0 < R_L < 1$), linear ($R_L = 1$) or unfavourable ($R_L > 1$):

The Freundlich model (Eq. 1-10) assumes that the adsorbent surface energy is related to heterogeneous, multilayer adsorption. The stronger binding sites are occupied first and the binding strength decreases with increasing degree of site occupation.

Eq. 1-10:
$$Q_e = K_F C_e^{1/n}$$

where Q_e (mg/g) is the amount of solute adsorbed per unit weight of adsorbent at equilibrium, C_e (mg/l) the equilibrium concentration of the solute in the bulk solution, K_F ($mg^{1-(1/n)}\ l^{1/n}/g$) is a measure for the relative adsorption capacity of the adsorbent and n is a measure for the intensity of the adsorption (favourability of adsorption) (Hamdaoui & Naffrechoux 2007). A value of n in the range 2 – 10 represents “good”, 1 – 2 “moderately difficult”, and < 1 “poor” adsorption characteristics (Hamdaoui & Naffrechoux 2007).

1.3.4.3 Adsorption kinetics

The adsorption of a substance on the surface of an activated carbon is time dependent and consists out of a seven step process which is depicted in Figure 1-8 (adapted from Le Cloirec (2002)).

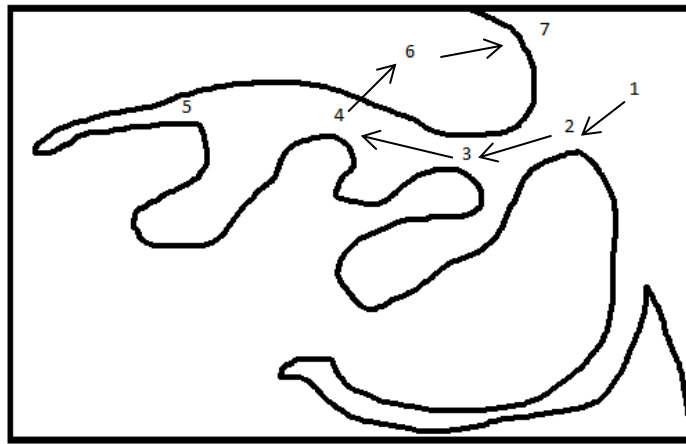


Figure 1-8: The mass transfer-adsorption process (Le Cloirec 2002)

The first step is bulk diffusion (1), the adsorbate needs to diffuse from the solution to the hydrodynamic layer of the activated carbon. The following step is the external mass transfer ((2) film diffusion) through the hydrodynamic layer surrounding the activated carbon particle. After the external mass transfer delivering the adsorbate to the external activated carbon surface, internal mass transfer ((3) intraparticle diffusion) conveys the adsorbate. This transfer may occur through the pore fluid or along the pore wall (Chowdhury et al. 2013). The fourth step (4) is the very quickly adsorption producing an exothermic reaction in the range of 0 – 60 kJ/mol ($-\Delta H$) (Chowdhury et al. 2013, Le Cloirec 2002). After adsorption, the molecules diffuse (5) very slowly on the adsorbent surface to their final location. Steps (6) and (7) are the thermal conduction from heat generated by the exothermic reaction through the solid to the solution and to the solution respectively (Le Cloirec 2002).

As the first and the fourth step are fast, the total rate of the adsorption process is thought of as a two-step mass transfer process (of external and internal mass transfers) (Chowdhury et al. 2013, Le Cloirec 2002). Since these diffusion steps act in series, the slowest step is the rate limiting step of the adsorption process. Investigation of the kinetics is necessary to determine the rate-limiting mass-transfer mechanisms, uptake rates and to

evaluate the mass transfer parameters. Together with the equilibrium data the kinetic results are essential input data for determining contact times in adsorption reactors.

In order to study the adsorption kinetics, jar testing or modelling predictions are used. In both methods a defined mass of activated carbon is brought into a solution with known volume (V_L) and concentration (C_0). The resulting concentration change is measured in function of the time. Model predictions are of limited value as no widely accepted model exists for target organic contaminant removal (Chowdhury et al. 2013). In this work the experimental data (from jar testing) are fitted using the pseudo-first-order model (Eq. 1-11) and the pseudo-second-order model (Eq. 1-12)).

Eq. 1-11:
$$Q_t = Q_e - Q_e e^{-K_f t}$$

Eq. 1-12:
$$Q_t = \frac{Q_e^2 K_s t}{1 + Q_e K_s t}$$

Where Q_e is the equilibrium adsorption capacity (mg/g), K_f (1/h) and K_s (g/mg h) are the pseudo-first-order model and pseudo-second-order model rate constants respectively. The pseudo-second-order model predicts the behaviour over the entire range of the adsorption process and is in agreement with a rate controlling step in the adsorption mechanism (Hameed & Rahman 2008, Li et al. 2013). The pseudo-first-order model is generally only applicable over the initial stage of adsorption (Hameed & Rahman 2008, Li et al. 2013).

1.3.4.4 Adsorption dynamics

The adsorption dynamics are an important feature for fixed-bed adsorbers as this is a time and distance-dependent (not steady-state) process. In contrast to slurry reactors, fixed bed adsorbers are better suitable for granular activated carbon. During adsorption, an adsorption front is created as displayed in Figure 1-9. The carbon above this front is in equilibrium with the influent concentration. Due to the dispersion and mass transfer kinetics a mass transfer zone is created. Below the mass transfer zone the concentration is zero. The shape of the mass transfer zone is dependent on the adsorption rate and the shape of the equilibrium curve (Worch 2012). The mass transfer zone moves through the system. In time a gradual increase in concentration of the target compound is seen at the output until a complete breakthrough (concentration in = concentration out of the target compound).

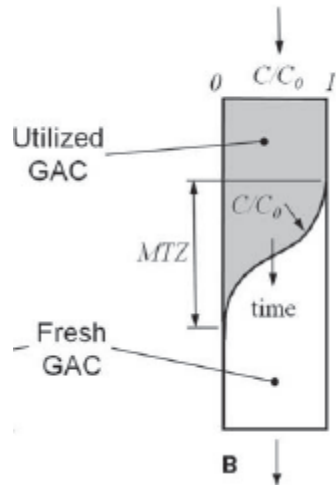


Figure 1-9: Unsteady-state fixed bed adsorber concentration profile (Chowdhury et al. 2013)

The distribution of mass transfer zone is mainly influenced by the mass transfer resistances of the activated carbon as the dispersion effect is usually negligible under typical fixed-bed adsorber conditions (Worch 2012). The dynamic adsorption is determined by Pilot-Scale testing, Bench-Scale testing or by model predictions. Pilot-Scale testing is the currently most used and accepted method predicting the adsorption dynamics. However, this is an expensive and time consuming process. The model prediction is of limited value in evaluating the performance as no widely accepted empirical models are available to predict the performance. The use is also limited due to the dependence of the specific activated carbon, the adsorbate and the dissolved organic molecules in solution. A Bench-Scale (rapid small-scale column) test is available to reduce the amount of samples. The rapid small-scale column test is a downscaled version of the fixed-bed adsorber. However, the results of this test are not completely matching the full-scale data due to two problems: first (1) the adsorbate diffusion is dependent on the activated carbon particle size, secondly (2) the bench test exhibits a larger adsorption capacity. (Chowdhury et al. 2013). Despite, these problems this rapid low cost simulation gives very useful information in the design process of a pilot fixed bed installation.

1.4 Techno-economic assessment

Many innovative technologies, research topics and products have a (potential) faultless technical performance, however many of them fail due to economic reasons at market introduction. Investigation of the economics during the development stage could save a lot of money invested in non-feasible technologies (and projects) and drive this towards other innovative technologies or direct the focus towards the parameters that influence the economic performance. (It may not be worth to investigate the improvement of a parameter that only influences the economic performance of the whole process slightly, while other parameters needs more attention on its improvement to improve the economics.) Unfortunately, at this moment there is no systematic economic analysis tool that integrates technical and economic calculations. The economic calculations are often added ex-post, and detailed information and the effect of the parameters on the economic performance is in many cases not provided. A techno-economic assessments address this problem (also called techno-economic analysis, techno-economic evaluation). It is a rather new concept and its use is significantly increasing since 2010, however no clear accepted definition is accepted. Furthermore, no standards are provided on how to perform a techno-economic assessment. In literature some efforts have been made to provide a definition such as Smura et al. (2007), Kantor et al. (2010) and NABC (2016). In this dissertation, we will use the definition provided by Kuppens (2012): *"A techno-economic assessments is the evaluation of the technic performance or potential and the economic feasibility of a new technology that aims to improve the social or environmental impact of a technology currently in practice, and which helps decision makers in directing research and development or investments."*

Based on the work of Kuppens (2012) a techno-economic assessment needs to answer three questions: (1) How does the technology work? (2) Is the technology profitable? (3) Is the technology desirable? Strictly following the definition, only question 1 and 2 are addressed as a techno-economic assessment consists out of an integrated technological (i.e., mass and energy balance) and economic (i.e., investment analysis) evaluation. Van Dael et al. (2014) added a sustainability analysis to address question 3 and defines this as an extended techno-economic assessment. By applying this methodology chances of missed opportunities or failed market introductions will be diminished (Van Dael et al. 2014).

Chapter: 1

It is advised to perform techno-economic analysis as soon as possible in the research and development phase of a new process as it can provide (Van Dael et al. 2014):

1. initial assessment on the barriers (operational and technical) to overcome,
2. optimal sizing of the project
3. desirable product yields and waste management
4. indication of the (preliminary) feasibility or the main factors (financial or technical) that limit its feasibility.

Van Dael et al. (2014) provides a general framework for a techno-economic assessment methodology and describes four phases. A techno-economic assessment is performed in an iterative way with a go-no-go basis after every iteration. First, a market study is performed. This provides information regarding competition and customers, market size and needs, alternatives, costs and revenues and the legislation. This first phase, provides a lot of information needed in the following phases. It can also be used to convince investors, policymakers or customers. Second, a preliminary process design is defined and translated into mass and energy balances. Third, the information is integrated directly in a dynamic model which estimates capital and operational costs and revenues. This information is used to calculate projected discounted cash flows. Fourth, a risk analysis is performed to identify potential technical and non-technical barriers. As a fifth phase an environmental analysis can be added to assess the desirability of the project. Based on the results, risk reduction strategies can be formulated and the techno-economic assessment steps can be repeated. A techno-economic assessment will thus enhance the chances of success and diminishes costs from development to market introduction.

1.5 Research questions

The aim of this dissertation is to answer the question whether industrial organic waste streams (i.e., brewer's spent grain, melamine formaldehyde and particle board) are interesting renewable resources for the profitable production of nitrogenised activated carbons. The main research question that needs to be answered at the end of this PhD project is therefore:

What is the potential of brewer's spent grain and particle board waste streams to be profitably valorised as a precursor for activated carbon?

In order to make this research question operational, it is divided into sub questions.

Subquestion1:

Can the production of activated carbon from the selected waste streams be profitable? And what are the key variables for the profitability of the production of activated carbon from the waste streams?

Before investing a lot of time and money in the production and assessment of activated carbons, one should first assess the economic potential of the precursors for the production of activated carbon. In addition, the identification of the crucial variables for rendering the production of activated carbon from the waste streams profitable need to be determined. For this purpose, a preliminary economic feasibility study needs to be carried out for a process design especially developed for the production of activated carbon from the selected waste streams. After developing a process diagram of an activated carbon production unit, the net present value of the cash flows generated by an investment in co-pyrolysis and char activation has to be calculated. The minimum selling price of the produced AC needs to be determined, taking into account uncertainties by performing Monte Carlo Sensitivity analysis. Finally, this preliminary economic feasibility study will be used to identify the key variables for the profitability of the production of activated carbon from the precursors.

Subquestion 2:

How can high quality activated carbons from the selected precursors be produced and what is the best production strategy?

This subquestion is closely related with subquestion 1 and implies an exploration of the possible activated carbon production techniques. This knowledge will be used in the development of the process design and the development of a lab-scale pyrolysis and activation reactor.

Subquestion 3:

What are the characteristics and the quality of the produced activated carbons?

To find an answer on this question, first the characteristics of the waste materials need to be investigated followed by the effect of the temperature and time of steam activation on the yield and features and properties (surface properties and porous nature) of the produced activated carbons. The performance of these will be evaluated by batch adsorption experiments in function of different parameters like time, temperature, ionic strength and pH using phenol and three pharmaceuticals as target compounds.

2 Material and methods

Chapter 2 summarizes the experimental approach and strategy of this research. Section 2.1 describes the studied waste materials briefly. The analytical techniques used for the characterisation of the waste materials are described in Section 2.2. Section 2.3 gives an overview of the different pyrolysis and activation routes used in this research. The next section (Section 2.4) describes the different characterisation techniques to analyse the obtained activated carbons, while the methodology of the adsorption studies (Nitrogen adsorption study, phenol adsorption and pharmaceutically active compounds adsorption in aqueous solution) is discussed in Section 2.5. A schematic overview of the experimental approach and strategy is shown in Figure 2-1.

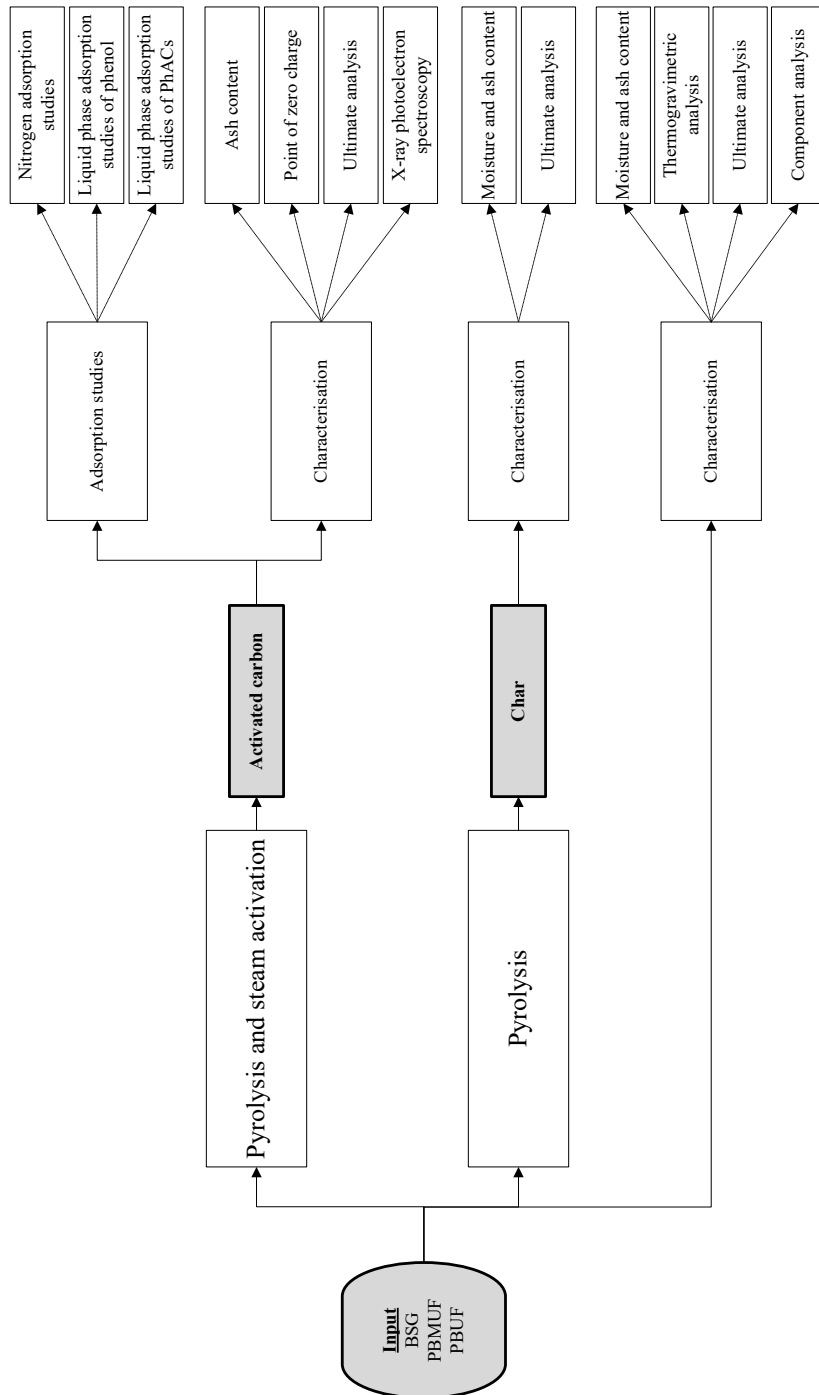


Figure 2-1: Schematic overview of the experimental approach

2.1 Waste Materials

The general focus of this research is directed towards the production of in-situ nitrogenised activated carbon by pyrolysis and steam activation of three waste materials: i.e., brewer's spent grain (BSG), particle board (PB) glued with urea formaldehyde (UF) and glued with melamine urea formaldehyde (MUF). In addition, the use of co-pyrolysis followed by steam activation of particle board with melamine formaldehyde for the production of high in-situ nitrogenised activated carbons with enhanced nitrogen content is investigated.

2.1.1 Brewer's spent grain

Fresh wet BSG was delivered by AB Inbev (Leuven, Belgium). The BSG was immediately oven dried at a temperature of 105 ± 3 °C until constant weight to prevent microbial degradation. After drying the BSG was crushed and sieved (≤ 2.0 mm). For the thermogravimetric, moisture, ash and ultimate characterisation of the input materials particle size was further reduced by milling (≤ 0.25 mm) with a IKA Werke Yellow Line A10 mill. (Further explanation of the techniques can be found in paragraph 2.2.)

2.1.2 Particle board samples

Two different particle board samples were obtained (confidentially) as panels: i.e., water-resistant particle board (glued with MUF) and standard particle board (glued with UF). The panels have been sawn to strips of 1 cm and then cut (≤ 2.0 mm) with a high-speed rotary cutting mill (Retsch SM 100). For the thermogravimetric, moisture, ash and ultimate characterisation of the input materials particle size was further reduced by milling (≤ 0.25 mm) with a IKA Werke Yellow Line A10 mill.

2.1.3 Melamine formaldehyde glue

MF waste (particle size ≤ 2.0 mm) is supplied by Sadepan Chimica (Genk, Belgium). For the thermogravimetric, moisture, ash and ultimate characterisation of the input materials particle size was further reduced by milling (≤ 0.25 mm) with a IKA Werke Yellow Line A10 mill.

2.2 Waste characterisation

Prior to the pyrolysis and activation experiments the waste materials are characterized by thermogravimetric and ultimate analysis. In addition, the composition of BSG is determined.

2.2.1 Moisture and ash content

The moisture content of the samples is determined according to ASTM E 1756 - 01 by oven drying at a temperature of 105 ± 3 °C until constant weight. ASTM E 1755 - 01 is applied for the determination of the ash content by dry oxidation at 575 ± 25 °C for a minimum of 3 h. Both methods are performed in quadruplicate. The presented faults are calculated by standard deviation (1 sigma).

2.2.2 Thermogravimetric analysis

Thermogravimetric analysis (TGA) is a thermal analysis method by which the weight loss of a sample is continuously recorded against temperature or time under a controlled heating rate and gas atmosphere. The weight loss, caused by volatilization and/or decomposition reaction, provides useful information about the thermal degradation behaviour of the waste materials. However in contrast to lab-scale or industrial processes, secondary reactions and other heat and mass transfer effects are much less prominent due to the low sample size (Raveendran et al. 1996). Differential thermogravimetric (DTG) profiles can be derived from the respective TG curves, and plot the weight change as a function of temperature (time). In this study, TGA is performed using a DuPont Instruments 951 Thermogravimetric Analyser. About 10mg of sample is weighed into a quartz crucible. The sample is heated with a heating rate of 10 °C/min from room temperature (RT) to a pre-set temperature under nitrogen atmosphere (80 ml/min) to 900 °C. At 900 °C, an isothermal period of 10 min is applied and the gas-flow is switched to oxygen atmosphere (80 ml/min).

2.2.3 Ultimate analysis

Ultimate or elemental analysis (EA) is used to determine the CHNS- and O-content (wt%). Around 3 mg of a (dry) sample is introduced into a tin container (for CHNS-determination). For accurate sulphur contents 5 - 10 mg vanadiumpentoxide can be added to the sample as combustion catalyst. In this research, the instrument is programmed to use longer oxygen injection times (from 5 to 10 s) rather than using vanadiumpentoxide. Based on extensive testing both methods yielded the same results. The instrument is calibrated using BBOT (2,5-bis (5-tert-butyl-benzoxazol-2-yl) thiophene). All samples are analysed in quadruplicate by a Thermo Electron FlashEA1112 elemental analyser of Thermo Electron Corporation for CHNS. O-content is calculated by difference as: $O = 100\% - (C + H + N + S + \text{ash})$. The presented faults are calculated by standard deviation (1 sigma).

2.2.4 Component analysis

The chemical composition (hemicellulose, cellulose and lignin) of the brewer's spent grain is assessed by an adapted Van Soest and Wine gravimetric method (Faithfull 2002) after ethanol extraction (according to ASTM E 1690 – 01). Since extractives in biomass can interfere with the Van Soest en Wine method, the biomass is extracted with ethanol to remove non-structural materials (that can include waxes, fats, resins, tannins, gums, sugars, starches, and pigments) (ASTM 2004). The extraction makes it easier to wet the material for the analysis of structural components in the biomass. The gravimetric Van Soest and Wine method consists out of four wet-chemical treatments. Firstly (1), the acid detergent fiber (ADF) and the neutral detergent fiber (NDF) are determined after removal of the interfering compounds. Secondly (2), the ADF sample is oxidized by KMnO_4 to obtain the amount of lignin. Then, the resulting sample (cellulose + ash) is ignited to obtain the cellulose content. Finally, hemicellulose is determined from the difference between the ADF and the NDF percentage. The fat content was determined by diethyl ether extraction of the brewers spent grain (Santos et al. 2003). All steps were performed in quadruplicate. Prior to analysis, the BSG is dried overnight at 105°C to remove moisture. A possible interference can occur during the drying step causing Maillard reactions products which are detected and analysed as lignin (Faithfull 2002). The presented faults are calculated by standard deviation (1 sigma).

2.3 Char and Activated carbon Production

Pyrolysis and steam activation are executed with the semi-continuous Lab-built pyrolysis reactor manufactured in stainless steel (AISI 304) which is discussed in more detail in Chapter 3. To achieve as much similarity as possible with industrial activated carbon production process input materials are used as described in Section 2.1. During the entire process, the materials are in constant motion with the aid of the rotator to ensure an adequate heat transfer and mixing of the sample inside the pyrolysis volume. Prior to heating, the reactor and input materials (40 g, particle board and melamine formaldehyde glue where not dried before introduction, the dried brewer's spent grain was dried as described in section 2.1.1, however during storage it had adsorbed 2.7 wt% moisture) are flushed by N_2 -gas (80 ml/min) to guarantee an oxygen poor environment. Chars are produced by heating the samples at $10^\circ\text{C}/\text{min}$ up to the desired temperature of 800°C or 850°C followed by an isothermal period of 30 min under N_2 -atmosphere (80 ml/min). Activated carbons are produced by

heating the samples at 10 °C/min up to the desired temperature of 800 °C or 850 °C followed by an isothermal period of 30 or 45 min under steam atmosphere (by introduction of different known quantities of water into the reactor). The different pyrolysis and activation routes are displayed in Figure 2-2. The produced gases exit the reactor and are burned in the flame of a Bunsen burner.

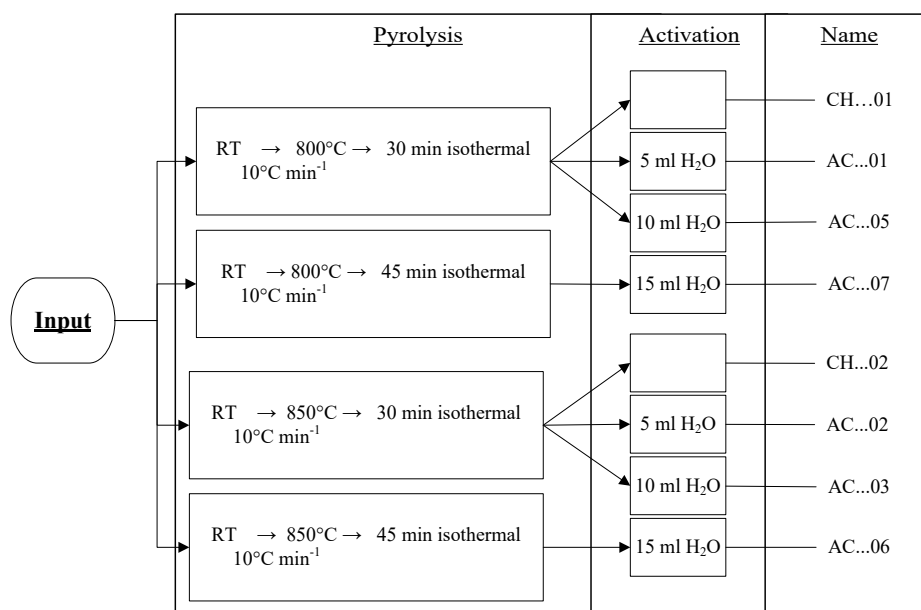


Figure 2-2: Pyrolysis and activation routes

After the experiment, the yield of the pyrolysis products is calculated as follows:

- The char/activated carbons are collected from the reactor, introduced into a storage vessel and directly weighted afterwards. During cooling down the reactor N₂-gas is flushed in the reactor to avoid uptake of moisture or other molecules. No corrections were made for initial moisture in the waste samples to represent industrial conditions.
- The gas yield is calculated by difference.
- The reported yield are the average of minimum six experiments

Only the fraction between 63 μm – 1 mm of chars and activated carbons is used in the subsequent characterization and adsorption studies. The labelling of the activated carbon samples is done by replacing the dots in Figure 2-2 by BSG, PBMUF and PBUF for brewer's spent grain, particle board glued with

melamine urea formaldehyde and glued with urea formaldehyde respectively.

2.4 Activated carbon characterization

2.4.1 Ash content

ASTM E 1755 – 01 is used for the determination of the ash content by dry oxidation at 575 ± 25 °C for a minimum of 3 h and performed in quadruplicate. The presented faults are calculated by standard deviation (1 sigma).

2.4.2 Point of zero charge

The point of zero charge (pH_{PZC}) is estimated by a modified mass titration of Noh & Schwarz (1990). 2.0 g AC was put in 20 ml 0.1 M KNO_3 solution in a closed vessel. After 24 h shaking in a thermostat shaker, the equilibrium pH values of the mixtures were measured electronically (calibrated combined pH electrode) and the limiting pH was taken as the pH_{PZC} . An extensive discussion of the method is given in (Vandevenne et al. 2013).

2.4.3 Acid-basic groups

The basic and acid groups on the AC surface are measured by an acid-base titration method based on (Velghe et al. 2012). To determine the number of basic and acid groups, 200 mg AC was put in contact with 25 ml 0.100 M HCl or NaOH solution respectively. Titration is done with 0.100 M NaOH or HCl in a nitrogen atmosphere by a Metrohm 794 Basic Titrino.

2.4.4 Ultimate analysis

Elemental analysis (EA) is performed in quadruplicate for CHNS-content. O-content is calculated by difference as described in Section 2.2.3.

2.4.5 X-ray photoelectron spectroscopy

X-ray photoelectron spectroscopy (XPS) measurements are performed to determine the carbon, nitrogen and oxygen functionalities on the surface of the activated carbons. Experiments are performed using an XPS customized SPECS system with monochromatic (XPS Microlab 350) Al $K\alpha$ (1486,74 eV) X-ray radiation set at 175 W and 14 kV. The atomic concentrations were calculated from the photoelectron peak areas, using Shirley background subtraction. Deconvolution of the main peak of the C1s, N1s and O1s spectra

is performed by an iterative least-square fitting algorithm. Chemical structural assignments of each component were made taking into account the binding energies reported by Lorenc-Grabowska et al. (2012), Zhou et al. (2007), Arrigo et al. (2008). Experiments are performed by the Mazovian Centre for Surface Analysis, Institute of Physical Chemistry' Polish academy of sciences, Poland.

2.5 Adsorption experiments

2.5.1 Nitrogen adsorption studies (porosity characteristics)

The porosity characteristics of the activated carbons e.g., 'Brunauer, Emmet and Teller' (BET) surface areas, total porosity volume (V_T), micropore volume (V_{mic}) and mesopore volume (V_{mez}) are analysed by nitrogen (77 K) adsorption using an Autosorb AS-1 from Quantachrome. Before analysis the samples are outgassed for 16 h at 200 °C in high vacuum. Experiments are performed by 'Department Chemistry', Laboratory for Adsorption and Catalysis, University Antwerp, Belgium.

The specific surface area of the activated carbons is estimated by the Brunauer, Emmett and Teller (BET) gas adsorption method (Brunauer et al. 1938). The micropores are characterised by the Dubinin – Radushkevich method (volume micropores V_{DR}) and the t-plot method using the De Boer method (micropore surface S_{micro} and extremal surface S_{ext}). By using the Dubinin – Radushkevich method the characteristic adsorption energy (E_0) can be estimated. The average micropore (L_0) is calculated using the Stoeckli equation. The total mesopore volume is estimated by converting the adsorbed volume of nitrogen at a relative pressure of 0.96 into the equivalent liquid volume at 77K. The mesopore volume is then estimated by subtracting the micropore volume (V_{DR}) from the total pore volume.

2.5.2 Liquid phase adsorption studies of phenol

During all Liquid phase adsorption studies no pretreatment has been done like degassing or heating of the activated carbons.

2.5.2.1 Adsorption isotherm studies

The batch phenol adsorption on the selected activated carbons against two commercial activated carbons (Filtrisorb F400 and Norit GAC 1240) is evaluated by introducing 25 ml of a 100 ppm (initial concentration C_0) unbuffered phenol solution with different quantities of activated carbon (5, 10, 20, 30, 40, 60 and 100 mg) in a hermetically closed flask. Analytical

grade phenol and Milli-Q water (18.2 MΩ/cm conductivity) is used. The flasks are placed in a thermostatic water bath (25°C) and shaken for 24 h. It is assumed that equilibrium is reached in this time period. The solution is filtered and the residual phenol concentration (C_e) is analysed using a Pharmacia Biotech Ultraspec 2000 UV-VIS spectrophotometer at 270 nm and the pH is measured. Calibration is carried out using a number of phenol standard solutions (concentration range: 1 ppm, 5 ppm, 10 ppm, 30 ppm, 50 ppm, 80 ppm and 100 ppm) and a correction factor is determined for each pH value to counteract the lower adsorption due to the dissociation of phenol in the solution (discussed in detail in section 6.4.1). Milli-Q water, subjected to a similar procedure as the unknown samples is used as a blank and adsorbent-free controls are run in parallel. Each experiment was done in quadruplicate. Once C_e is determined the amount of phenol adsorbed on the AC at equilibrium can be calculated using Eq. 2-1.

Eq. 2-1:
$$q_e = \frac{(C_0 - C_e)V}{m_{AC}}$$

with q_e the mass of phenol adsorbed per mass unit of AC (mg/g), C_0 the initial phenol concentration (mg/l), C_e the phenol concentration at equilibrium (mg/l), V the volume adsorbate (phenol solution) (l) and m_{AC} the AC mass (g). In this work the equilibrium data are fitted by two two-parameter models: the Langmuir and Freundlich model (discussed in Section 1.3.4.1.)

2.5.2.2 Adsorption kinetic studies

The adsorption kinetics are investigated (in duplicate) by varying the contact time from 0.5 h – 24 h in the batch adsorption mode using 25 ml of a 100 ppm unbuffered phenol solution with 50 mg of AC. The phenol concentration is measured as described in section 2.5.2.1. The amount of phenol adsorbed in the corresponding time interval (q_t) is calculated by

Eq. 2-2:
$$q_t = \frac{(C_0 - C_t)V}{m_{AC}}$$

The experimental data were fitted (using the pseudo-first-order model model) and the pseudo-second-order model. The theoretical background is discussed in Section 1.3.4.3.

2.5.2.3 Effect of initial pH, ionic strength and standard water

The effect of acidity degree/pH on the phenol adsorption is studied (in triplicate) by introducing 20 mg AC in 25 ml of a 100 ppm phenol solution and varying the pH of the phenol solution in the range of (0.5 – 13.5) by

introducing appropriate amounts of HCl or KOH respectively, additionally maintaining the ionic strength at 0.1 M by adding various amounts of KCl. The hermetically closed flasks are shaken for 24 h in a thermostatic water bath (25 °C). The phenol concentration is measured as described in section 2.5.2.1.

To study the effect of the ionic strength on the phenol adsorption five different phenol solutions are made with varying concentrations of KCl (0, 0.001, 0.01, 0.1 and 1 M). 25 ml of these solutions are added to 20 mg AC, after 24 h shaking in a water bath (25 °C) the residual phenol concentration is determined as described in section 2.5.2.1. The experiments are performed in triplicate.

To investigate the phenol adsorption in a more realistic water medium, a reconstituted standard water based on ISO 6341, representative of those generally occurring in the environment, is made using "*OECD series on testing and assessment number 29: Guidance document on transformation/dissolution of metals and metal compounds in aqueous media*". The chemical composition of the reconstituted standard water (for tests carried out at pH 8) is as follows: NaHCO₃ 65.7 mg/l, KCl 5.75 mg/l, CaCl₂·2H₂O 294 mg/l, MgSO₄·7H₂O 123 mg/l. The solution is air buffered at pH 8 in which the concentration of CO₂ provides a natural buffering capacity sufficient to maintain the pH within an average of ± 0.2 pH units over a period of one week (OECD Environment 2001). A 100 ppm phenol solution is made with this water and added to 20 mg AC. After 24 h shaking in a water bath (25 °C) the residual phenol concentration is determined as described in section 2.5.2.1. The experiments are performed in triplicate.

2.5.2.4 Dynamic phenol adsorption and effect of temperature

For a better understanding of the adsorption process a Lab-built thermostatic slurry batch reactor connected with a computer controlled Pharmacia Biotech Ultraspec 2000 UV-VIS spectrophotometer (Figure 2-3) is used. 100 mg of adsorbent is weighted and placed in a double walled vessel with 50 ml 100 ppm phenol solution. The slurry is agitated by means of an IKA RW20 n overhead stirrer fitted by a Screw Type Stir Element at 150 rpm. By means of a glass fritted filter a stream of filtered solution is withdrawn with a Hiedolph pumpdrive 5001 peristaltic pump (set at 35 rpm) to a Lab-built measuring cell (Quartz, path length 2.3 mm) mounted in a computer controlled UV-VIS spectrophotometer. The absorbance of the solution is measured at 270 and 286 nm every minute and stored using a self-developed LabView programme. The liquid is transferred back to the slurry reactor. In the system design the volume of the measuring loop is very small

in comparison with the total solution. The measurements are performed in twofold at a temperature of 15, 20, 25 and 30 °C.

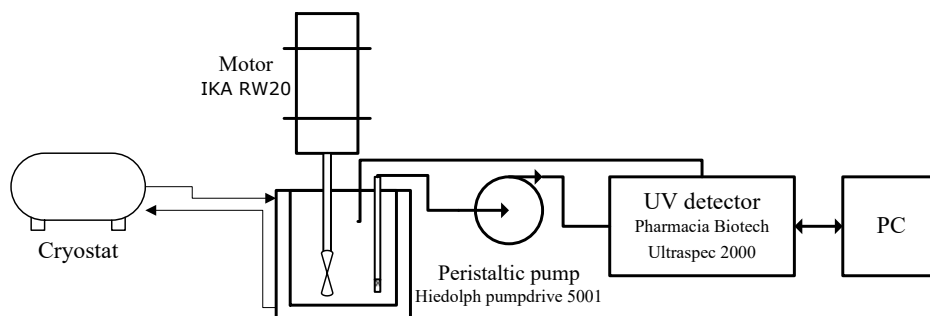


Figure 2-3: Set-up dynamic adsorption

2.5.2.5 Column adsorption experiments

To simulate the performance of the selected activated carbons in an activated carbon filter a small scale column test (Figure 2-4) is developed to predict their adsorption characteristics. The Lab-built test apparatus is constructed out of a thermostatic fixed-bed glass column (10 mm internal diameter) connected with two PC controlled TR 100 burettes from Schott instruments and a computer controlled Pharmacia Biotech Ultraspec 2000 UV-VIS spectrophotometer. Prior to introduction in the test column the AC is wetted (degassed) with reconstituted standard water based on ISO 6341 (see section 2.5.2.3) for a minimum of 48h at room temperature. To avoid air pockets in the carbon bed, the degassed carbon is introduced to the column as a slurry, keeping a thin layer of reconstituted standard water above the bed (Legros 1966). Also all connecting tubing and void spaces must be filled with the liquid before starting the experiment. From a solution reservoir (containing the phenol stock solution) the column is alternating fed (for a continuous flow and to achieve high volumes without standstill of the liquid) by the TR 100 burettes at a predetermined flow rate. For safety reasons a Swagelok SS Poppet Check Valve of 1.8 bar is installed to release pressure in the event of column plugging. The column is fed from the bottom to the top to avoid channelling and to ensure an uniform streaming (Worch 2012). The effluent is measured by a computer controlled Pharmacia Biotech Ultraspec 2000 UV-VIS spectrophotometer at 270 and 286 nm every 30 seconds, the data are automatically stored by to a home-made LabVIEW programme.

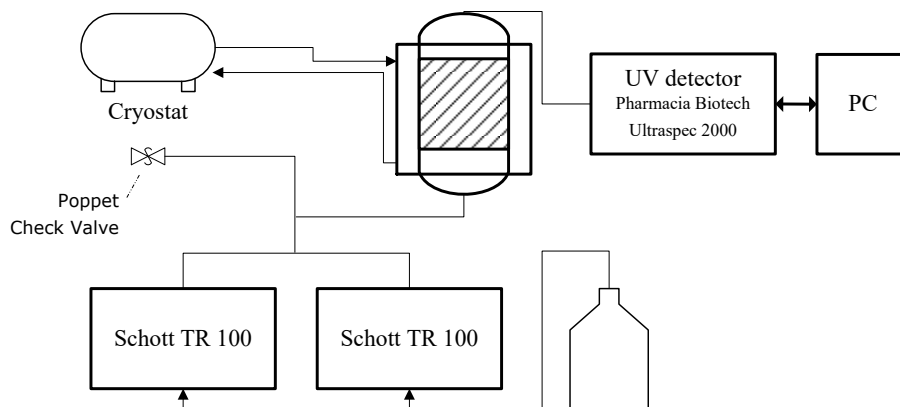


Figure 2-4: Column adsorption set-up

2.5.3 Liquid phase adsorption studies of pharmaceutically active compounds (PhAC's)

For the evaluation of the potential of the developed sorbents for the remediation of water polluted PhAC's (Diclofenac (DCF), Ibuprofen (IBP), Sulfamothoxazole (SMX)), in three sequential types of assays are performed e.g.,: Screening assay, Equilibrium assay and a kinetic assay. During assay studies no pretreatment has been done like degassing or heating of the activated carbons.

2.5.3.1 Screening assay

In the screening assay the produced activated carbons along with the reference activated carbon are evaluated as potential sorbents for the selected pharmaceuticals. 20 mg of sorbent is added to 25 ml of the target pharmaceutical compound solutions (40 mg/l). The compound solutions are prepared in Milli-Q water without pH adjustment. After a contact time of 24 h (shaking) in a water bath (25 °C), the pH of the solution is measured. The residual concentration is determined by collecting an aliquot from the solution and filtered through a 0.45 µm PTFE membrane filter in a 2 ml vial, and analysed using a high-performance liquid chromatograph (Agilent 1100) equipped with a photo diode array detector and a Zorbax SB-C18 column from Agilent (75 * 4.5 mm; 3.5 µm). A gradient elution of 0.1% H₃PO₄:acetonitrile (75:25, v/v) for 1 min followed by 0.1% H₃PO₄:acetonitrile (70:30, v/v) at a constant flow of 1 ml/min for 9 min is

applied. The pharmaceutical compounds are measured at a wavelength of 195 nm and eluted from the column at 2.37 (SMX), 8.51 (DCF) and 8.80 (IBP) min respectively. Calibration is carried out using a number of standard solutions prepared in methanol (concentration range: 0.5, 1, 5, 10, 50 and 100 ppm). Milli-Q water, subjected to a similar procedure as the unknown samples is used as a blank and adsorbent-free controls are run in parallel. The screening assay is used to select the three best performing activated carbons and the best performing reference carbon.

2.5.3.2 Equilibrium assay

Equilibrium absorption studies of the selected AC's from the screening assay are performed using batch experiments. PhAC's solutions (40 ppm) are made reconstructed fresh water medium; 25 ml of these solution is brought into contact with different quantities of AC (5, 10, 20, 30, 40, 60 and 100 mg) in hermetically closed flasks. After 24 h shaking in a water bath at 25 °C, the pH of the solutions is measured and the residual concentration is measured with the aid of HPLC as described in section 2.5.3.1. Reconstructed water (blank) and adsorbent-free controls are run in parallel.

2.5.3.3 Kinetic assay

25 mg of the selected AC's is weighted and placed in the double walled slurry batch reactor connected with a computer controlled Pharmacia Biotech Ultraspec 2000 UV-VIS spectrophotometer (as described in section 2.5.2.2). 50 ml of PhAC solution, 40 ppm in reconstructed water, is added and the concentration is measured at both 254 and 278 nm for DCF and SMX, and at 210 and 230 nm for IBF until equilibrium.

2.6 Techno-economic assessment

To investigate the techno-economic performance of the solution proposed and to direct the research to the best options for the production of high value activated carbon and toward the crucial variables a techno-economic assessment from the point of view of a private investor is performed. For this purpose, a market study is carried out to investigate the costs and revenues, market size, availability of the input streams, A process diagram of an activated carbon production technique (co-pyrolysis combined with physical activation) is developed. A dynamic economic model is developed to calculate the cash-flows resulting for an investment in the technology. These serve as a basis for calculating the net present value by discounting the future yearly incoming and outgoing cash flows using a predetermined discount rate. Also the internal rate of return (the discount

rate at which the net present value equals zero) is calculated. Because the internal rate of return is a percentage, it can only be used as a decision rule for selecting projects when there is only one alternative to a status quo. When there are a group of mutually exclusive projects that differ in size this is not a good evaluation criteria. Therefore, the net present values is preferred.

In order to have an idea about the impact of uncertainties on the net present value, Monte Carlo Sensitivity analysis is performed. The sensitivity analysis repeatedly calculates the net present value corresponding to numerous random draws for the value of uncertain variables following a presupposed distribution. The selected variables are allowed to change following a triangular distribution characterized by a most likely, a minimum and a maximum value. Monte Carlo simulations are performed, in which each run of the Monte Carlo simulation draws a random value for each of these variables, between the minimum and maximum value and in accordance with the selected distribution. Each run results in a NPV corresponding to the values drawn for each of the nine uncertain variables. Numerous runs (10 000 per ratio in this research) of the Monte Carlo Simulation result in a NPV distribution. Because no large data sets or historical data are available for the uncertainties, it is impossible to objectively assign probability distributions. For this reason a triangular distribution is chosen which is an adequate solutions as literature is insufficient as described by Haimes (2004). Monte Carlo simulations typically result in a distribution of net present that can be declared by the degree of uncertainty of each individual variable. Each variable with its corresponding range of values and distribution is partly responsible for the total uncertainty of the net present value. The variables with the highest influence on net present value sensitivity should be identified and should be the subject for further research so that they can be controlled when putting the project into practice. In our study 10 000 runs are carried out using the @Risk software from Palisade Decision Tools.

Finally, these uncertainties have been taken into account when calculating the minimum selling price at which the activated carbon should be sold in order to guarantee a 95 % chance on a positive NPV.

3 Development of the pyrolysis/activation reactor

Within the research group "Applied and Analytical Chemistry", different pyrolysis reactors are available which can be used for pyrolysis and subsequent steam activation. The first reactor is a horizontal tubular reactor designed for a horizontal Nabertherm oven (see Figure 3-1), applied in the studies of Smets et al. (2013), Smets (2013), Lievens et al. (2009), Lievens et al. (2008a) and Lievens et al. (2008b).

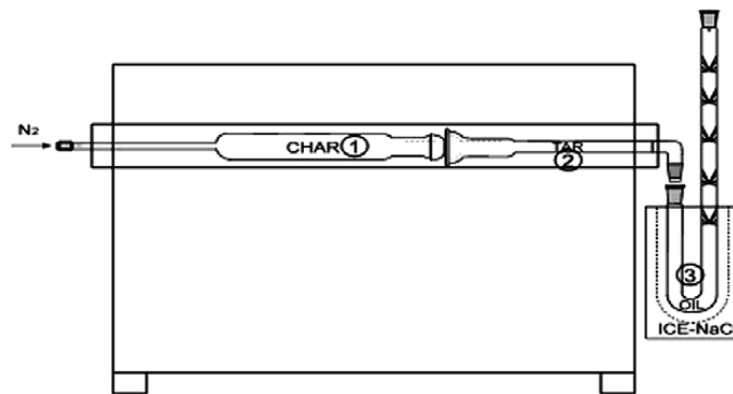


Figure 3-1: Horizontal tubular pyrolysis reactor set-up.

The second available reactor is a horizontal tubular reactor for steam activation developed by Stals (2011).

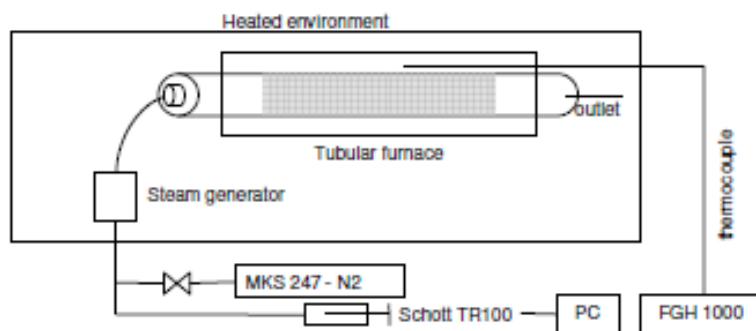


Figure 3-2: Steam activation setup

Both reactors can be programmed to heat the sample to a certain temperature with a predetermined heating rate. In both cases the samples are introduced in a quartz reactor. When the desired temperature is reached, the temperature is held isothermally and the gas inlet is switched to steam. In the first reactor, water is injected directly (with a programmable Schott TR 100 automatic burette) into the quartz reactor, with steam formation. In the second reactor, the automatic burette pumps water into a steam generator forming steam which is passed through the quartz tube.

The goal of this research is to produce sufficient amounts of activated carbon with good quality on a repetitive manner resembling industrial synthesis for small scale laboratory testing. The horizontal tubular reactors described above however have several limitations. Both reactors have a rather small internal volume. So by performing a pyrolysis and subsequent steam activation only a very small amount of activated carbon is produced. Therefore, in previous research the reactors are used for activation starting from char instead of biomass. In addition, both reactors are static. As a result the heat transfer inside the bed of biomass is rather poor, the temperature inside the bed is not uniform during heating, after pyrolysis (around 800 °C) the fixed bed is not packed anymore which results in channelling of the steam, and the activated carbon is polluted with quartz wool. Furthermore, the thermocouple is inserted between the quartz reactor and the oven and not directly into the sample.

To meet the need for a pyrolysis / activation reactor which is suitable to produce sufficient amounts of activated carbon on a laboratory resembling industrial plants a new and improved reactor is developed. The requirements of the new reactor are:

1. Produce sufficient amounts of activated carbon
2. Perform pyrolysis and subsequent steam activation without interrupting the process, starting from biomass.
3. Uniform heat transfer inside the pyrolysis / activation volume
4. Uniform temperature inside the biomass / char
5. No pollution of the activated carbon
6. Uniform activation of the char
7. Measuring the temperature of the biomass / char / activated carbon
8. Closely related to industrial activated carbon production plant

Based on the knowledge of industrial activated carbon production plants, the laboratory reactor is designed to be closely related to the rotary kiln reactor concept. Within the research group different ovens and heating jackets are available as a heating source for the reactor. Based on their specifications

Chapter: 3

the Nabertherm oven is chosen. First a 3-D model (see Figure 3-3) is sketched in SolidWorks. The model is evaluated and finally built.



Figure 3-3: 3-D model pyrolysis and activation reactor (above), manufactured reactor in comparison with the quartz reactors (below).

The difference in sizes between the different reactors can be seen in Figure 3-3. The active part (i.e., the actual pyrolysis and activation) part of the different reactors has a volume of around 290 cm³ (around 40 – 60 g of input), 114 cm³ (max 20 g of input), 8cm³ (max 4 g) clearly indicating the difference in size.

Figure 3-4 shows the semi-continuous Lab-built pyrolysis reactor set-up manufactured in stainless steel (AISI 304) which is developed for the pyrolysis and steam activation. A rotator is used to ensure an adequate heat

Chapter: 3

transfer and mixing of the sample inside the pyrolysis volume. The reactor is heated using a furnace (Nabertherm) controlled by a programmed FGH 1000 controller. Temperature feedback to the controller is supplied by a type K thermocouple, inserted directly in the pyrolysis volume. To ensure an oxygen-deficient environment during pyrolysis experiments the reactor was flushed with nitrogen gas. During steam activation, water was injected by a PC controlled Schott TR 100 burette.

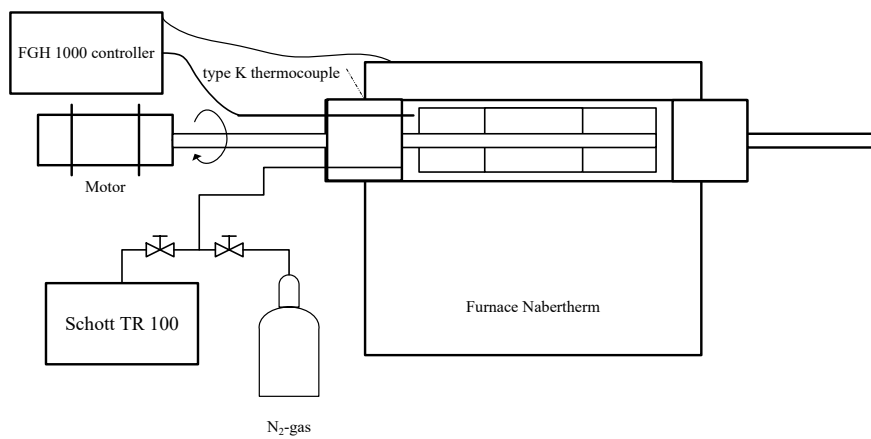


Figure 3-4: Home-built pyrolysis / activation set-up

4 Preliminary techno-economic analysis

The results of this chapter have been published:

VANREPPELEN, Kenny; KUPPENS, Tom; THEWYS, Theo; CARLEER, Robert; YPERMAN, Jan & SCHREURS, Sonja (2011) Activated carbon from co-pyrolysis of particle board and melamine (urea) formaldehyde resin: a techno-economic evaluation. In: CHEMICAL ENGINEERING JOURNAL, 172(2-3). p. 835-846. [Article - cat: A1 - Validation: ecom 2012 (*)]

4.1 Introduction

During the production of melamine (urea) formaldehyde resins (MF, MUF both further abbreviated as MF in this chapter) for the production of particle board (PB) a considerable amount of waste resin is produced that cannot be re-used or recycled at this moment.

In addition, classical thermo-chemical conversion (e.g., combustion) of wood waste containing these aminoplasts resins might cause pollution because it results in the production of toxic gases like ammonia, isocyanic and hydrocyanic acid and nitrous oxides (Girods et al. 2008a, Girods et al. 2009b, Girods et al. 2008b).

A sustainable solution is more and more required to avoid environmental problems and landfilling costs, and to turn this waste stream in a rather profitable material resource. A possible opportunity, is the production of high value activated carbon after thermal treatment in an oxygen deficient environment and subsequent activation.

Activated carbons are produced for a large number of dedicated applications both as structural and functional materials. Activated carbons are generally used for air, water and gas purification, chemical and pharmaceutical processing, food processing, decolourization, solvent vapour recovery, fillers in rubber production, refractory materials, catalysis and catalyst support (Bandosz 2009, Marsh & Rodríguez-Reinoso 2006a, Menéndez-Días & Martín-Gullón 2006).

Marsh & Rodríguez-Reinoso (2006a) estimated the world annual production capacity of activated carbon to be around 400 kt in 2006, excluding countries without accurately known figures like China and some other Eastern countries. Furthermore the market is increasing constantly, due to the environmental awareness and the growing industrialization. Girods et al.

(2009a) expect a growth of 5.2 % per year to 1.2 Mt by 2012. In Europe, Japan and the USA the growth is 1 % to 5% per year, whereas this rate is much higher in the developing countries. The price of activated carbon is a function of demand, quality, production cost, etc.. A typical price range is 1.4 kUSD/t to 6 kUSD/t, but for very special carbons the price can increase to 20 kUSD/t (Marsh & Rodríguez-Reinoso 2006a, Ng et al. 2003). Girods et al. (2009a) state that the average cost of activated carbon from the major producers was on average 2.5 kUSD/t.

Activated carbon is structurally a non-graphitic carbonaceous material of fused aromatic rings grouped into layers in a turbostatic structure with a disordered stacking of the layers connected with Van der Waals interactions (Bandosz 2009, Menéndez-Días & Martín-Gullón 2006). Almost any carbonaceous solid material can be converted into AC. In spite of this there are some limitations. The raw materials must not go through a fluid or pseudo fluid state because then the solid tends to form an ordered structure (Menéndez-Días & Martín-Gullón 2006). The wide range of applications exists thanks to the high volume of pores, high surface area and the variety of surface chemistry of activated carbons. The final properties of the activated carbons are related to the precursor material and the activation process (physical or chemical). Activation happens in a medium to high temperature atmosphere, which removes solid mass and thus creates a porous structure (Menéndez-Días & Martín-Gullón 2006). It is stated that the physicochemical properties of the activated carbons are strongly influenced by the presence of heteroatoms like oxygen, nitrogen, sulfur, etc. In normal conditions the amount of nitrogen in the activated carbon is negligible (Bandosz 2009, Menéndez-Días & Martín-Gullón 2006). Several published results however, demonstrate the positive effect of nitrogen incorporation as a key parameter for the adsorption properties of the activated carbon (Bandosz & Ania 2006), especially for the removal of acid gases like hydrogen sulfide, sulfur dioxide and phenolic compounds (Girods et al. 2009a, Girods et al. 2008a, Girods et al. 2009b). Nitrogen incorporation can also play a significant role for the catalytic activity and dispersion of carbon supported catalysts (Bandosz & Ania 2006). According to Girods et al. (2008a) the value of such a nitrogenised activated char from particle board (in 2006) is on average 2.5 kUSD/t (\approx 2.0 kEUR/t), whereas normal activated carbons are sold (in 2008) at prices between 0.8 kEUR/t and 1.7 kEUR/t (\approx 1.2 kUSD/t to 2.5 kUSD/t) (Infomil 2011). According to Infomil (2011), impregnated activated carbons (i.e., including pick-up of the saturated carbon) have a higher selling price (in 2008) of 4.0 kEUR/t to 6.0 kEUR/t (\approx 5.9 kUSD/t to 8.8 kUSD/t) due not only to higher costs incurred by the impregnation step but also because of better performance.

Because the chemical properties of the particle board and melamine (urea) formaldehyde waste materials result in in-situ nitrogen incorporation during char formation and activation, the production cost of nitrogenised activated char is considerably reduced in comparison with post impregnation of nitrogen containing components on activated carbon. In addition, these waste materials have the economic advantage of representing a negative cost (Girods et al. 2008b) for a waste processing company, which means that the latter does not have to pay for obtaining resources such as particle board and melamine (urea) formaldehyde waste, but instead receives a gate fee for processing the waste material.

The objective of this work is to identify the crucial variables for rendering the production of activated carbon from particle board and melamine (urea) formaldehyde waste profitable. For this purpose, a preliminary economic feasibility study has been carried out for a process design especially developed for the production of activated carbon from particle board and melamine (urea) formaldehyde waste. After developing a process diagram of an activated carbon production technique (co-pyrolysis combined with physical activation), the net present value of the cash flows generated by an investment in co-pyrolysis and char activation has been calculated. The minimum selling price of the produced activated carbon has been determined, taking into account uncertainties by performing Monte Carlo Sensitivity analysis. Finally, this preliminary economic feasibility study is used to identify the key variables for the profitability of the production of activated carbon from particle board and melamine (urea) formaldehyde waste.

4.2 Process design

The preliminary process design for the production of activated carbon from particle board waste co-pyrolysed with melamine (urea) formaldehyde is shown in Figure 4-1. The process can be divided in four parts: pretreatment, pyrolysis, activation and packaging. After shipping the raw materials to the activated carbon production facility, they are first mixed and milled into a smaller particle size (a few millimetre), dried and transported to a silo. It is difficult to predict the moisture content of the incoming waste. Girods et al. (2008a) determined the moisture in wood board to be about 7 %. Next, the grinded and dried waste will be transported to a rotary pyrolysis furnace (operating at 800 °C). Here the waste is pyrolysed in an oxygen-free environment for a few minutes (2-5 min). The developed chars (solid fraction) are then transported to a second rotary kiln furnace where they are activated during 30 min at a temperature of 800 °C in the presence of steam as activation agent. The pyrolysis and activation are carried out in two

separate but connected furnaces to achieve a continuous system. Both the pyrolysis and activation kiln have a cross-sectional area occupied by material which is 10 % of the cylinder's length to ensure an adequate heat transfer and mixing (Boateng & Barr 1996, Lima et al. 2008). The produced pyrolysis gases and aerosols are conducted to a thermal combustor followed by a cyclone for complete combustion at a temperature of around 1000 °C with a residence time of at least 2.5 s. This reduces formation of harmful compounds or promotes their breakdown (Choy et al. 2005). By using a multiple zone oxidiser the formation of NO_x can be further controlled by managing the oxygen inflow in the different zones, but this is not implemented at this stage. The hot flue gases are used as a heat source for pyrolysis/activation and the steam generator. After cooling, the produced activated carbon is transported to a storage silo before screening and packaging. The remaining gases are cooled to recover water from the steam generator. After cooling they are discarded. A palletisation device and an extra gas cleaning unit before emission can also be installed, but are at the moment not incorporated in this analysis. The possible extra investment costs for this equipment can be found in recent literature e.g., Lemmens et al. (2004) and Lima et al. (2008).

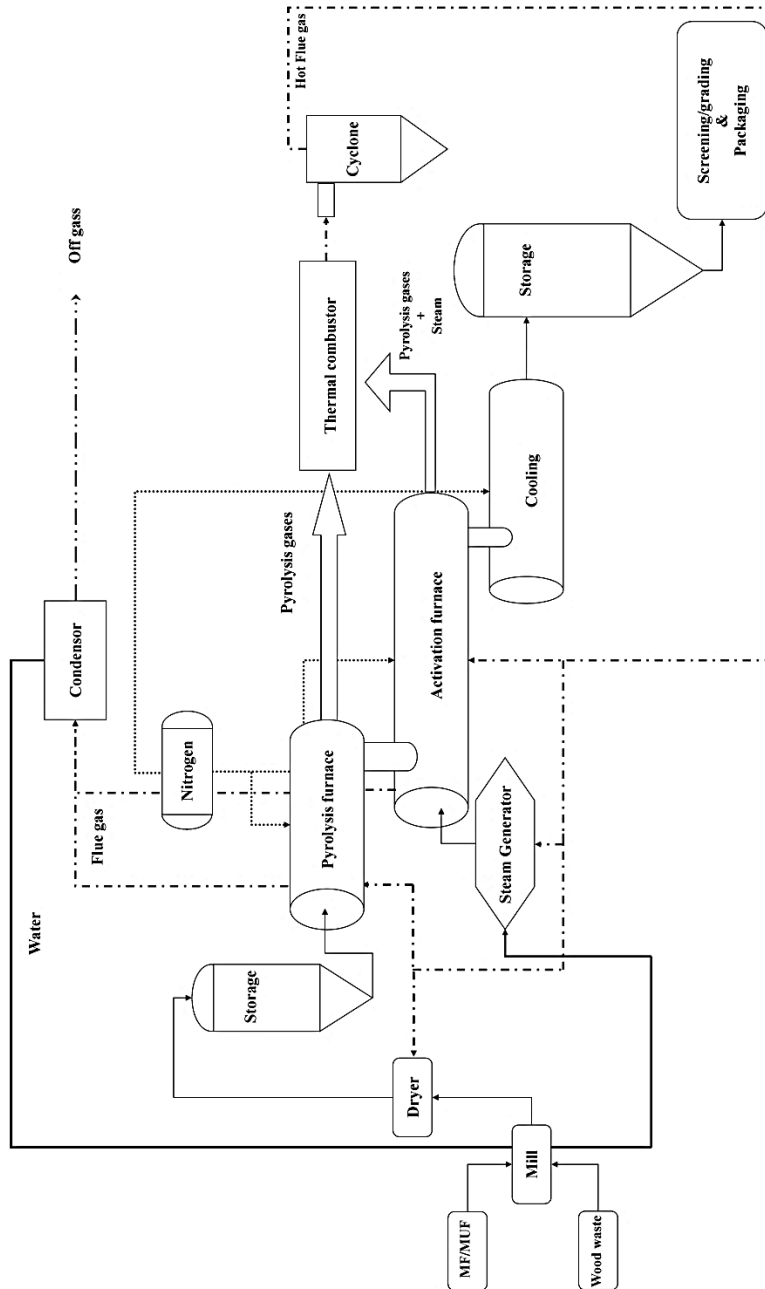


Figure 4-1: Process flow

4.3 Economic feasibility model

Poor capital investment decisions can alter the future stability of an organisation. Investors deal with this problem by using investment decision rules which evaluate the profitability of the project or investment. Biezma & Cristóbal (2006) have categorized many various investment criteria methods. Two of these criteria, the net present value (NPV) and the internal rate of return (IRR), are used to evaluate the economics of the melamine (urea) formaldehyde - particle board pyrolysis/activation. The NPV is the best criterion for selecting or rejecting an investment, either industrial or financial (Lorie & Savage 1955, Vernimmen et al. 2005). The NPV is today's value of current and future cash flows, which are the result of an investment using a predetermined discount rate (Horngren et al. 2003, Vernimmen et al. 2005). The NPV is calculated with Eq. 4-1 (Horngren et al. 2003, Kuppens et al. 2010, Thewys & Kuppens 2008, Vernimmen et al. 2005).

Eq. 4-1:
$$NPV = \sum_{n=1}^T \frac{CF_n}{(1+i)^n} - I_0$$

With:

- CF_n = Cash Flows generated in year n;
- I_0 = initial total capital investment (see Table 4-1 row 19) in year 0;
- T = the life span of the investment;
- i = discount rate.

The cash flow in a given year is the difference between revenues (R) and expenditure (E) after tax (t) generated by the investment. To calculate the cash flow, depreciation (D) also needs to be taken into account because it lowers tax payments (Kuppens et al. 2010, Thewys & Kuppens 2008). According to Kuppens et al. (2010) and Thewys & Kuppens (2008) cash flows can be calculated using the following equation:

Eq. 4-2:
$$CF_n = (1 - t) * (R - E) + t * D$$

The discount rate of the invested money is set at 9 % incorporating the market interest rate and some risk premium (Kuppens et al. 2010, Ochelen & Putzeijs 2008a). Taxes on profits to be paid amount up to 33 % in Belgium (t= 0.33). The life span of a reactor is described as 20 years (Bridgwater et al. 2002, Kuppens et al. 2010, Thewys & Kuppens 2008). All the results are based on an operation of the reactor of 7 000 hours per year. In general, when the NPV is positive, the investment is a good decision.

The IRR is the discount rate (i) at which the present value of expected cash inflows from a project equals the present value of expected cash outflows of the project. In other words, it is the discount rate that makes the NPV equal to zero. It is frequently used in financial markets because it gives the return that the investor can expect for a given level of risk (Vernimmen et al. 2005). If the IRR is lower than the required return (discount rate) then the project should be rejected.

Additionally the minimal selling price of the activated carbon has been calculated. This is the minimal price at which the activated carbon should be sold so that the NPV breaks even or in other words the NPV equals at least 0.

In order to have an idea about the impact of uncertainties on the NPV, Monte Carlo Sensitivity analysis is performed. The sensitivity analysis repeatedly calculates the NPV corresponding to numerous random draws for the value of uncertain variables following a presupposed distribution. Monte Carlo simulations typically result in a distribution of NPVs that can be declared by the degree of uncertainty of each individual variable. Each variable with its corresponding range of values and distribution is partly responsible for the total uncertainty of the NPV. The variables with the highest influence on NPV sensitivity should be identified and should be the subject for further research so that they can be controlled when putting the project into practice. In our study 10 000 runs are carried out using the @Risk software from Palisade Decision Tools.

Finally, these uncertainties have been taken into account when calculating the minimum selling price at which the activated carbon should be sold in order to guarantee a 95 % chance on a positive NPV.

4.4 Model assumptions

The first step in NPV calculation is the estimation of the initial investment expenditure. For preliminary economic feasibility analysis, the Percentage of Delivered-Equipment cost is commonly used, with an expected accuracy of 20 % to 30 % (Peters et al. 2004).

Before an industrial facility can be put into operation, a large sum of money needs to be spent on the necessary machinery, equipment and their delivery: i.e., the cost of delivered equipment. The total capital investment however also consists of costs of the building itself, the land on which the equipment is installed, piping, electrical systems, etc. These are all direct plant costs. But also indirect plant costs have to be taken into account: such as costs for engineering, legal expenses, contingencies, etc. The sum of

Chapter: 4

these investment costs, i.e., the cost for delivered equipment, the direct plant costs and the indirect plant costs are called fixed-capital investment. The amount of money required for a stock of raw materials and cash kept on hand, i.e., the working capital, should be added for estimating the total capital investment. The working capital and the direct and indirect plant costs are expressed as a percentage of the delivered equipment cost. The percentages determined by Peters et al. (2004) are used in the calculation and are displayed in Table 4-1. All costs have been updated to 2009, based on the US Dollar / Euro exchange ratio provided by European Central Bank (2010) and the Marshall and Swift Index (Chemical Engineering 2010) see Eq. 4-3.

Eq. 4-3: $Cost\ of\ Equipment\ (2009) = cost\ of\ Equipment\ (year) * \frac{Cost\ index\ (2009)}{Cost\ index\ (year)}$

Table 4-1: Multiplying factor for the Delivered-equipment cost

Cost component		Percent of equipment cost
Direct costs	Delivered Equipment	100
	Installation	39
	Piping (installed)	31
	Instrumentation and controls (installed)	26
	Electrical systems (installed)	10
	Buildings (including services)	29
	Yard improvements	12
	Service facilities (installed)	55
	Land	6
		Direct plant costs (DPC)
Indirect costs	Engineering, supervision	32
	Construction expenses	34
	Legal expenses	4
	Contractor's fee	19
	Contingency	37
	Indirect plant costs (IPC)	126
	Fixed-capital investment	434
	Working capital (15% of total capital investment)	76
	Total capital investment	509

4.4.1 Total capital investment

The total investment cost for production of the activated carbon is determined by the Percentage of Delivered-Equipment cost method. The equipment cost information was provided by literature (Table 4-2). A delivery allowance of 10 % on the purchased equipment cost is used (Peters et al. 2004).

Table 4-2: Major equipment cost and their scaling factors used

Item	Sizing parameter	Unit cost year	Reference
Crusher	2 t/h	44.94 kUSD (2002)	(Choy et al. 2005)
Dryer	10 t/d	51.27 kUSD (2002)	(Choy et al. 2005)
Silo (raw material)	500 m ³	380 kEUR (2009)	(Dutch Association of Cost Engineers 2009)
Nitrogen storage tank	1.92 m ³	19.26 kUSD (2002)	(Choy et al. 2005)
Pyrolysis and activation reactor	/	equation 8	
Steam boiler and condenser	3 781 kg/h	116.84 kUSD (2002)	(Choy et al. 2005)
Thermal combustor	1 000 Nm ³ /h	40 kEUR (2004)	(Lemmens et al. 2004)
Cyclone	1 000 Nm ³ /h	1.5 kEUR (2004)	(Lemmens et al. 2004)
Silo (activated carbon)	500 m ³	380 kEUR (2009)	(Dutch Association of Cost Engineers 2009)
Screening and Grading	139.9 kg/h	25.0 kUSD (2005)	(Lima et al. 2008)
Packing of activated carbon	139.9 kg/h	25.0 kUSD (2005)	(Lima et al. 2008)

One of the problems in cost estimating is that cost data are not always available for the particular size or capacity involved. Predictions can be made by using Eq. 4-4 which is known as the six-tenths factor rule and is widely

used in approximations of equipment and even total process costs (Peters et al. 2004).

Eq. 4-4: $Cost\ of\ unit\ (new) = cost\ of\ unit\ (ref.) \left(\frac{capacity\ (new)}{capacity\ (ref.)} \right)^{capacity\ exponent}$

The actual value of the cost capacity exponent in equation 4 can vary from less than 0.3 to greater than 1.0. Yassin et al. (2009) stated that the capacity exponent is in the range of 0.6 – 0.8 for gasification and pyrolysis facilities. In this calculation a capacity exponent of 0.7 is used as suggested by Henrich et al. (2009), Tock et al. (2010) and Gassner & Marechal (2009).

The equipment cost of the pyrolysis and activation reactor (which is on its turn a pyrolysis reactor) is derived from the fixed-capital investment (FCI) of a pyrolysis plant presented by Bridgwater et al. (2002) in Eq. 4-5 with $Q_{feed\ input\ pyrolysis}$ the flow ratio of the feed (ton dry matter per hour):

Eq. 4-5: $FCI\ pyrolysis\ plant = 40.8 * 10^3 * (Q_{feed\ input\ pyrolysis} * 10^3)^{0.6194}$

Eq. 4-5 calculates the cost of the fast pyrolysis reactor, the feeding system and liquids recovery. Eq. 4-5 is a result of a regression from 14 cost data performed by Bridgwater et al. (2002), and the data are assumed to be first plant costs from a novel technology. This is important, because there can and probably will be a considerable cost reduction from the 'learning effect'. Henrich et al. (2009) state that, if the same type of facility is designed, built and operated several times the investment and operating costs decrease exponentially with the number of built plants. According to Henrich et al. (2009), it is reasonable to set the total capital investment at about two-thirds of the first plant cost. In this chapter the first plant cost is used. Therefore, it may be inferred that a rather pessimistic investment cost scenario is applied.

Because Bridgwater et al. (2002) used other and less factors to calculate the indirect plant cost and direct costs, the fixed capital investment of the pyrolysis plant is recalculated to the equipment cost. Bridgwater et al. (2002) stated that the total plant cost is 169% of the direct plant cost. The percentages of the direct cost factors that Bridgwater et al. (2002) used are not defined, but the factors can be found in Peters et al. (2004). So they are assumed to be 39 % for erection, 31 % for piping, 26 % for instruments, 10 % for electrical systems, 55 % for civil works and 29 % for structures and buildings. The expenses for lagging are included under the equipment

installation and piping costs like Peters et al. (2004) suggested. The equipment cost of the pyrolysis reactor can thus be calculated by Eq. 4-6¹.

$$\text{Eq. 4-6: } \textit{Equipment cost pyrolysis reactor} = \frac{\textit{Direct plant cost}}{290\%} = \frac{\textit{FCI pyrolysis plant}}{490.1\%}$$

It is also important to note that the feed input of the activation reactor is related to the feed input of the pyrolysis reactor as defined in Eq. 4-7:

$$\text{Eq. 4-7: } Q_{\textit{feed input activation}} = Y_{\textit{Char}} * Q_{\textit{feed input pyrolysis}}$$

With Y_{Char} the char yield from the pyrolysis step which can be found in Table 4-4 and $Q_{\text{feed input activation}}$ the input of the activation reactor in t/h dry matter.

From the foregoing discussion the total equipment cost for the pyrolysis and activation reactor can be calculated by combining Eq. 4-5, Eq. 4-6 and Eq. 4-7 to form Eq. 4-8.

Eq. 4-8:

$$\textit{Equipment cost reactor} = \frac{40,8 * 10^3 * \left[\left(Q_{\textit{feed input pyrolysis}} * 10^3 \right)^{0,6194} + \left(Y_{\textit{Char}} * Q_{\textit{feed input pyrolysis}} * 10^3 \right)^{0,6194} \right]}{490.1\%}$$

The formula is used in the assumption that condensable gases (pyrolysis liquids) will not be condensed (i.e., direct diversion to the combustion system), but instead the activated carbon needs to be cooled. Therefore it is assumed that the cost of the liquids recovery of Bridgwater et al. (2002), is the same as for the activated carbon cooling.

The produced gases can be considered as a mixture of flammable (and toxic) compounds at enhanced temperature. From an energy and environmental point of view there is a need to (re)use this heat or "combustion" energy and decompose or separate the toxic compounds. Thermal treatment of the volatile combustible gases will be performed by a direct fired thermal

¹ $\textit{Direct plant cost} = \textit{equipment cost pyrolysis reactor} * (100\% + 39\% + 26\% + 31\% + 10\% + 29\% + 55\%) = 290\% * \textit{equipment cost pyrolysis reactor}$

$$\textit{Direct plant cost} = \frac{\textit{FCI pyrolysis plant}}{169\%}$$

oxidizer combined with a cyclone. The temperature of the combustion chamber is maintained at $\sim 1\,000\text{ }^{\circ}\text{C}$ with a residence time of minimum 2.5 s. This reduces the formation of NO_x and harmful materials, like dioxins, will be destroyed (Choy et al. 2005). For complete combustion, the flue gases pass through a cyclone where possible solid particles are separated out. Lemmens et al. (2004) calculated a cost estimate for these systems. Where a maximum cost of 40 kEUR and 1.5 kEUR for a gas stream of $1\,000\text{ Nm}^3/\text{h}$ for the combustion chamber and the cyclone is used respectively.

4.4.2 Expenditure

The total expenditure of the project consists of the operating cost and the yearly interest payments. Thewys & Kuppens (2008) assumed that an investment is financed by means of a loan with a yearly interest of 4.60 % in Belgium. The macro-economic database Belgostat (2010) gives an average initial interest provision for more than 5 years of 3.9 % on new credits (in 2009) for the euro area for an amount of more than 1 MEUR. In this model an interest rate of 4.0 % is applied as a realistic compromise. The annual operating costs of pyrolysis and activation consist of maintenance, labour, insurance, overhead, delivered feed, energy and water costs which are generally expressed as a percentage of the total fixed-capital investment (Thewys & Kuppens 2008) except the last three items.

A summary of literature percentages to calculate the annual operating cost is displayed in Table 4-3.

In this model, maintenance is accounted for 3 %, overhead and insurance for 2 % of the total plant cost. The labour costs are calculated with **Eq. 4-9** based on Bridgwater et al. (2002). The calculation is in function of the flow rate of the dry feed (t/h) $Q_{\text{feed input pyrolysis}}$ and will always be rounded up.

Eq. 4-9: Labour cost = $1,04 * ([1 + Y_{Char}] * Q_{\text{feed input pyrolysis}})^{0,475} * 3 \text{ shifts} * \text{annual salary}$

FPS Economy (2010) states that the annual salary of one person, employed in the industrial sector in Belgium was on average 48 kEUR in 2004. By using the annual nominal unit labour cost data from Eurostat (2010) the average annual salary in industry is estimated to be around 55 kEUR in the year 2009. In this model it is assumed that 3 shifts are sufficient for a good and secure operation of the activated carbon production facility.

Table 4-3: Summary of the fixed annual operating factors

Annual operating cost	expressed as	Reference
Maintenance	3% of Fixed-capital investment	(Caputo et al. 2005, Islam & Ani 2000, Kuppens et al. 2010, Thewys & Kuppens 2008)
	5% of Fixed-capital investment (for a gasification system)	(Choy et al. 2005, Gassner & Marechal 2009, Yassin et al. 2009)
	3% of Fixed-capital investment (for a combustion process)	(Yassin et al. 2009)
	4% of Fixed-capital investment	(Peacocke & Bridgwater 2004)
	6% of Fixed-capital investment	(Ko et al. 2004)
	2.5 % of Fixed-capital investment	(Bridgwater et al. 2002)
	2% of Fixed-capital investment	(Lima et al. 2008)
Insurance	2% of Fixed-capital investment	(Islam & Ani 2000, Thewys & Kuppens 2008)
	1% of Fixed-capital investment	(Ko et al. 2004)
Insurance and general	1% of Fixed-capital investment	(Caputo et al. 2005)
Overheads	4% of Fixed-capital investment	(Peacocke & Bridgwater 2004)
	2% of Fixed-capital investment	(Islam & Ani 2000, Thewys & Kuppens 2008)

The delivered feed cost consists of the cost of the particle board waste and the melamine (urea) formaldehyde waste. For processing particle board waste a gate fee of 70 EUR/t (Girods et al. 2009a) is paid, which is an incoming cash flow for the activated carbon production plant. Disposing of melamine (urea) formaldehyde waste to a landfill site costs a melamine (urea) formaldehyde factory 220 EUR/t (including transport) in Belgium. This

could mean that this waste also represents an income stream for the activated carbon production facility, as the melamine (urea) formaldehyde factory is already satisfied when it has to pay less than 220 EUR/t for disposing its melamine (urea) formaldehyde waste stream. In this model the cost of the melamine (urea) formaldehyde is set at 0 EUR/t to have a worst case scenario.

To provide an oxygen free environment, nitrogen gas is applied to act as a purging gas. In this study a rate of 8 kg nitrogen gas per ton feed input (based on Ko et al. (2004)) with a cost of 2.5 EUR/kg is applied.

Bridgwater et al. (2002) used 18.5 m³ water per ton input material for cooling the produced pyrolysis liquid and Ko et al. (2004)) used 13.5 m³ water per ton input material to generate steam for the activation and cooling water for the produced pyrolysis liquid. The quantity of cooling water (from surface water 20 °C) needed to cool the produced activated carbon from 800 °C to 20 °C is 13 t/h. In this calculation it is assumed that the specific heat capacity of activated carbon is equal to the specific heat capacity of graphite (709 kJ/(t.°C)) and the maximum temperature of cooling water that needs to be discharged is 30 °C as defined by the Belgian legislation. Here, the water requirements are assumed to be 15 m³ water per ton input material with a cost of 1.5 EUR/m³.

Another utility required in the process is energy which can be split in two parts, power and heat requirements. Ko et al. (2004) estimated that a 1.25 t/h processing plant producing activated carbon uses 200 kW electricity. So it is assumed that for a 1 t/h facility the electricity consumption is 160 kW. In this estimation the price of electricity is set at 0.0725 EUR/kWh. The heat of pyrolysis for municipal solid waste is calculated by Baggio et al. (2008) as 1.8 MJ/kg. For biomass a range of 2 MJ/kg to 3.47 MJ/kg can be found in literature (Beckham & Graham 1994, Diebold & Bridgwater 2003, Polagye et al. 2007, Reed & Gaur 1997). In our case a value of 2.5 MJ/kg for both the pyrolysis and the activation step is taken. In the activation step steam is also needed. Heating water from 20 °C to 800 °C requires 5.5 MJ/kg. For the drying process 2.67 MJ/kg water in the wood is needed. In most pyrolysis reactors (for the production of pyrolytic oil) the required heat is provided by the combustion of the gas and/or the char. In this application, as explained before in section 4.4.1, only activated carbon and gases (as by-product) are produced. The gases will be thermally destroyed and provide the required heat.

4.4.3 Revenues

It is expected that the activated carbon can be sold at a price between 1 kEUR/t and 4.5 kEUR/t AC. Net present values have been calculated for processing capacities of 1 t/h and 2 t/h waste in different ratios of melamine (urea) formaldehyde resin and particle board waste. Different ratios result in different yields (see Table 4-4) and different qualities and hence different costs are incurred.

Table 4-4: Estimated yields of the input feed

	OMF-5PB	1MF- PB	2MF-3PB	3MF-2PB	4MF-1PB
Yield Char ^a (wt%)	50%	43%	36%	29%	22%
Yield Activated carbon ^a (vis-à-vis char, (wt%))	50%	48%	47%	45%	44%

^a Girods et al. (2009a) determined the carbon yield after pyrolysis (400 °C) typically 50% and again 50% after pyrolysis combined with steam activation (800 °C). Own laboratory experiments on MF give a yield of 15 and 42 wt% respectively (800 °C).

Table 4-4 provides a guideline for the char and activated carbon yields. It is shown that the activated carbon yield increases when the share of PB increases in the mixture. So the highest yield is obtained by the 0 MF – 5 PB ratio and the lowest by the 4 MF – 1PB.

In some countries subsidies can be applied such as ecological (governmental) premium, a discount for waste treatment, ..., recovery and selling of other possible by-products, possible production of green electricity and heat. However, these are not taken into account in this process because these are mostly meant as temporary regulations, which differ from country to country.

4.5 Results and Discussion

4.5.1 Economic evaluation of the base case

The NPVs corresponding to a 1 t/h processing facility are outlined in Figure 4-2 as a function of the selling price of activated carbon and the MF - PB ratios. The total investment and operating costs for this facility are displayed in Table 4-5. A higher activated carbon yield (i.e., less MF in the feed mix) and thus a larger installation are the cause of slightly higher investment and operating (without feed cost) costs. This small increase is compensated by the income provided by the gate fee of the waste and higher yield (revenue) of AC: i.e., in the 0 MF – 5 PB ratio the gate fee (490 kEUR/year) is responsible for a decrease of 30 % of the total operating cost (1 726 kEUR/year – 490 kEUR/year = 1236 kEUR/year). The analysis of Table 4-5 and Figure 4-2 illustrates that the lower operating costs and higher activated carbon yields in the successive range (4 MF – 1 PB → 0 MF – 5 PB) of ratios are responsible for the higher NPV.

The minimal selling price (NPV = 0 EUR, break-even point) of the produced activated carbon can be found in Table 4-5 and Figure 4-2. By increasing the share of PB in the ratio the minimal selling price for activated carbon that needs to be achieved gradually decreases from 4.2 kEUR/t to 1.7 kEUR/t which corresponds respectively to a 4 MF – 1 PB and a 0 MF – 5 PB ratio.

The accompanying IRRs are presented Table 4-6. Only the cases in the green box (full line) where the IRR is higher than the discount rate can be accepted. The 2 MF – 3 PB, 1 MF – 4 PB and 0 MF – 5 PB feed mixture appear to be the most likely to result in an acceptable investment project (i.e., when IRR > 9 %). When the major share in the mix comes from MF waste (i.e., 4 MF – 1 PB or 3 MF – 2 PB) an investment is only acceptable for a high activated carbon price. A clear view on the situation can be made by combining Figure 4-2, Table 4-5 and Table 4-6.

For example: a 1 t/h processing facility with a feed mixture of 1 unit MF and 4 units PB would yield a NPV of the cash flows of 4.2 MEUR, an IRR of 14 % and a yearly output of 1.4 kt activated carbon when selling the product at a price of 2.5 kEUR/t. The minimum selling price of this mixture yielding at least a NPV of 0 EUR is 2.0 KEUR/t. A feed mixture of 3 MF and 2 PB however requires a higher minimum selling price of at least 3.2 kEUR/t in order to operate break even.

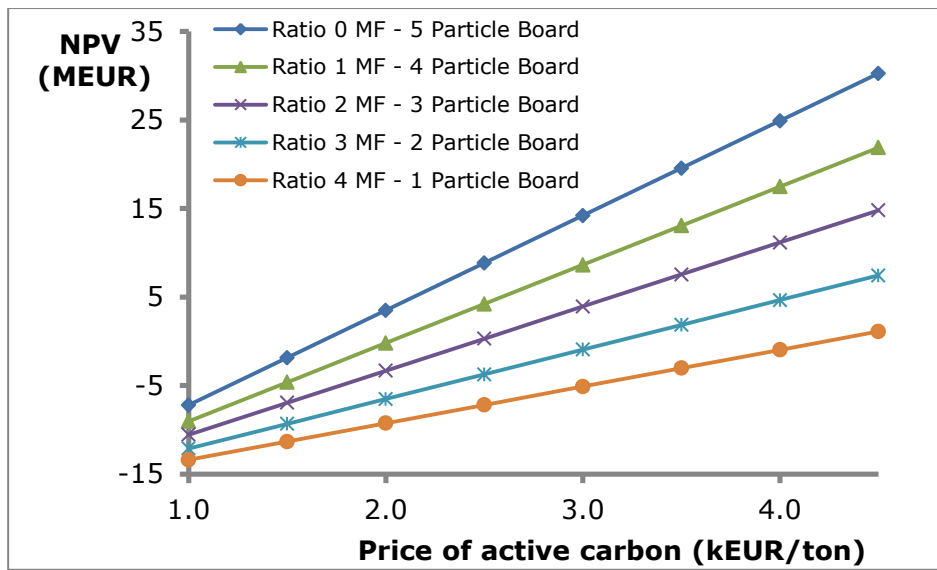


Figure 4-2: Net Present value for a 1 t/h processing facility

Table 4-5: Summary of costs for the production of Activated Carbon by this model

1 t/h	4 MF- 1 PB	3 MF - 2 PB	2 MF - 3 PB	1 MF - 4 PB	0 MF - 5 PB
Total capital investment	10 221 KEUR	10 764 KEUR	11 263 KEUR	11 733 KEUR	12 180 KEUR
Operating cost (without feed cost)	1 547 KEUR	1 595 KEUR	1 641 KEUR	1 684 KEUR	1 726 KEUR
Gate fee delivered feed	98 KEUR	196 KEUR	294 KEUR	392 KEUR	490 KEUR
Total operating cost	1 449 KEUR	1 399 KEUR	1 347 KEUR	1 292 KEUR	1 236 KEUR
Produced Activated carbon	678 t/year	914 t/year	1184 t/year	1445 t/year	1750 t/year
Minimal selling price activated carbon	4.2 KEUR/t	3.2 KEUR/t	2.5 EUR/t	2.0 KEUR/t	1.7 KEUR/t

Table 4-6: IRR for the 1 t/h feed input factory

activated carbon selling price	4 MF- 1 PB	3 MF - 2 PB	2 MF - 3 PB	1 MF - 4 PB	0 MF - 5 PB
1.0 kEUR/t	< 0%	< 0%	< 0%	< 0%	< 0%
1.5 kEUR/t	< 0%	< 0%	< 0%	3%	6.80%
2.0 kEUR/t	< 0%	< 0%	4.60%	8.80%	13%
2.5 kEUR/t	< 0%	3.70%	9.40%	14%	18%
3.0 kEUR/t	1%	7.80%	14%	18%	23%
3.5 kEUR/t	4.50%	11%	18%	23%	28%
4.0 kEUR/t	7.60%	15%	21%	27%	33%
4.5 kEUR/t	10%	18%	25%	31%	38%

4.5.2 Economic impact of the nitrogen content of the activated carbon

When looking at the previous analysis (and Figure 4-2, Table 4-4, Table 4-5 and Table 4-6) one could argue that it is only useful to study the 0 MF – 5 PB ratio. Because this mix has the lowest minimal selling price of 1.7 kEUR/t and the highest output of activated carbon (1.7 kt/year), it results in higher NPVs compared to mixes with a higher share of MF. However, the quality of the resulting activated carbon needs to be considered. Badosz (2009), Marsh & Rodríguez-Reinoso (2006a), Menéndez-Días & Martín-Gullón (2006) state that a higher nitrogen content corresponds to a better performance of the activated carbon resulting in higher attainable selling prices. It can be seen that the nitrogen content of the resulting activated carbon decreases in the successive range (4 MF – 1 PB → 0 MF – 5 PB) of ratios. Girods et al. (2009a) have produced an activated carbon from PB with a nitrogen content of 1.5 wt% to 2 wt% with an estimated value of 2.0 kEUR/t. They state that a higher nitrogen content could be obtained by optimizing the activation conditions, and hence probably better adsorption properties and thus yield a higher value. Therefore, if activated carbon production from pure PB is optimized, a somewhat higher selling price – with an expected maximum of 2.5 kEUR/t corresponding to an NPV of 8.8 MEUR can be achieved.

In our case of mixing the PB with MF, activated carbon with an even higher nitrogen content could easily be achieved. In recent literature, the estimated selling value of specialty (impregnated) carbons is in the range of 4.0 – 6.0 kEUR/t (incl. pick-up of the saturated carbon and selling prices of 2008) (Infomil 2011). An example of such a specialty activated carbon is impregnation with NaOH to trap acidic components. Our case, provides the incorporated nitrogen for the basic properties of the activated carbon thus a similar sales value can be expected. In addition, in some “extra specialty” cases even higher prices can be achieved.

Therefore, one should take the nitrogen content into account, which is the highest in the feed mixture of 4 MF – 1 PB and gradually decreases as the share of MF in the ratio decreases. It means that the mixtures with a higher share of MF have a higher chance of reaching a selling price of 4.0 kEUR/t to 6 kEUR/t. From Figure 4-2 and Table 4-5, it can be seen that, a feed mixture of 3 MF and 2 PB requires a higher minimum selling price of at least 3.2 kEUR/t in order to break even. However, this mixture is more likely to reach a sales value of 5.0 kEUR/t with a NPV of 10.2 MEUR (compared to pure PB NPV of 8.8 MEUR). In the case of 2 MF – 3 PB a NPV of 18.4 MEUR is achieved. However, its nitrogen content will be lower, so this price (of 5.5 kEUR/t) may not be achievable. A key point is that the mixture of 4 MF – 1

PB at a selling price of 6.0 kEUR obtains a NPV of 7.3 MEUR. This is somewhat smaller than the pure PB in the situation of a selling price of 2.5 kEUR/t, at a price of 2.0 kEUR/t the NPV of the pure PB (3.5 MEUR) is lower. Taken the expected price of the 0 MF – 5 PB (between 2.0 kEUR/t and 2.5 kEUR/t) into account, it is possible to select the ratios in function of their selling prices which yield an equal or more positive result than this mixture. These ratios with their accompanying IRRs are presented in Table 4-6. In the shaded area in the case of a price of 2.0 kEUR/t and in the dashed box in the case that the maximum selling price (2.5 kEUR/t) for the activated carbon of the pure PB is reached. As illustrated by Table 4-6, the 4 MF – 1 PB ratio neither appears in the shaded area, nor in the dashed box. This ratio would only be comprised in the shaded area if Table 4-6 would be expanded to prices of 5.5 kEUR/t and more. The 4 MF – 1 PB ratio would only appear in the dashed box if Table 4-6 is expanded to contain prices above 6.5 kEUR/t. It is important to keep this in mind, as the 4 MF – 1 PB ratio is potentially interesting if higher nitrogen content can be scientifically proved, which means that these high selling prices can be attained.

4.5.3 Economies of scale

Another important factor affecting the NPV is the processing capacity, i.e., the hourly flow ratio of the input material ($Q_{\text{feed input pyrolysis}}$). Doubling the processing rate of the activated carbon plant from 1 ton waste per hour to 2 ton waste per hour results in higher NPVs (compare Figure 4-3 to Figure 4-2). This is a consequence of the economies of scale that are incorporated in the total equipment cost equation (Eq. 4-8). As the power exponent in equation 8 is smaller than one ($0.6194 < 1$), doubling the processing capacity (in other words multiplying $Q_{\text{feed input pyrolysis}}$ by 2) does not result in a proportional increase of the total equipment cost. Doubling the processing rate thus augments the total capital investment with only 57 % instead of 100 %. Consequently, also the total operating costs – which partly depend on the height of the total capital investment – increase with only 39 % to 52 % (depending on the mix ratio of MF and PB waste). As a consequence the break-even selling price of activated carbon decreases on average with 24 %.

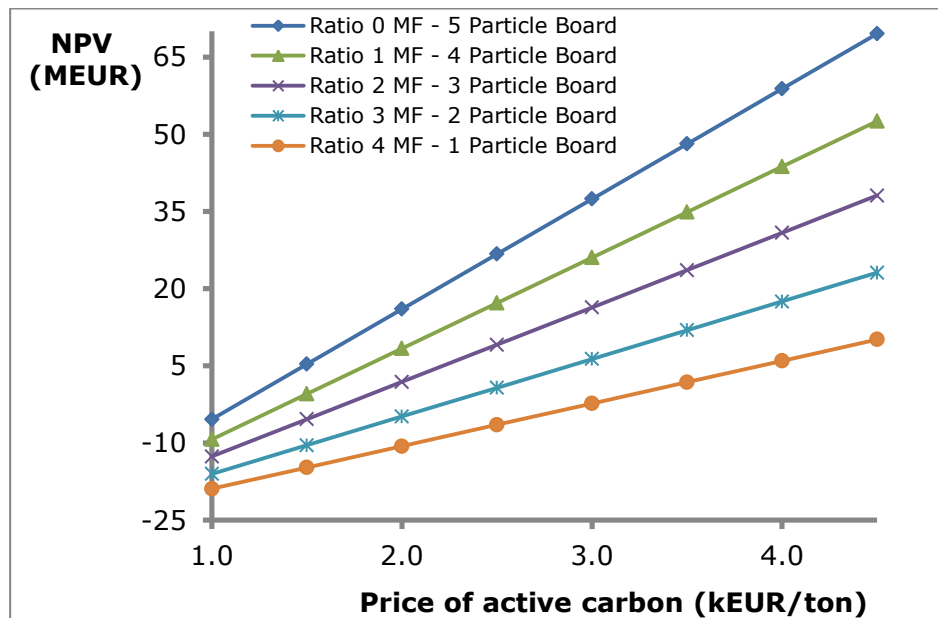


Figure 4-3: Net Present value for a 2 t/h processing facility

4.5.4 Share of expenditure items in total expenditure

Figure 4-4 presents the share of the distinct expenditure items expressed as an average percentage for all ratios of the total discounted expenses (over 20 years). The total capital investment represents on average the major share of 42.9 % (with a maximum deviation down of 0.9 % and a maximum deviation up of 0.7 %). Staff and maintenance present the main operating costs with respectively a share of 11 % (with a maximum deviation down of 0.7 % and a maximum deviation up of 0.8 %) and 10 % (with a maximum deviation down and up of 0.2 %) of the total expenses. The interest payments amount to 8 % (- 0.2 %; + 0.1 %) of the total expenditure closely followed by insurance, overhead, liquid nitrogen, water and electricity. The fixed operating costs (insurance, overhead, interest payments, maintenance) are considered as unchanging during the life time of the project (20 years). The impact of the total capital investment and the cash flows generated by the staff cost, liquid nitrogen, water and electricity on the NPV will be analysed in section 4.5.5 by means of Monte Carlo Sensitivity analysis.

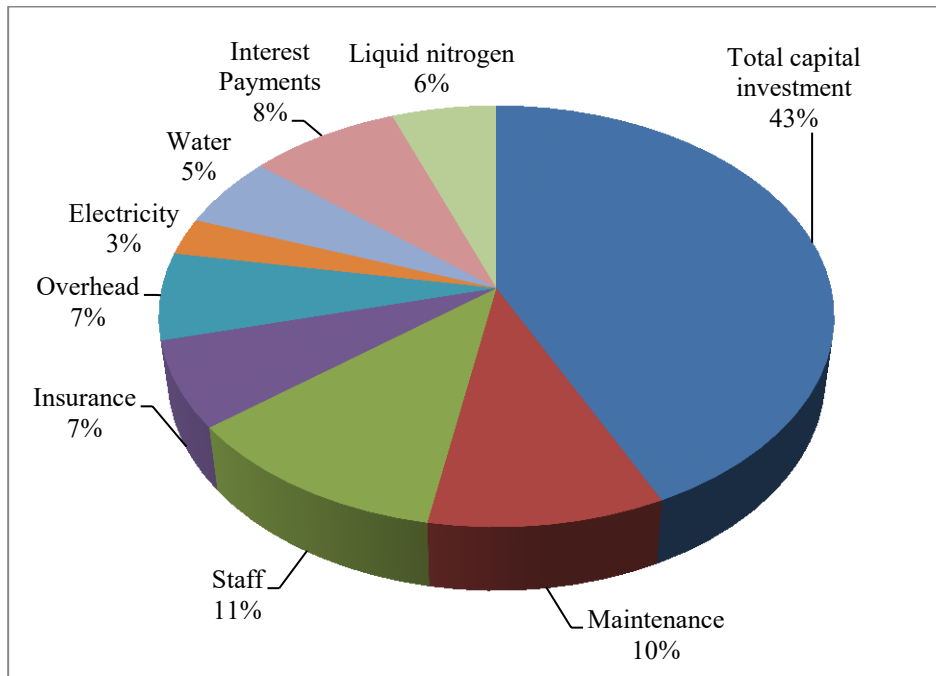


Figure 4-4: Importance of the distinct expenditure items

4.5.5 Monte Carlo Sensitivity analysis

As described in section 4.3, results are only valid in the case of 100 % certainty of the base case variables. Some variables however are uncertain by definition, other variables might strongly influence the NPV if their value changes slightly. Nine main variables that are expected to affect the economic attractiveness of the production plant are selected. The variables, listed in Table 4-7, are allowed to change following a triangular distribution characterized by a most likely, a minimum and a maximum value. Monte Carlo simulations are performed, in which each run of the Monte Carlo simulation draws a random value for each of these variables, between the minimum and maximum value and in accordance with the selected distribution. Each run results in a NPV corresponding to the values drawn for each of the nine uncertain variables. Numerous runs (10 000 per ratio in this research) of the Monte Carlo Simulation result in a NPV distribution.

Table 4-7: Variables with their profitability distribution

Input variable	Profitability Distribution	Most likely value	Variance of the distribution
Delivered feed cost	Triangular	dependent of the ratio	± 10 %
Discount rate	Triangular	9 %	± 10 %
Electricity cost	Triangular	0.0725 EUR/kWh	± 10 %
Cost of water	Triangular	1.5 EUR/m ³	± 10 %
Char output (%) (pyrolysis)	Triangular	See Table 4-4	± 10 %
Activated carbon output (%) (activation)	Triangular	See Table 4-4	± 10 %
Staff cost/shift	Triangular	55 kEUR	± 10 %
Total Capital Investment	Triangular	dependent of the ratio	± 10 %
Liquid nitrogen	Triangular	2.5 EUR/kg	± 10 %

Figure 4-5 illustrates this distribution, characterized by the mean of the Monte Carlo analysis with their respective standard deviations for the 1 t/h processing plant. Similar results for the other input rates can be calculated.

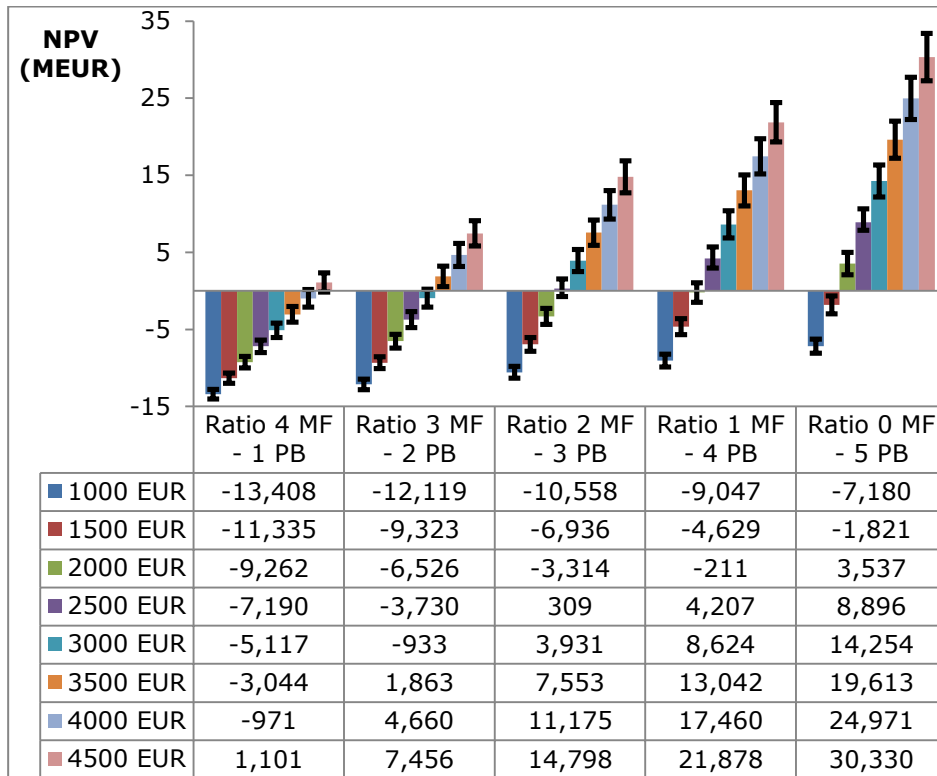


Figure 4-5: Mean NPV Output after Monte Carlo analysis

Table 4-8: Percentage of Monte Carlo Simulation Runs that gain a positive NPV

activated carbon selling price	4 MF- 1 PB	3 MF - 2 PB	2 MF - 3 PB	1 MF - 4 PB	0 MF - 5 PB
1.0 KEUR/t	0	0	0	0	0
1.5 KEUR/t	0	0	0	0	2
2.0 KEUR/t	0	0	0	42	100
2.5 KEUR/t	0	0	62	100	100
3.0 KEUR/t	0	17	100	100	100
3.5 KEUR/t	0	96	100	100	100
4.0 KEUR/t	16	100	100	100	100
4.5 KEUR/t	85	100	100	100	100

Table 4-9: Minimal selling price at which the activated carbon should be sold to guarantee a 95% chance on a positive NPV

1 t/h	4 MF- 1 PB	3 MF - 2 PB	2 MF - 3 PB	5 MF - 4 PB	0 MF - 5 PB
Minimal selling price activated carbon	5.0 kEUR/t	3.7 kEUR/t	2.9 EUR/t	2.5 kEUR/t	2.5 kEUR/t

By means of Monte Carlo simulations also the probability of obtaining a positive NPV is calculated. The results are listed in Table 4-8. For example, a 1 MF – 4 PB ratio that yields an activated carbon quality with a sales value of only 2.0 kEUR/t has a 42 % chance on a positive NPV. If the product is of better quality and can be sold at 2.5 kEUR/t or more, 100 % of the cases have a positive NPV. The green full line box summarizes the ratios and selling prices that would yield at least in 95 % of the cases a positive NPV. These are the most promising scenarios for an activated carbon production facility put into practice. Comparing the selected cases (full line green box) of Table 4-8 and Table 4-6 the scenario of the ratio 2 MF – 3 PB with a selling price of 2.5 kEUR/t and the 4 MF – 1 PB at a selling price of 4.5 kEUR/t are supplementary rejected by the Monte Carlo simulation, because the chance on a negative NPV is higher than 5%. The minimal price corresponding to this minimal 95 % chance on a positive NPV is determined (see Table 4-9).

These selling prices are somewhat higher than the values defined in the base case (see Table 4-5) because the latter did not consider uncertainties in the assumed values of the base case variables. Based on these results one can say that it is, from an economical point of view, not interesting to study the 4 MF – 1 PB and ratios with an even higher MF portion. Nevertheless, in order to analyse these results, one should follow the same consideration (expected price of the 0 MF – 5 PB ratio) as in section 4.5.1.

The shaded area in Table 4-8 represents the scenarios which yield an equal or more positive NPV than the 0 MF – 5 PB mixture (from the Monte Carlo simulation (Table 4-5) at a price of 2.0 kEUR/t and in the dashed box the cases where the maximum price (2.5 kEUR/t) for this ratio is applied. For the 3 MF - 2 PB and the 4 MF – 1 PB ratio the dashed box starts at a sales value of 5.5 kEUR/t and at 6.5 kEUR/t for respectively. In addition, for the 4 MF – 1 PB ratio the shaded area starts at 5.5 kEUR/t. The conclusions in paragraph 4.5.1 thus still hold.

Nevertheless, we need to keep in mind that these results represent a rather worst case scenario, with a zero income from the MF-waste and first plant costs. In normal conditions the MF waste will probably yield a gate fee and will make the projections more positive. Another important fact is the likelihood of producing a specialty carbon of very high added value 4.0 – 6.0 kEUR/t (as described in section 4.5.5).

4.5.6 Identification of the key variables

Finally, the sensitivity of the NPV to the diverse input variables is determined, in order to identify the crucial process parameters for further investigation. The sensitivity of the NPV for a given variable is defined as the extent to which the variability of the NPV is dependent to the variability of the variable under consideration. For each variable of Table 4-7 an average NPV sensitivity is given in Figure 4-6 for a 1 t/h facility. The coefficients on the graph are normalized by the standard deviation of the output and the standard deviation of the input and not in actual euro's. The higher the coefficient of an input variable (the longer the bar), the greater the impact that the selected variable has on the NPV. The variability of the NPV for every factor can be calculated by using Eq. 4-10.

Eq. 4-10:
$$\text{sensitivity} = \frac{\frac{\Delta \text{NPV}}{\sigma_{\text{NPV}}}}{\frac{\Delta \text{variable}}{\sigma_{\text{variable}}}}$$

A positive value (the bar extending to the right) means that an increase in the variable leads to an increasing NPV. In the case of a negative sign the NPV decreases by an increase of the variable. (1) The char and activated carbon yield are on average the most determining factors for the NPV variability, both have an average sensitivity of 0.55. This means that for every k fraction of a standard deviation increase in char/activated carbon yield, the NPV will increase by 0.55 k standard deviations of the NPV. (2) The total capital investment is on average the 3rd most important variable in declaring the NPV's sensitivity. A key point is that, depending on the mix ratio and the activated carbon selling price, the investment cost is sometimes more important than the activated carbon and char yield, but the three main variables are always the char yield, the activated carbon yield and investment expenditure. The negative average sensitivity results of the discount rate and the delivered feed costs clearly indicate that a lower discount rate and a higher gate fee for the waste respectively result in a higher NPV. (3) The cost of water, liquid nitrogen, electricity and staff have also negative sensitivity factors. However these are almost negligible relative to the total capital investment, discount rate, char and activated carbon yield.

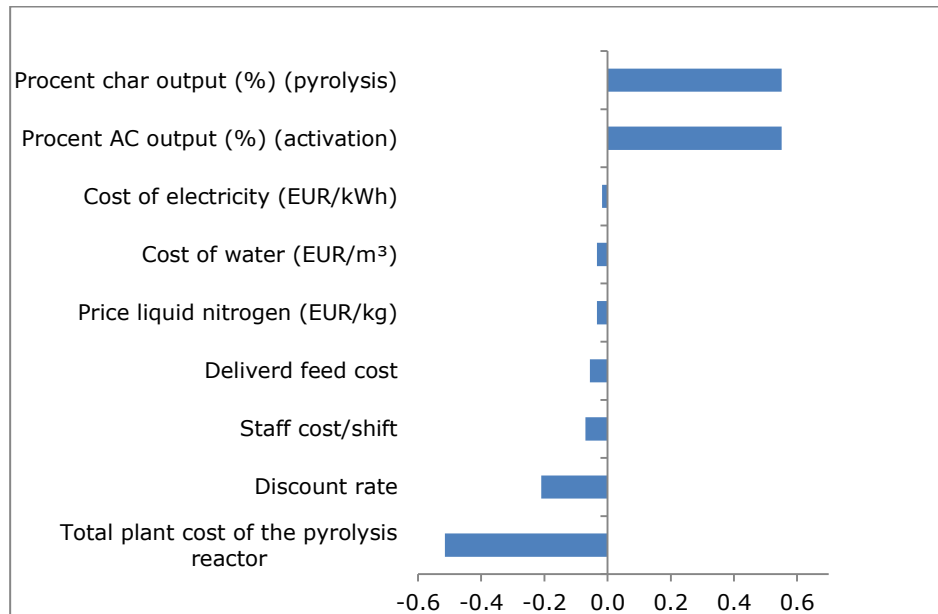


Figure 4-6: Average sensitivity of the crucial variables on the NPV for a 1 t/h facility

4.6 Conclusion

A feasibility study to process MF and PB waste for the production of activated carbon has been performed. A preliminary process design has been based on various literature sources, for an input feed of 1 t/h and different mixing ratios of the two waste products. The economic feasibility of the preliminary process design has been investigated, by calculating the NPV and IRR of the cash flows incurred by an investment in a pyrolysis and activation plant for the production of AC. A sensitivity analysis has been performed in order to determine the most crucial variables that influence the profitability of the investment.

Really encouraging results are obtained for a profitable production of AC, as the current assumptions start from a rather pessimistic scenario: e.g., a zero gate fee for the MF waste (which will probably be higher in practice). Besides that, the in-situ incorporation of nitrogen can result in a high quality product which can be sold at a high price or even in a niche market. In addition, the value or usefulness of the activated carbon production plant is enhanced by its ability to reuse two waste streams. Also the processing capacity plays a significant role. A larger manufacturing plant is able to produce carbons at a lower cost despite the higher initial investment. By doubling the input rate to

Chapter: 4

2 t/h (dry matter) a reduction of average 24% of the minimal selling price is obtained.

The sensitivity analysis reveals that the activated carbon plant economies are very sensitive to the investment cost, the product yield and the activated carbon selling price which is an indication for product quality.

Future research needs to focus on these prime properties to create a marketable high value product.

5 Screening of activated carbon produced by co-pyrolysis and steam activation from particle board and melamine formaldehyde resin

The results of this chapter have been published:

VANREPELEN, Kenny; KUPPENS, Tom; THEWYS, Theo; SCHREURS, Sonja; YPERMAN, Jan & CARLEER, Robert (2011) Activated carbon by co-pyrolysis and steam activation from particle board and melamine formaldehyde resin: production, adsorption properties and techno economic evaluation. In: Guzović, Zvonimir & Ban, Marko & Matijašević, Sunčana (Ed.) The 6th Dubrovnik Conference on Sustainable Development of Energy, Water and Environment Systems: Book of Abstracts & online CD Proceedings: vol. 6. [cat: C1]

VANREPELEN, Kenny; KUPPENS, Tom; THEWYS, Theo; SCHREURS, Sonja; CARLEER, Robert & YPERMAN, Jan (2011) Activated Carbon by Co-Pyrolysis and Steam Activation from Particle Board and Melamine Formaldehyde Resin: Production, Adsorption Properties and Techno Economic Evaluation. In: 6th Dubrovnik Conference on Sustainable Development of Energy, Water and Environmental Systems, Dubrovnik, 25-29 september. [Paper - cat: C2]

Vanreppelen, Kenny; Schreurs, Sonja; Carleer, Robert & Yperman, Jan (2012) Activated carbon by co-pyrolysis and steam activation from particle board and melamine formaldehyde resin. In: 2nd Symposium 'Cluster Milieu', Diepenbeek, Belgium, 30 January 2012. [Presentation - cat: C2]

VANREPELEN, Kenny; SCHREURS, Sonja; KUPPENS, Tom; THEWYS, Theo; CARLEER, Robert & YPERMAN, Jan (2013) Activated Carbon by Co-pyrolysis and Steam Activation from Particle Board and Melamine Formaldehyde Resin: Production, Adsorption Properties and Techno Economic Evaluation. In: JOURNAL OF SUSTAINABLE DEVELOPMENT OF ENERGY, WATER AND ENVIRONMENT SYSTEMS, 1 (1), p. 41-57. [Article - cat: A2]

5.1 Abstract

One of the top strategic objectives and research areas in Europe is recovering wood from processing and end of life products. However, there are still several 'contaminated' wood products that are not or only partly reused/recycled.

Particle board waste which is contaminated with aminoplasts is one of these products. In addition, a considerable amount of aminoplast waste resin is produced for the production of particle board that cannot be re-used or recycled. The chemical properties of these wastes (high nitrogen content of 5.9 wt% and 54.1 wt% for particle board and melamine formaldehyde resin respectively) make them ideal precursors for the production of nitrogenised activated carbon. The profitability of the produced activated carbon is investigated by calculating the net present value, the minimum selling price and performing a Monte Carlo Sensitivity analysis. Encouraging results for a profitable production are obtained even though the current assumptions start from a rather pessimistic scenario.

5.2 Introduction

The world population has increased significantly since the start of the industrial revolution and thereby also the waste production and the depletion of the world's resources. In an ideal society there is no waste generation, however in today's society large quantities of waste cannot be eliminated. Improper management of this waste can lead to serious health threats as a result of fires, explosions, and contamination of air, soil, and water (Demirbas 2011). Sustainable management needs to reduce the amount of waste that is discharged to the environment. These advanced waste management systems include prioritized management strategies to minimize environmental problems and preserve resources (Demirbas 2011). In decreasing order of importance and with respect to the final disposition of the waste, these strategies are (Demirbas 2011):

- Minimization or prevention of waste
- Recycling of waste
- Thermal treatment with energy recovery
- Land filling

It is thus necessary to search for new recycling/reengineering methods for waste products that are still landfilled or burned.

Recovering wood from processing and end of life products is recognised as one of the top strategic objectives and research areas in Europe (Daian & Ozarska 2009). This recovered wood provides a high volume resource for recycled products and new advanced materials, with further enhancing the environmental profile of wood (Daian & Ozarska 2009). One could say that, it is not necessary to maximize the utilisation of wood because it is the most abundant biodegradable and renewable material available on this planet (Daian & Ozarska 2009). However, there are numerous reasons to maximize its utilization like economic concerns, social preoccupation with the climate change

and greenhouse gas emissions as well as threats to forests due to adverse effect of climate change, pollution abatement and efficient savings of fossil primary energy (Daian & Ozarska 2009, Dornburg & Faaij 2006, Dornburg et al. 2006).

There are already different recycling and reengineering practices for clean wood like fuel briquettes, animal bedding, mulch, salvaged timber, recycling into particle board, etc. However there are still some wood products that are not or only partly reused/recycled. One of these products is particle board (PB) which is chemically contaminated with aminoplasts (melamine formaldehyde (MF), melamine urea formaldehyde (MUF) and urea formaldehyde). These products can be partly recycled in the production of 'new' PB; loss of mechanical properties of the final product will not allow to use significant quantities of board off-cuts and wood dust (chips between 3 mm – 50 mm) as an incoming wood stream (BFM 2003, Daian & Ozarska 2009). In Australia for example the panel board off-cuts (on average 8 % of the PB is wasted as off cuts) and wood streams contaminated with glues are currently not used (Daian & Ozarska 2009). In the UK 75 % of the wood waste from the furniture industry consists of board off-cuts and sawdust (Bromhead 2005). In addition the produced furniture ends up eventually as waste. In the UK, the end of life furniture (board materials account for 80 % in weight) is estimated between 1.9 and 2.2 Mtonnes BFM (2004). The annual production of new PB in 2004 by the European PB industry was 34.3 million m³ (Federation 2011).

Furthermore a considerable amount of aminoplast waste resin is produced for the production of particle board (PB) that cannot be re-used or recycled at this moment.

In addition, combustion of wood waste containing these aminoplasts resins might cause pollution because it results in the production of toxic gases like ammonia, isocyanic and hydrocyanic acid and nitrous oxides (Girods et al. 2008a, Girods et al. 2009b, Girods et al. 2008b, Girods et al. 2008c, Vanreppelen et al. 2011). To avoid environmental problems and landfilling costs, and to turn this waste stream into a rather profitable material resource, a sustainable solution is mostly required. Based on the properties of the waste sources (e.g., PB and MF) the production of high value nitrogenised activated carbon (AC) is considered as a possible opportunity.

The aim of this work is to evaluate the profitability of AC production from PB and MF waste based on preliminary research results and an economic feasibility study before up scaling the research. For this purpose a process design and an economical model has been developed in a previous work (see Chapter 4, Vanreppelen et al. (2011)). After production of AC from different blends of PB and MF a low concentration phenol adsorption test has been carried out. Based

on the obtained results, the Net Present Value (NPV) of the cash flows generated by an investment in an AC production facility and the minimum selling price of this AC has been calculated. The key variables for the profitability of the AC plant are identified. Finally, Monte Carlo Sensitivity analysis is carried out to take uncertainties into account.

5.3 Methodology

5.3.1 Economic feasibility model

The feasibility of the AC production facility is investigated by building a cost-benefit model (in EUR 2009) and a process design for estimating the total capital investment, the production costs, the possible revenues and the NPV based on various literature sources. This model is extensively detailed in Chapter 4 (which is also published as Vanreppelen et al. (2011)). An overview of the economic strategy is presented in Figure 5-1.

Investors use various investment criteria to evaluate the profitability of an investment before they want to invest. According to Vernimmen et al. (2005) the NPV is the best criterion for selecting or rejecting an investment, either industrial or financial. By using the NPV the expected profit is estimated using today's value of current and future cash flows generated by the AC production plant during a certain time period using a predetermined discount rate (Kuppens et al. 2010). The NPV formula is given in **Eq. 5-1**:

$$\text{Eq. 5-1:} \quad NPV = \sum_{n=1}^T \frac{CF_n}{(1+i)^n} - I_0$$

With: T = life span of the reactor (20 years (Bridgwater et al. 2002, Kuppens et al. 2010, Thewys & Kuppens 2008)), I_0 = initial total capital investment in year zero, CF_n = Cash Flows generated in year n, i = discount rate is set at 9 % incorporating the market interest rate and some risk premium (Ochelen & Putzeijs 2008b).

The cash flow in a given year can be calculated by using **Eq. 5-2** (Kuppens et al. 2010, Thewys & Kuppens 2008). It is the difference between revenues (R) and expenditure (E) after tax (t) generated by the investment taking depreciation into account because it lowers tax payments. To calculate the cash flow, depreciation (D) also needs to be taken into account because it lowers tax payments (Kuppens et al. 2010, Thewys & Kuppens 2008).

$$\text{Eq. 5-2:} \quad CF_n = (1 - t) * (R - E) + t * D$$

All the results of the base case (1 ton/h installation) are based on an average operation time of the reactor of 7 000 hours per year without

shutdown due to maintenance; etc. (80% operating + 20% maintenance, etc.). In general, when the NPV is positive, the investment is a good decision.

The NPVs are only valid if the calculated revenues and expenses are 100% certain. Because all the different variables are the most likely values obtained from literature, these are prone to uncertainty. Monte Carlo Sensitivity analysis is performed to have an idea about the impact of these uncertainties on the NPV. For each run of the simulation, a random value of all the uncertain variables is drawn following a presupposed distribution resulting in a NPV. In this study 10,000 runs are carried out using the @Risk software from Palisade Decision Tools. The total uncertainty of the NPV can be explained by the corresponding range of values and the obtained distribution.

Finally, taking into account all these uncertainties the minimum selling price at which the AC should be sold in order to guarantee a 95 % chance on a positive NPV is calculated.

5.3.2 Sample preparation

The PB samples are prepared from industrial water-resistant PB panels (glued with MUF) which have been sawn to strips of 1 cm and then cut (≤ 2.0 mm) with a high-speed rotary cutting mill (Retsch SM 100). The provided waste samples of MF have particle size ≤ 2.0 mm. For characterisation of the input materials they are further reduced in size by milling to ≤ 0.5 mm with a IKA Werke Yellow Line A10 mill. Prior to pyrolysis and characterisation the samples are oven dried (110 °C) and mixed.

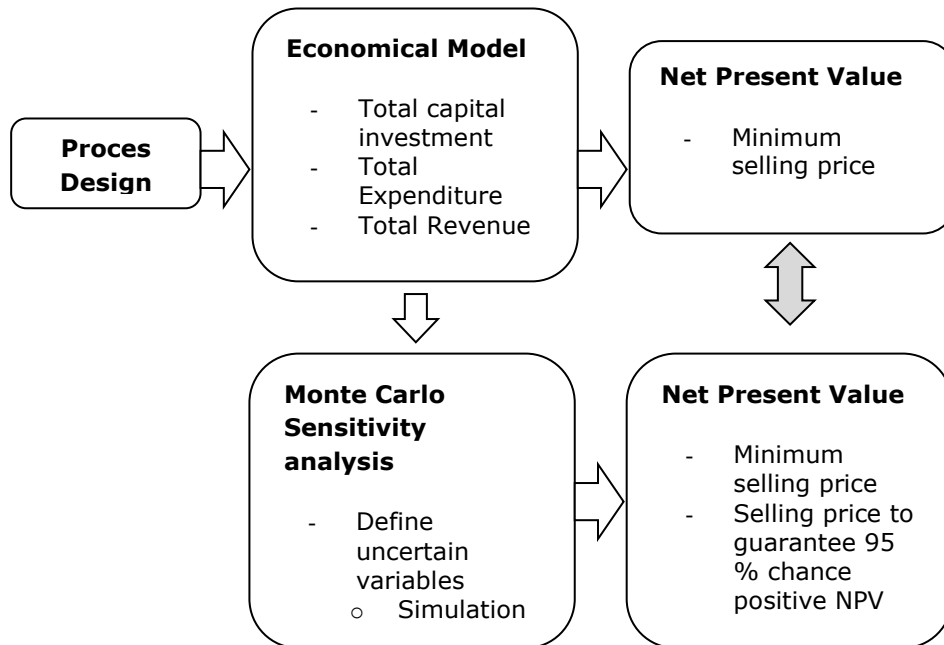


Figure 5-1: Economical strategy

5.3.3 Characterisation of the input materials

The PB and MF samples are determined by a DuPont Instruments 951 thermal analyser (TGA). The input materials are heated in inert atmosphere (with a N₂-gas flow of 30 ml/min⁻¹) from room temperature to 800 °C at a ramp of 20 °C/min followed by an isothermal period of 10 min, then heated to 900 °C at a ramp of 20 °C/min. The ash residue of the pure PB and MF are analysed by the TGA with the following temperature program: heating from room temperature to 800 °C at a ramp of 20 °C/min in N₂-flow (30 ml/min), then 10 min isothermal in O₂-flow (30 ml/min), heating to 900 °C at a ramp of 20 °C/min in O₂-flow (30 ml/min). The elemental composition (C, H, N, S) of the samples is analysed by a Thermo Electron FlashEA1112 elemental analyzer. BBOT (2,5-bis (5-tert-butyl-benzoxazol-2-yl) thiophene) is used to calibrate the instrument. O-content is determined by difference.

5.3.4 Preparation of the activated carbon

The waste blends (2 g – 5 g) are pyrolysed in triplicate in a horizontal quartz tube reactor (Nabertherm see chapter 3), with a heating rate of 20 °C/min from room temperature to 800 °C under nitrogen atmosphere (30 ml/min) followed by a 30 min isothermal activation under steam atmosphere (water

flow of 2ml/h directly injected in the reactor). The produced gases are combusted.

5.3.5 Batch adsorption experiments

The phenol adsorption of the different activated carbons against a commercial AC (Norit GAC 1240) were evaluated by introducing 50 ml of a 100 mg/l unbuffered phenol solution with different quantities of AC in a hermetically closed flask. The phenol was of analytical grade and Milli-Q Millipore water (18.2 M Ω /cm conductivity) was used. The flasks were placed in a thermostatic water bath (25°C) and stirred for 24 h. It is assumed that equilibrium is reached in this time period. The solution was filtered and the residual phenol concentration was analysed using a Pharmacia Biotech Ultraspec 2000 UV-VIS spectrophotometer at 270 nm. Calibration is carried out using a number of phenol standard solutions (concentration range: blank, 1 mg/l, 5 mg/l, 10 mg/l, 30 mg/l, 50 mg/l, 80 mg/l and 100 mg/l). Each experiment was done in quadruplicate, with an average scatter in the results of 5%.

5.4 Results and discussion

5.4.1 Characterisation of the input material

The thermal behaviour of PB and MF is investigated by TGA-analysis in N₂-atmosphere. In the literature, limited information is provided concerning the thermal degradation of the MF. The TG and DTA curves of PB and MF (Figure 5-2) show respectively a small weight loss of 2 wt% and 3 wt% because of fixed moisture (25 – 150 °C) followed by a major weight loss step. For PB this corresponds to the degradation of hemicellulose, cellulose and lignin and can be observed from 194 °C – 385 °C (weight loss of 62 wt%), followed by a further slow degradation until a fixed carbon content of 13 wt% (at 800 °C). For MF a small loss (5 wt%) is observed from 125 °C till 372 °C. Girods et al. (2008a) found mainly N-compounds such as isocyanic acid and ammonia as degradation products below 350 °C. Additionally a loss of 35 wt% (between 372 °C – 424 °C and) is observed with a maximum degradation rate at 400 °C. In this temperature range the detected degradation products are formaldehyde, methanol, amines, ammonia and sublimated melamine (Girods et al. 2008a). In the temperature range starting at 424 °C the resin undergoes extensive degradation. Devallencourt et al. (1995) assumed that the resin progressively deaminates forming cyameluric structures in the range of 410 °C – 525 °C with release of HCN and CH₃CN. Above 660 °C the MF resin undergoes extensive degradation with production of HCN, CO, CO₂ (Devallencourt et al. 1995). A fixed carbon

content at 800°C of 11 wt% is determined after switching to an oxidative atmosphere.

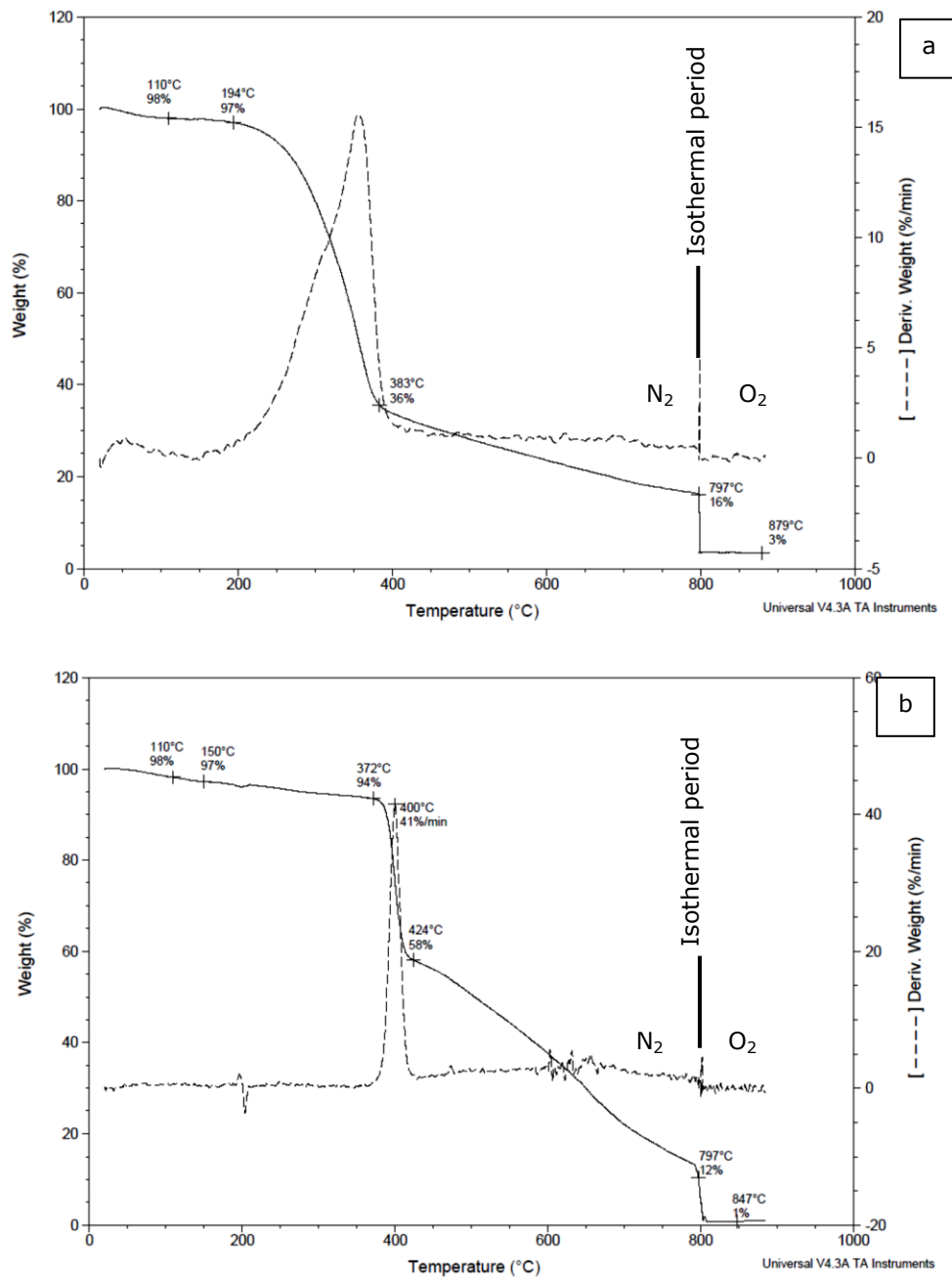


Figure 5-2: TGA of PB (a) and MF (b)

Ultimate analysis is carried out on the pure products and is presented in Table 5-1. The chemical properties i.e., the high nitrogen content of PB (5.9 wt%) and MF (54.1 wt%) waste materials indicates that pyrolysis and subsequent activation will result in in-situ production of nitrogenised activated carbons.

Table 5-1: Ultimate analysis

	PB – MF (5/0)	PB – MF (0/5)
Ultimate analysis (%)(dry and ash free)		
C	46 ± 3	37.2 ± 0.4
N	5.9 ± 0.4	54.1 ± 0.6
H	5.9 ± 0.4	4.70 ± 0.04
S	0.9 ± 0.4	Not detected
O*	41 ± 4	4 ± 1
N/C molar ratio	0.13	1.45
O/C molar ratio	0.89	0.11

* Calculated by difference

5.4.2 Pyrolysis and activation experiments

Pyrolysis and steam activation is performed on different blends of PB and MF resin. The effect on the product distribution is shown in Table 5-2. An average char yield of 27 wt% is obtained after pyrolysis. The mix ratio PB – MF has no effect on the char yield. For the successive range of ratios [PB – MF (5/0) → PB – MF (2/3)], the char yield is lower than predicted in Vanreppelen et al. (2011). In the case of PB – MF (1/4) a higher yield is observed. It can be seen that the resulting AC yield after activation decreased in the successive range [PB – MF (5/0) → PB – MF (1/4)] with a burn-off between 18.5 wt% and 59 wt%. Nevertheless, the char yields are lower (with exception of PB – MF (1/4)) than predicted in Vanreppelen et al. (2011) and higher AC yields are achieved for all the ratios except for the pure PB which is somewhat lower.

The chemical composition of the produced activated carbons with their standard deviations is given in Table 2. By increasing the fraction of MF in the mixture a significant higher N-content is obtained with an increase of 84% from 2.2 wt% for PB – MF (5/0) to 14 wt% PB – MF (1/4) respectively.

Table 5-2: AC yield and ultimate analysis

	0 MF - 5 PB	1 MF - 4 PB	2 MF - 3 PB	3 MF - 2 PB	4 MF - 1 PB
Pyrolysis products (wt%)					
- char	27.0 ± 0.5	28.0 ± 0.3	28.0 ± 0.7	26.1 ± 0.9	27.4 ± 0.9
- gases	73	72	72	74	73
Activation (wt%)					
- activated carbon	22 ± 0.4	21 ± 0.7	19 ± 0.6	15 ± 0.9	11 ± 0.6
% burn-off	18.5	25	32	42	59
- gases	78	78.6	80.7	84.7	89.1
Ultimate analysis (%) (dry and ash free)					
C	91 ± 1	85 ± 4	86 ± 2	83 ± 2	83.4 ± 0.7
N	2.24 ± 0.04	4.3 ± 0.2	7.35 ± 0.07	9.6 ± 0.3	14 ± 1
H	1.14 ± 0.06	1.32 ± 0.06	1.3 ± 0.1	1.5 ± 0.2	1.65 ± 0.08
S	0.1 ± 0.1	0.07 ± 0.01	0 ± 0	0 ± 0	0 ± 0
O (calculated by difference)	6 ± 1	8 ± 4	6 ± 2	6 ± 3	1.4 ± 0.8
N/C atomic ratio	0.02	0.05	0.09	0.12	0.17
O/C atomic ratio	0.07	0.09	0.07	0.07	0.02

5.4.3 Low concentration phenol adsorption

Phenol is an important raw material and/or product of the chemical and allied industries (Srivastava et al. 2006). Phenol and phenolic compounds are very toxic with a fixed low admissible level following the Flemish regulation of ≤ 0.1 mg/l of surface water for the production of drinking water, ≤ 0.05 mg/l of surface swimming water and 0.5 mg/l of groundwater (VLAREM-II 2013). It is well known that activated carbons containing nitrogen-containing surface groups, have a basic nature and thus have enhanced adsorption capacity toward phenol (Girods et al. 2009a). To evaluate the performance of the produced AC, phenol adsorption tests have been performed.

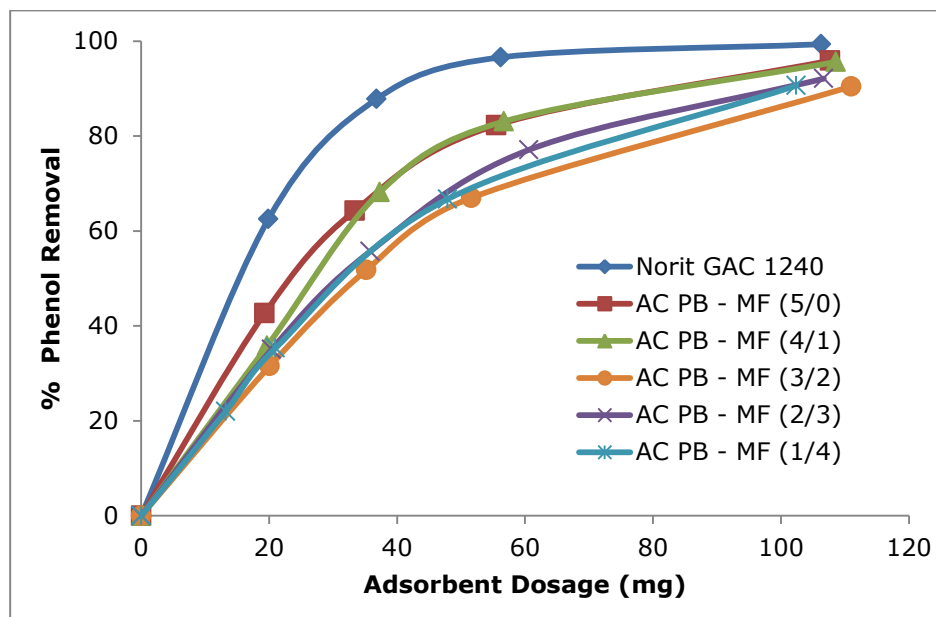


Figure 5-3: Effect of adsorbent dosage (1 mg/l, 5 mg/l, 10 mg/l, 30 mg/l, 50 mg/l, 80 mg/l and 100 mg/l activated carbon; 50 ml of a 100 mg/l unbuffered phenol solution)

The effect of the adsorbent dosage on the phenol removal against a commercial AC (Norit GAC 1240) is shown in Figure 5-3. It can be seen that the performance of AC PB – MF (5/0 & 4/1) are similar but somewhat lower than the commercial AC. At an adsorbent dosage of 0.1 g, phenol removal efficiency for all the produced carbons is higher than 90 %.

When combining Figure 5-3 and Table 5-2 no correlation can be found with the incorporated N. However, samples AC PB – MF (5/0 & 4/1) have an intermediate behaviour in comparison with Norit GAC 1240 and the other activated carbons. This indicates to a nonlinear behaviour with increasing MF. This is probably due to a decrease of surface area by blocking of pores (Drage et al. 2007, Rivera-Utrilla et al. 2011, Seredych et al. 2008).

5.4.4 Economic evaluation base case

Based on the economic model and process design proposed in Chapter 4 the total capital investment is estimated by using the Percentage of Delivered-Equipment cost method and various literature sources. The pyrolysis and activation reactor are calculated as a first plant cost. The total expenditure consists of two parts, namely the operating cost and the yearly interest payments. It is assumed that the investment is financed by means of a loan with a yearly interest of 4.0 %. The operation costs are divided into the following categories: maintenance, insurance, overhead, labour, nitrogen gas, delivered feed, energy and water costs which are generally expressed as a percentage of the total fixed-capital investment for the first three (Kuppens et al. 2010, Thewys & Kuppens 2008) (see also Chapter 4). Table 5-3 provides a guideline for the calculation of the annual operating costs for the all eight items. In this model, a gate fee of 70 EUR/t (Girods et al. 2009a) for processing the PB waste is paid. In Belgium a MF factory pays 220 EUR/t for disposing its waste to a landfill site (including transport). However in this model the cost for MF is set at 0 EUR/t to have a worst case scenario.

NPVs have been calculated for different blends of PB and MF resin waste for a processing capacity of 1 t/h. These different ratios result in different yields (see Table 5-2), different qualities and hence different costs are incurred. The total capital investment and the total expenditure for this facility are displayed in

Table 5-4. The total capital investment is about the same for every facility except for the pure MF resin (PB – MF 0/5). Compared to the predicted values in Chapter 4, the lower char yields (with exception of PB – MF (1/4)) result in a lower total capital investment than predicted in Chapter 4.

Table 5-3: Guideline for calculating the annual operating costs (from ref (Vanreppelen et al. 2011) and Chapter 4)

Annual operating costs	
Maintenance	3 % of Fixed-capital investment
Overhead	2 % of Fixed-capital investment
Insurance	2 % of Fixed-capital investment
Labour costs	labour costs = Total staff members (rounded up) * 55 kEUR/year Total staff members = 1,04 * $([1 + Y_{Char}] * Q_{feed\ input\ pyrolysis})^{0,475}$ * 3 shifts
Delivered feed cost	dependent on the mix ratio
Water	per ton input material 15 m ³ with a price of 1.5 EUR/m ³
Energy	
- Power	1 t/h facility the electricity consumption is 160 kW with a price of 0.0725 EUR/kWh
- Heat	provided by combustion of the gases
Nitrogen gas	8 kg nitrogen gas per ton input material a cost of 2.5 EUR/kg

There is a very small difference in the sum of the operating costs and the yearly interest payments for all the ratios. Due to the gate fee from the delivered feed, the total expenditure cost decreases with a decrease of MF in the mixture. The total expenditure is similar to the total investment cost and is lower than predicted with exception of the PB – MF (1/4) ratio. The corresponding NPVs for selling prices between 1 kEUR/t and 4.5 kEUR/t are presented in Figure 5-4. The minimum selling price (NPV = 0 EUR) of the produced AC can be found in Figure 5-4 and

Table 5-4. Figure 5-5 shows the discounted cumulative cash flow of an AC production facility operating at 1 t/h and a selling price of 2.5 kEUR/t. With increasing share of MF the minimum selling price increases from 1.6 kEUR/t until 3.9 kEUR/t. Girods et al. (2009a) estimated the selling price of AC from PB (N-content 1.5 wt% - 2 wt%) to be around 2.0 kEUR/t. They state that by optimising their activation conditions a higher N-content could be obtained and hence yield a higher quality (better adsorption properties) and thus yield a higher value.

Table 5-4: Total capital investment, annual expenditure and minimum selling price for the production of AC

	0 MF - 5 PB	1 MF - 4 PB	2 MF - 3 PB	3 MF - 2 PB	4 MF - 1 PB
Total capital investment	10,420 KEUR	10,503 KEUR	10,572 KEUR	10,455 KEUR	10,605 KEUR
Expenditure					
→ Gate fee delivered feed	490 KEUR	392 KEUR	330 KEUR	196 KEUR	98 KEUR
→ Operating cost + yearly interest	1,581 KEUR	1,586 KEUR	1,589 KEUR	1,573 KEUR	1,579 KEUR
→ Total	1,091 KEUR	1,194 KEUR	1,295 KEUR	1,377 KEUR	1,481 KEUR
Minimum selling price	1.6 KEUR/t	1.8 KEUR/t	2.0 KEUR/t	2.6 KEUR/t	3.9 KEUR/t

Vanreppelen et al. (2011) expect that optimized AC from PB could yield a selling price of maximum 2.5 kEUR/t. When looking at Figure 5-4,

Table 5-4 and Figure 5-5 in the interval 2.0 kEUR/t- 2.5 kEUR/t only the ratios where the share of PB is greater than the share of MF are profitable. For example the pure PB would yield a NPV of the cash flows of 3.6 MEUR - 8.4 MEUR when the product is sold at a price of 2.0 kEUR/t and 2.5 kEUR/t respectively. The payback time for this AC production facility is 11 and 7 years respectively.

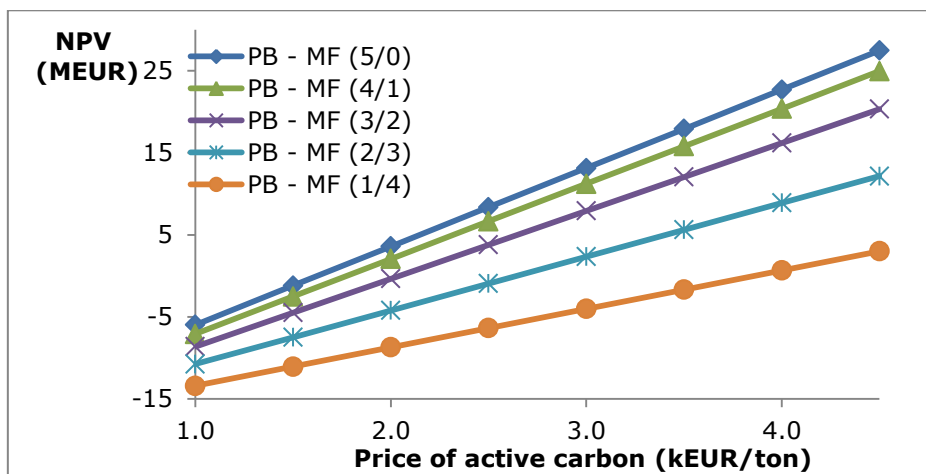


Figure 5-4: NPV for a 1 t/h production facility

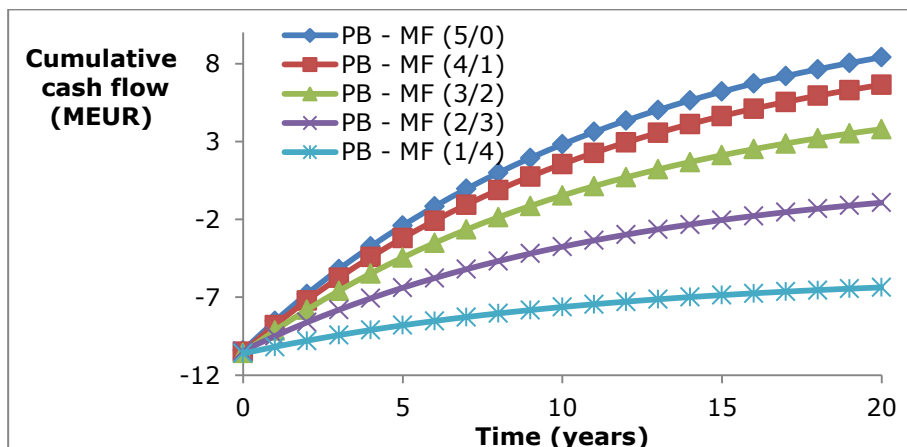


Figure 5-5: Payback time for a 1 t/h production facility at a selling price of 2.5 kEUR/t

5.4.5 Economic impact of the gate fee for MF

By combining the previous economic analysis, the AC yields from Table 5-2 and the preliminary phenol adsorption test (Figure 5-3) one could argue that it is only useful to study the pure PB. Moreover, the possible gate fee from the MF waste needs to be considered. The minimum gate fee for MF waste needs to be calculated to match at least the NPV of AC from PB (3.6 MEUR at a selling price of 2.0 kEUR/t).

When a gate fee of 180 EUR/t is paid for processing the MF waste, the PB – MF (4/1) mix ratio is economical at least equally attractive as the AC from pure PB. Taking the landfill cost into account, a MF production facility is already satisfied to pay less than 220 EUR/t. In addition two waste streams are reused and so the value of the AC production facility is enhanced.

5.4.6 Economic impact of the nitrogen content

Recent literature (Budaeva & Zoltoev 2010, Girods et al. 2009a, Seredych et al. 2009, Vanreppelen et al. 2011) states that nitrogen incorporation is a key parameter for the adsorption properties of AC, especially for the removal of acid gases and phenolic compounds. Such a nitrogenised AC could yield a very high selling price (as high as 4 kEUR/t– 6 kEUR/t) as discussed in Chapter 4 (published as Vanreppelen et al. (2011)). When looking at the N incorporation (Table 5-2) in the produced AC, high N-contents have been achieved. Analysing the phenol adsorption test at low phenol concentration (see Figure 5-3), these high N-content carbons perform somewhat lower than the commercial AC.

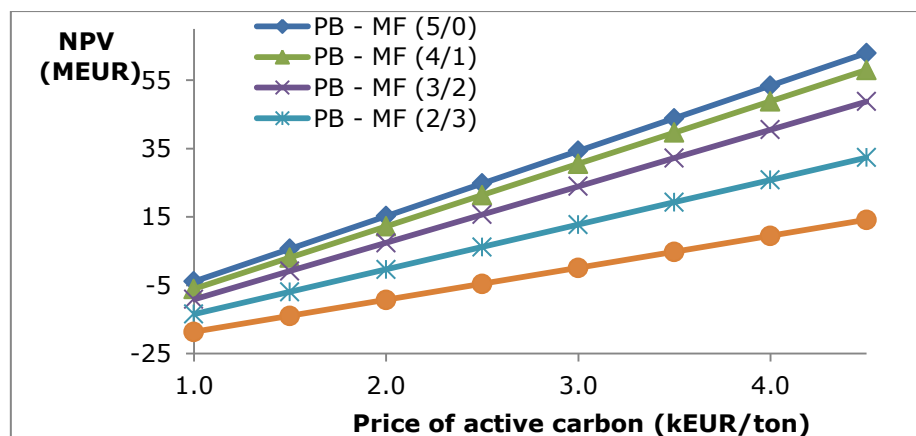


Figure 5-6: NPV for a 2 t/h waste processing facility

Nevertheless, at higher phenol concentrations better performances and thus a higher value could be obtained according to Girods et al. (2009a). It is thus necessary to further investigate other concentrations, target molecules, char characteristics and activation routes to judge thoroughly the economic feasibility of the different mixing ratios.

5.4.7 Economies of scale

Another important factor determining the profitability of the process is the processing capacity. As a consequence of the economies of scale, which are incorporated in the total equipment cost equation, doubling the processing capacity augments the total capital investment with only 57%. The total expenditure with only 36 % to 53 % and the break-even selling price decreases on average with 22.5 % to 25.9% (compare Figure 5-4 [1 t/h] with Figure 5-6 [2 t/h]).

5.4.8 Monte Carlo Sensitivity analysis

The economic viability of the AC production facility, i.e., the calculated NPVs, is also dependent on the accuracy of the predicted variables of the base case. Nevertheless some of these values are uncertain by definition, additionally other variables might strongly influence the NPV if their value changes slightly.

In order to investigate the effect of possible changes of the variables on the NPV a Monte Carlo Sensitivity analysis is performed. Ten variables are selected and listed below:

- Total Capital Investment
- Electricity Cost
- Water Cost
- Delivered feed cost
- Discount rate
- Liquid nitrogen cost
- Char output
- AC output
- Staff cost / shift
- Annual working hours facility

The selected variables are now allowed to change with 10 % above or below their initial value following a triangular distribution (characterized by a most likely, a minimum and a maximum value). Monte Carlos simulation calculates numerous (10,000 per ratio) NPVs, for which in each run of the simulation a random value for each variable is drawn from the triangular distribution.

The minimum selling prices in order to guarantee a 95 % chance on a positive NPV are calculated from the NPVs distributions. This distribution for a 1 t/h processing plant is characterized by the mean with their respective standard deviations as shown in Figure 5-7. In the successive range [PB – MF (5/0) → PB – MF (4/1)] the minimum selling prices are respectively 2.0 kEUR/t, 2.2 kEUR/t, 2.5 kEUR/t, 3.1 kEUR/t, 4.5 kEUR/t. These are somewhat higher than defined in the base case (

Table 5-4). The results indicate that in the 2.0 kEUR/t to 2.5 kEUR/t price range no supplementary ratios are rejected compared to the base case. At the expected selling price of 2.0 kEUR/t only the AC produced from pure PB is profitable in order to guarantee a 95 % chance on a positive NPV. The mean NPV calculated for the Monte Carlo simulation at this price is 3,5 MEUR.

Nevertheless, the same considerations (gate fee, N-content and economies of scale) as in the base case need to be taken into account to analyse these results.

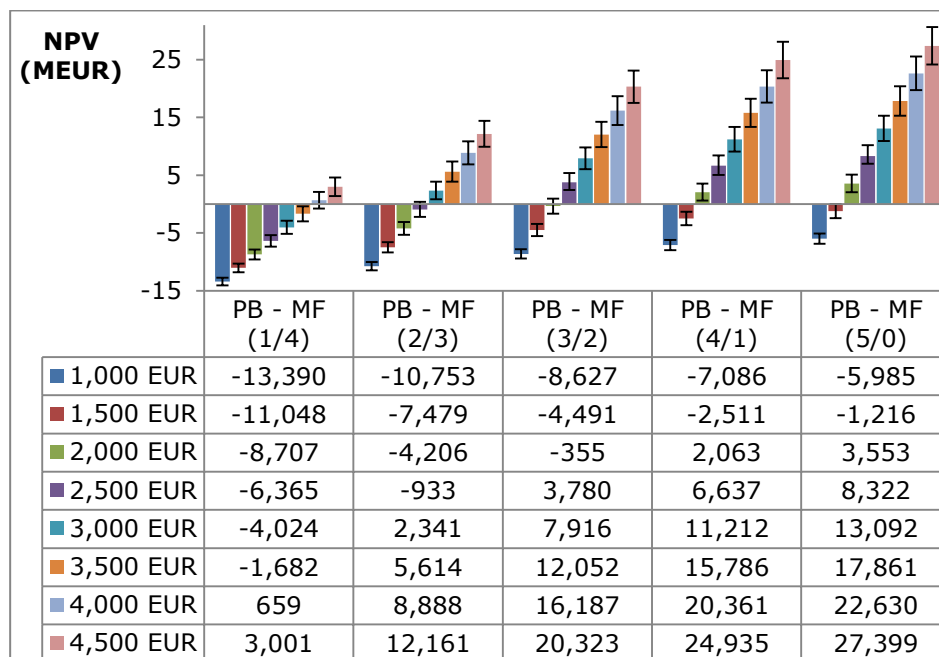


Figure 5-7: NPV distribution

Finally, the average sensitivity of the NPV (normalized by the standard deviation of the output and the standard deviation of the input as defined in Vanreppelen et al. (2011)) (Figure 5-8) to the ten selected variables is

determined. A positive value means that the NPV increases and a negative value means that the NPV decreases by an increase in the variable. The char and AC yields are almost independent of the ratio and are on average the most determining factors. The total annual hours of production is on average the third most important factor. The sensitivity of this variable increases by an increase of the selling price and by an increase in the share of PB. The Total Capital Investment (fourth most important factor) closely follows the sensitivity of the latter. The sensitivity increases by an increase in the share of MF and decreases as the selling price increases. The other variables have a negative sensitivity and are almost negligible compared to first four variables, except for the discount rate.

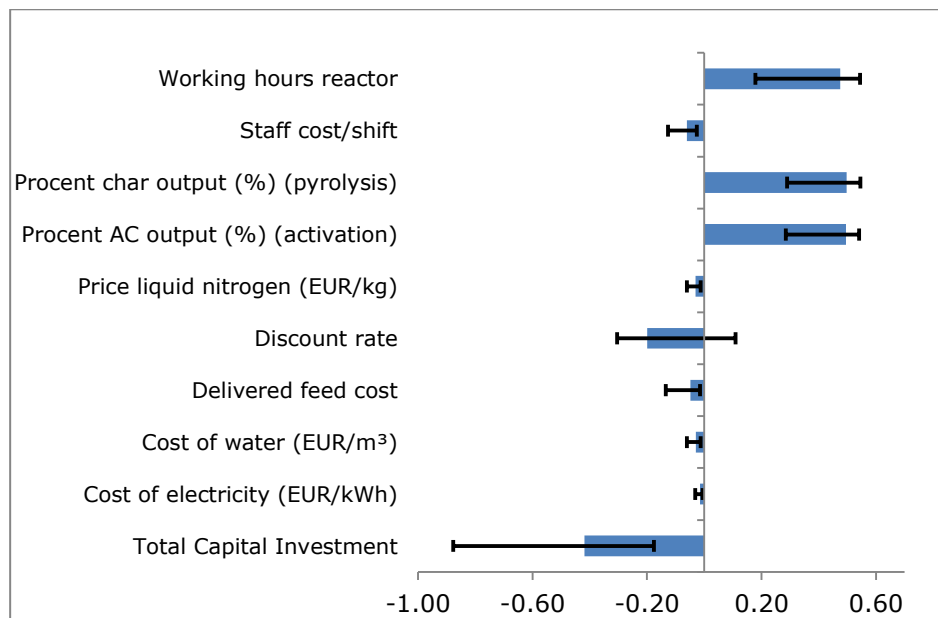


Figure 5-8: Average sensitivity for a 1 t/h processing facility

5.5 Conclusion

To evaluate the feasibility of an AC production facility which processes MF and PB waste, pyrolysis and steam activation experiments have been carried out. Starting from five different blends of PB and MF waste, enhanced activated carbons with a nitrogen content ranging from 2.24 wt% up to 14 wt% are obtained. Pure PB yields the highest amount of AC (22 wt%). The quality of the produced AC (steam activated) is determined by low concentration batch adsorption experiments for the removal of phenol from aqueous solutions (starting from 100 mg/l).

Based on the obtained results and a feasibility model (with a rather pessimistic scenario: e.g., first plant cost) previously developed, really encouraging results are obtained for a profitable production of AC and scaling up the research. However, it is necessary to further investigate other concentrations, target molecules, char characteristics and activation routes to thoroughly judge the economic feasibility of the different mixing ratios and to obtain higher AC qualities.

The economic feasibility depends largely on the annual working hours, char and AC yield, the product quality and the total capital investment.

6 Waste particle board as a renewable source for the production of activated carbon

The results obtained from the preliminary techno-economic analysis in chapter 4 and the screening of the activated carbon produced from the different blends of particle board and melamine formaldehyde waste in chapter 5 reveal encouraging results for a profitable production. However, despite the possibilities of developing a specialty activated carbon from blends of particle board and melamine formaldehyde, experiments were not continued based on the lower phenol adsorption capacity (see section 5.4.3). However, this does not exclude possible profitable (specialty) applications such as electric double layer capacitors, specialty sorbents, ...

During the research, the choice was made to develop activated carbons from particle board glued with urea formaldehyde and urea melamine formaldehyde as it is expected to be useful in a broader range of adsorption applications.

The results of this chapter will be submitted for publication.

6.1 Abstract

Nitrogenised activated carbon prepared from particle board samples glued with aminoplast adhesives (urea formaldehyde or melamine urea formaldehyde), are investigated for the removal of phenol from aqueous solutions. Several activated carbons are prepared under different pyrolysis and steam activation profiles, to develop different carbons with well-developed porosity characteristics. Yields between 9 and 20 wt% are obtained. Based on a preliminary phenol adsorption experiment six activated carbons are selected for further characterisation by N₂ adsorption/desorption (BET surface area between 794 and 1656 m²/g), x-ray photoelectron spectroscopy, acid/base character, point of zero charge (12.21 – 12.82) and elemental analysis (nitrogen contents between 0.96 – 1.73 wt%). Phenol adsorption experiments in function of several environmental conditions and variables like solution pH, ionic strength, temperature and a standard fresh water medium in comparison with two commercial carbons are investigated.

Kinetic data are determined in batch and dynamic adsorption mode. The equilibrium isotherms are described by the non-linear Langmuir and Freundlich models, revealing adsorption capacities of minimum 116 mg phenol per g activated carbon. The kinetic (pH monitored) results are fitted using the pseudo-first and pseudo-second order model. The results give insight on the adsorption mechanism with the in-situ formation and adsorption of phenolate revealing favourable fast adsorption rates.

6.2 Introduction

Today's economic system is based on the linear "take-make-consume-dispose" model which relies on large quantities of easily accessible resources. Natural resources, underpin the global economy and our quality of life. If current trends continue, the global population is expected to grow by 30 % to around 9 billion people by 2050 (European Commission 2011). Even the most conservative projections for global economic growth for the next decade suggest that the demands for coal, oil, iron ore and other natural resources will rise by at least a third (Ellen MacArthur Foundation 2013). In order to cope with the resulting increasing environmental pressure and rapid depletion of resources, resource efficiency and a shift towards a circular biobased economy will be key to securing growth and jobs. One part of the transition to a more circular economy is turning today's waste into a resource.

In this research a renewable alternative input stream, which fits in a circular biobased economy, for the production of nitrogenised activated carbon is searched. In normal conditions the amount of nitrogen is negligible in activated carbons produced from normal input streams like virgin wood, coconut and coal. However, results have demonstrated that nitrogen incorporation is a key parameter for the adsorptive properties of activated carbon (Bandosz 2009, Bandosz & Ania 2006, Rivera-Utrilla et al. 2011). The introduction significantly increases the surface polarity and acid/base properties (basic surface groups) of the resulting activated carbon. In contrast to oxygen groups, nitrogen surface groups are not formed spontaneously on the surface of carbons by contact with air. They have to be introduced in some way, during the production process or by the raw material itself.

The use of waste particle board (PB) is seen as a solution which fits both worlds. In this wood material every fibre is impregnated by urea formaldehyde (UF) or melamine urea formaldehyde resins (MUF) (abbreviated as PBUF and PBMUF respectively) which provide a source of nitrogen. As every product, particle board has a limited service life. Garcia & Freire (2014) estimated the average service life to be around 10 years for

wood-based panels. Reuse of this material is often limited due to the harsh environments where particle boards have been used (BFM 2004, Harwell 2010). Also recycling of the panels is not endless as the size of the wood particles often is reduced and these particles are getting dirty. For example, the use of reject panels and off-cuts for the production of new particle board panels is usually less than 5 % because of the desired chip geometry and the final panel properties (Wrap 2007). The world production of particle board in 2013 was 99.28 Mm³, with Europe (47.7 %) as major producer followed by America (34.6 %) and Asia (15.5 %) (FAOStat 2015).

The objective of this research is dual. The first objective is the preparation and characterisation of activated carbons from particle board samples glued with urea formaldehyde and melamine urea formaldehyde. The second objective is to investigate the adsorption properties of the prepared activated carbons for phenol from aqueous solution in function of different parameters like time, temperature, ionic strength and pH. During all experiments the pH change of the solution is measured to reveal the adsorption mechanism.

6.3 Methods and materials

Two different particle board samples: i.e., water-resistant particle board (glued with MUF) and standard particle board (glued with UF) were obtained as panels. The panels have been sawn to strips of 1 cm and then cut (≤ 2.0 mm) with a high-speed rotary cutting mill (Retsch SM 100). For the thermogravimetric, moisture, ash and ultimate characterisation of the input materials particle size was further reduced by milling (≤ 0.25 mm) with a IKA Werke Yellow Line A10 mill.

An overview of the experimental approach and strategy is shown in Figure 6-1.

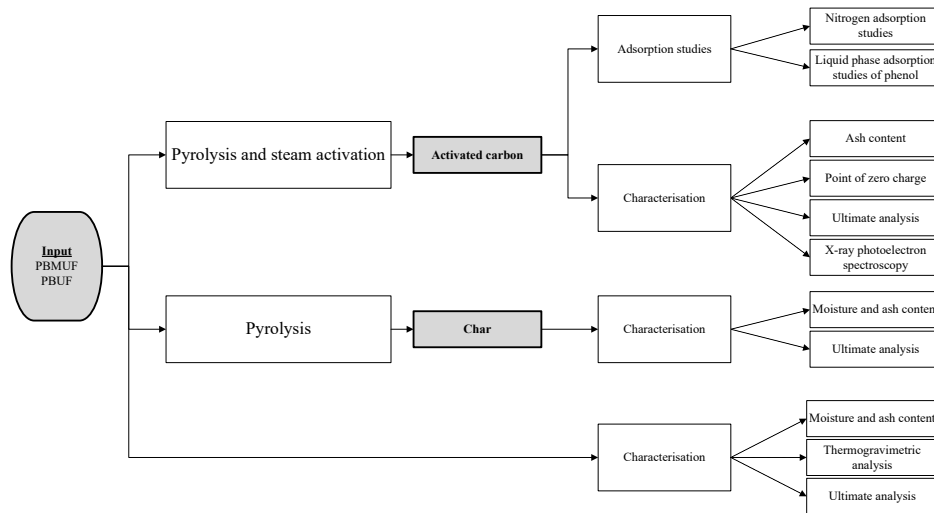


Figure 6-1: Experimental approach and strategy for the production and characterization of activated carbons from particle board

The moisture content of the samples is determined according to ASTM E 1756 – 01 by oven drying at a temperature of 105 ± 3 °C until constant weight. ASTM E 1755 – 01 is applied for the determination of the ash content by dry oxidation at 575 ± 25 °C for a minimum of 3 h. Both methods are performed in quadruplicate. TGA is performed using a DuPont Instruments 951 Thermogravimetric Analyser. About 10mg of sample is weighed into a quartz crucible. The sample is heated with a heating rate of 10 °C/min from room temperature (RT) to a pre-set temperature under nitrogen atmosphere (80 ml/min) to 900 °C. At 900 °C, an isothermal period of 10 min is applied and the gas-flow is switched to oxygen atmosphere (80 ml/min). Ultimate analysis (EA) is used to determine the CHNS- and O-content (wt%). Around 3 mg of a (dry) sample is introduced into a tin container (for CHNS-determination). The instrument is calibrated using BBOT (2,5-bis (5-tert-butyl-benzoxazol-2-yl) thiophene). All samples are analysed in quadruplicate by a Thermo Electron Flash EA1112 elemental analyser of Thermo Electron Corporation for CHNS. O-content is calculated by difference as: $O = 100\% - (C + H + N + S + \text{ash})$. Pyrolysis and steam activation are executed with the semi-continuous home-built pyrolysis reactor manufactured in stainless steel (AISI 304) which is discussed in more detail in Chapter 3. To achieve as much similarity as possible with industrial activated carbon production process, input materials are used as described in Section 2.1. Prior to heating, the reactor and input materials are flushed by N_2 -gas (80 ml/min) to guarantee an oxygen poor environment. Chars are produced by heating the samples at 10 °C/min up to the desired temperature of 800 °C or 850 °C followed by an isothermal period of 30 min

under N₂-atmosphere (80 ml/min). Activated carbons are produced by heating the samples at 10 °C/min up to the desired temperature of 800 °C or 850 °C followed by an isothermal period of 30 or 45 min under steam atmosphere (by introduction of different known quantities of water into the reactor). The different pyrolysis and activation routes are displayed in Figure 2-2. The produced gasses exit the reactor and are burned in the flame of a Bunsen burner.

In a screening assay the produced activated carbons along with the reference activated carbon are evaluated as potential sorbents for the phenol. 20 mg of sorbent is added to 25 ml unbuffered phenol solution (prepared in Milli-Q water without pH adjustment). After a contact time of 24 h (shaking) in a water bath (25 °C), residual concentration is determined as described further in this section. The three best performing activated carbons are selected from each particle board sample for further analysis.

The ash content is determined by dry oxidation at 575 ± 25 °C for a minimum of 3 h and performed in quadruplicate (ASTM E 1755 - 01). The point of zero charge (pH_{PZC}) is estimated by a modified mass titration of Noh & Schwarz (1990). 2.0 g AC was put in 20 ml 0.1 M KNO₃ solution in a closed vessel. After 24 h shaking in a thermostat shaker, the equilibrium pH values of the mixtures were measured electronically (calibrated combined pH electrode) and the limiting pH was taken as the pH_{PZC}. To determine the number of basic and acid groups, 200 mg AC was put in contact with 25 ml 0.100 M HCl or NaOH solution respectively. Titration is done with 0.100 M NaOH or HCl in a nitrogen atmosphere by a Metrohm 794 Basic Titrino (based on Velghe et al. (2012)). Elemental analysis (EA) is performed in quadruplicate for CHNS-content. X-ray photoelectron spectroscopy (XPS) measurements are performed to determine the carbon, nitrogen and oxygen functionalities on the surface of the activated carbons. Experiments are performed using an XPS customized SPECS system (XPS Microlab 350) with monochromatic Al K α (1486,74 eV) X-ray radiation set at 175 W and 14 kV. The atomic concentrations were calculated from the photoelectron peak areas, using Shirley background subtraction. Deconvolution of the main peak of the C1s, N1s and O1s spectra is performed by an iterative least-square fitting algorithm. Chemical structural assignments of each component were made taking into account the binding energies reported by Lorenc-Grabowska et al. (2012), Zhou et al. (2007), Arrigo et al. (2008). Experiments are performed by the Mazovian Centre for Surface Analysis, Institute of Physical Chemistry' Polish academy of sciences, Poland. The BET surface areas, total porosity volume (V_T), micropore volume (V_{mic}) and mesopore volume (V_{mez}) are analysed by nitrogen (77 K) adsorption using an Autosorb AS-1 from Quantachrome. Before analysis the samples are outgassed for 16 h at 200 °C in high vacuum. Experiments are performed by

'Department Chemistry', Laboratory for Adsorption and Catalysis, University Antwerp, Belgium. The specific surface area of the activated carbons is estimated by the Brunauer, Emmett and Teller (BET) gas adsorption method (Brunauer et al. 1938). The micropores are characterised by the Dubinin – Radushkevich method (volume micropores V_{DR}) and the t-plot method using the De Boer method (micropore surface S_{micro} and extremal surface S_{ext}). By using the Dubinin – Radushkevich method the characteristic adsorption energy (E_0) can be estimated. The average micropore diameter (L_0) is calculated using the Stoeckli equation. The total mesopore volume is estimated by converting the adsorbed volume of nitrogen at a relative pressure of 0.96 into the equivalent liquid volume at 77K. The mesopore volume is then estimated by subtracting the micropore volume (V_{DR}) from the total pore volume.

The batch phenol adsorption on the selected activated carbons against two commercial activated carbons (Filtrisorb F400 and Norit GAC 1240) is evaluated by introducing 25 ml of a 100 ppm (initial concentration C_0) unbuffered phenol solution with different quantities of activated carbon (5, 10, 20, 30, 40, 60 and 100 mg) in a hermetically closed flask. Analytical grade phenol and Milli-Q water (18.2 M Ω /cm conductivity) is used. The flasks are placed in a thermostatic water bath (25°C) and shaken for 24 h. It is assumed that equilibrium is reached in this time period. Each experiment was done in quadruplicate. In this work the equilibrium data are fitted by two two-parameter models: the Langmuir and Freundlich model (discussed in Section 1.3.4.1.). The adsorption kinetics are investigated (in duplicate) by varying the contact time from 0.5 h – 24 h in the batch adsorption mode using 25 ml of a 100 ppm unbuffered phenol solution with 50 mg of AC. The amount of phenol adsorbed in the corresponding time interval (q_t) is calculated by Eq. 2-2 and fitted (using the pseudo-first-order model and the pseudo-second-order model. The theoretical background is discussed in Section 1.3.4.3. The effect of pH on the phenol adsorption is studied (in triplicate) by introducing 20 mg AC in 25 ml of a 100 ppm phenol solution and varying the pH of the phenol solution in the range of (0.5 – 13.5) by introducing appropriate amounts of HCl or KOH respectively, additionally maintaining the ionic strength at 0.1 M by adding various amounts of KCl. The hermetically closed flasks are shaken for 24 h in a thermostatic water bath (25 °C). To study the effect of the ionic strength on the phenol adsorption five different phenol solutions are made with varying concentrations of KCl (0, 0.001, 0.01, 0.1 and 1 M). 25 ml of these solutions are added to 20 mg AC, after 24 h shaking in a water bath (25 °C). The experiments are performed in triplicate. To investigate the phenol adsorption in a more realistic water medium, a reconstituted standard water based on ISO 6341, representative of those generally occurring in the environment, is made using *“OECD series on testing and assessment number 29: Guidance*

document on transformation/dissolution of metals and metal compounds in aqueous media". The chemical composition of the reconstituted standard water (for tests carried out at pH 8) is as follows: NaHCO₃ 65.7 mg/l, KCl 5.75 mg/l, CaCl₂·2H₂O 294 mg/l, MgSO₄·7H₂O 123 mg/l. The solution is air buffered at pH 8 in which the concentration of CO₂ provides a natural buffering capacity sufficient to maintain the pH within an average of ± 0.2 pH units over a period of one week (OECD Environment 2001). A 100 ppm phenol solution is made with this water and added to 20 mg AC. After 24 h shaking in a water bath (25 °C) the residual phenol concentration is determined. The experiments are performed in triplicate.

After the assigned adsorption time the solutions are filtered and the residual phenol concentration (C_e) is analysed using a Pharmacia Biotech Ultraspec 2000 UV-VIS spectrophotometer at 270 nm and the pH is measured. Calibration is carried out using a number of phenol standard solutions (concentration range: 1 ppm, 5 ppm, 10 ppm, 30 ppm, 50 ppm, 80 ppm and 100 ppm) and a correction factor is determined for each pH value to counteract the lower adsorption due to the dissociation of phenol in the solution (discussed in detail in section 6.4.1). Milli-Q water, subjected to a similar procedure as the unknown samples are used as blanks and adsorbent-free controls are run in parallel. Once C_e is determined the amount of phenol adsorbed on the AC at equilibrium can be calculated using Eq. 2-1.

Dynamic phenol adsorption and effect of temperature are monitored by a home-build thermostatic slurry batch reactor connected with a computer controlled Pharmacia Biotech Ultraspec 2000 UV-VIS spectrophotometer (Figure 2-3). 100 mg of adsorbent is weighted and placed in a double walled vessel with 50 ml 100 ppm phenol solution. The slurry is agitated by means of an IKA RW20 overhead stirrer fitted by a Screw Type Stir Element at 150 rpm. By means of a glass fritted filter a stream of filtered solution is withdrawn with a Heidolph pumpdrive 5001 peristaltic pump (set at 35 rpm) to a home-build measuring cell (Quartz, path length 2.3 mm) mounted in a computer controlled UV-VIS spectrophotometer. The absorbance of the solution is measured at 270 and 286 nm every minute and stored using a home-made LabView programme. The liquid is transferred back to the slurry reactor. The measurements are performed in twofold at a temperature of 15, 20, 25 and 30 °C.

6.4 Results and discussion

6.4.1 Characterisation of the particle board samples

Both particle board samples (glued with urea formaldehyde: PBUF; glued with melamine urea formaldehyde: PBMUF) are analysed thermogravimetrically to gain a better understanding of their pyrolytic behaviour (See Figure 6-2). The initial weight losses (20 – 200 °C) of 3.6 wt% and 7.1 wt% for PBMUF and PBUF respectively. They are due to the loss of fixed moisture and the start of decomposition of extractives. Both samples start to lose their largest weight loss from 200 °C until a temperature of around 380 °C due to the degradation of hemicellulose, cellulose, lignin and resin. The weight loss in function of time in this region is the highest for PBUF. Also a shift of 10 °C of the maximum in the derivative curve of PBMUF versus PBUF is noticed. This is probably due to the superposition of the melamine glue on the decomposition peaks of cellulose and lignin. In the following temperature region the sample glued with urea-formaldehyde (PBUF) is quite stable with a small weight loss in comparison with PBMUF (particle board glued with melamine urea formaldehyde). Based on the results obtained by Devallencourt et al. (1995) and Girods et al. (2008a) the decrease in the case of the particle board glued with melamine urea formaldehyde may be explained by the fact that, the melamine forms cyameluric structures in the temperature range of 410 -525 °C which are integrated in the carbon matrix. With increasing temperature this integrated melamine condensate undergoes extensive degradation leaving weak spots in the carbon matrix which on their turn decompose.

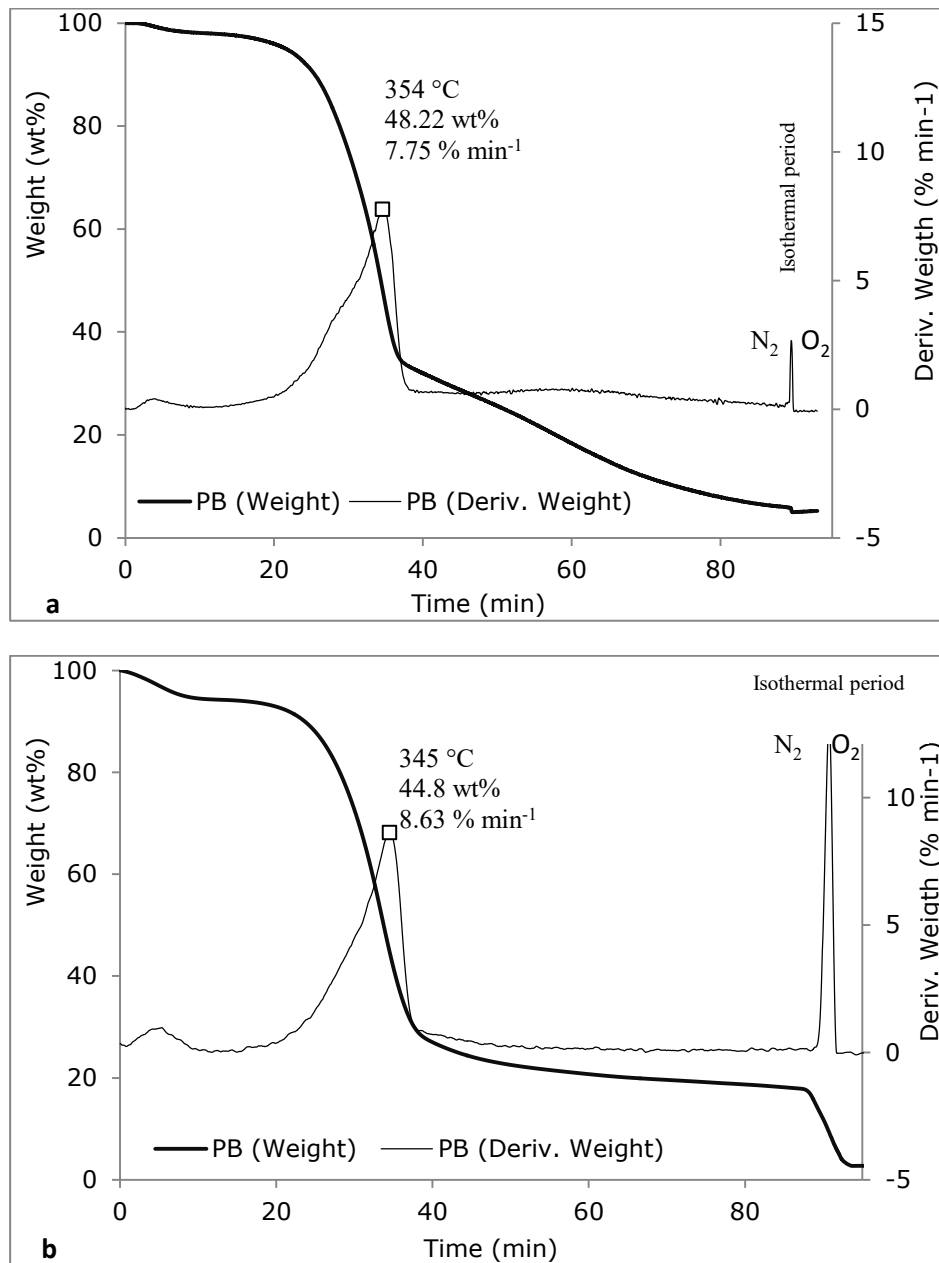


Figure 6-2: Thermo-gravimetric analysis
a) particle board glued with melamine formaldehyde (PBMUF) and
b) particle board glued with urea formaldehyde PBUF

As can be seen from the elemental analysis in Table 6-1 high nitrogen contents of 5.3 and 4.1 wt% are present in the particle board samples. Carbon and oxygen are identified as the main elements of the samples. Both samples have a small ash content of 3.0 and 1.8 wt% while the moisture content of the samples is around 7.3 wt% which is in agreement with the findings (wt%) of Girods et al. (2008a).

Table 6-1: Elemental analysis particle board samples

	PBMUF (wt%)	PBUF (wt%)
%N	5.3 ± 0.6	4.1 ± 0.2
%C	44.9 ± 0.8	50 ± 3
%H	5.9 ± 0.1	6.3 ± 0.4
%S	< DL	< DL
%O*	40.9 ± 0.2	37.7 ± 3.6
Ash	3.0 ± 0.2	1.8 ± 0.1
Moisture	7.6 ± 0.1	7.1 ± 0.1

* **Calculated by difference** %O = 100% – % N – % C – % H – % S – % ash;
< DL = < detection limit

6.4.2 Activated carbon yield

The particle board samples are (undried) pyrolysed after shredding and activated under different temperature and activation profiles as described in section 2.3. The obtained activated carbon and char yields are shown in Table 6-2. It can be seen that the yield of the activated carbons, taking into account the standard deviation and moisture content, are similar for all the experiments except AC...06 where PBUF yields a 30% lower value. Based on the TGA, this was not expected. The char yields obtained in the TGA (Figure 6-2) are for PBUF 18.8 (800 °C) and 18.2 wt% (850 °C) which are ~ 20% lower than the yields in the pyrolysis reactor. For PBMUF the char yields from the TGA experiments are 8.2 (800 °C) and 6.8 wt% (850 °C). These values are significant lower than the obtained yields for the pyrolysis experiments (23.8 and 25.0 wt% respectively). The longer residence times of the evolved gasses, and thus higher amount of secondary reactions in combination with the bigger particle diameters are thought to be a possible explanation. For the activations at a temperature of 800 °C the burn-off increases significantly from 19 to 44 % for PBUF and from 26 to 40 % for PBMUF. Increasing the temperature to 850 °C increases the burn-off of the samples. For PBUF a maximum burn-off of 62 % is achieved. The PBMUF sample yield a burn-off of 52 %.

Table 6-2: Activated carbon yields from particle board samples

			PBMUF		PBUF	
			Yield (wt%)	Burn-off (%)	Yield (wt%)	Burn-off (%)
CH...01	800°C	- ml 30 min	23.8 ± 0.5		24.1 ± 0.4	
AC...01		5 ml 30 min	17.6 ± 0.8	26	19.6 ± 1.2	19
AC...05		10 ml 30 min	16.2 ± 0.4	32	15.5 ± 0.6	36
AC...07		15 ml 45 min	14.4 ± 1.1	40	13.5 ± 2.0	44
CH...02	850°C	- ml 30 min	25.0 ± 0.4		24.0 ± 0.7	
AC...02		5 ml 30 min	17.6 ± 0.4	30	18.0 ± 0.4	25
AC...03		10 ml 30 min	13.3 ± 1.0	47	13.1 ± 1.1	45
AC...06		15 ml 45 min	12.1 ± 1.6	52	9.4 ± 0.5	62

6.4.3 Activated carbon screening for phenol adsorption

In order to evaluate the carbons ability to adsorb phenol a screening of the produced carbons is performed (Table 6-3). The char samples have as good as no adsorption capacity. With increasing activation the adsorption capacity increases. For both samples AC...03, AC...06 and AC...07 yield the highest adsorption capacities and are selected for further investigation.

Table 6-3: Activated carbon phenol adsorption screening assay

			PBMUF	PBUF
			Phenol removal (%)	Phenol removal (%)
CH...01	800°C	- ml 30 min	0.1	0.4
AC...01		5 ml 30 min	50	60
AC...05		10 ml 30 min	53	68
AC...07		15 ml 45 min	61	70
CH...02	850°C	- ml 30 min	0.2	0.2
AC...02		5 ml 30 min	57	67
AC...03		10 ml 30 min	73	75
AC...06		15 ml 45 min	58	72

6.4.4 Correction factor

As phenol (pKa 9.98) is a weak acid, it can dissociate dependent on the solution pH, forming its ionized form namely phenolate. This ability does not only affect the adsorption process, it also has an important effect on its direct UV spectroscopic determination as they have different extinction coefficients. In this research a correction factor based on the solution pH is determined for the direct UV adsorption method to counteract the lower adsorption due to the dissociation of phenol in comparison with the calibration solutions. The molar fraction of phenol and phenolate in function of the solution pH can be calculated by Eq. 6-1.

Eq. 6-1:
$$\frac{C_{phenol}}{C_{phenolaat+phenol}} = \frac{1}{1+10^{(pH-pK_a)}}$$

Using the law of Lambert-Beer, the extinction coefficients (for our system) and Eq. 6-1 the total concentration of phenol and phenolate is determined to yield the same adsorption result as the calibration solution with its specific pH. The fraction of the necessary concentration at a specific pH and the concentration of the calibration solution (pH 6.6) gives the correction factor for every pH as shown in Figure 6-3.

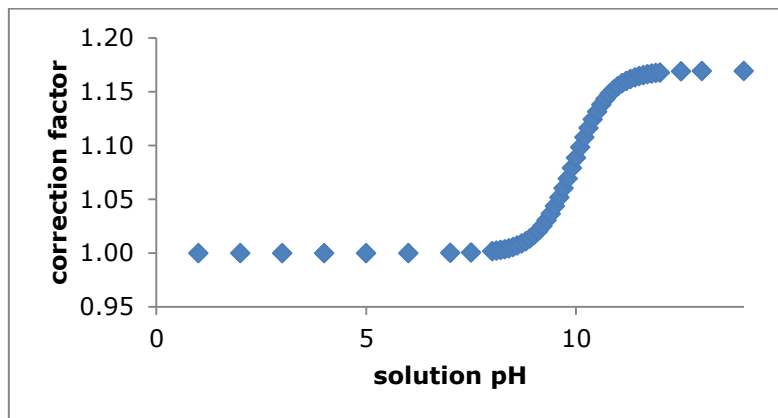


Figure 6-3: Correction factor phenol determination in function of the solutions pH

The correction factor can thus be used to recalculate the measured adsorption to the adsorption which would be measured if the solution pH would match the calibration solution pH. To give a workable result the correction factor is modelled into a second order model (Eq. 6-2, $R^2 = 0.999998$).

Eq. 6-2:
$$\text{Correction factor} = 0.0266 * \left(1 - \frac{1}{1+10^{(pH-pK_a)}}\right)^2 + 0.1425 * \left(1 - \frac{1}{1+10^{(pH-pK_a)}}\right) + 1$$

6.4.5 Activated carbon characterisation*6.4.5.1 Nitrogen adsorption isotherm*

The nitrogen adsorption-desorption isotherms at 77 K for the selected activated carbons are shown in Figure 6-4. Based on the shape of the isotherms and the hysteresis loops qualitative information can be obtained according to the IUPAC classification (Sing et al. 1985). The isotherms are classified as type IV isotherms. This type is given by mesoporous adsorbents where the adsorption in the mesopores is determined by the adsorbent-adsorptive interactions and also by the interactions between the molecules in the condensed state. The initial monolayer-multilayer adsorption on the mesopore walls is followed by pore condensation (where the N₂-gas condenses to a liquid like phase in a pressure less than the saturation pressure of the bulk liquid). The steep initial part of the isotherm ($p/p_0 : 0 - 0.05$) is assigned to micropore filling. The steeper the gradient the narrower the micropores. The second part of the isotherm ($p/p_0 > 0.4$), a gradually increasing build-up with increasing relative pressure is seen. Close to a relative pressure of 1 the amount adsorbed rises steeply. This behaviour is explained by multilayer adsorption and capillary condensation in the mesopores. The presences of a hysteresis loop is also an indication of mesopores in the activated carbons. The hysteresis occurs when the pore width exceeds a certain critical with, which is dependent on the adsorption system and temperature. The adsorption-desorption hysteresis loops are classified as type H4 according to IUPAC recommendations (Sing et al. 1985). This type of hysteresis loop is attributed to adsorption in narrow slit-like pores (Choma & Jariniec 2006). The closure of the hysteresis loop at a relative pressure of $p/p_0 \sim 0.4$ indicates the presence of small mesopores.

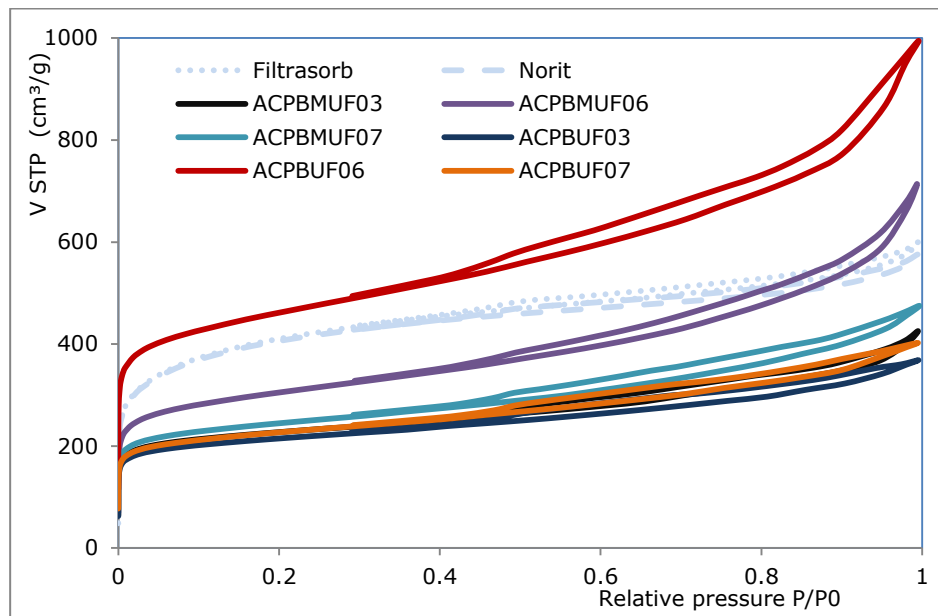


Figure 6-4: Nitrogen adsorption-desorption isotherms at 77 K for the selected activated carbons from particle board

The pore size distribution of the micropores, determined by means of the Density Functional Theory (DFT), is shown in Figure 6-5. The pore size distribution reveals that all carbons exhibit the same distribution. Even the carbons AC...03 and AC...07 differ only slightly, despite their differences in temperature and steam activation, AC...06 yields higher pore volumes. When comparing the two particle board samples, it can be seen that the samples with urea formaldehyde glue (PBUF) exhibit higher mesopore volumes (2.5 – 8.5 nm). The micropore volumes (0.5 – 2.5 nm) are similar except for ACPBUF06 which has a significant higher micropore volume. All samples have four major peaks in the micropores region at 0.98, 1.06, 1.17 and 1.27 nm. In the small mesopore range three major peaks can be seen at 3.67, 4.90 and 5.3 nm.

For effective adsorption the pore size of the adsorbent needs to be above 1.2 (Pelekani & Snoeyink 2000), 1.7 (Kasaoka et al. 1987) times the second widest dimension of the adsorbate or 1.5 – 2 times the adsorbates largest diameter according to Lorenc-Grabowska et al. (2012). With molecular dimensions of 0.57 * 0.43 nm, the obtained pore size distribution results reveal that the produced carbons based on their pore sizes are possible candidates for good phenol adsorption.

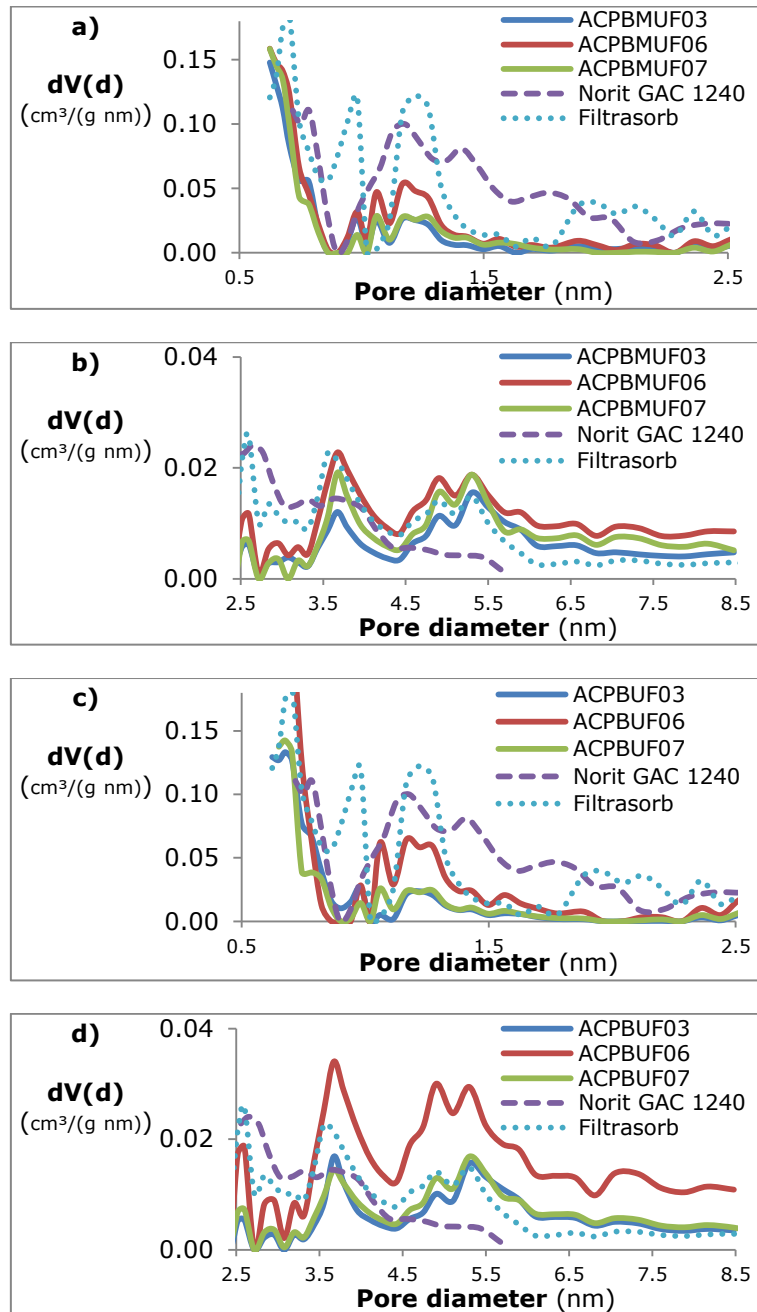


Figure 6-5: Pore size distribution of the activated carbons determined by DFT method for a, b) PBMUF (a: micropores, b: mesopores) ; c, d) PBUF (c: micropores, d: mesopores)

The results of the porosity characterisation are presented in Table 6-4. The specific surface area of the activated carbons is estimated by the Brunauer, Emmett and Teller (BET) gas adsorption method (Brunauer et al. 1938). The micropores are characterised by the Dubinin – Radushkevich method (volume micropores V_{DR}) and the t-plot method using the De Boer method (micropore surface S_{micro} and extremal surface S_{ext}). By using the Dubinin – Radushkevich method the characteristic adsorption energy (E_0) can be estimated. The average micropore (L_0) is calculated using the Stoeckli equation. The total mesopore volume is estimated by converting the adsorbed volume of nitrogen at a relative pressure of 0.96 into the equivalent liquid volume at 77K. The mesopore volume is then estimated by subtracting the micropore volume (V_{DR}) from the total pore volume. The BET analysis reveal good correlation coefficients of more than 0.999 for all samples. All samples have a high surface area starting from 794 and 840 m^2/g for the carbons produced with the lowest activation time (ACPBUF03 and ACPBMUF03). As the activation time increases the **BET surface area** increases. When comparing the samples produced at 800 °C and 850 °C with an activation time of 45 minutes the surface area increases significant. Similar BET and micropore volumes are obtained for the samples 800 °C, 45 min activation and 850 °C, 30 min activation. It is also interesting to see that the carbons from particle board with melamine urea formaldehyde (PBMUF) exhibit higher BET surface areas than those of urea formaldehyde (PBUF) except for the carbon produced at 850 °C, 45 min activation (ACPBUF06). Here a very high BET surface area of 1656 m^2/g (higher than commercial carbons) is obtained. With increasing activation time also the **average micropore surface (S_{micro})** increases for the activated carbons samples from particle board glued with urea formaldehyde. For the ACPBMUF samples the differences in micropore surface are negligible as there is an error of 5 – 10% on the sorption data. Similar or slightly higher **external surface areas (S_{ext})** are obtained for the samples produced at 850 °C, 30 min activation and 800 °C, 30 min activation. When increasing the activation time to 45 min at 850°C (ACPB...06) the external surface area increases significantly. This increase is most profound for the carbons from particle board with urea formaldehyde (~3 times higher). When looking at the micro- and mesopore volume, the V_{DR}/V_{Meso} ratio decreases with increasing activation, indicating that the mesopores gaining a larger contribution to the total pore volume by increasing activation. The latter is also observed in the broadening of the **average micropore diameter (L_0)**. The reference activated carbons exhibit a much larger average micropore width and lower characteristic adsorption energy than the produced carbons. The characteristic adsorption energy decreases with increasing activation of the samples.

Table 6-4: Porosity characteristics: BET analysis (S_{BET}), t-plot analysis for micropore (S_{micro}) and external surface (S_{ext}) based on De Boer, and micropore characterization based on the Dubinin-Radushkevich method (V_{T} , V_{DR} , V_{Meso} , L_0 and E_0)

	S_{BET} (m ² /g)	S_{micro} (m ² /g)	S_{ext} (m ² /g)	V_{T} (cm ³ /g)	V_{DR} (cm ³ /g)	V_{Meso} (cm ³ /g)	L_0 (nm)	E_0 (kJ/mo l)
ACPBUF03	794	422	225	0.528	0.328	0.206	1.1	20.8
ACPBUF06	1656	781	644	1.337	0.683	0.654	1.4	19.3
ACPBUF07	834	499	191	0.582	0.338	0.244	1.2	20.5
ACPBUMF03	840	434	254	0.569	0.341	0.228	1.2	20.5
ACPBUMF06	1096	442	506	0.909	0.453	0.456	1.6	18.3
ACPBUMF07	900	430	317	0.665	0.364	0.300	1.2	20.3
Norit GAC 1240	1468	532	725	0.827	0.599	0.228	2.6	15.5
Filtrisorb F400	1483	833	432	0.859	0.604	0.256	2.6	15.5

6.4.5.2 Surface functionalities

The presence and types of surface functional groups is, combined with the porous texture of carbons, an important factor to be considered in the adsorption of phenols. The surface chemistry of the activated carbons is considered as the main factor in the adsorption mechanism from phenol in aqueous solutions (Moreno-Castilla 2004). It has been shown that activated carbons having a basic nature, reveal an enhanced adsorption capacity towards phenol whatever their textural characteristics are (Girods et al. 2009a). To have an idea of the basic nature of the selected activated carbons, the pH_{PZC} is determined and the basic and acid groups on the AC surface are measured by the acid-base titration method. Table 6-5 reveals very high pH_{PZC} values for the produced activated carbons between 12.21 and 12.82 in comparison with the reference carbons. When comparing the samples between each other, the particle board samples with urea formaldehyde all exhibit higher values. Also with increasing temperature and activation time the pH_{PZC} value increases (AC...07 \rightarrow AC...03 \rightarrow AC...06). This highly basic character is also reflected in the basic and acid groups on the carbon surfaces.

Table 6-5. pH_{PZC} and amount of acid / basic groups mounted on the activated carbon surfaces

	pH_{PZC}	Acid groups (mmol/g)	Basic groups (mmol/g)
ACPBUF03	12.67	0.3850	1.6005
ACPBUF06	12.82	0.6721	1.6777
ACPBUF07	12.76	0.4396	1.6005
ACPBUMF03	12.21	0.6472	1.7379
ACPBUMF06	12.37	0.3968	1.8673
ACPBUMF07	12.28	0.6917	1.5437
Norit GAC 1240	11.76	0.9552	0.4753
Filtrisorb F400	11.54	0.5783	0.4666

The results of the deconvoluted X-ray photoelectron spectroscopy (XPS) spectra of the produced activated carbons are listed in Table 6-6, according to the binding energies reported by Zhou et al. (2007), Arrigo et al. (2008), Li (2012), Pietrzak (2009), Sánchez-Sánchez et al. (2015) and Lorenc-Grabowska et al. (2012).

The C1s signal reveals a carbon content of around 92 at% with a major graphitic carbon peak at a binding energy (284 – 285.6 eV) of around 76 at% for every carbon except for ACPBUF07 which has a contribution of 57 at%. The carbon content increases with increasing temperature and steam activation. Carbon covalently bonded with oxygen and nitrogen in hydroxyl, ether groups, C-N and C=N are also present in high quantities.

The N1s spectra are deconvoluted into five different types of N-containing species. The total amount of the atomic nitrogen concentration on the surface of the activated carbons decreases with increasing production temperature and steam activation (AC...07 → AC...03 → AC...06). In general, most of the surface nitrogen is present as quaternary N followed by imine, amine, amide and pyridinic nitrogen groups except for ACPBUF07 where pyridinic-N-oxide or ammonia groups are the second most abundant groups. The reference carbons in contrast only have a small percentage and only one (quaternary nitrogen for Filtrasorb F400) or two (quaternary nitrogen and pyridinic nitrogen for Norit GAC 1240) nitrogen groups present on their surface namely quaternary nitrogen.

The O1s spectra are deconvoluted into three peaks, which can be attributed to the following functional groups: C-OH, C-O-C, C=O in esters, amides,

Chapter: 6

anhydrides and are the most abundant on the surface followed by chemisorbed O₂ and H₂O. The third peak is attributed to C=O groups on the surface. The total atomic oxygen percentage for the produced activated carbons are higher than that of the reference carbons.

As an example the C1s, N1s and O1s spectra of ACPBUF06 are displayed in Figure 6-6

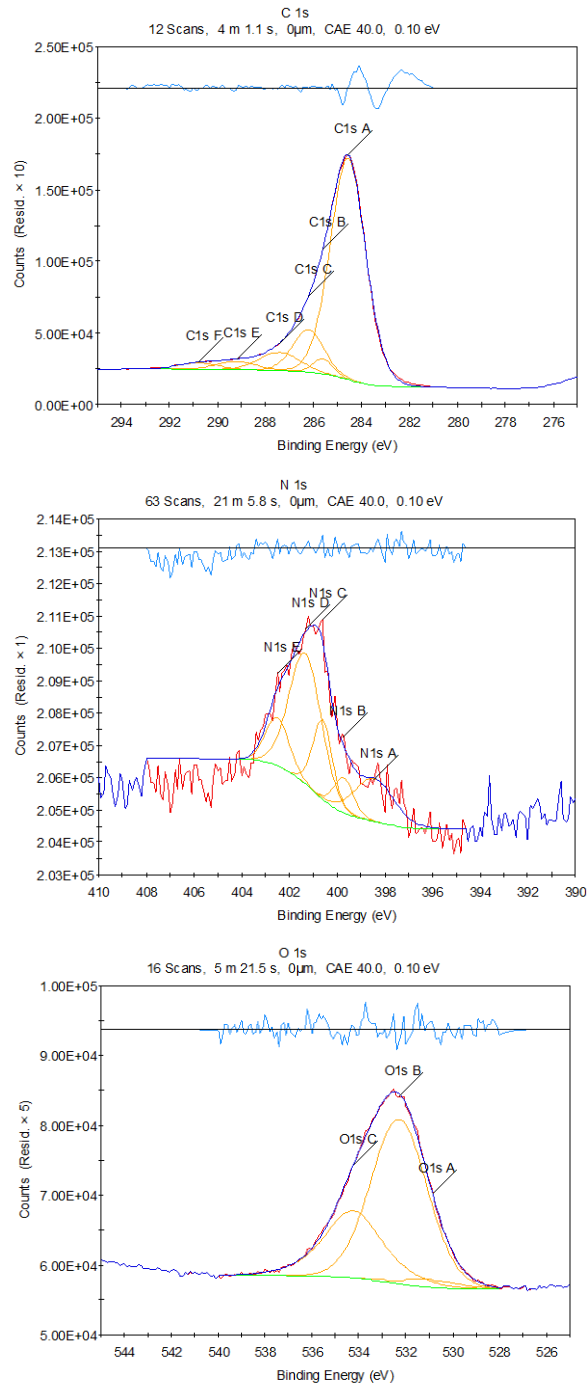


Figure 6-6: C1s, N1s and O1s XPS spectra of ACPBUF06

Table 6-6: Carbon, Oxygen and Nitrogen atomic concentration and the surface functionalities distribution derived from the C1s, O1s and N1s spectra

Binding energy (eV)	Filtrisorb F400	Norit GAC 1240	ACPBMUF07			ACPBMUF06			ACPBMUF03										
			ACPBMUF07	ACPBMUF06	ACPBMUF03	ACPBMUF07	ACPBMUF06	ACPBMUF03	ACPBMUF07	ACPBMUF06	ACPBMUF03								
C surface concentration (at%)																			
C-C (aromatic and aliphatic, $\pi \rightarrow \pi^*$ delocated bondings)	94.53	94	92.32	94.12	90.49	91.42	93.3	92.3	66.31	69.2	17.42	69.06	65.29	67.73	69.17	69.6			
C-C graphitic carbon (located bondings)	0.12	0.63	35.58	2.63	2.73	2.93	2.46	1.98											
Single C-O bond (C-OH, C-O-C, Csp ³) or C=N (aromatic rings), C-N	12.95	10.7	24.1	11.58	10.23	8.32	10.01	9.13											
C=O, C=N, $\pi \rightarrow \pi^*$ shake-up satellite	7.27	7.68	9.75	6.27	6.67	6.56	6.42	6.33											
Carboxyl, ester or N=C-O	3.68	-	2.54	2.6	2.83	2.9	2.76	2.39											
COOR, C=C ($\pi \rightarrow \pi^*$ delocated bondings)	290.3																		
carbonate groups and/or adsorbed CO and CO ₂	291.2	-	2.93	1.98	2.74	2.98	2.48	2.92											

Binding energy (eV)	Filtrisorb F400	Norit GAC 1240	ACPBUF07	ACPBUF06	ACPBUF03	ACPBMUF07	ACPBMUF06	ACPBMUF03
N surface concentration (at%)								
	0.17	0.3	0.55	0.34	0.56	0.99	0.56	0.61
N-6 (pyridinic)	-	0.08	0.07	0.06	0.11	0.26	0.11	0.12
N-5 (pyrrolic and pyridonic)	-	-	0.06	0.03	0.02	0.02	0.01	0.02
Imine, amine and amide	-	-	0.01	0.06	0.17	0.26	0.11	0.18
N-Q (quaternary N in aromatic graphene structure)	0.17	0.22	0.25	0.15	0.17	0.34	0.25	0.22
Pyridinic-N-oxide or ammonia	-	-	0.16	0.04	0.09	0.11	0.08	0.07
O surface concentration (at%)								
	3.95	4.28	6.2	5.01	7.85	6.64	5.1	5.99
C=O	0.62	0.7	0.15	0.15	0.92	1.32	0.33	0.35
C-OH, C-O-C, C=O in esters, amides, anhydrides	-	-	4.53	3.34	5.93	3.98	3.51	4.48
C=O (esters, anhydrides), -OH (alcohols) C-O-C (ethers)	2.16	2.66	-	-	-	-	-	-
Chemisorbed O ₂ , H ₂ O	1.17	0.92	1.52	1.52	1	1.34	1.26	1.16

When looking at the elemental composition of the bulk of the activated carbons (

Chapter: 6

Table 6-7) nitrogen contents between 0.96 and 1.73 wt% are revealed. For the samples glued with melamine formaldehyde (ACPBMUF) the nitrogen content increases while the oxygen content decreases with increasing temperature and steam activation. For the ACPBUF samples, the nitrogen content decreases in favour of the oxygen content. When comparing with the elemental composition of respectively Filtrasorb F400 and Norit GAC 1240, very high nitrogen and oxygen contents are obtained.

Table 6-7. Ultimate analysis (on dry base)

	ACPBUF07	ACPBUF06	ACPBUF03	ACPBUMUF07	ACPBUMUF06	ACPBUMBUF03
% N	1.29 ± 0.04	1.0 ± 0.1	1.2 ± 0.1	1.3 ± 0.1	1.7 ± 0.2	1.4 ± 0.1
% C	84.65 ± 2.64	72.8 ± 2.2	81.6 ± 4.8	76.2 ± 1.7	73.5 ± 2.6	80.5 ± 1.7
% H	1.16 ± 0.10	1.1 ± 0.1	1.0 ± 0.1	0.86 ± 0.01	0.8 ± 0.1	0.9 ± 0.1
% S	< DL	< DL	< DL	< DL	< DL	< DL
% O*	1.17 ± 1.03	5.0 ± 2.3	3.3 ± 2.8	6.1 ± 1.7	2.7 ± 2.5	5.4 ± 1.7
N/C atomic ratio	0.015	0.014	0.015	0.017	0.023	0.017
O/C atomic ratio	0.014	0.069	0.040	0.080	0.037	0.067

* Calculated by difference %O = 100% - %N - %C - %H - %S - %ash;
 < DL = below detection limit; Filtrasorb F400 on a dry base (Velghe et al. 2012): N
 0.7 wt%, C 83.4 wt%, H 0.7 wt%, O 1.4 wt% and 6.2 wt% ash; Norit GAC 1240 on
 a dry base (Vandewijngaerden et al. 2010) N 0.7 wt%, C 87.0 wt%, H 0.4 wt%, O
 2.5 wt% and 9.4 wt% ash

6.4.6 Liquid phase adsorption studies of phenol

6.4.6.1 Kinetics of adsorption

The adsorption of phenol on the activated carbons as a function of time is shown in Figure 6-7. The experimental data were fitted using the pseudo-first-order model (Eq. 1-11) and the pseudo-second-order model (Eq. 1-12).

Eq. 1-11:
$$Q_t = Q_e - Q_e e^{-K_f t}$$

Eq. 1-12:
$$Q_t = \frac{Q_e^2 K_s t}{1 + Q_e K_s t_e}$$

Where Q_e is the equilibrium adsorption capacity (mg/g), K_f (1/h) and K_s (g/mg h) are the pseudo-first-order model and pseudo-second-order model rate constants respectively. The data obtained by the two models are given in Table 6-8.

Table 6-8. Comparison of the pseudo-first-order and pseudo-second-order model by non-linear regression analysis

	Pseudo-first-order			Pseudo-second-order		
	Q_e (mg/g)	K_f (1/h)	R^2	Q_e (mg/g)	K_s (g/mg h)	R^2
ACPBMUF03	43.3	0.988	0.892	47.5	0.0323	0.961
ACPBMUF06	39.5	0.871	0.890	43.4	0.0311	0.959
ACPBMUF07	36.5	1.13	0.858	40.5	0.0412	0.945
ACPBUF03	44.3	1.31	0.924	48.2	0.0425	0.982
ACPBUF06	43.0	2.32	0.927	46.5	0.0764	0.973
ACPBUF07	43.3	1.29	0.923	47.6	0.0390	0.974
Fitrasorb F400	50.1	0.386	0.987	57.2	0.00840	0.988
Norit GAC 1240	50.3	0.520	0.990	56.6	0.0123	0.986

The results show that the kinetic data are better fitted by the pseudo-second order model (higher R^2 values). The K_s values for the activated carbons from particle board are 3 – 6 times higher than those of the reference carbons indicating a much faster phenol adsorption which is also visible in Figure 6-7. Over 50 % of the equilibrium adsorption capacity is reached after 30 minutes (for ACPBMUF06 even 67 %), in contrast to 30 % for the reference carbons (50 % after 1.5 – 2 h).

It is also interesting to see that the carbons produced from particle board have a type IV isotherm behaviour with a small plateau around 1 – 2 hours of adsorption. Figure 6-8 gives an insight between the calculated adsorption

capacities (Q_t) by the pseudo-second-order model and the experimental values.

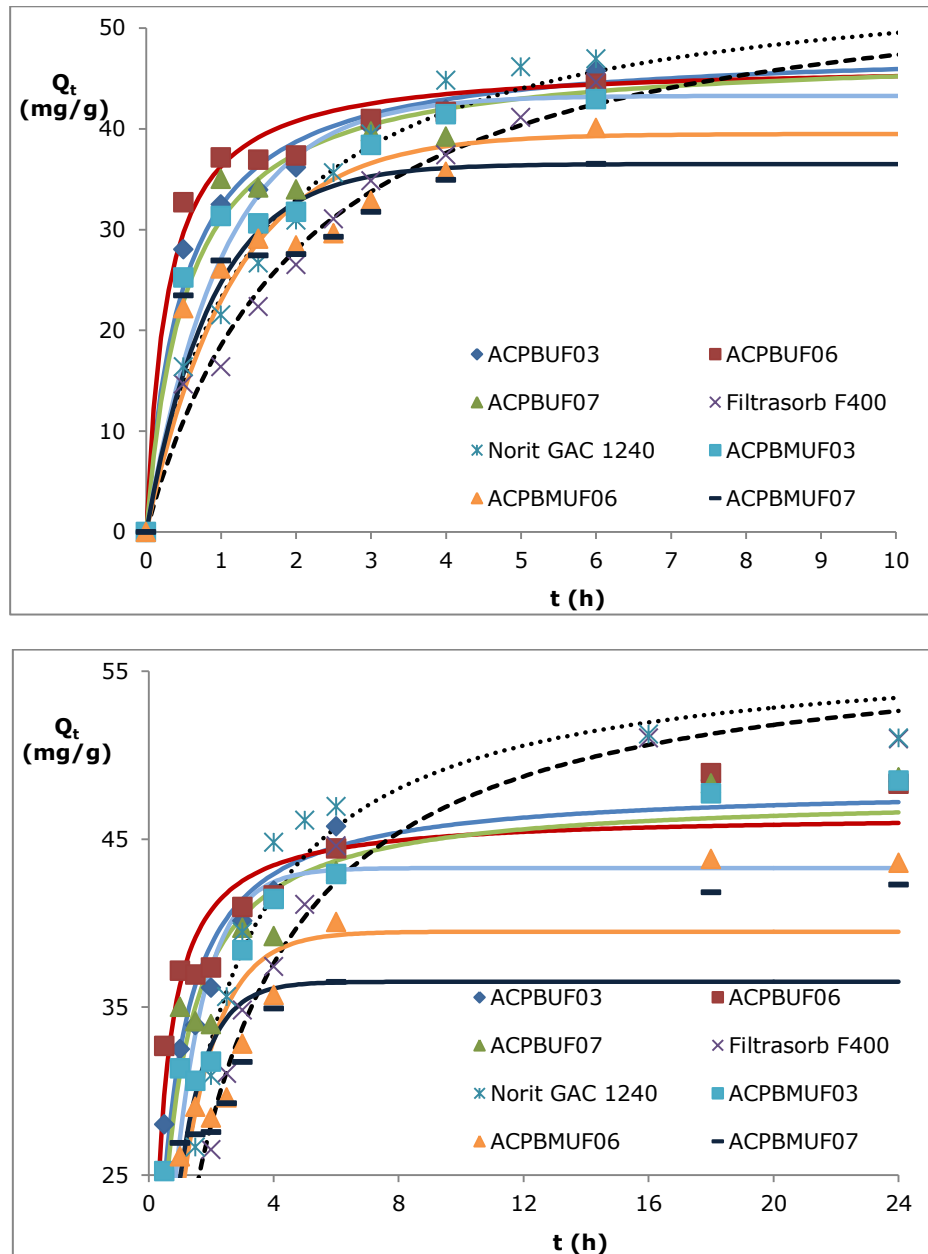


Figure 6-7. Effect of contact time on the phenol removal (Filled and dashed lines refer to the pseudo-second-order model)

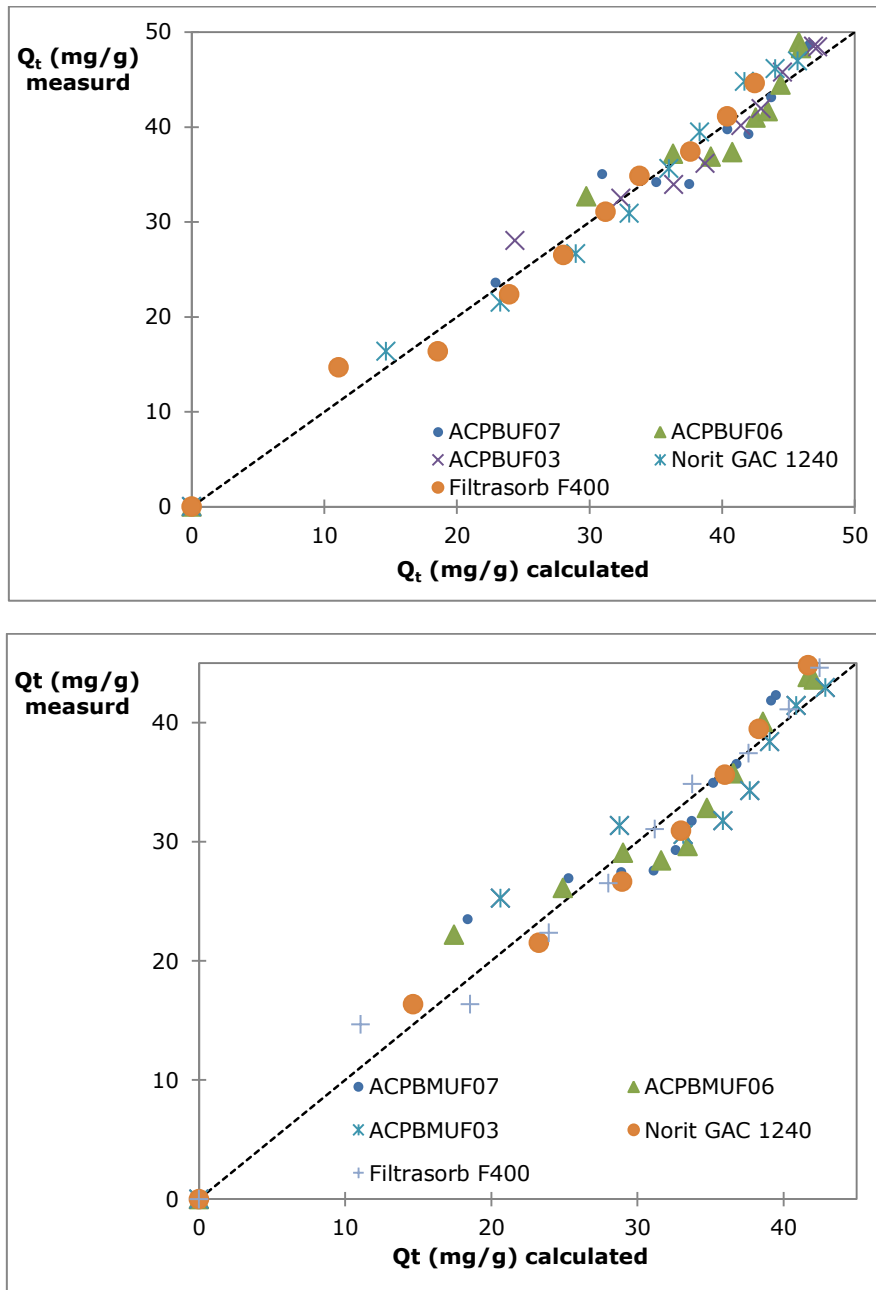
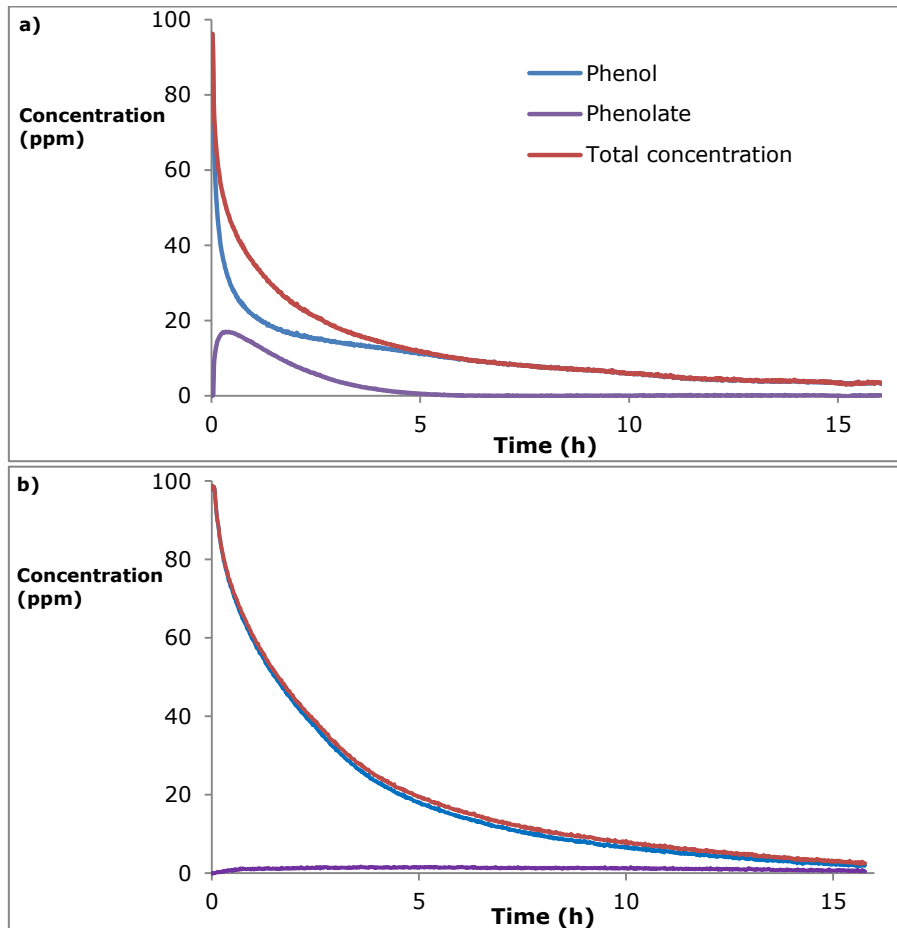


Figure 6-8. Deviation between calculated (pseudo-second-order) and experimental adsorption capacities

6.4.6.2 *Dynamic adsorption experiments*

To gain a better understanding of the adsorption process, the phenol, phenolate and total concentration (phenol + phenolate) and pH are continuously monitored in time. For this purpose a dynamic adsorption module is developed as described in section 2.5.2.4. The developed module also better corresponds to the operations of an industrial slurry reactor (batch). The dynamic adsorption experiments on the activated carbons from particle board (ACPBMUF and ACPBUF) reveal an interesting process going on during the adsorption as shown in Figure 6-9 (ACPBMUF07 is depicted, all produced carbons yield similar observations). The adsorption process is very fast in the initial stage with a rapid decrease of the total phenol concentration. In addition, the introduction of activated carbon induces a fast increase of phenolate. Furthermore, it is observed that the increase of phenolate concentration is lower than the decrease of the phenol concentration. Also the solution pH increases immediately from 6.4 - 6.7 to around 10 - 11 and remains constant at this value over time. After 0.5 h a maximum in phenolate concentration is reached. The decrease in phenol concentration slows down after around 0.5h, which is in contrast to the fast decrease in phenolate concentration. This fast decrease can be explained by the electrostatic attraction of the negatively charged phenolate ions and the positively charged ($\text{pH} < \text{pH}_{\text{PZC}}$) carbon surface at the solution pH. In the third part of the graph a further slow decrease in total concentration is seen. This process (formation of phenolate shown in Figure 6-9) is not observed in case of the reference carbons as the pH of the solution just slightly increases to a pH of around 8 for both Filtrasorb F400 and Norit GAC 1240. Despite this, they have also a high basic pH_{PZC} of 11.7 and 11.5 respectively. When looking further to the surface functionalities (section 6.4.5.2), the observed process could probably be assigned to the high amount of nitrogen and basic groups on the surface of the particle board activated carbons as described in section 6.4.5.2.



**Figure 6-9: Kinetic evolution of the phenol and phenolate concentration with
a) activated carbon from particle board (ACPBMUF07) and
b) reference activated carbons (Norit GAC 1240)**

The results of the dynamic kinetic adsorption are analysed by pseudo-first-order model and pseudo-second-order model respectively. The results in Table 6-9 indicate that the pseudo-first-order model is not able to describe the kinetic data for the activated carbons from particle board with low R^2 . The pseudo-second-order model performs better, however still low R^2 values are obtained (<0.974), indicating that more than 1 process is responsible for the adsorption. The adsorption results of the reference activated carbons are well described by the pseudo-second-order model.

Table 6-9. Comparison of the kinetic constants obtained by non-linear regression analysis of the pseudo-first-order and pseudo-second-order model

	Pseudo-first-order			Pseudo-second-order		
	Q _e (mg/g)	K _s (g/mg h)	R ²	Q _e (mg/g)	K _s (g/mg h)	R ²
ACPBMUF03	43.1	0.671	0.828	46.9	0.0240	0.919
ACPBMUF06	47.3	0.510	0.906	51.9	0.0162	0.964
ACPBMUF07	44.6	1.05	0.880	47.5	0.0390	0.973
ACPBUF03	47.3	0.639	0.903	51.4	0.0207	0.974
ACPBUF06	45.6	0.475	0.872	50.4	0.0149	0.942
ACPBUF07	58.0	0.545	0.877	63.5	0.0139	0.956
Fitrasorb F400	49.8	0.684	0.949	54.2	0.0199	0.997
Norit GAC 1240	46.9	0.388	0.984	53.4	0.0989	0.998

The temperature effect on the adsorption capacity and the mechanism is tested by performing the dynamic test at four different temperatures namely 15, 20, 25 and 30 °C. Based on the results, no increase or decrease in adsorption capacity is noticed by varying the temperature in this range.

6.4.6.3 Adsorption equilibria

The adsorption isotherms for phenol on the produced carbons are shown in Figure 6-10. The equilibrium data (experimental values) are nonlinear modelled with the Langmuir (Eq. 1-8) and Freundlich (Eq. 1-10) equations in order to determine the model parameters.

Eq. 1-8:
$$Q_e = \frac{Q_m K_L C_e}{1 + K_L C_e}$$

Eq. 1-10:
$$Q_e = K_F C_e^{1/n}$$

The results are shown in Table 6-10 and the best fitted model (based on R²; marked with green) is also shown in Figure 6-10. According to the Giles classification, the obtained isotherms belong to the L-type (Langmuir class) (Giles et al. 1960). Implying that the adsorbed molecules are most likely flat adsorbed and/or there is no strong competition with the solvent i.e., water in this case.

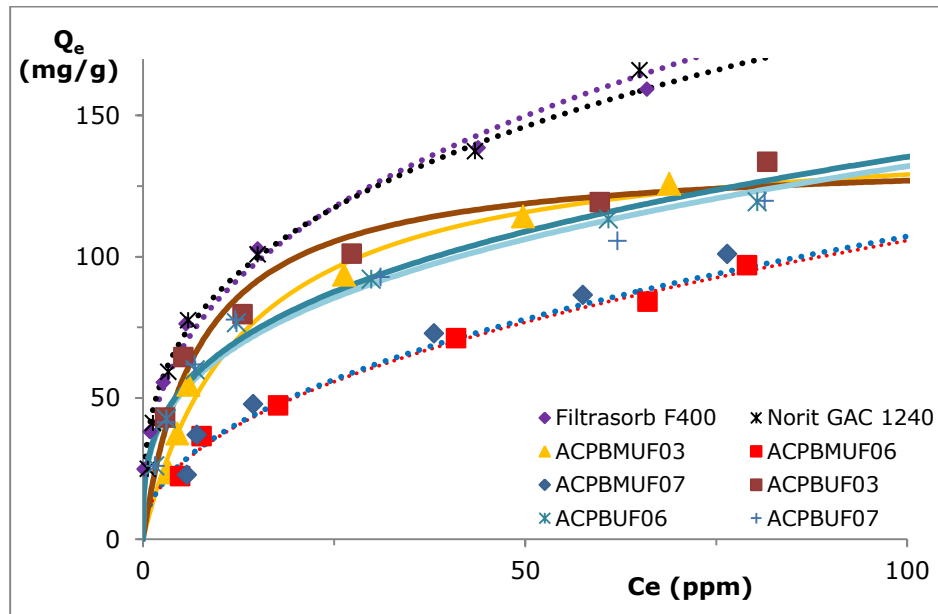


Figure 6-10: Adsorption equilibrium isotherm of phenol

Both the separation factor R_L (Eq. 1-9) and the Freundlich n factor indicate that the phenol adsorption is favourable. A comparison of the R^2 and SSE values of the nonlinear regression indicates that for the particle board activated carbons glued with urea formaldehyde (ACPBUF), Langmuir model yields a better fit. Also ACPBMUF03 (one of the samples glued with urea melamine formaldehyde) is better fitted by this model. The reference carbons and the other produced carbons (ACPBMUF06 and ACPBMUF07) are better fitted by the Freundlich model. In addition, both carbons (ACPBMUF06 and ACPBMUF07) perform less than the other carbon materials. Based on the results, relative high Langmuir monolayer capacities are obtained for the produced carbons. The samples ACPBUF03 and ACPBMUF03 produced at 850 °C with 30 min of steam activation give the best results. During the experiments even for very low activated carbon dosages the pH of the solution increased significantly (see Table 6-11).

Table 6-10. Isotherm parameters + R_L

	Langmuir					Freundlich			
	Q_m (mg/g)	K_L (l/mg)	R_L (Eq 1-9)	R^2	SSE	K_F ($mg^{1-1/n}$ /g)	n	R^2	SSE
ACPBMUF03	145.9	0.077	0.117	0.989	155	21.1	2.3	0.977	324
ACPBMUF06	116.4	0.045	0.186	0.983	129	12.6	2.2	0.993	48
ACPBMUF07	123.9	0.044	0.187	0.985	121	12.8	2.2	0.991	72
ACPBUF03	136.2	0.14	0.0695	0.984	248	32.4	3.1	0.978	339
ACPBUF06	124.2	0.14	0.0672	0.989	142	31.1	3.2	0.984	201
ACPBUF07	120.1	0.16	0.0615	0.989	137	31.8	3.2	0.975	297
Filtrisorb F400	165.7	0.16	0.0608	0.969	787	38.1	2.9	0.993	148
Norit GAC 1240	159.7	0.18	0.0530	0.967	1019	42.4	3.2	0.998	38

The adsorption of phenol onto activated carbon occurs via a complex interplay of electrostatic and dispersion interactions. In literature three possible mechanisms are postulated namely (Lorenc-Grabowska et al. 2012, Nabais et al. 2009):

- π - π dispersion interactions between the phenol aromatic ring and the delocalised π electrons present in the aromatic graphene structure;
- electron-donor-acceptor complex formation between the surface electron donor groups and the phenol molecule acting as acceptor;
- hydrogen bond formation.

In addition, electrostatic interaction can play a significant role if phenolate is present in the solution which is determined by the pH_{PZC} .

In this case as the isotherms all behave like L-type isotherms (following the Giles classification), hydrogen bond formation is excluded from the possible mechanisms. If hydrogen bond formation would be one of the possible mechanisms the isotherms should behave as S-type because of the strong competition between water and phenol molecules at low phenol concentrations in this case. Further it is clear that the π - π dispersion interaction and electron-donor-acceptor complex formation can occur simultaneously if adsorption centers are not located too close to each other. Because of the positive surface charge of the activated carbons during the experiments ($\text{pH}_{\text{solution}} < \text{pH}_{\text{pzc}}$) it is assumed that electrostatic attraction is the main mechanism. The π - π dispersion interactions will almost not occur as the π -electrons of the aromatic graphene layers which act as Lewis basic centres and thus accept/interact with protons of the aqueous solution becoming positively charged. The partly positive charged phenol ring will thus be repulsed. Furthermore, the positive basic sites will withdraw π -electrons of the aromatic system. The electron-donor-acceptor complex formation mechanism is also hindered by the positive charge of the surface. The eventually negative charge (electron donor) resulting from the dissociation of the acidic groups is countered by the surplus of positive surface charge. The phenol molecules are believed to be mostly adsorbed in the vertical interaction by electrostatic interactions of the partly negative charged oxygen on the phenol ring and the negatively charged oxygen of the phenolate. However, locally the different mechanism could occur as the activated carbons have heterogeneous surfaces.

6.4.6.4 *Effect of ionic strength and pH*

The effect of the **ionic strength** on the adsorption capacity of the activated carbons is shown in Figure 6-11. Adding a small amount of salt (KCl) in the solution increases the adsorption capacity of the carbons levelling off to a plateau. Theoretically, if the electrostatic forces between the carbons and the adsorbate are attractive (like in this research), the adsorption capacity decreases by an increase in ionic strength (Al-Degs et al. 2008). The experimental data from this study do not follow this convention, as the adsorption of phenol and phenolate increased by adding salt to the system. This can be explained by two possible mechanisms. The first is the salting-out effect, by decreasing the solubility of phenol in water. The KCl dissociates to monovalent ions, which tightly bind water molecules into well-organized ionic atmospheres decreasing the volume of the aqueous solution macroscopically by electrostriction, decreasing the aqueous solubility of the

phenol and thus intensify the diffusion process into the carbon surface (Lazo-Cannata et al. 2011). The other possible mechanism is the increasing dimerization of phenol molecules by the addition of salt as is reported for active dyes by Al-Degs et al. (2008). The increase is most profound for ACPBMUF and long activation times (i.e., AC...06 and AC...07). However ACPBUF are still performing better in high ionic strength solutions.

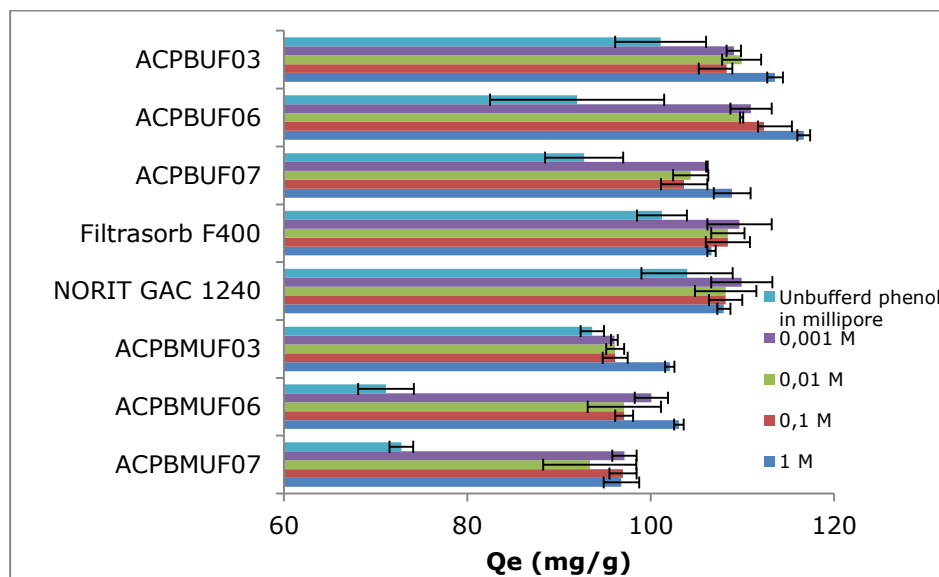


Figure 6-11: Effect of the ionic strength on the removal of phenol

The adsorption of pollutants from an aqueous medium is highly dependent on the pH_{Solution} by affection the adsorbents surface charge and the degree of ionization of the adsorbate. The **effect of pH** on phenol removal with the adsorbents is shown in Table 6-11. The pH is measured before, during and after the adsorption process. It is found that the produced activated carbon immediately affects the pH after addition to the solution towards its pH_{PZC} . When looking at Table 6-11, two pH ranges can be detected, above and below the point of zero charge designating a turning point of the carbons surface charge. For pH_{Solution} values lower than the pH_{PZC} , the carbon surface is positively charged; for higher values the net surface charge is negative. By increasing the difference between the pH and pH_{PZC} , the surface charge density also increases. Lowering the solution pH slowly decreases the phenol removal capacity of the sorbents. From Table 6-11, two distinct areas (below and above a final pH of 10) of different behaviour are observed. By analysing the behaviour below pH of 10, the optimum pH for phenol removal is found to be around 9.5 – 10. Decreasing the pH, the removal only decreases slowly for the carbon samples with melamine urea formaldehyde (ACPBMUF). For

the samples with urea formaldehyde (ACPBUF) the decrease is more significant to the extent of 20% less phenol removal. However, all keep a phenol removal of around 70 % at a pH of around 1.8. At this pH (1.8), there is no dissociation of phenol molecules, it is believed that the phenol molecule adsorb in the vertical position with their partial negative charge on the oxygen molecule towards the positive carbon surface. Increasing the pH, will increase the phenol dissociation, enhancing the adsorption by electrostatic interaction (adsorption in the vertical position). In addition, the hindrance by hydrogen protons in the solution decreases. The second trend is observed at pH values higher than 10. As the pH_{Solution} increases, the net positive surface charge decreases to zero at the point of zero charge, decreasing the electrostatic interaction and decreasing the phenol adsorption. However, even at a pH higher (above 13, more than 99.9 % of phenol ionization) than the point of zero charge there is still 20 - 30 % phenol removal.

Table 6-11. Equilibrium phenol removal at different pH values

pH_{solution}	ACPBU07	ACPBU06	ACPBU03	ACPBUM07	ACPBUM06	ACPBUMF03
<i>pH_{initial}</i>	1.79	1.77	1.76	1.8	1.84	1.81
pH _{final}	68.3	75.1	72.6	69.2	71.7	71.3
% phenol removal						
<i>pH_{initial}</i>	6.17	9.46	9.32	9.72	9.68	9.83
pH _{final}	9.41	95.7	93.4	74.5	74.3	75.4
% phenol removal						
<i>pH_{initial}</i>	8.34	9.71	9.66	9.65	9.53	9.67
pH _{final}	9.4	96	93.5	74.75	79	77.9
% phenol removal						
<i>pH = pK_a phenol = 9.98 (phenol ionisation = 50 %, 25°C)</i>						
<i>pH_{initial}</i>	10.34	10.71	10.68	10.67	10.61	10.62
pH _{final}	10.4	10.71	10.68	10.67	10.61	10.62
% phenol removal						
<i>pH_{pzc} net surface charge = 0</i>	12.8	12.8	12.7	12.3	12.4	12.2
<i>pH_{initial}</i>	13.55	13.3	13.23	13.2	13.22	13.23
pH _{final}	13.3	13.3	13.23	13.2	13.22	13.23
% phenol removal						
	30.2	30.6	32.2	21.6	24.3	25.3

To give an insight into the adsorption capacity of the produced carbons in a more realistic water sample. The effect of a standard fresh water medium with phenol as solution is investigated. The results are displayed in Table 6-12. The solution is buffered at pH 8.1 by equilibrium with air. By introduction of activated carbon, the pH_{Solution} increases marginal especially in contrast to the unbuffered phenol solution and the solutions from Table 6-11. The removal efficiencies are a little bit affected by the standard solution. However, no trend could be detected, some carbons have a little higher (ACPBMUF03) or lower (ACPBUF03, ACPBUF06) removal efficiency. the other are unaffected by the use of fresh water medium.

Table 6-12. Effect of standard water on the removal efficiency of phenol

	pH_{initial}	pH_{final}	Removal efficiency (%)	Removal efficiency unbufferd phenol solution (%)
ACPBMUF03	8.1	8.36	83.7	75.4
ACPBMUF06	8.1	8.84	75.8	74.3
ACPBMUF07	8.1	8.43	75.6	74.5
ACPBUF03	8.1	8.68	87.6	93.4
ACPBUF06	8.1	8.70	87.6	95.7
ACPBUF07	8.1	8.30	84.2	85.9

6.5 Conclusion

In this study a new valorisation method for waste particle board is developed. Two different particle board samples are characterised for their elemental composition and thermogravimetric behaviour. Both samples reveal high nitrogen contents of 5.33 and 4.09 wt% for the sample glued with melamine urea formaldehyde and urea formaldehyde respectively. The thermogravimetric analysis shows good pyrolysis properties for the production of activated carbon.

Different activated carbons are produced in a lab-scale pyrolysis and activation reactor by applying several heat and steam activation profiles on the particle board samples. AC yields from 9.4 – 20 wt% were obtained with the undried ($\sim 7 - 7.5$ wt% moisture) particle board samples. In order to evaluate the carbons ability to adsorb phenol, first of all a screening of the produced carbons is performed. For both particle board samples 3 activated carbons are selected for further characterisation and phenol adsorption experiments.

All selected samples have a high BET surface area starting from 794 and 840 m^2/g for the carbons produced with the lowest activation time to 1656 m^2/g (higher than reference activated carbons) The micro- and mesopore volume ($V_{\text{DR}}/V_{\text{Meso}}$) ratio decreases with increasing activation, indicating that the mesopores gaining a larger contribution to the total pore volume by increasing activation. The latter is also observed in the broadening of the average micropore diameter (L_0). The pore size distribution reveals that all carbons exhibit the same pore distribution. Analysis of the surface functionalities reveal highly basic carbons ($\text{pH}_{\text{PZC}} > 12$) with nitrogen contents of 0.96 – 1.73 wt%. The x-ray photoelectron spectroscopy sheds a light on the distribution and presence of the different oxygen and nitrogen groups. Mainly C-OH, C-O-C, C=O in esters, amides and anhydrides and quaternary N respectively. The phenol adsorption isotherm data are non-linearly modelled by Langmuir and Freundlich equations. The produced carbons give high phenol adsorption capacities of around 125 mg/g. Dynamic adsorption experiments of the particle board activated carbons reveal an interesting process. From the moment of activated carbon introduction, the pH increases immediately from 6.4 - 6.7 to around 10 – 11 promoting phenolate formation and stays constant at this value over time. The adsorption of phenol is thus an interplay between adsorption of phenol, phenolate and in-situ phenolate formation. The experiments reveal a very fast removal of total phenol (phenol and phenolate) with over 50% removal in the first 50 minutes. The adsorption capacity is only slightly affected by the pH below the pH_{PZC} . Higher pH values negatively affect the adsorption

Chapter: 6

capacity significant. Addition of salt to the solution has a small positive effect and remains rather constant over large salt concentrations.

It can be concluded that the produced activated carbons from particle board have good adsorptive characteristics for the removal of phenol from aqueous solutions in different environments.

7 Activated carbon from pyrolysis of brewer's spent grain: Production and Adsorption properties

Since the goal of this research is the development of activated carbon using several waste streams, a third highly abundant residue, namely brewers spent grain, is studied. The choice of this residue is based on the high nitrogen content, which is expected to be beneficial for adsorption, as discussed in section 1.3.3.2.

The results of this chapter have partly been published:

VANREPELEN, Kenny; VANDERHEYDEN, Sara; KUPPENS, Tom; SCHREURS, Sonja; YPERMAN, Jan & CARLEER, Robert (2014) Activated carbon from pyrolysis of brewer's spent grain: Production and adsorption properties. In: Waste Management & Research, 32 (7), p. 634-645. [Article - cat: A1]

VANREPELEN, Kenny; VANDERHEYDEN, Sara; KUPPENS, Tom; SCHREURS, Sonja; CARLEER, Robert & YPERMAN, Jan (2013) Activated Carbon from Pyrolysis of Brewer's Spent Grain: Production and Adsorption Properties. In: Ban, M.; Duić, N.; Guzović, Z.; Markovska, N; Schneider, D.R.; Klemeš, J.J.; Varbanov, P.; Ababneh, A.; Østergaard, P.A.; Connolly, D.; Kafarov, V.; Krajačić, G.; Lund, H.; Mathiesen, B.V.; Mohsen, M.; Möller, B.; Perković, L.; Sikdar, S.K.; Vujanović, M. (Ed.). Proceedings of the 8th Conference on Sustainable Development of Energy, Water and Environment Systems (SDEWES 2013). [Paper - cat: C1]

VANREPELEN, Kenny; VANDERHEYDEN, Sara; KUPPENS, Tom; SCHREURS, Sonja; CARLEER, Robert & YPERMAN, Jan (2013) Activated Carbon from Pyrolysis of Brewer's Spent Grain: production and Adsorption Properties. In: 8th Conference on Sustainable Development of Energy, Water and Environment Systems, Dubrovnik, 22-27/09/2013. [Presentation - cat: C2]

7.1 Abstract

Brewer's spent grain (BSG) is a low cost residue generated by the brewing industry. Its composition (high nitrogen content 4.35 wt. %, fibres, ...) makes it very useful for the production of added value in-situ nitrogenised activated carbon (AC). The composition of BSG revealed high amounts of

cellulose (21 wt. %), hemicellulose (49 wt. %) and lignin (11 wt. %). Fat, ethanol extractives and ash accounted for 8.17, 4.7 and 3.2 wt. % respectively. Different activated carbons were produced in a lab-scale pyrolysis/activation reactor by applying several heat and steam activation profiles on BSG. AC yields from 16.1 – 23.6 wt. % with high N-contents (> 2wt. %) were obtained. The efficiency of the prepared activated carbons for phenol adsorption was studied as a function of different parameters: pH, contact time and carbon dosage relative to two commercial activated carbons (Filtrisorb F400, Norit GAC 1240). The equilibrium isotherms were described by the non-linear Langmuir and Freundlich models and the kinetic results were fitted using the pseudo-first-order model and the pseudo-second-order model. The feasibility of an AC production facility (onsite and offsite) which processes BSG for different input feeds is evaluated based on a techno-economic model for estimating the net present value (NPV). Even though the model assumptions start from a rather pessimistic scenario encouraging results for a profitable production of AC using BSG are obtained.

7.2 Introduction

Brewer's spent grain (BSG) is a widely available, low cost residue representing around 85% of the total by-products generated by the brewing industry. BSG are the remains (husk, pericarp-seed coat layers) from the barley malt after the mashing process. It is a lignocellulosic material rich in fibres (60 wt. % dry matter) and proteins (20 wt. % dry matter) (Mussatto et al. 2006). On average 14 – 20 kg of wet BSG (20 – 25 wt. % dry matter) is produced per 100 l beer (Deconinck et al. 2001, Mussatto et al. 2006). For Europe (EU27 in 2011) with a total beer production of 38400 Ml (Eurostat 2011) the average production capacity was around 5.38 – 7.68 Mt of wet BSG. Worldwide the annual generation of BSG is estimated at 30 Mt (Cook 2011).

Traditionally this material has been landfilled or sold as animal feed (mostly for ruminants which can cope with the high fibre content (Cook 2011)). However, BSG is difficult to store because of the rapid deterioration due to microbial activity and therefore it is not always suitable for food applications. In addition, the environmental implications of increased methane emission due to this hard to digest material are gaining attention (Cook 2011).

Despite its potential as a valuable and renewable resource for industrial exploitation, it has received little attention as a marketable product yet. Its chemical composition (high nitrogen content, fibres, ...) makes BSG very useful for the production of high added value in-situ nitrogenised activated carbon (AC). The in-situ nitrogen presence will result in a considerably reduced production cost in comparison with post impregnation of nitrogen

containing components on AC (Vanreppelen et al. 2011). Furthermore, the gases (condensable and non-condensable) produced during the pyrolysis and activation step can be used as a source of chemicals or renewable energy. In normal conditions the amount of nitrogen in AC is negligible (Bandosz 2009, Girods et al. 2009a). However, it is demonstrated that nitrogen incorporation is seen as a key parameter for the adsorption properties of activated carbons, especially for the removal of phenolic compounds (Girods et al. 2009a, Girods et al. 2008a, Lorenc-Grabowska et al. 2012, Przepiorski 2006).

Phenol is considered a priority pollutant due to its toxicity even at low concentrations. In addition, the presence of phenol in natural water can lead to the formation of other toxic substituted compounds during disinfection and oxidation processes (Busca et al. 2008). The fixed low admissible level of phenol following the Flemish regulation is 0.1 mg/l for surface water for the production of drinking water, ≤ 0.05 mg/l for surface swimming water and 0.5 mg/l for groundwater (VLAREM-II 2013). Major sources of phenol pollution in the aquatic environment are pharmaceuticals, plastics, pulp and paper industries (0.1–1600 mg/l), refineries (6–500 mg/l), coking operations (28–3900 mg/l), coal processing (9–6800 mg/l), manufacture of petrochemicals (2.8–1220 mg/l), steel plants, rubber proofing, ... (Busca et al. 2008). Various physicochemical and biological treatment techniques have been employed for the removal of phenol from waste water such as solvent extraction, ozone oxidation, biodegradation, etc. but the most effective and frequently used procedure is adsorption on activated carbons (Busca et al. 2008, Girods et al. 2009a).

The objective of this study was to prepare, characterise, investigate the feasibility and measure the phenol adsorption properties of activated carbons derived from BSG as a function of different experimental parameters such as initial pH, contact time and carbon dosage relative to two commercial activated carbons (Fitrasorb F400 and Norit GAC 1240).

7.3 Methods and materials

An overview of the experimental approach and strategy is shown in Figure 7-1.

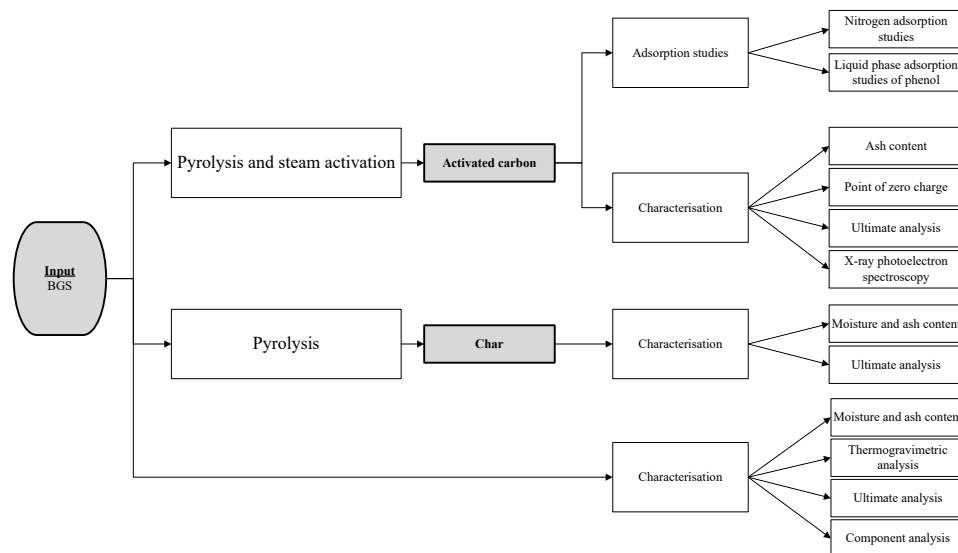


Figure 7-1: Experimental approach and strategy for the production and characterization of activated carbons from particle board

The moisture content of the samples is determined according to ASTM 1756 – 01 by oven drying at a temperature of 105 ± 3 °C until constant weight. Ash content is determined by ASTM E 1755 – 01 by dry oxidation at 575 ± 25 °C for a minimum of 3 h. Both methods are performed in quadruplicate. TGA is performed using a DuPont Instruments 951 Thermogravimetric Analyser. About 10 mg of sample is weighed into a quartz crucible. The sample is heated with a heating rate of 10 °C/min from room temperature (RT) to a pre-set temperature under nitrogen atmosphere (80 ml/min) to 900 °C. At 900 °C, an isothermal period of 10 min is applied and the gas-flow is switched to oxygen atmosphere (80 ml/min). CHNS- and O-content (ultimate analysis (EA)) is determined in quadruplicate by a Thermo Electron FlashEA1112 calibrated using BBOT (2,5-bis (5-tert-butyl-benzoxazol-2-yl) thiophene)). Around 3 mg of a (dry) sample is introduced into a tin container (for CHNS-determination O-content is calculated by difference as: $O = 100\% - (C + H + N + S + \text{ash})$). The chemical composition (hemicellulose, cellulose and lignin) of the brewer's spent grain is assessed by an adapted Van Soest and Wine gravimetric method (Faithfull 2002) after ethanol extraction (according to ASTM E 1690 – 01) performed in quadruplicate.

Pyrolysis and steam activation are executed with the semi-continuous Lab-built pyrolysis reactor manufactured in stainless steel (AISI 304) which is discussed in more detail in Chapter 3. To achieve as much similarity as possible with industrial activated carbon production process input materials

are used as described in Section 2.1. Prior to heating, the reactor and input materials are flushed by N₂-gas (80 ml/min) to guarantee an oxygen poor environment. Chars are produced by heating the samples at 10 °C/min up to the desired temperature of 800 °C or 850 °C followed by an isothermal period of 30 min under N₂-atmosphere (80 ml/min). Activated carbons are produced by heating the samples at 10 °C/min up to the desired temperature of 800 °C or 850 °C followed by an isothermal period of 30 or 45 min under steam atmosphere (by introduction of different known quantities of water into the reactor). The different pyrolysis and activation routes are displayed in Figure 2-2. The produced gasses exit the reactor and are burned in the flame of a Bunsen burner. ASTM E 1755 – 01 is used to determine the ash content (performed in quadruplicate).

Batch phenol adsorption on the produced activated carbons against two reference activated carbons (Filtrisorb F400 and Norit GAC 1240) is evaluated by introducing 25 ml of a 100 ppm (initial concentration C₀) unbuffered phenol solution with different quantities of activated carbon (5, 10, 20, 30, 40, 60 and 100 mg) in a hermetically closed flask. Analytical grade phenol and Milli-Q water (18.2 MΩ/cm conductivity) is used. The flasks are placed in a thermostatic water bath (25°C) and shaken for 24 h. It is assumed that equilibrium is reached in this time period. Residual concentration is determined as described further in this section. Each experiment was done in quadruplicate. In this work the equilibrium data are fitted by two two-parameter models: the Langmuir and Freundlich model (discussed in Section 1.3.4.1.). The three best performing activated carbons are further analysis.

The point of zero charge (pH_{PZC}) is estimated by a modified mass titration of Noh & Schwarz (1990). 2.0 g AC was put in 20 ml 0.1 M KNO₃ solution in a closed vessel. After 24 h shaking in a thermostat shaker, the equilibrium pH values of the mixtures were measured electronically (calibrated combined pH electrode) and the limiting pH was taken as the pH_{PZC}. The number of basic and acid groups is determined by bringing 200 mg AC in contact with 25 ml 0.100 M HCl or NaOH solution respectively. After 24 h the solutions are titrated with 0.100 M NaOH or HCl in a nitrogen atmosphere by a Metrohm 794 Basic Titrino (based on Velghe et al. (2012)). Elemental analysis (EA) is performed in quadruplicate for CHNS-content. X-ray photoelectron spectroscopy (XPS) measurements are performed to determine the carbon, nitrogen and oxygen functionalities on the surface of the activated carbons. Experiments are performed using an XPS customized SPECS system with monochromatic Al K_α (1486,74 eV) X-ray radiation set at 175 W and 14 kV. The atomic concentrations were calculated from the photoelectron peak areas, using Shirley background subtraction. Deconvolution of the main peak of the C1s, N1s and O1s spectra is

performed by an iterative least-square fitting algorithm. Chemical structural assignments of each component were made taking into account the binding energies reported by Lorenc-Grabowska et al. (2012), Zhou et al. (2007), Arrigo et al. (2008). Experiments are performed by the 'Mazovian Centre for Surface Analysis, Institute of Physical Chemistry' Polish academy of sciences, Poland. The BET surface areas, total porosity volume (V_T), micropore volume (V_{mic}) and mesopore volume (V_{mez}) are analysed by nitrogen (77 K) adsorption using an Autosorb AS-1 from Quantachrome. Before analysis the samples are outgassed for 16 h at 200 °C in high vacuum. The specific surface area of the activated carbons is estimated by the Brunauer, Emmett and Teller (BET) gas adsorption method (Brunauer et al. 1938). The micropores are characterised by the Dubinin – Radushkevich method (volume micropores V_{DR}) and the t-plot method using the De Boer method (micropore surface S_{micro} and extremal surface S_{ext}). By using the Dubinin – Radushkevich method the characteristic adsorption energy (E_0) can be estimated. The average micropore (L_0) is calculated using the Stoeckli equation. The total mesopore volume is estimated by converting the adsorbed volume of nitrogen at a relative pressure of 0.96 into the equivalent liquid volume at 77K. The mesopore volume is then estimated by subtracting the micropore volume (V_{DR}) from the total pore volume.

The adsorption kinetics are investigated (in duplicate) by varying the contact time from 0.5 h – 24 h in the batch adsorption mode using 25 ml of a 100 ppm unbuffered phenol solution with 50 mg of AC. The amount of phenol adsorbed in the corresponding time interval (q_t) is calculated by Eq. 2-2 and fitted (using the pseudo-first-order model and the pseudo-second-order model). The theoretical background is discussed in Section 1.3.4.3. The effect of pH on the phenol adsorption is studied (in triplicate) by introducing 20 mg AC in 25 ml of a 100 ppm phenol solution and varying the pH of the phenol solution in the range of (0.5 – 13.5) by introducing appropriate amounts of HCl or KOH respectively, additionally maintaining the ionic strength at 0.1 M by adding various amounts of KCl. The hermetically closed flasks are shaken for 24 h in a thermostatic water bath (25 °C). To study the effect of the ionic strength on the phenol adsorption five different phenol solutions are made with varying concentrations of KCl (0, 0.001, 0.01, 0.1 and 1 M). 25 ml of these solutions are added to 20 mg AC, after 24 h shaking in a water bath (25 °C). The experiments are performed in triplicate. To investigate the phenol adsorption in a more realistic water medium, a reconstituted standard water based on ISO 6341, representative of those generally occurring in the environment, is made using "OECD series on testing and assessment number 29: Guidance document on transformation/dissolution of metals and metal compounds in aqueous media". The chemical composition of the reconstituted standard water (for tests carried out at pH 8) is as follows: NaHCO_3 65.7 mg/l, KCl 5.75 mg/l,

CaCl₂·2H₂O 294 mg/l, MgSO₄·7H₂O 123 mg/l. The solution is air buffered at pH 8 in which the concentration of CO₂ provides a natural buffering capacity sufficient to maintain the pH within an average of ± 0.2 pH units over a period of one week (OECD Environment 2001). A 100 ppm phenol solution is made with this water and added to 20 mg AC. After 24 h shaking in a water bath (25 °C) the residual phenol concentration is determined. The experiments are performed in triplicate.

After the assigned adsorption time the solutions are filtered and the residual phenol concentration (C_e) is analysed using a Pharmacia Biotech Ultraspec 2000 UV-VIS spectrophotometer at 270 nm and the pH is measured. Calibration is carried out using a number of phenol standard solutions (concentration range: 1 ppm, 5 ppm, 10 ppm, 30 ppm, 50 ppm, 80 ppm and 100 ppm) and a correction factor is determined for each pH value to counteract the lower adsorption due to the dissociation of phenol in the solution (discussed in detail in section 6.4.1). Milli-Q water, subjected to a similar procedure as the unknown samples are used as blanks and adsorbent-free controls are run in parallel. Once C_e is determined the amount of phenol adsorbed on the AC at equilibrium can be calculated using Eq. 2-1.

Dynamic phenol adsorption and effect of temperature is determined by a home-build thermostatic slurry batch reactor connected with a computer controlled Pharmacia Biotech Ultraspec 2000 UV-VIS spectrophotometer (Figure 2-3). 100 mg of adsorbent is weighted and placed in a double walled vessel with 50 ml 100 ppm phenol solution. The slurry is agitated by means of an IKA RW20 n overhead stirrer fitted by a Screw Type Stir Element at 150 rpm. By means of a glass fritted filter a stream of filtered solution is withdrawn with a Heidolph pumpdrive 5001 peristaltic pump (set at 35 rpm) to a home-build measuring cell (Quartz, path length 2.3 mm) mounted in a computer controlled UV-VIS spectrophotometer. The absorbance of the solution is measured at 270 and 286 nm every minute and stored using a home-made LabView programme. The liquid is transferred back to the slurry reactor. The measurements are performed in twofold at a temperature of 15, 20, 25 and 30 °C.

7.4 Results and discussion

7.4.1 Characterisation of the input material

The obtained fresh wet BSG has a moisture content of 74.5 ± 0.1 wt %. BSG basically consists of the husk-pericarp-seed coat layers from the malted barley grain after the mashing process. The chemical composition and EA of the (dried) BSG are listed in Table 7-1. After drying the main components are hemicellulose (49 wt %), cellulose (21 wt %) and lignin (11 wt %). Fat, extractives and ash are 8.17, 4.7 and 3.2 wt% respectively. Elemental analysis (on dry BSG) reveals a high nitrogen content of 4 wt% which is an indication for a possible in-situ production of nitrogenised activated carbons. The TG and DTA (Differential thermal analysis) curves of (dry) BSG (Figure 7-2) show a small weight loss of 5 wt% due to the loss of fixed moisture and the start of decomposition of extractives (25 – 200 °C). Most of the weight loss occurs in the range 200 – 500 °C. In this range two significant weight loss peaks can be seen which correspond to the degradation of hemicelluloses and cellulose superimposed on the slow degradation of lignin. The fixed carbon amounts to 16.3 wt% (600 °C without ash). The char yield at a temperature of 800 and 850 °C is 18.9 and 18.6 wt% respectively.

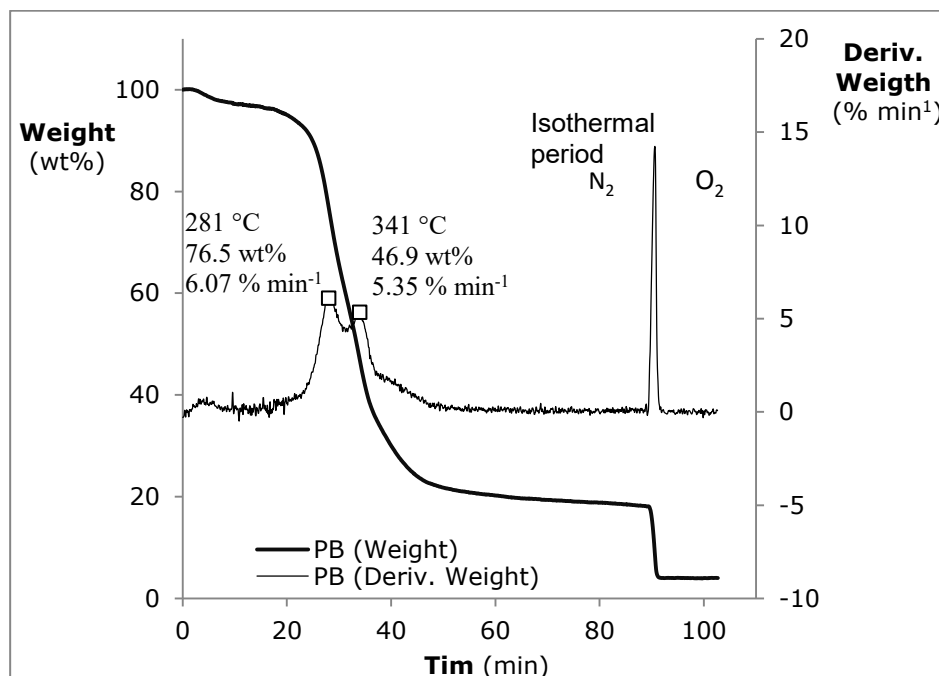


Figure 7-2: TGA/DTG curves of BSG

Table 7-1. Chemical composition and EA of BSG

	BSG (wt%)		
Cellulose	21 ± 2	%N	4.4 ± 0.2
Hemicellulose	48.8 ± 0.7	%C	50 ± 1
Lignin	11.3 ± 0.4	%H	6.9 ± 0.2
Fat	8.2 ± 0.1	%S	< DL
Ethanol extractives	4.7 ± 0.3	%O*	36 ± 1
Ash	3.2 ± 0.1		
Undetermined	3 ± 2		

* Calculated by difference %O = 100% - %N - %C - %H - %S - %ash;
< DL = below detection limit

7.4.2 Activated carbon yield and characterization

The yield combined with the obtained quality is an important measure for a feasible AC production from a given precursor. The effect of the different pyrolysis and steam activation profiles (from Figure 2-2) on the production distribution is shown in Figure 7-3. It can be seen that the AC yield from dried BSG (remaining moisture content of 0.64 ± 0.03 wt%) for the pyrolysis at 800°C decreases from 23.5 - 19.2 wt% by increasing steam activation, and from 20.4 - 16.0 wt% for the pyrolysis at 850 °C. This corresponds to a burn-off between 9.0 - 25.7 wt% and 19.3 - 36.6 wt% for the steam activation at 800 °C and 850 °C respectively. The char yields (25.9 wt% at 800 °C and 25.3 wt% at 850 °C) are significant higher than predicted by the TGA results (18.9 wt% at 800 °C and 18.6 wt% at 850 °C).

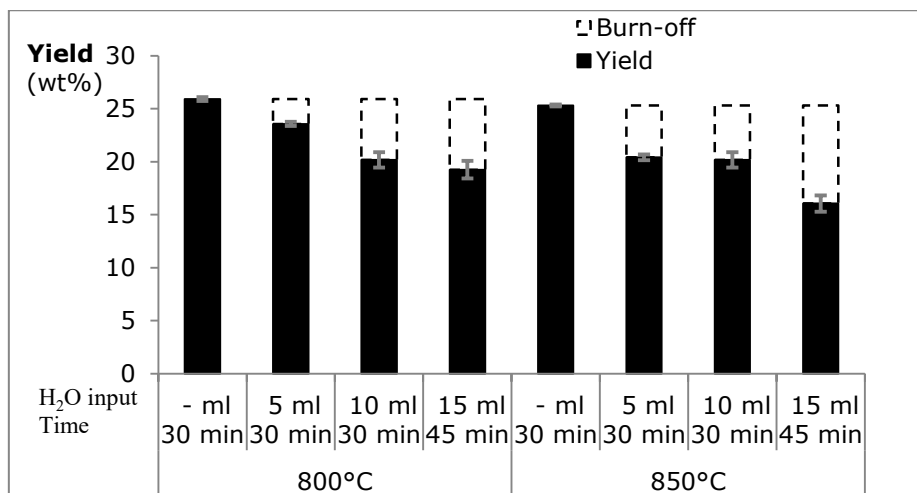


Figure 7-3. Pyrolysis and ACBSG yield

The composition of the obtained chars and activated carbons (on a dry basis) is investigated by elemental analysis, the results with their standard deviations (6 experiments) are given in Table 7-2. It can be seen that the N-content of the chars decreases with increasing pyrolysis temperature from 4.35 wt% (for BSG) to 3.84 (800 °C) and 3.44 wt% (850 °C). The subsequent steam activation results in a further reduction of the N-content to 2.49 and 2.13 wt%. The C-content (~70%) strongly increases (on average 45%) in comparison with the BSG. When looking at the char and activated carbons the C-content decreases with increasing steam activation amount and time, however no significant difference between both pyrolysis temperatures can be detected. For the H-content there is an increase for the ACBSG01 and ACBSG02 compared with the char samples when the steam activation is performed for 30 minutes with the injection of 5 ml H₂O into the reactor. Stronger steam activation diminishes the concentration but it still remains higher than in the char samples. The produced chars retain also a high O-content of on average 7 wt% which further increases by activation (>10%). Ash content further increases as a function of the steam activation amount and contact time.

Table 7-2. Ultimate analysis

	CHBSG01	ACBSG01	ACBSG05	ACBSG07	CHBSG02	ACBSG02	ACBSG03	ACBSG06
% N	3.8 ± 0.1	3.2 ± 0.2	2.7 ± 0.1	2.549 ± 0.033	4.3 ± 0.02	2.12 ± 0.04	2.16 ± 0.04	2.13 ± 0.04
% C	76 ± 1	72 ± 2	71 ± 1	71 ± 1	77 ± 1	72.6 ± 0.2	70 ± 2	71 ± 1
% H	1.2 ± 0.1	1.6 ± 0.1	1.6 ± 0.1	1.5 ± 0.2	1.2 ± 0.03	1.4 ± 0.1	1.3 ± 0.1	1.2 ± 0.1
% S	< DL	< DL	< DL	< DL	< DL	< DL	< DL	< DL
% Ash	11.7 ± 0.1	13.1 ± 0.4	14.4 ± 0.5	14.6 ± 0.3	12.0 ± 0.1	15.1 ± 0.3	15.4 ± 0.3	18 ± 1
% O*	7 ± 1	10 ± 2	10 ± 2	11 ± 1	7 ± 1	9.9 ± 0.3	11 ± 3	9 ± 1
N/C atomic ratio	0.05	0.04	0.04	0.04	0.04	0.03	0.03	0.03
O/C atomic ratio	0.1	0.14	0.15	0.15	0.09	0.14	0.16	0.12

* Calculated by difference %O = 100% - %N - %C - %H - %S - %ash;
< DL = below detection limit

7.4.3 Phenol adsorption

Adsorption equilibrium data are key information in understanding and explaining an adsorption process (Hamdaoui & Naffrechoux 2007). The isotherm reflects the relationship between the amount of a solute adsorbed at constant temperature and its equilibrium concentration in the solution providing essential physicochemical data for assessing the applicability of the adsorption process (Yousef et al. 2011). In this work the equilibrium data are fitted by two two-parameter models: the Langmuir (Eq. 1-8) and Freundlich model (Eq. 1-9).

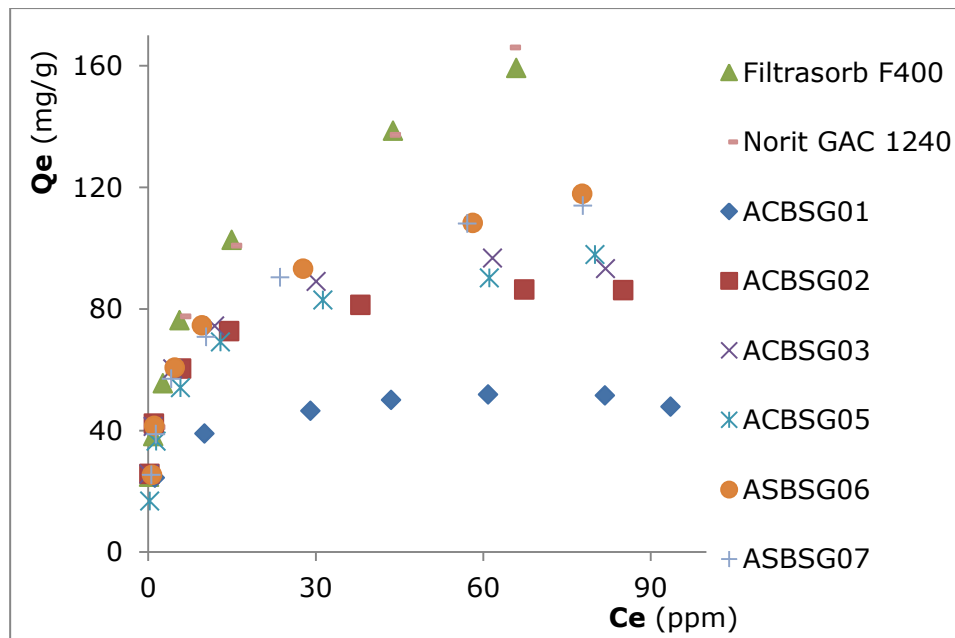


Figure 7-4. Comparison of adsorption isotherms of phenol onto different BSG activated carbons

Figure 7-4 presents the equilibrium adsorption isotherms of phenol from aqueous solution onto activated carbons prepared from BSG following the pyrolysis and activation routes (as presented in Figure 2-2). The equilibrium data (experimental values) are nonlinear modelled with the Langmuir and Freundlich equations in order to determine the model parameters. The results are shown in Table 7-3. It can be seen from Table 7-3 and Figure 7-4 that the applied pyrolysis temperature has the same influence on the adsorption capacity: the higher the activation temperature, the higher the

adsorption capacity. Nevertheless they are comparable, except for the large difference found between ACBSG01 and all other activated carbons. The steam activation has a pronounced effect on the adsorption capacity of the produced adsorbents. An increase in steam during the activation step gives rise to an improved adsorption capacity. The pH of the solution increased from on average 6.5 - 6.9 (unbuffered phenol solution) to 7.1 with 5 mg of activated carbon to around 8 for 100 mg of activated carbon. For the commercial activated carbons this was from 7.2 to 8.1 and 7.3 to 8.8 for Norit GAC 1240 and Filtrasorb F400 respectively. The produced activated carbons have a very good performance, however they are not as good as the reference activated carbons (Filtrasorb F400 and Norit GAC 1240) in terms of maximum adsorption capacity. Moreover, not only the maximum adsorption capacity is of importance, the required carbon dosage to achieve sufficient phenol removal is also crucial as determined in Figure 7-5. It can be seen that all activated carbons have very high removal efficiencies (even for ACBSG01) at a dosage of 4 g/l. At lower dosages the impact of the steam activation on the removal efficiency can be seen. The tendency is the same as for the adsorption capacity, more steam improves the removal efficiencies (ACBSG01 performs again clearly worse).

By analysing the experimental data using the non-linearized form of the Langmuir equation it is shown that the adsorption of phenol onto the AC is a favourable process ($0 < R_L < 1$). This is also indicated by the magnitude of n ($2 < n < 10$) given by the non-linearized form of the Freundlich equation. Based on the n values the adsorption intensity of the activated carbons from brewer's spent grain is higher than the adsorption of phenol by the commercial activated carbons. Comparison of the R^2 values shows that the Freundlich model fits the experimental data the best except for ACBSG01 where both isotherms are comparable with a slight preference for Langmuir (based on a lower SSE value except for ACBSG01).

Table 7-3. Isotherm constants

	Langmuir					Freundlich			
	Q_m (mg/g)	K_L (l/mg)	R_L (Eq.1-9)	SSE	R^2	K_F ($\text{mg}^{1-(1/n)}$ $\text{l}^{1/n}/\text{g}$)	n	SSE	R^2
ACBSG01	50.3	0.657	0.015	46	0.980	26.5	6.6	149	0.976
ACBSG02	81.9	1.09	0.009	294	0.961	42.1	5.8	38	0.984
ACBSG03	91.0	0.796	0.012	420	0.957	43.5	5.2	55	0.981
ACBSG05	94.2	0.306	0.031	263	0.975	33.3	4.0	113	0.985
ACBSG06	111.7	0.312	0.031	501	0.962	38.7	3.9	163	0.988
ACBSG07	111.3	0.270	0.035	412	0.968	36.8	3.8	136	0.992
Filtrisorb F400	165.7	0.156	0.061	787	0.969	38.1	2.9	143	0.993
Norit GAC 1240	159.7	0.180	0.053	1019	0.967	42.4	3.2	93	0.998

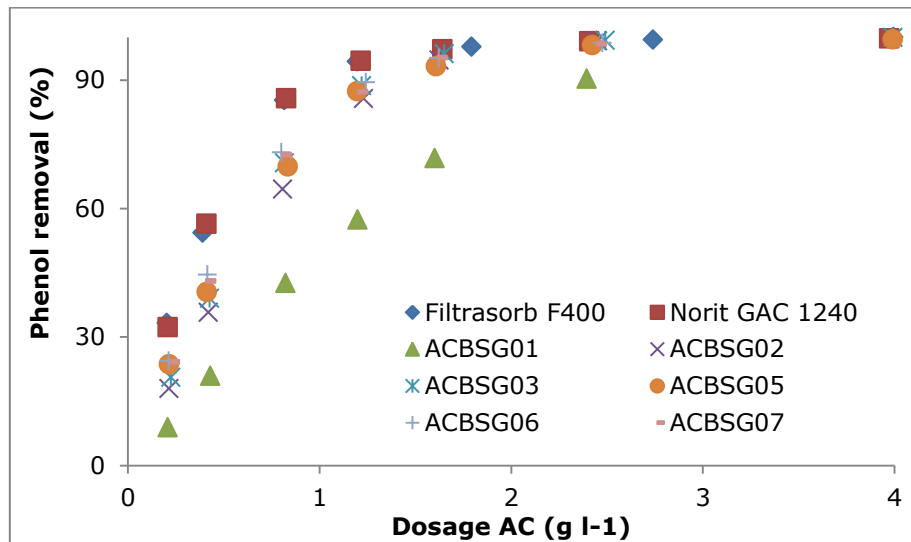


Figure 7-5. Effect of AC dosage on phenol removal

Based on Table 7-3, Figure 7-4 and Figure 7-5 the 3 best performing prepared activated carbons (ACBSG05, ACBSG06 and ACBSG 07) are selected and compared with the commercial activated carbons to investigate the effect of contact time and the effect of pH onto the adsorption. It can be argued that ACBSG03 is similar as ACBSG05. However due to the lower production temperature needed for its production i.e., 800 °C instead of 850°C, ACBSG05 is chosen. By further investigation of Figure 7-3 for the selected activated carbons, the relative adsorption capacity (K_F) of ACBSG07 and ACBSG06 is in the same range as the commercial activated carbons. ACBSG05 is a little bit lower. The maximum adsorption capacity from the produced carbons obtained by Langmuir is on average two third of those of the commercial activated carbons.

7.4.4 Porosity

Valuable information about the porous structure of the produced activated carbons can be obtained by the analysis of nitrogen (or another gas) adsorption and desorption isotherms. The nitrogen adsorption-desorption isotherms at 77 K for the selected activated carbons are shown in Figure 7-6. First of all qualitative information can be obtained from the shape of the isotherms and the hysteresis loops according the IUPAC classification (Sing et al. 1985).

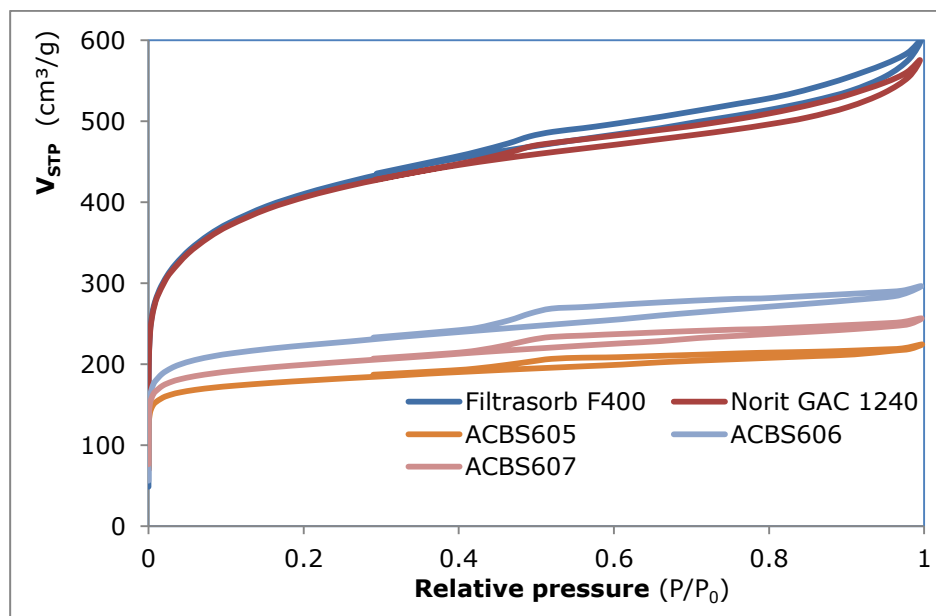


Figure 7-6: N₂ adsorption-desorption isotherms at 77K

All brewer's spent grain isotherms behave as type I(a) isotherms, although there is a small contribution of slit shaped pores. Type I(a) isotherms are concave with a steep uptake in the low pressure region. They are found in microporous materials having mainly narrow micropores ($< 1\text{nm}$). The amount of adsorbed N_2 -gas has a limiting value governed by the accessible micropore volume. The steep uptake is due to enhanced adsorbent-adsorptive interaction in narrow micropores (molecular dimension). The presence of a hysteresis loop is an indication of mesopores in the activated carbons. The adsorption-desorption hysteresis loops are classified as type H4 according to IUPAC recommendations (Sing et al. 1985). This type of hysteresis loop is attributed to adsorption in narrow slit-like pores (Choma & Jariniec 2006). The closure of the hysteresis loop at $p/p_0 \sim 0.4$ indicates the presence of small mesopores.

Based on the isotherms, quantitative information can be obtained like pore size distribution, Brunauer, Emmett and Teller (BET) specific surface area and the pore volumes of the samples (see Table 7-4 and Figure 7-6). The specific surface area of the activated carbons is estimated by the BET gas adsorption method (Brunauer et al. 1938) in the relative pressure range between 0.005 - 0.11 and 0.008 - 0.15 for the activated carbons from brewer's spent grain and reference carbons respectively. The micropores are characterised by the Dubinin - Radushkevich method (volume micropores V_{DR}) and the t-plot method using the De Boer method (micropore surface S_{micro} and external surface S_{ext}). By using the Dubinin - Radushkevich method the characteristic adsorption energy (E_0) can be estimated. The average micropore (L_0) is calculated using the Stoeckli equation. The total mesopore volume is estimated by converting the adsorbed volume of nitrogen at a relative pressure of 0.96 into the equivalent liquid volume at 77K. The mesopore volume is then estimated by subtracting the micropore volume (V_{DR}) from the total pore volume. The BET analysis reveal good correlation coefficients of more than 0.9999 for all samples. As observed in Figure 7-6 and calculated in Table 7-4 the **BET surface (apparent surface) increases** with increasing activation (from ACBSG05 to ACBSG07 and to ACBSG06). The obtained BET surface for the activated carbons from brewer's spent grain is around half (686 - 836 m^2/g) of the BET surface from the reference activated carbons (1468 -1483 m^2/g). Higher and longer activation times (ACBSG05 \rightarrow ACBSG07 \rightarrow ACBSG06) increases the BET surface, **micropore (V_{DR}), mesopore (V_{Meso}) and the pore volumes (V_{T})** of all the samples. The $V_{\text{DR}}/V_{\text{T}}$ ratio decreased from 0.81 to 0.78, indicating that the mesopores gaining a larger contribution to the total pore volume by increasing activation. The latter is also observed in the broadening of the **average micropore diameter (L_0)**. In contrast to the reference activated carbons the produced carbons have a very small (≤ 0.5 times) average pore diameter. The activated carbons from brewer's spent grain exhibit very small

external surface areas (S_{ext}) which increases slightly with increasing activation from 100 for ACBSG05, 121 m²/g for ACBSG07 to 151 m²/g for ACGSG06. The low external surface area in combination with a large microporous surface contribution also indicates type I(a) isotherms as discussed previously. No clear correlation can be found between the pore volumes and the adsorption capacity for the carbons from brewer's spent grain.

Table 7-4: Porosity characteristics: BET analysis (S_{BET}), t-plot analysis for micropore (S_{micro}) and external surface (S_{ext}) based on De Boer, and micropore characterization based on the Dubinin-Radushkevich method (V_T , V_{DR} , V_{Meso} , L_0 and E_0)

	S_{BET} (m ² /g)	S_{micro} (m ² /g)	S_{ext} (m ² /g)	V_T (cm ³ /g)	V_{DR} (cm ³ /g)	V_{Meso} (cm ³ /g)	L_0 (nm)	E_0 (kJ/mo l)
ACBSG05	686	422	100	0.335	0.274	0.060	0.9	23.5
ACBSG06	836	506	151	0.439	0.342	0.097	1.3	19.9
ACBSG07	758	461	121	0.382	0.304	0.078	1.0	22.2
Norit GAC 1240	1468	532	725	0.827	0.599	0.228	2.6*	15.5
Filtrisorb F400	1483	833	432	0.859	0.604	0.256	2.6*	15.5

* The empirical correlation (Stoeckli formula) is only valid for L_0 values between 0.5 and 2.0 nm

The pore size distribution of the micropores (Figure 7-7) is determined by means of the Density Functional Theory (DFT). The pore size distribution reveals that the activated carbons from brewer's spent grain consists out of primarily pores with a diameter between 1 and 1.1 nm. Followed by two secondary micropores 0.82 – 0.97 nm and 1.12 – 1.32 nm. In addition a wider micropores are found around 2 nm. An increase in temperature and activation increases the amounts of the micropores, without an enlargement of the micropores. The pore size distribution in the range of 2.5 – 8.5 show four peaks: at 3.7 nm, 4.9 nm, 5.3 nm and 5.8 nm. As with the micropores the stronger activation and higher temperature increases their volume without enlarging the pores. When comparing with the pore size distribution of the commercial activated carbons, a very discrete distribution is obtained by the activation and pyrolysis of brewer's spent grain.

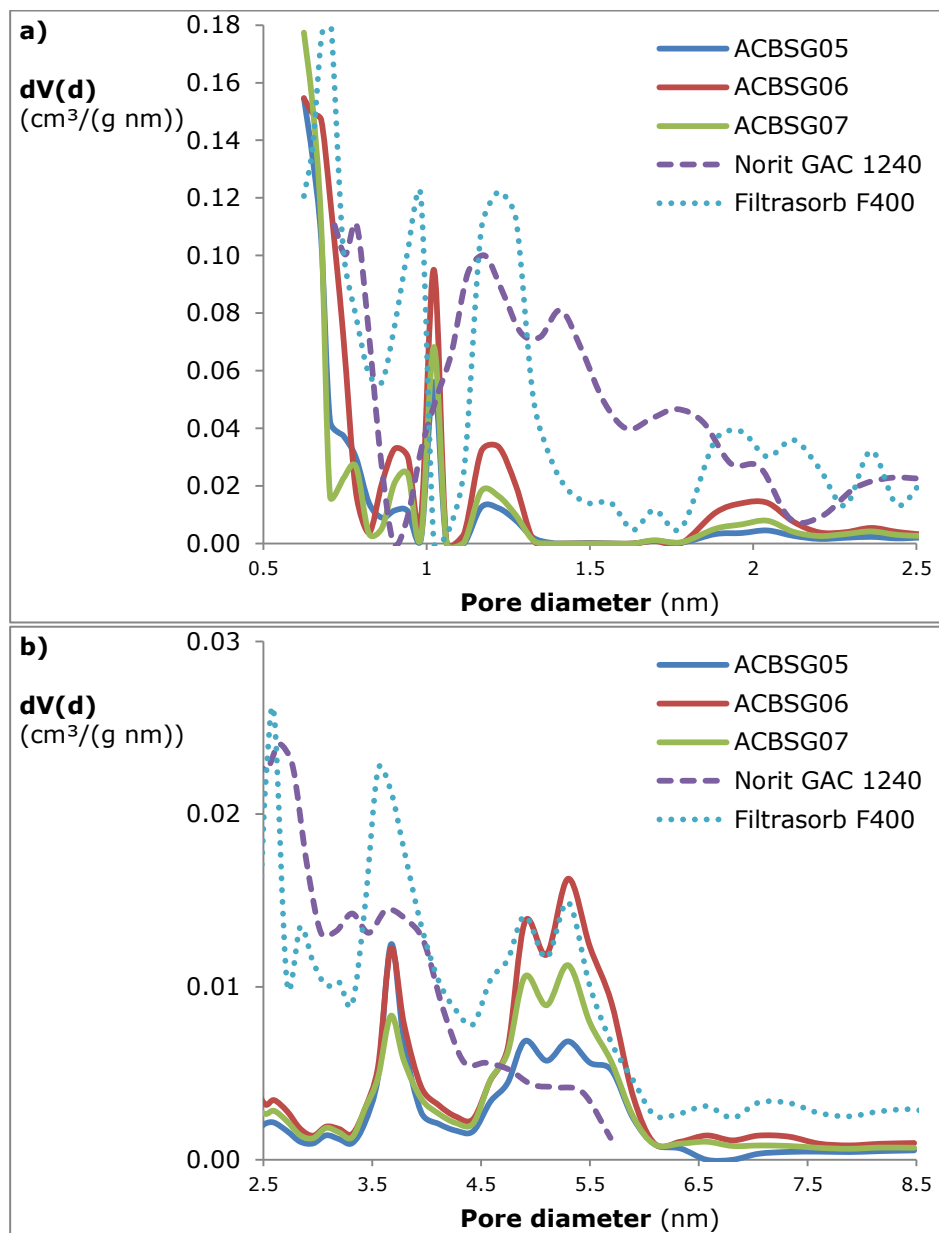


Figure 7-7: Pore size distribution of the activated carbons determined by DFT method for a) micropores; b) mesopores (2.5 – 8.5 nm)

7.4.5 Surface functionalities

In literature, it has been shown that activated carbons having a basic nature show enhanced adsorption capacity towards phenol whatever their textural characteristics are (Girods et al. 2009a). To have an idea of the basic nature of the selected activated carbons, the pH_{PZC} is determined and the basic and acid groups on the AC surface are measured by the acid-base titration method (see Table 7-5). In addition, X-ray photoelectron spectroscopy is performed on the samples. The pH_{PZC} for the activated carbons produced from BSG are 10.6, 10.8, 10.7 for ACBSG05, ACBSG06, ACBSG07 respectively and for the reference activated carbons 11.8 and 11.5 for Norit GAC 1240 and Filtrasorb F400 which are slightly higher, showing the basic character of the surface. However the amount of basic groups is significant higher for the ACBSGs. This is probably due to the higher amount of N (more than double) in the ACBSGs (EA of Filtrasorb F400 on a dry base (Velghe et al. 2012): N 0.7 wt%, C 83.4 wt%, H 0.7 wt%, O 1.4 wt% and 6.2 wt% ash; EA of Norit GAC 1240 on a dry base: N 0.7 wt%, C 87.0 wt%, H 0.4 wt%, O 2.5 wt% and 9.4 wt% ash (Vandewijngaarden et al. 2010)). As expected, the total surface acidity of the ACBSGs increased by increasing activation. The amount of basic groups decreases from ACBSG07 > ACBSG06 > ACBSG05.

Table 7-5. pH_{PZC} and amount of acid and basic group mounted on the surface

	pH_{PZC}	Acid groups (mmol/g)	Basic groups (mmol/g)
ACBSG05	10.6	0.7030	0.6468
ACBSG06	10.8	0.9588	0.7888
ACBSG07	10.7	0.7799	0.8036
Norit GAC 1240	11.8	0.9552	0.4753
Filtrasorb F400	11.5	0.5783	0.4666

The surface functionalities distribution and the carbon, oxygen and nitrogen atomic concentration of the activated carbons (Table 7-6) is investigated by X-ray photoelectron spectroscopy. The deconvolution of the C1s, N1s and O1s spectra by an iterative least-square fitting algorithm is used to provide a general picture of the concentration and distribution of the different functional groups taking into account the binding energies reported by Zhou et al. (2007), Arrigo et al. (2008) and Lorenc-Grabowska et al. (2012). Only small differences in carbon, nitrogen and oxygen content on the surface are detected for the carbons with an average atomic concentration of around 93 at%, 1.5 at% and 5.4 at% respectively. Despite the small changes the same trend as observed in the bulk concentration (elemental analysis, section

7.4.2) is noticed. The carbon content increases with increasing temperature and activation, while the oxygen and nitrogen content decreases. The C1s core level spectrum consists out of a major graphitic carbon peak at 284.4 eV and four different types of carbon atoms linked with nitrogen or oxygen namely, carbon in phenolic, alcohol, ether or C=N groups (286.0–286.3 eV); carbon in carbonyl, quinone or C-N groups (287.3–287.6 eV); carboxyl, ester and N=C-O groups (288.8–289.1 eV) and (290.5–291.2 eV) carbon in carbonate groups and/or adsorbed CO and CO₂. From the carbon bonding distribution in Table 7-6 it can be seen that a longer activation (e.g., ACBSG06, ACBSG07) gives rise to a higher aromatic structure i.e., larger graphitic peak. This graphitic peak accounts for more than half of the total surface concentration rising to 63 and 66 at% (67.5 and 71 % of the total carbon concentration) for ACBSG06 and ACBSG07 respectively. The less activated sample ACBSG05 has a higher contribution of phenolic, alcohol, ether or C=N groups (286.0–286.3 eV) and carbon in carbonyl, quinone or C-N groups (287.3–287.6 eV). This is also noticeable in the O1s spectra, the atomic concentration of oxygen is the highest in the case of ACBSG05. When combining the C1s and O1s spectra information on the oxygen functionalities on the surface can be obtained. Four different peaks are found by deconvolution of the spectra. The C-OH, C-O-C, C=O in esters, amides, anhydrides are the most abundant on the surface followed by the C-O-C in esters and anhydrides. Chemisorbed O₂ and H₂O varies between 13 and 9 % of the oxygen functionalities. The total atomic concentration of oxygen is the lowest for ACBSG06 and increases by lower heating and activation profiles. As for nitrogen, the temperature has an effect on the atomic surface concentration. The carbons prepared at 800 °C have a concentration around 1.56 at% which decreases to 1.29 at% by a pyrolysis temperature of 850 °C. Most of the surface nitrogen is present as quaternary nitrogen in all carbons. In contrast to literature (Lorenc-Grabowska et al. (2012)), the higher temperature carbon has a lower concentration of quaternary and pyridinic-N (N-6) concentration (ACBSG06 versus ACBSG07). The higher temperature gives rise to an increase in imine, amine and amide groups, which is probably promoted by the burning of the surface by steam. This could explain the higher amount of acidic groups determined in Table 7-5. The higher amount of basic groups in Table 7-5 for ACBSG07, could possibly be attributed to the high amount of pyridinic (N-6) groups present on the surface.

For reference the C1s, N1s and O1s spectra of the sample ACBSG07 is provided in Figure 7-8.

Table 7-6. XPS analysis of selected ACBSGs: Carbon, Oxygen and Nitrogen atomic concentration and the surface functionalities distribution derived from the C1s, O1s and N1s spectra

	Binding energy (eV)	ACBSG05	ACBSG06	ACBSG07
<i>C surface concentration (at%)</i>		92.65	93.76	93.11
C-C (aromatic and aliphatic, $\pi \rightarrow \pi^*$ delocated bondings)	284.4	50.34	63.24	66.29
Single C-O bond (C-OH, C-O-C, Csp ³) or C=N (aromatic rings), C-N	286.0	23.41	18.61	16.95
C=O, C=N, $\pi \rightarrow \pi^*$ shake-up satellite	287.4	10.86	4.61	4.21
Carboxyl, ester or N=C-O	289.1	5.52	4.41	3.73
carbonate groups and/or adsorbed CO and CO ₂	291.2	2.52	2.89	1.93
<i>N surface concentration (at%)</i>		1.54	1.29	1.58
N-6 (pyridinic)	398.1	0.32	0.28	0.44
N-5 (pyrrolic and pyridonic)	400.6	0.27	0.35	0.27
Imine, amine and amide	399.5	0.2	0.1	0.14
N-Q (quaternary N in aromatic graphene structure)	401.5	0.52	0.41	0.58
Pyridinic-N-oxide or ammonia	403.4	0.23	0.15	0.15
<i>O surface concentration (at%)</i>		5.81	4.95	5.32
C=O	530.6	0.5	0.32	0.58
C-OH, C-O-C, C=O in esters, amides, anhydrides	532.2	2.99	2.72	2.95
C-O-C in esters and anhydrides	533.8	1.59	1.28	1.31
Chemisorbed O ₂ , H ₂ O	535.8	0.73	0.63	0.48

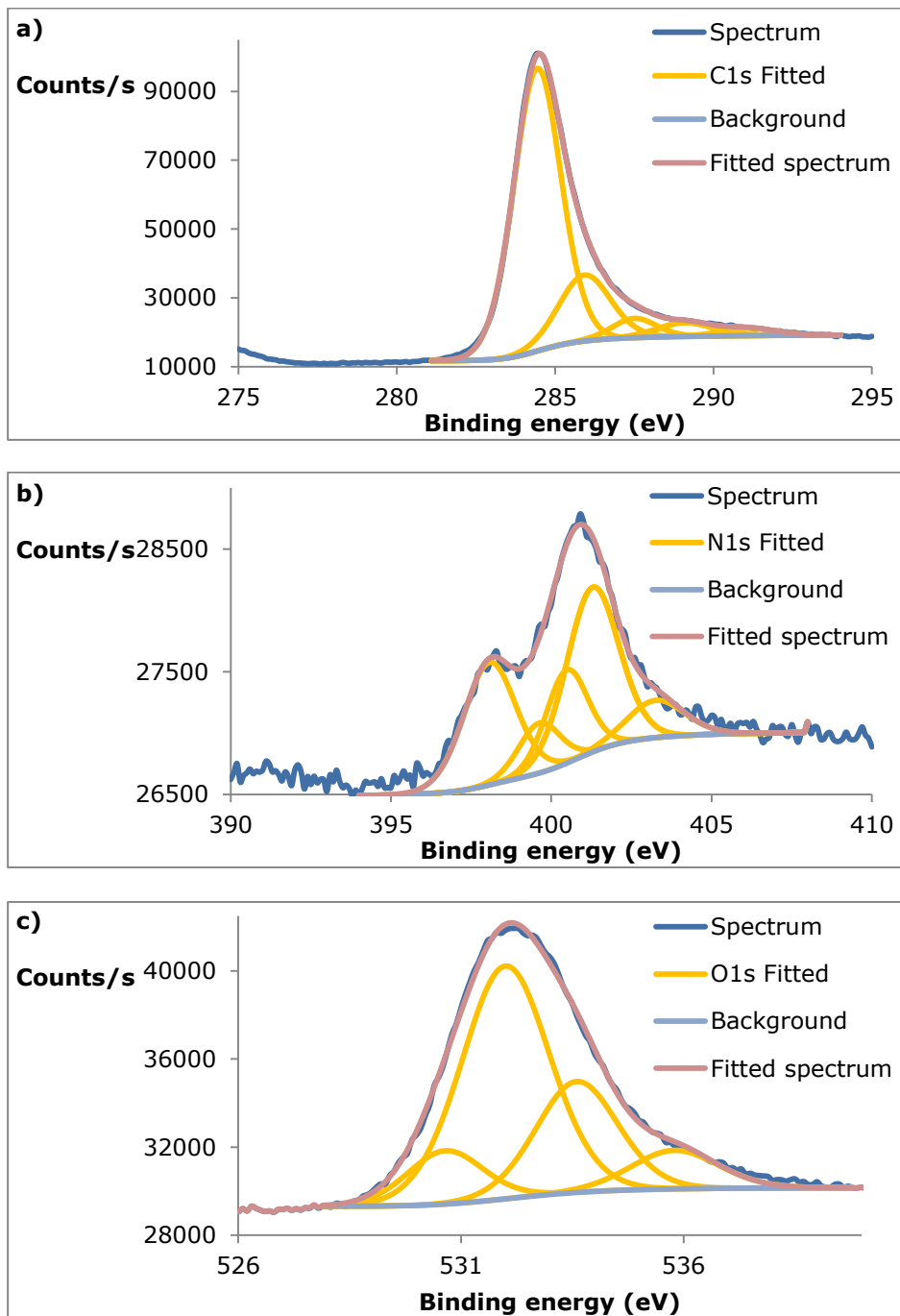


Figure 7-8: C1s, N1s and O1s XPS spectra of ACBSG07

7.4.6 Effect of contact time

Adsorption kinetics (shown in Figure 7-9) of phenol (25 ml 100 ppm phenol solution and 50 mg AC) are important for understanding the uptake rates of phenol on the surface of adsorbents and for determining the equilibrium times of adsorption. The experimental data were fitted (using the pseudo-first-order model (Eq. 1-11) and the pseudo-second-order model (PSO model) (Eq. 1-12).

$$\text{Eq. 1-11:} \quad Q_t = Q_e - Q_e e^{-K_f t}$$

$$\text{Eq. 1-12:} \quad Q_t = \frac{Q_e^2 K_s t}{1 + Q_e K_s t_e}$$

Where Q_e is the equilibrium adsorption capacity (mg/g), K_f (1/h) and K_s (g/mg h) are the pseudo-first-order model and pseudo-second-order model rate constants respectively. The PSO model predicts the behaviour over the entire range of the adsorption process (Hameed & Rahman 2008, Li et al. 2013). The pseudo-first-order model is generally only applicable over the initial state of adsorption (Hameed & Rahman 2008, Li et al. 2013). Table 7-7 lists the results of the kinetic constants of the models. The results indicate that the adsorption system followed the pseudo-second-order model with a high R^2 for all activated carbons. This could indicate that the rate-limiting step may be chemisorption (El-Naas et al. 2010, Hameed & Rahman 2008, Ho & McKay 1998). For Filtrasorb F400 and Norit GAC 1240 pseudo-first-order model fits equally. The results show that 16 h is sufficient to reach steady state. Around 80 – 90% of phenol is removed within the first 5 – 6 h. It is very interesting to see that the activated carbons from BSG all exhibit much higher removal rates than the commercial Norit GAC 1240 and Filtrasorb F400.

Table 7-7. Comparison of the pseudo-first-order and pseudo-second-order model by non-linear regression analysis

	Pseudo-first-order			Pseudo-second-order		
	Q_e (mg/g)	K_f (1/h)	R^2	Q_e (mg/g)	K_s (g/mg h)	R^2
ACBSG05	44.1	1.05	0.943	48.6	0.0332	0.989
ACBSG06	44.3	1.49	0.939	48.2	0.0495	0.988
ACBSG07	44.9	1.27	0.944	49.0	0.0417	0.988
Filtrisorb F400	50.1	0.386	0.987	57.2	0.0084	0.988
Norit GAC 1240	50.3	0.520	0.990	56.6	0.0123	0.986

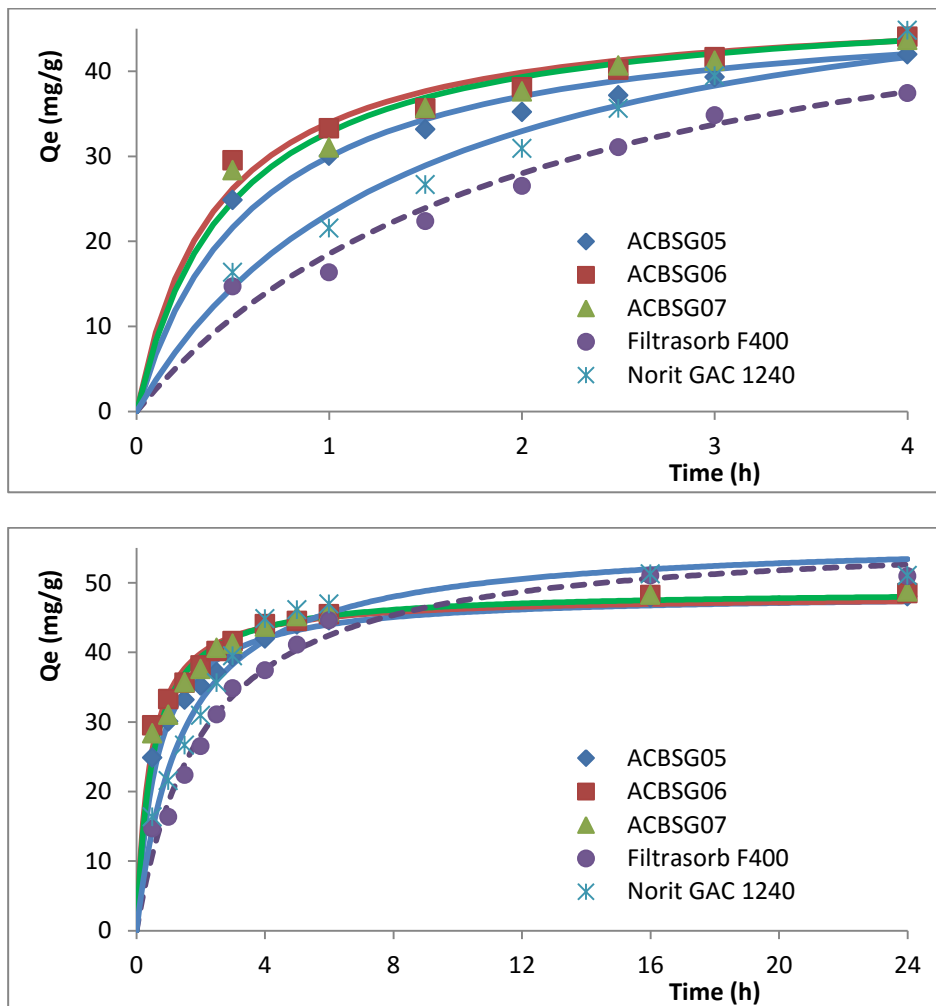


Figure 7-9. Effect of contact time on the phenol removal: pseudo-second-order model fitted to the experimental data points

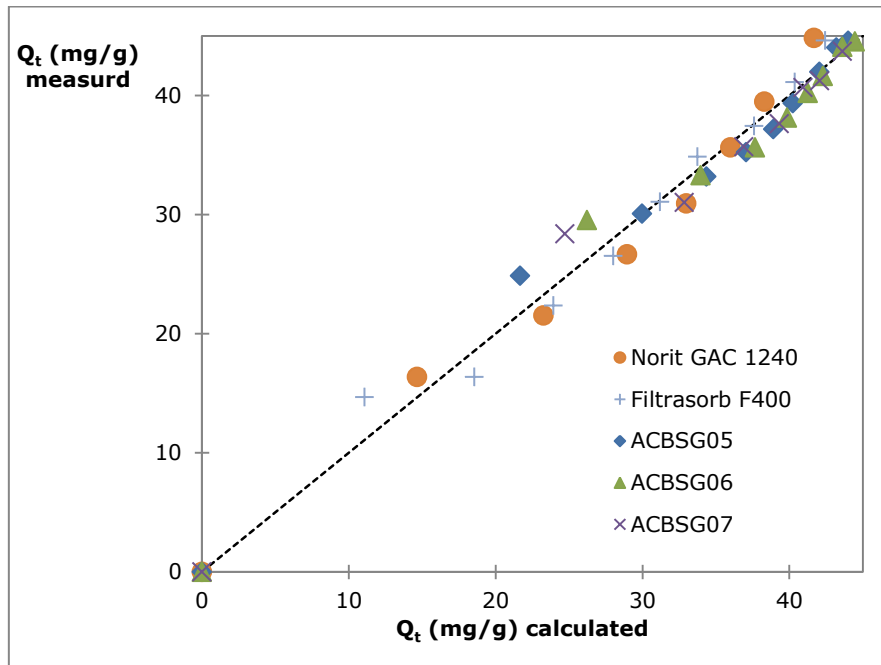


Figure 7-10. Deviation between the calculated by the pseudosecond-order model and the experimental adsorption capacity (Q_t)

7.4.7 Effect of pH, ionic strength and standard water

The **pH** is another key parameter in the adsorption of phenol since ionization of phenol (pK_a 9.98, 25°C) is strongly influenced by acidity, and thus its chemical form, neutral or negative loaded, in solution.

Figure 7-11 shows the effect of the initial pH (pH_i) on the adsorption of phenol (25 ml 100 ppm phenol, 20 mg AC). It can be concluded that the best adsorption results are obtained when the pH_i is around 8. For a pH_i lower than 8, the adsorption capacity will decrease rather slowly. This can be explained by the shielding effect of the hydrogen ions in the solution which will be attracted by the π -electrons of the phenolic ring and the positive charges on the AC surface. For pH_i higher than 11, a sudden drop (of adsorption capacity) is observed. This is probably due to electrostatic repulsion between the negative surface charge of the activated carbons ($pH_i > pH_{PZC}$ (Table 7-5)) and the negative charged phenolate ion ($pH > pK_a$). In addition, the adsorbed phenol molecules repulse each other.

The optimum range for phenol adsorption on the produced activated carbons is within a pH of 6 – 10 with a maximum at pH 8.

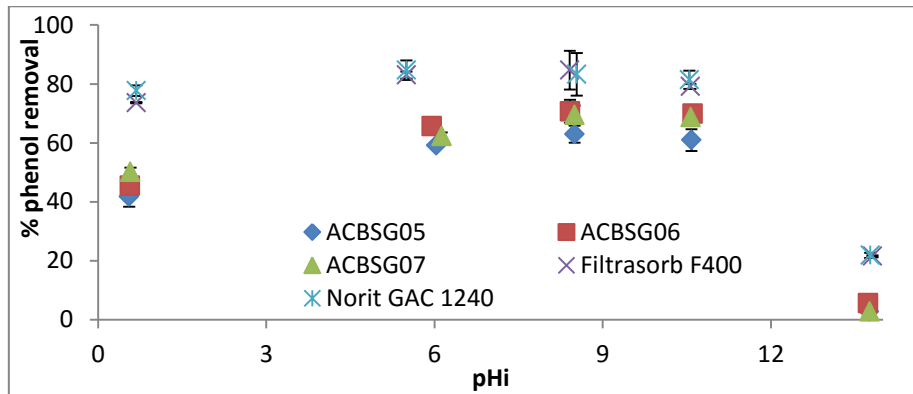


Figure 7-11. Effect of initial pH on the phenol removal

The effect of **ionic strength** (KCl) and a **standard water solution** of phenol on the adsorption capacity of the produced activated carbon is shown in Figure 7-12. The ionic strength of the solution does not have an influence on the adsorption capacity. From this result it can be deduced that the adsorption mechanism is probably not electrostatic: as the electrostatic forces between the carbons and the adsorbate are attractive, the adsorption capacity decreases by an increase in ionic strength (Al-Degs et al. 2008). When using the standard water phenol solution the adsorption capacity is a little bit lower (10 – 20 %). For the reference carbons no effect is seen.

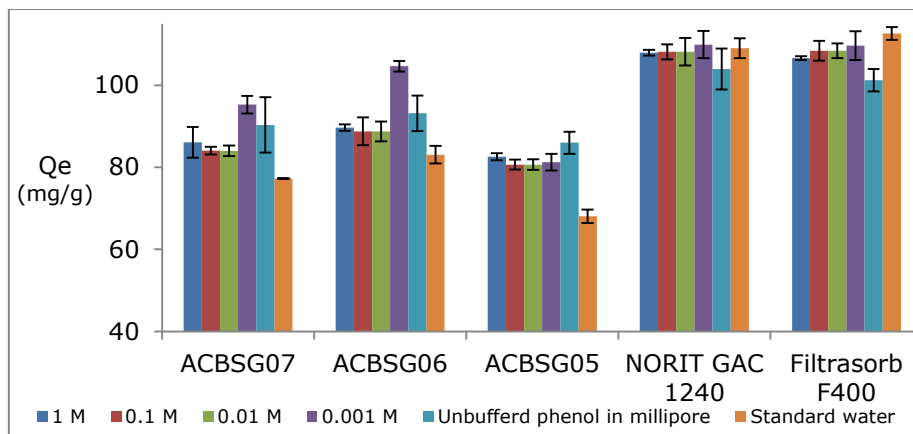


Figure 7-12: Effect of ionic strength and standard water on the phenol adsorption capacity

7.4.8 Economic evaluation

Except the quality and characteristics of the activated carbon it is also of utmost importance to investigate the feasibility of an AC production facility from Brewer's spent grain. This is investigated by the techno-economic model and process design proposed previously (Vanreppelen et al. 2011) for estimating the total capital investment, the production costs, the possible revenues and the NPV (all costs have been updated to 2011). By analysing the results it is necessary to keep in mind that the economic model is based on rather pessimistic assumptions (e.g., a first plant cost, not utilizing rest heat and recoverable chemicals from the produced gasses, etc.).

A brewery has two possibilities to valorise the brewer's spent grain as activated carbon. The first option is to produce the activated carbon onsite and thus build an activated carbon production facility near the brewery. In this case the brewery process quantity for activated carbon production is limited to its own BSG production capacity, an additional major advantage is a 0 EUR/t feed cost. In our case it is assumed that a brewery produces around 76 kt/year brewer's spent grain (25.5 wt% dry matter). The second possibility is to sell the brewer's spent grain at 38 EUR/t (= 149.12 EUR/t dry BSG in Belgium 2012) to an external activated carbon producer (who also built a complete new installation). This offsite facility has the advantage of buying brewer's spent grain from more breweries and is not limited in process quantity. Farmers often collect the brewer's spent grain free of charge (White et al. 2008). Nevertheless, by using this high selling price, a rather worst case scenario is applied.

Total capital investment, annual expenditure, minimum selling price and NPVs have been calculated for the **onsite** production facility for a processing capacity of 1 t/h (= 1/3 of 76 kton or 25.3 kton) and 2 t/h (54.9 kton) (Table 7-8 and Figure 7-13).

From Table 7-8 it can be seen that the total capital investment and total expenditure is about the same for every activated carbon from brewer's spent grain within one (i.e., 1 ton/h, 2 ton/h) processing capacity due to the little difference in yield (see Figure 7-3).

Based on the quality of the produced activated carbon (high adsorption rate and phenol removal capacity) the expected selling price is estimated (based on (Girods et al. 2009a, Girods et al. 2008a, Infomil 2011, Kuppens 2012, Vanreppelen et al. 2011)) to be around 2.0 - 2.5 kEUR/t. From Figure 7-13 it can be inferred that for a 1 t/h processing facility onsite it would not be feasible to produce ACBSG06. ACBSG05 and ACBSG07 are feasible when the selling price is minimum 2.2 kEUR/t and 2.3 kEUR/t resulting in a NPV of 2.7

MEUR and 1.7 MEUR respectively at a selling price of 2.5 kEUR/t. As a consequence of the economies of scale, doubling the processing capacity augments the total capital investment and total expenditure with only 46 % and 47 % respectively. The break-even selling price decreases on average with 21 %. The NPVs increases from 2.7 – 13.4 MEUR and 1.7 – 11.4 MEUR in the selected price range respectively. Nevertheless, loss of income from selling the brewer's spent grain needs to be incorporated in the selection criteria. For the processing of 1 t/h (25.3 kton) the loss of income is around 960 kEUR (not discounted). Incorporating this still feasible NPV's are obtained for the production of ACBSG05 and ACBGS07.

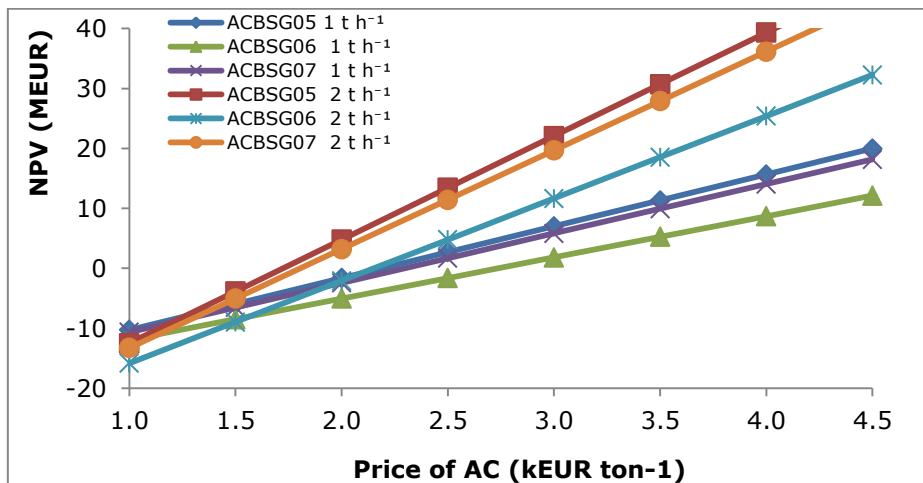


Figure 7-13: NPV for a 1 t/h and 2 t/h onsite production facility

Table 7-8: Total capital investment, annual expenditure and minimum selling price for the production of AC onsite

BSG production onsite 1 t/h				
		ACBSG05	ACBSG06	ACBSG07
Total investment	capital	10,365 kEUR	10,301 kEUR	10,359 kEUR
Expenditure				
-	Feed cost	0 EUR	0 EUR	0 EUR
-	Operating cost + yearly interest	1,653 kEUR	1,642 kEUR	1,651 kEUR
-	Total	1,653 kEUR	1,642 kEUR	1,651 kEUR
Minimum selling price		2.2 kEUR/t	2.7 kEUR/t	2.3 kEUR/t
BSG production onsite 2 t/h				
		ACBSG05	ACBSG06	ACBSG07
Total investment	capital	15,178 kEUR	15,084 kEUR	15,169 kEUR
Expenditure				
-	Feed cost	0 EUR	0 EUR	0 EUR
-	Operating cost + yearly interest	2.428 kEUR	2.411 kEUR	2.425 kEUR
-	Total	2.428 kEUR	2.411 kEUR	2.425 kEUR
Minimum selling price		1.7 kEUR/t	2.2 kEUR/t	1.8 kEUR/t

The results for the **offsite** facility for 1 and 2 t/h are shown in Figure 7-14 and Table 7-9. It is clear that in the selected price range there is no AC from BSG that can be produced on a feasible manner based on this (pessimistic) model. This is due to the high expenditure cost, 63 % and 77% higher than the onsite facility of 1 t/h and 2 t/h resulting from the very high feed cost (149 EUR/t dry BSG). Nevertheless, the offsite facility has also the advantage of unlimited supply of BSG. By calculating a 5 t/h facility the

Chapter: 7

minimum selling price for ACBSG05, ACBSG06 and ACBSG07 is 2.1 kEUR/t, 2.6 kEUR/t and 2.1 kEUR/t respectively. This makes the production facility profitable for ACBSG05 and ACBSG07 even in the rather pessimistic scenario.

However, in this calculation the produced gasses are not fully incorporated since only a part is used for the production of the desired heat. For example, the rest heat can be sold or supplied to other factories nearby and thus generate income and improve the feasibility.

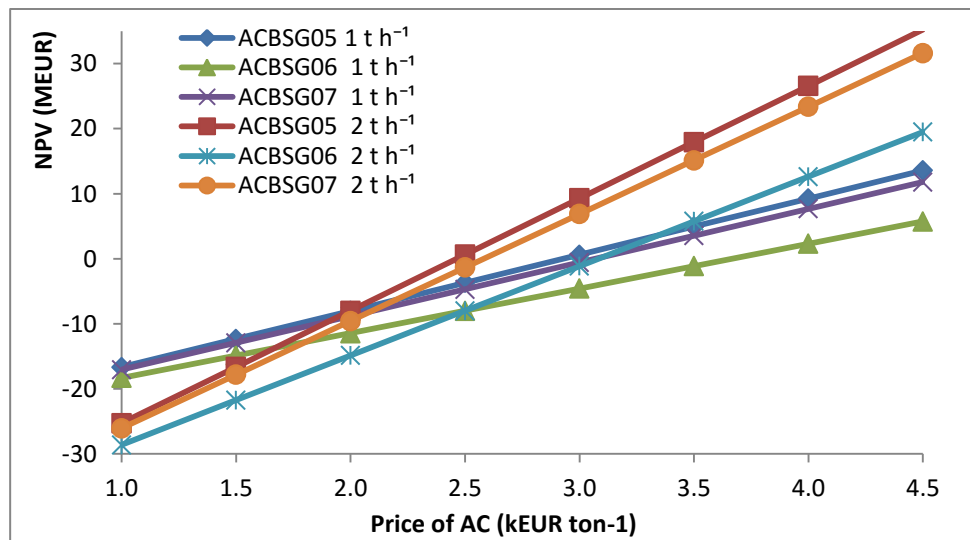


Figure 7-14: NPV for a 1 t/h and 2 t/h offsite production facility

Table 7-9: Total capital investment, annual expenditure and minimum selling price for the production of AC offsite

BSG production offsite 1 t/h				
		ACBSG05	ACBSG06	ACBSG07
Total investment	capital	10.365 kEUR	10.301 kEUR	10.359 kEUR
Expenditure				
- Feed cost		1.044 kEUR	1.044 kEUR	1.044 kEUR
- Operating cost + yearly interest		1.653 kEUR	1.642 kEUR	1.651 kEUR
- Total		2.697 kEUR	2.686 kEUR	2.695 kEUR
Minimum selling price		2.9 kEUR/t	3.7 kEUR/t	3.1 kEUR/t
BSG production offsite 2 t/h				
		ACBSG05	ACBSG06	ACBSG07
Total investment	capital	15.178 kEUR	15.084 kEUR	15.169 kEUR
Expenditure				
- Feed cost		1.879 kEUR	1.879 kEUR	1.879 kEUR
- Operating cost + yearly interest		2.429 kEUR	2.411 kEUR	2.425 kEUR
- Total		4.308 kEUR	4.290 kEUR	4.304 kEUR
Minimum selling price		2.5 kEUR/t	3.1 kEUR/t	2.6 kEUR/t

7.5 Conclusion

Brewer's spent grain (BSG) is a widely available, low cost residue representing around 85% of the total by-products generated by the brewing industry. Its composition (high nitrogen content 4.35 wt%, fibres, ...) makes BSG very useful for the production of high added value in-situ nitrogenised activated carbon. The in-situ nitrogen presence will result in a considerably

reduced production cost in comparison with post impregnation of nitrogen containing components on AC. In addition, nitrogenised activated carbon is seen as a key parameter for the adsorption properties of activated carbons, especially for the removal of phenolic compounds.

Different activated carbons were produced in a lab-scale pyrolysis and activation reactor by applying several heat and steam activation profiles on Brewer's spent grain. Activated carbon yields from 16.1 – 23.6 wt% were obtained. The effectiveness of the high nitrogen content activated carbons prepared from brewer's spent grain towards phenol in aqueous solution was evaluated by performing isothermal adsorption studies (100 ppm phenol) relative to two reference activated carbons (Filtrisorb F400 and Norit GAC 1240). The prepared activated carbons show high N-contents ranging from 2.12 wt% up to 3.84 wt% compared to 0.7 wt% for the reference activated carbons. It was observed that a higher activation temperature resulted in a higher adsorption capacity, nevertheless they are comparable except for the one obtained at 800°C and 5 ml H₂O of steam activation (ACBSG01). The steam activation has a strong influence on the adsorption capacity. The Langmuir and Freundlich data show that adsorption is a favourable process. The Freundlich model fits the results the best. Based on the isothermal adsorption studies 3 activated carbons (800 °C and 10 ml H₂O of steam activation (ACBSG05), 850 °C and 15 ml H₂O of steam activation (ACBSG06), 800 °C and 10 ml H₂O of steam activation (ACBSG07)) were selected which have similar removal efficiencies than the reference carbons. The adsorption capacities (Q_m 50.3 – 111.3 mg/g based on Langmuir) are lower than those of the reference activated carbons (Q_m 160 – 166 mg/g based on Langmuir). Nevertheless, the kinetics revealed that the produced activated carbons have higher adsorption rates than the reference carbons. After 5 – 6 h 80 – 90 % of phenol is removed. The optimum range for phenol adsorption on the produced activated carbons is within a pH of 6 – 10 with a maximum at pH 8.

The feasibility of an activated carbon production facility (onsite and offsite) which processes brewer's spent grain for different input feeds is evaluated based on a previously developed techno-economic model (Vanreppelen et al. 2011). Even though the current model assumptions start from a rather pessimistic scenario (e.g., a first plant cost, etc.) encouraging results for a profitable onsite production of AC using BSG by-products are obtained. The minimal selling prices for a 2 t/h is for ACBSG05 and ACBSG07 1.7 en 1.8 kEUR/t. When taking into account that the investment cost is based on a first plant cost of a fluidized bed pyrolysis reactor the total investment cost could dramatically be reduced. Furthermore, subsidy and other financial benefits, utilising rest heat, ... would alter the results of the activated carbon production facility towards lower minimal selling prices.

8 Adsorption screening of pharmaceutically active compounds

The results of this chapter will be submitted for publication.

8.1 Abstract

Pharmaceutically active compounds are being identified as emerging contaminants and are frequently detected in environmental waters such as drinking, surface and ground water. Three pharmaceutical active compounds (Ibuprofen, Diclofenac and Sulfamethoxazole), are selected based on their medium to high risk to the aquatic life and their frequent use and/or their use over long period of time. The removal of the selected target compounds from aqueous solutions is investigated using high valuable activated carbons prepared from industrial waste and by-products. Based on the results of the screening assay, three activated carbons and one reference carbon is selected for further investigation by an equilibrium and kinetic assay. The equilibrium and kinetic assay reveal high and fast adsorption capacities up to 180 mg/g exceeding the reference carbon.

8.2 Introduction

Pharmaceutically active compounds (PhAcs) are developed to promote health and wellbeing for humans and animals. However, recently, pharmaceutically active compounds and their metabolites have been identified as emerging contaminants and are frequently detected in environmental waters such as drinking, surface and ground water (Al-Khateeb et al. 2014, Delgado et al. 2012, Jung et al. 2013b, Khraishah et al. 2014, Rivera-Utrilla et al. 2013). A first entering route of pharmaceutically active compounds into environmental waters is via excreta, as a considerable amount of the dose taken is not adsorbed by the body (Baccar et al. 2012). In addition, large amounts of unused (overtime) human and veterinary drugs are flushed down the toilet into the sewage system (Baccar et al. 2012, Feng et al. 2013). For example, in Germany 60 – 80 % of the pharmaceuticals (9.5 – 12.8 ktonnes) are being disposed by flushing or by normal household waste each year (Feng et al. 2013). Pharmaceuticals are specially designed for a long shelf-life and are resistant and persistent in aquatic ecosystems (Calisto et al. 2015). Most of the active compounds are not or slightly affected by the wastewater treatments plants (biological or conventional chemical processes) (Al-Khateeb et al. 2014, Baccar et al. 2012, Calisto et al. 2015, Feng et al. 2013, Jung et al. 2013b, Rivera-Utrilla et al. 2013, Verlicchi et al. 2012). It

is known that pharmaceuticals (and pharmaceutically active compounds) may not only target human or animal specific metabolic pathways but can also affect non-target organisms (Feng et al. 2013). Even at very low concentrations they may cause subtle, chronic effects on ecosystems (Al-Khateeb et al. 2014, Verlicchi et al. 2012). In addition, they pose a potential long-term risk due to their bio-accumulation in aquatic and terrestrial organisms (Al-Khateeb et al. 2014). Even, very little is currently known about the synergetic, chronic exposure to trace levels of multiple pharmaceutically active compounds and other chemicals (Delgado et al. 2012, Feng et al. 2013, Rivera-Utrilla et al. 2013). Paradoxically, the increasing consumption of pharmaceuticals, is increasing the exposure and is causing a threat to our health. The removal of these compounds is an emerging and real issue in water treatment plants and drinking water preparation (Delgado et al. 2012, Feng et al. 2013). A significant amount of research is focussed during the last decade on the removal of pharmaceutical active compounds by conventional water treatment options such as flocculation, filtration, activated sludge, chlorination revealing the ineffective removal of these compounds (Calisto et al. 2015, Rivera-Utrilla et al. 2013).

Due to its versatility and efficiency, adsorption on activated carbon it is seen as the most promising and interesting solution for removing the pharmaceutically active compounds (Baccar et al. 2012, Mestre et al. 2014). The main advantage of activated carbon is the ability to remove the drugs without generating toxic or pharmacologically active compounds (Rivera-Utrilla et al. 2013). As part of the transition to a more circular economy, three residues (brewer's spent grain, particle board glued with urea formaldehyde and particle board glued with melamine urea formaldehyde) are selected as precursors for the production of high value activated carbon for the remediation of water contaminated with pharmaceutical active compounds. Brewer's spent grain (BSG) represents around 85% of the total by-products generated by the brewing industry (Aliyu & Bala 2011, Cook 2011, Gupta et al. 2010, Mussatto 2013, Mussatto et al. 2006). Traditionally this material has been landfilled or sold as animal feed (Cook 2011, Gupta et al. 2010). However, BSG is difficult to store, increases methane emission due to this hard to digest material (Cook 2011) and the numbers of agricultural businesses are decreasing, resulting in a considerable decline in prices for brewer's spent grain. Particle board is an engineered wood product made from woodchips, low grade logs such as thinnings, twisted/bowed logs, knots, branches, stumps, wood waste glued with aminoplast adhesives (urea formaldehyde and melamine urea formaldehyde). The resulting product is used for furniture, building, ... The world production of particle board in 2013 was 99.28 Mm³, with Europe (47.7 %) as major producer followed by America (34.6 %) and Asia (15.5 %) (FAOStat 2015). As every product,

particle board has a limited service life. Garcia & Freire (2014) estimated that the average service life is around 10 years for wood-based panels. Reuse of this material is often limited due to the harsh environments where particle boards have been used (BFM 2004, Harwell 2010). Also recycling of the panels is difficult as the size of the wood particles often is reduced (Harwell 2010). For example, the use of reject panels and off-cuts for the production of new particle board panels is usually less than 5 % because of the desired chip geometry and the final panel properties (Wrap 2007).

Three pharmaceutical active compounds are selected as target compounds based on their medium to high risk to the aquatic life and their frequent use and/or their use over long period of time namely: Ibuprofen (IBP), Diclofenac (DCF) and Sulfametoxazole (SMX) (Baccar et al. 2012, Feng et al. 2013, Verlicchi et al. 2012). All of them are defined by the Global Water Research Coalition (Voogt et al. 2009) as high priority pollutants. SMX, an antibiotic, can persist in the environment for more than a year (Rivera-Utrilla et al. 2013) and is seen as a compound with high risk to aquatic life (Verlicchi et al. 2012). The wide spread occurrence of antibiotics increases the potential of bacteria to become antibiotic-resistant. DCF and IBP, both anti-inflammatory and analgesic drugs, are hugely consumed and have high acute toxicity to aquatic life and birds (i.e., vultures) (Feng et al. 2013). In addition, IBP is suspected to have endocrine disrupting activity in human and wildlife (Feng et al. 2013).

In this research, high value activated carbons are used from brewer's spent grain and two particle board samples for the adsorption of SMX, DCF and IBP. For this purpose, different activated carbons are prepared (based on previous research, see chapters 5,7 and 6) after thermal treatment in an oxygen deficient environment and subsequent steam activation. The adsorption of the pharmaceutically active compounds is assayed (in comparison with two reference activated carbons) in three sequential types of assays: e.g., screening assay, equilibrium assay and kinetic assay.

8.3 Methods and materials

In the **screening assay** the produced activated carbons along with the reference activated carbons are evaluated as potential sorbents for the selected pharmaceuticals. 20 mg of sorbent is added to 25 ml of the target pharmaceutical compound solutions (40 mg/l). The compound solutions are prepared in Milli-Q water without pH adjustment. The screening assay is used to select the three best performing activated carbons and the best performing reference carbon. **Equilibrium assay** of the selected AC's from the screening assay are performed using batch experiments. pharmaceutically active compounds solutions (40 ppm) are made in

reconstructed fresh water medium; 25 ml of these solution is brought into contact with different quantities of AC (5, 10, 20, 30, 40, 60 and 100 mg) in hermetically closed flasks. Reconstructed water (blank) and adsorbent-free controls are run in parallel.

For both the screening and equilibrium assay the residual concentration and the pH of the solution are determined after a contact time of 24 h (shaking) in a water bath (25 °C). The residual concentration is determined by collecting an aliquot from the solution and filtered through a 0,45 µm PTFE membrane filter in a 2 ml vial, and analysed using a high-performance liquid chromatograph (Agilent 1100) equipped with a photo diode array detector and a Zorbax SB-C18 column from Agilent (75 * 4.5 mm; 3.5 µm). A gradient elution of 0,1 % H₃PO₄:acetonitrile (75:25, v/v) for 1 min followed by 0,1 % H₃PO₄:acetonitrile (70:30, v/v) at a constant flow of 1 ml/min for 9 min is applied. The pharmaceutically active compounds are measured at a wavelength of 195 nm and eluted from the column at 2.37 (SMX), 8.51 (DCF) and 8.80 (IBP) min respectively. Calibration is carried out using a series of standard solutions prepared in methanol (concentration range: 0.5, 1, 5, 10, 50 and 100 ppm). Milli-Q water, subjected to a similar procedure as the unknown samples is used as a blank and adsorbent-free controls are run in parallel.

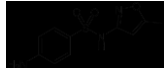
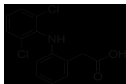
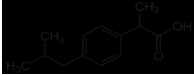
In the **Kinetic assay**; 25 mg of the selected AC's is weighted and placed in the double walled slurry batch reactor connected with a computer controlled Pharmacia Biotech Ultraspec 2000 UV-VIS spectrophotometer (as described in section 2.5.2.2). 50 ml of PhAC solution, 40 ppm in reconstructed water, is added and the concentration is measured at 254 and 278 nm for DCF and SMX, and at 210 and 230 nm for IBF until equilibrium.

8.4 Results and discussion

8.4.1 Screening assay

The potential of the different AC's for the adsorption of IBP, SMX and DCF are initially evaluated by a screening assay. Table 8-1 displays the structure and some physicochemical properties of the pharmaceutical active compounds under investigation

Table 8-1: Molecular structure, solubility and pK_a values of the PhACs (Jung et al. 2013a)

	<i>Structure</i>	pK _a	Water solubility (g/l)	Dimensions (l*/b*h; nm)
Sulfamethoxazole (C ₁₀ H ₁₁ N ₃ O ₃ S)		5.81	0.459	1.269*0.607*0.345
Diclofenac (C ₁₄ H ₁₁ Cl ₂ NO ₂)		4.15	0.004	1.014*0.719*0.484
Ibuprofen (C ₁₃ H ₁₈ O ₂)		4.52	0.049	1.098*0.531*0.433

The removal efficiencies of the produced carbons in comparison with two reference carbons namely Filtrasorb F400 and Norit GAC 1240 are evaluated for the three selected pharmaceutical active compounds after 24 h of contact time. The removal efficiencies of the different activated carbons for the pharmaceutical active compounds are displayed in Figure 8-1. The dashed boxes represent the removal efficiencies of the reference carbons for the different pharmaceuticals. The reference carbons remove between 86.4 and 91.2 % of SMX, 89.3 and 93.6 of DCF and 88.8 and 93.5 % of IBP for Filtrasorb F400 and Norit GAC 1240 respectively. Norit GAC 1240 consequently performs better, and is selected as reference activated carbon for the equilibrium and kinetic assay. The removal efficiencies of the produced carbons reveal a great influence of its production history. The results indicate that a lower pyrolysis temperature and a shorter steam activation results in lower removal efficiencies. The samples produced with a pyrolysis temperature of 850 °C and 45 min of steam activation (ACPBUF06, ACPBMUF06 and ACBSG06) show high removal which are similar or even

higher than those of the reference carbons and are selected for a more detailed study.

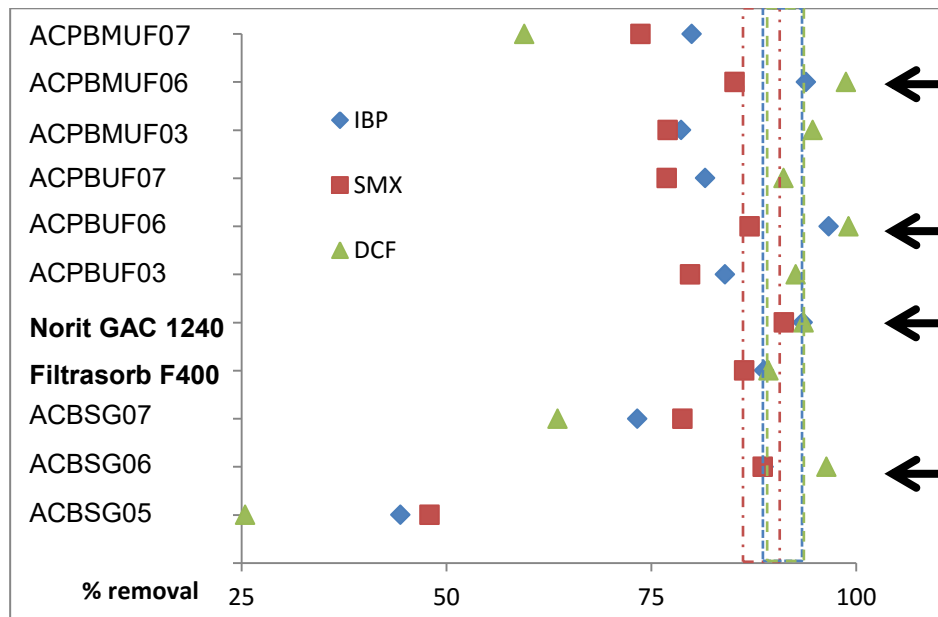


Figure 8-1: Screening assay for the adsorption of IBP, SMX and DCF on activated carbons produced from brewer's spent grain ACBSF) and particle board glued with melamine urea formaldehyde (ACPBUMUF) and urea formaldehyde (ACPBUF)

8.4.2 Equilibrium assay

Figure 8-2 illustrates the IBP, SMX and DCF adsorption isotherms on the selected carbons. Most of them belong to the L3/L4 type in the Giles classification (Giles et al. 1960), showing a steep initial rise and a concave curvature at low equilibrium concentration followed by a plateau. At higher equilibrium concentrations an upward curvature is seen, which is followed by a plateau in some cases.

For SMX and IBP the carbon from particle board glued with melamine urea formaldehyde (ACPBUMUF06) performs similar as the reference carbon, for DCF it performs significant higher. The particle board glued with urea formaldehyde (ACPBUF06) performs clearly the best for all pharmaceutical active compounds. The activated carbons experimentally produced from brewer's spent grain yield the lowest adsorption capacities. The initial pH

solution, 7.7, 7.9 and 8.1 for IBP, SMX and DCF respectively, increased in every experiment until maximum of 8.5, in the case of IBP the increase is limited to a pH of 8.2 (shown in Figure 8-3). In the case of the ACPBMUF06 the pH increases with increasing carbon dosage to 9.9, 9.8 and 9.8 for the solution of IBP, SMX and DCF respectively. For ACPBUF06 the pH increases to 9.4, 9.4 and 9.5. However, the pH steadily increased with increasing carbon dosage, the largest increase is realised in the carbon dosage of 0 – 1 g/l.

The obtained isotherms are nonlinear modelled with the Langmuir and Freundlich equation listed in Table 8-2. All selected activated carbons are best modelled by the Freundlich model. However, even this model is not able to fit the isotherms well. The reason should be found in the upward curvature of the Q_e - C_e plot at higher pharmaceutical active compounds concentration, what is not that usual. The Freundlich n values for ACPBMUF06 are significant higher compared to the adsorption of IBP and DCF reference activated carbon. For ACPBUF06 only for IBP a considerable higher n value compared to the reference activated carbon is found.

Based on the results (calculated from Figure 8-2 and the graph carbon dosage – C_e not shown in this dissertation), very low carbon dosages are necessary for completely removing the pharmaceutical active compounds. For IBP, carbon dosages are around 2, 2, 0.83 and 1.4 g/l for ACPBMUF06, ACBSG06, ACPBUF06 and Norit GAC 1240 respectively. For SMX no significant differences are found, with carbon dosages around 2 g/l for all carbons. In the case of DCF the carbon dosages are 1.1, more than 2 (estimated around 2.2), 0.9 and 1.4 g/l respectively for ACPBMUF06, ACBSG06, ACPBUF06 and Norit GAC 1240. Based on this result it is clear that ACPBUF06 performs the best in removing the selected pharmaceutical active compounds. This can also be concluded from the comparison of K_F values in Table 8-2. ACPBMUF06 performs second best followed by Norit GAC 1240. ACBSG06 performs the worst of all selected carbons especially for IBP with a K_F value of 15.3 versus 34.5 for Norit GAC 1240.

Table 8-2: Langmuir and Freundlich constants based on nonlinear modelling of the experimental equilibrium data points

	Langmuir				Freundlich		
	Q_m (mg/g)	K_L (l/mg)	R_L (calculated)	R^2	K_F ($\text{mg}^{1-(1/n)} \text{l}^{1/n}/\text{g}$)	n	R^2
ACPBMUF06							
IBP	101.4	0.41	0.05	0.877	43.4	4.01	0.913
SMX	117.9	0.27	0.08	0.947	32.4	2.59	0.986
DCF	159.1	0.86	0.03	0.860	69.2	3.46	0.905
ACPBUF06							
IBP	107.7	8.77	0.00	0.737	79.4	6.93	0.978
SMX	122.3	0.43	0.05	0.962	39.1	2.81	0.985
DCF	191.7	0.31	0.07	0.919	59.1	2.77	0.989
ACBSG06							
IBP	169.3	0.04	0.39	0.864	15.3	1.98	0.852
SMX	67.7	0.45	0.05	0.805	23.4	2.97	0.931
DCF	86.1	0.35	0.06	0.919	27.5	2.90	0.923
Norit GAC 1240							
IBP	136.0	0.30	0.07	0.915	41.2	2.77	0.942
SMX	101.0	0.44	0.05	0.867	34.5	2.89	0.967
DCF	127.0	0.29	0.08	0.885	36.1	2.70	0.971

Chapter: 8

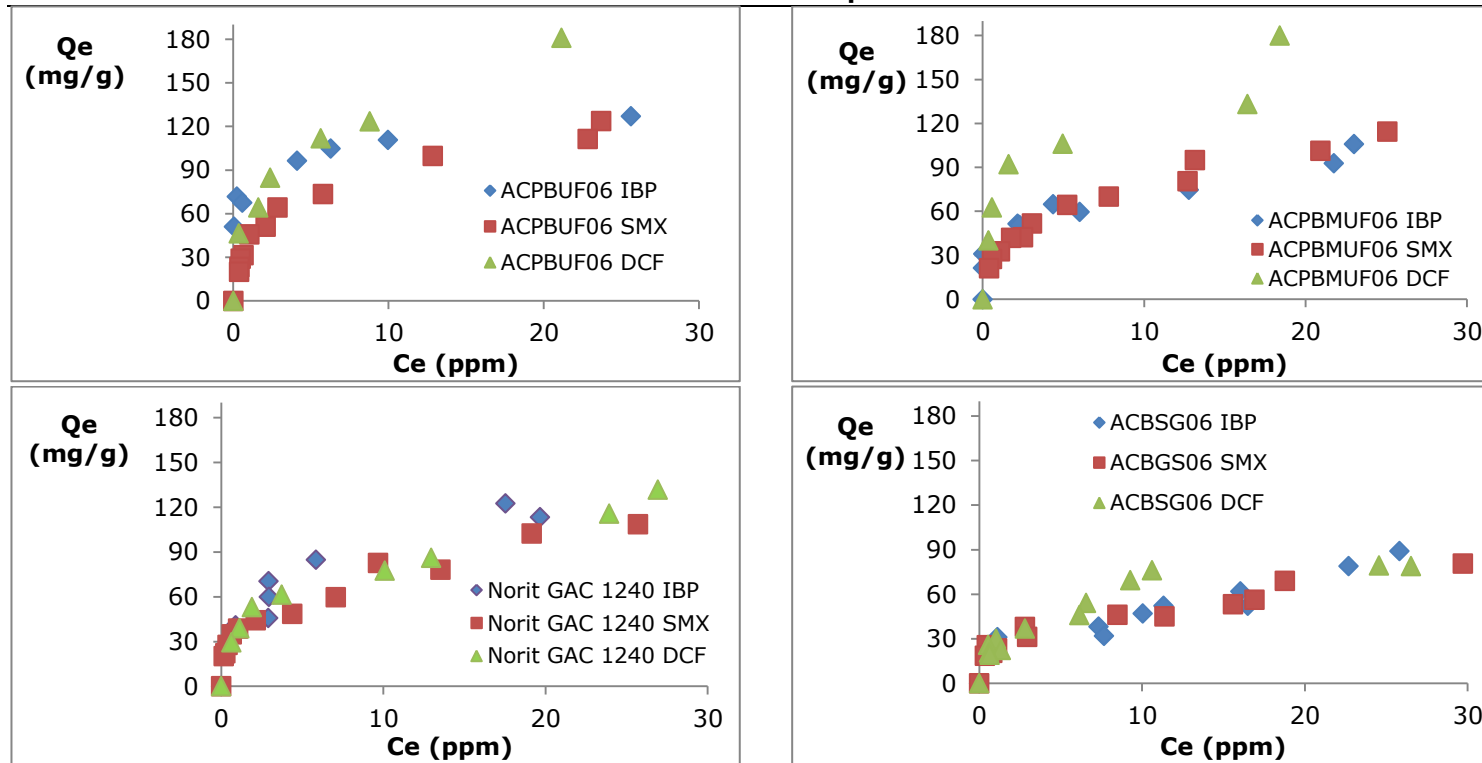


Figure 8-2: Equilibrium assay

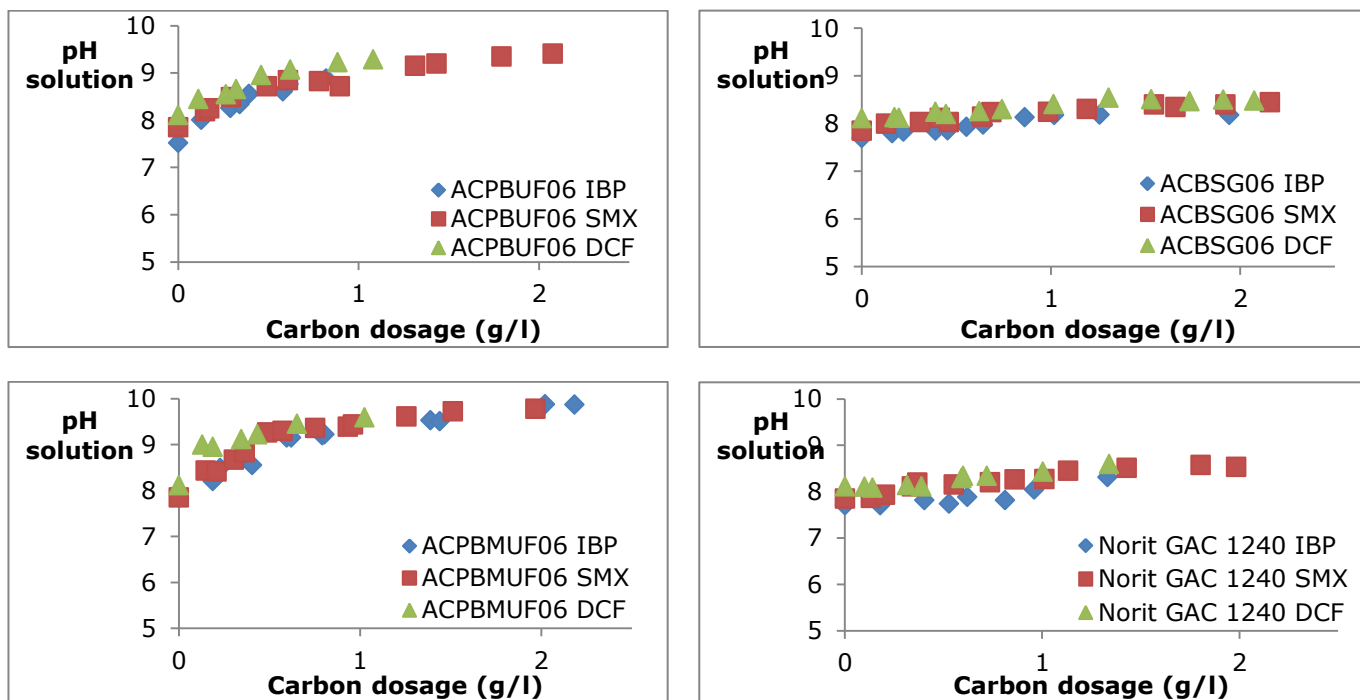


Figure 8-3: Final pH pharmaceutical active compounds solution in function of activated carbon dosage

8.4.3 Kinetic assay

The rate of adsorption of the different pharmaceutical active compounds in a standard fresh water medium on the selected activated carbons is evaluated by measuring the concentration change in function of the time. The residual pharmaceutical active compounds concentration in the fresh water medium in function of the time for the different produced activated carbons is displayed in Figure 8-5. The results of the nonlinear modelling with the pseudo-first-order model and the pseudo-second-order model (see Eq. 1-11 and Eq. 1-12 respectively) are listed in Table 8-3. The pseudo-first-order model has a somewhat lower R^2 values for all experimentally produced activated carbons and for the adsorption of SMX on Norit GAC 1240. The adsorption of IBP and DCF on Norit GAC 1240 yields a similar R^2 for the pseudo-first-order and pseudo-second-order model. The SSE values obtained for these adsorption experiments are used for further selection of the best fitting model. The SSE values for the pseudo-first-order model are 229 for IBP adsorption and 461 for DCF adsorption on Norit GAC 1240. The pseudo-second-order model obtains lower SSE values 119 and 158, for IBP and DCF respectively. Based on these results the pseudo-second-order model describes the experimental results the best. The graphs in Figure 8-5 indicate a faster adsorption rate for the produced activated carbons than the reference carbon. This is also observed in the higher K_f and K_s values obtained from the nonlinear modelling. The obtained Q_e values are for all activated carbons around 40 mg/g with a carbon dosage of 0.5 g/l. Norit GAC 1240 yields a little higher value for IBP and DCF. With the same carbon dosage in the equilibrium assay ACPBUF06 and ACPBMUF06 yield higher Q_e values. This is probably attributed to the experimental conditions as a small part of the produced activated carbons "crawls" up the wall of the beaker (during the kinetic assay). When using small quantities of activated carbon as in these experiments (25 mg activated carbon) this loss of activated carbon in solution becomes significant giving rise to lower modelled Q_e values. In the case of Norit GAC 1240 this effect of "crawling" is not observed. Nevertheless, Figure 8-5 and the K_s values in Table 8-3 demonstrate clearly that the PhACs uptake on the produced carbons is a much faster process (2 – 3 times) in comparison with the reference activated carbons.

Table 8-3. Comparison of the kinetic constants obtained by non-linear regression analysis of the pseudo-nth-order model

	Pseudo-first-order				Pseudo-second-order			
	Q _e (mg/g)	K _f (1/h)	R ²	SSE	Q _e (mg/g)	K _s (g/mg h)	R ²	SSE
ACPBMUF06								
IBP	32.6	0.66	0.955	1844	38.1	0.022	0.980	683
SMX	35.2	0.62	0.979	1062	41.9	0.018	0.993	280
DCF	33.1	0.93	0.940	1981	37.3	0.036	0.981	541
ACPBUF06								
IBP	37.2	0.70	0.953	2817	41.2	0.026	0.989	563
SMX	35.5	0.61	0.950	3077	39.8	0.022	0.984	799
DCF	35.3	0.87	0.924	3255	38.4	0.037	0.981	695
ACBSG06								
IBP	35.7	0.48	0.958	2425	40.6	0.016	0.994	283
SMX	36.7	0.73	0.927	2790	40.1	0.029	0.992	252
DCF	36.6	0.63	0.948	2412	40.6	0.023	0.996	163
Norit GAC 1240								
IBP	38.9	0.30	0.998	229	48.1	0.006	0.998	119
SMX	33.3	0.27	0.969	2453	41.2	0.007	0.983	1048
DCF	39.8	0.37	0.996	461	47.5	0.009	0.998	158

The results are analysed by the intraparticle diffusion model (Eq. 8-1) proposed by Weber & Morris (1963). The intraparticle diffusion equation is expressed as follows:

Eq. 8-1:
$$Q_t = kt^{0.5} + C$$

where k is the intraparticle diffusion rate constant and C represents the thickness of the boundary layer. As all the carbons for all the pharmaceutical active compounds give the same type of curves only the result of ACPBUF06 for the adsorption of DCF is shown in Figure 8-4. If the plot of Q_t and $t^{0.5}$ fits a straight line, the sorption process is exclusively controlled by intraparticle diffusion. All the plots are not linear in the first stage of adsorption (as a nonlinear behaviour of the $Q_e - t^{0.5}$ plot over a broad time interval is not an evidence for missing intraparticle diffusion impact on the adsorption kinetics (Worch 2012)) showing multi-linearity indicating that several steps are involved 1) The first sharper step is attributed by the boundary layer diffusion of pharmaceutical active compound molecules (diffusion through the solution towards the external surface of the carbon). 2) a gradual adsorption with intraparticle diffusion as rate controlling step. 3) the equilibrium stage. Based on the results intraparticle diffusion is not the rate limiting step because the different linear stages do not pass through the origin indicating some degree of boundary layer control.

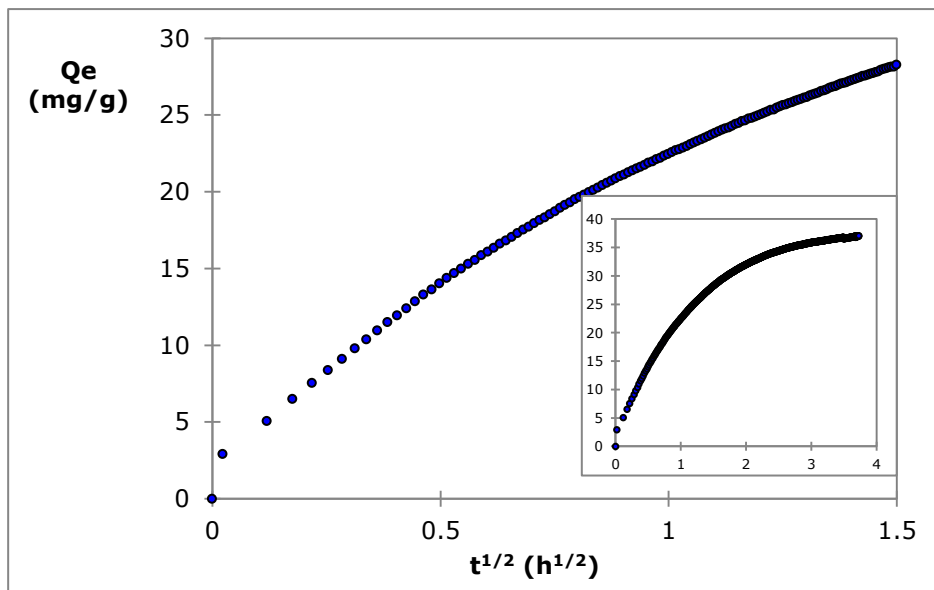


Figure 8-4: intraparticle diffusion for the adsorption of DCF on ACPBUF06

Based on the pore size distributions (Figure 7-7 and Figure 6-5) and the molecular dimensions, the selected carbons all exhibit the largest pore volumes between 1.2 and 2 times the molecular second widest dimension, proving that the porosity plays an important role in the adsorption process. Nevertheless, linking the Q_e values with the porous characteristics (pore size

distribution and the ratios of Q_e/V_{DR} , Q_e/S_{BET} and Q_e/V_{Meso} (Table 6-4 and Table 7-4) of the adsorbents, reveals that the porous features are not related with the adsorption capacity. The chemical features of the produced carbons have also a role in the adsorption uptake and mechanism. Based on the elemental analysis, the pH_{PZC} , the x-ray photoelectron spectroscopy and the amount of basic and acid groups (see section 6.4.5.2. and 7.4.5), the produced carbons have a heterogeneous, basic and more polar surface with a high amount of nitrogen surface groups. It is clear that the basic surface area of the carbons plays an important role in the adsorption process. At the pH of the equilibrium and kinetic assay, the basic carbons surface is positively charged attracting the negatively charged PhACs. Nevertheless, the pH_{PZC} and the amount of basic groups cannot be related to the uptake. For instance IBP adsorption is favoured in basic carbons and ACPBUF06 has the highest pH_{PZC} , however ACPBMUF06 represents the highest adsorption capacity, while ACPBMUF06 has a lower BET surface, meso and micropore volume and a somewhat lower point of zero charge. However, ACPBMUF06 has more basic groups which favour the adsorption of IBP. This could give an explanation. Nevertheless as conclusion, the unique combination of the basic nature, the surface groups and the porous nature of the produced carbons makes them excellent adsorbers for the tested pharmaceutical active compounds outperforming the reference carbons.

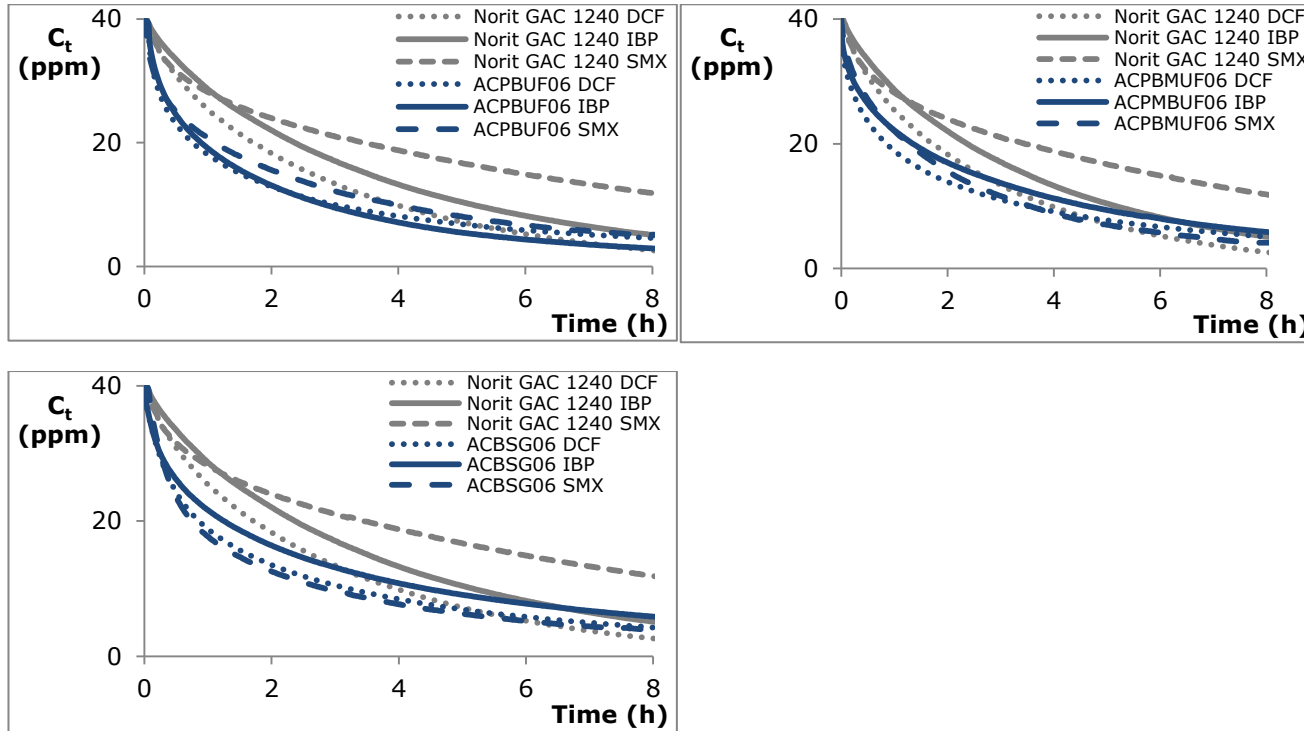


Figure 8-5: Residual concentration of PhACs in function of contact time for the different adsorbents

8.5 Conclusion

The potential of low-cost high-value activated carbons, obtained from particle board and brewer's spent grain for the removal of different pharmaceutically active compounds is investigated. Based on a preliminary screening assay three activated carbons are selected for further investigation in comparison with the best performing reference carbon. The equilibrium isotherms reveal high adsorption capacities. Complete removal of the investigated pharmaceutically active compounds is achieved even with low carbon dosages. In the case of DCF these carbon dosages are 1.1, more than 2 (estimated around 2.2), 0.9 and 1.4 g/l; for IBP, 2, 2, 0.83 and 1.4 g/l respectively for ACPBMUF06, ACBSG06, ACPBUF06 and Norit GAC 1240. For SMX no significant differences are found, with carbon dosages around 2 g/l for all carbons. The kinetic investigation of the pharmaceutically active compounds in a realistic fresh water medium, indicates high uptake rates (2-3 times faster than Norit GAC 1240) for the selected carbons. The results are fitted with acceptable R^2 and low SSE values by the pseudo-second-order model.

9 Summary and general conclusions

As the linear “take-make-consume-dispose” model is reaching the limits of its existence a rapid shift to a resource efficient biobased circular economy will be key to securing growth and jobs. If current trends continue, the global population is expected to grow by 30 % to around 9 billion people by 2050 (European Commission 2011). Even the most conservative projections for global economic growth for the next decade suggest that the demand for coal, oil, iron ore and other natural resources will rise by at least a third (Ellen MacArthur Foundation 2013). One part in the transition to a more circular economy is turning today’s waste and by-products into high value resources.

In this research, new input materials from industrial waste and by-products for the production of nitrogenised activated carbon replacing virgin resources like coals, fresh wood, coconut, ... are investigated. The dissertation includes a literature study relating to the circular economy, the selected waste products and activated carbon, a techno-economic analysis, the development of a pyrolysis/activation reactor, the characterisation of the selected waste products and produced activated carbons as well the adoptive properties for phenol and three selected pharmaceutical active compounds (i.e., ibuprofen, sulfamethoxazole and diclofenac).

First and foremost, a feasibility study (see Chapter 4) to process melamine formaldehyde and particle board waste for the production of activated carbon is performed. The goal of this study is to investigate if the eventual developed activated carbon could be profitable in an industrial production facility. For this purpose a preliminary process design is constructed based on various literature sources, for an input feed of 1 t/h and different mixing ratios of the two waste products i.e., melamine formaldehyde waste and particle board. The economic feasibility of the preliminary process design is investigated, by calculating the NPV and IRR of the cash flows incurred by an investment in a pyrolysis and activation plant for the production of activated carbon. A sensitivity analysis is performed in order to determine the most crucial variables that influence the profitability of the investment. Really encouraging results are obtained for a profitable production of activated carbon, as the current assumptions start from a rather pessimistic scenario: e.g., a zero gate fee for the melamine formaldehyde waste (which will probably be higher in practice). Besides that, the in-situ incorporation of nitrogen can result in a high quality product which can be sold at a high price or even in a niche market. In addition, the value or usefulness of the activated carbon production plant is enhanced by its ability to reuse two waste streams. Also the processing capacity plays a significant role. A larger

manufacturing plant is able to produce carbons at a lower cost despite the higher initial investment. By doubling the input rate to 2 t/h (dry matter) a reduction of average 24% of the minimal selling price is obtained. The sensitivity analysis reveals that the activated carbon plant economies are very sensitive to the investment cost, the product yield and the AC selling price which is an indication for product quality.

Based on the positive results obtained from the preliminary economic feasibility a screening of activated carbons produced by co-pyrolysis and subsequent steam activation of particle board and melamine formaldehyde samples is conducted (Chapter 5). Starting from five different blends of particle board (glued with melamine urea formaldehyde) and melamine formaldehyde waste, enhanced nitrogenised activated carbons with a nitrogen content ranging from 2.24 wt% up to 14 wt% are obtained. Pure particle board yields the highest amount of activated carbon (22 wt%). The quality of the produced activated carbon (steam activated) is determined by low concentration (100ppm) batch adsorption experiments for the removal of phenol from aqueous solutions. Based on the obtained results and the updated feasibility model (with a rather pessimistic scenario: e.g., first plant cost), really encouraging results are obtained for a profitable production of activated carbon and scaling up the research for the production of activated carbon from particle board waste.

To satisfy the need for a pyrolysis / activation reactor which is suitable to produce sufficient amounts of activated carbon on a laboratory scale resembling industrial plants, a new and improved reactor is developed (Chapter 3). As a first step in the development, all the criteria of the new reactor are listed and based on these a 3-D model is drawn. The model is evaluated, improved and finally made and applied in the research (for the production of chars and activated carbons).

A new valorisation method i.e., the production of activated carbon for waste particle board is developed (Chapter 6). Two different particle board samples (glued with melamine urea formaldehyde or glued with urea formaldehyde) are characterised for their elemental composition and thermogravimetric behaviour. Both samples reveal high nitrogen contents of 5.33 and 4.09 wt% for the sample glued with melamine urea formaldehyde and urea formaldehyde respectively. The thermogravimetric analysis shows good pyrolysis properties for the production of activated carbon. Different activated carbons are produced in the newly developed pyrolysis and activation reactor by applying several heat and steam activation profiles on the particle board samples. AC yields from 9.4 – 20 wt% were obtained with the undried (~7 -7.5 wt% moisture) particle board samples. In order to evaluate the carbons ability to adsorb phenol first of all a screening of the

produced carbons is performed. Samples AC...03, AC...06 and AC...07 yielded the highest adsorption capacities and are selected for further characterisation and phenol adsorption experiments. Nitrogen adsorption-desorption isotherms at 77 K reveal type IV isotherms with type H4 adsorption-desorption hysteresis loops classified according to IUPAC recommendations. BET analysis reveals good correlation coefficients of more than 0.999 for all samples. All samples have a high surface area starting from 794 and 840 m²/g for the carbons produced with the lowest activation time to 1656 m²/g (higher than reference carbons) The micro- and mesopore volume (V_{DR}/V_{Meso}) ratio decreases with increasing activation, indicating that the mesopores gaining a larger contribution to the total pore volume by increasing activation. The latter is also observed in the broadening of the average micropore diameter (L_0). The pore size distribution reveals that all carbons exhibit the same pore distribution. Even the carbons AC...03 and AC...07 differ only slightly, despite their differences in temperature and steam activation. Analysis of the surface functionalities reveal highly basic carbons (point of zero charge > 12) with nitrogen contents of 1 – 1.7 wt%. The x-ray spectroscopy data detected information on the distribution and presence of the different oxygen and nitrogen groups. The adsorption isotherm study shows that all isotherms can be classified as L-type according to the Giles classification excluding hydrogen bond formation as possible adsorption mechanism. The isotherm data are modelled by the non-linear Langmuir and Freundlich equations. The produced carbons give high phenol adsorption capacities of around 125 mg/g. For the direct measurement of phenol (phenol + phenolate) with UV-VIS spectroscopy a method for the determination of a correction factor is developed. To gain a better understanding of the adsorption process, the phenol, phenolate and total phenol concentration (phenol + phenolate) and pH is continuously monitored in time revealing an interesting process going on during the adsorption with the in-situ formation and adsorption of phenolate during the experiments. From the moment of carbon introduction, the pH increases immediately from 6.4 a 6.7 to around 10 – 11 promoting in-situ phenolate formation and remains constant at this value over time. The adsorption of phenol is thus an interplay between adsorption of phenol, phenolate and the phenolate formation. The experiments reveal a very fast removal of total phenol (phenol and phenolate) with over 50% removal in the first 50 minutes. The adsorption capacity is only lightly affected by the pH below the point of zero charge. higher pH values negatively affect the adsorption capacity significant. Addition of salt to the solution has a small positively effect and remains constant over large salt concentrations. It can be concluded that the produced activated carbons from particle board have good adsorptive characteristics for the removal of phenol from aqueous solutions in different environments.

The use of brewer's spent grain (Chapter 7) for the production of activated carbon by pyrolysis and subsequent steam activation in the newly developed reactor up to temperatures of 850 °C and 45 min of steam activation is investigated. First the brewer's spent grain is characterized by component analysis, thermogravimetric analysis and elemental analysis. The results reveal high amounts of cellulose (20.8 wt%), hemicellulose (48.78 wt%) and lignin (11.3 wt%) and lower quantities of fat, ethanol extractives and ash (8.2 wt%, 4.7 wt% and 3.2 wt% respectively). Thermogravimetric analysis reveal that most of the weight loss occurred in the range 200 – 500 °C with two significant weight loss peaks at 281 °C and 341 °C. At 850 °C 18 wt% of char is obtained. By applying several heat and steam activation profiles on the brewer's spent grain different activated carbons are produced with yields varying between 16.1 – 23.6 wt%. The effectiveness of the high nitrogen content activated carbons prepared from brewer's spent grain towards phenol in aqueous solution is evaluated by performing isothermal adsorption studies (100 ppm phenol) relative to two reference activated carbons (Filtrisorb F400 and Norit GAC 1240). The prepared activated carbons show high N-contents ranging from 2.1 wt% up to 3.8 wt% compared to 0.7 wt% for the reference activated carbons. It is observed that a higher activation temperature resulted in a higher adsorption capacity, nevertheless they are comparable except for the one activated carbon obtained at 800°C and 5 ml H₂O of steam activation (ACBSG01). The steam activation has a strong influence on the adsorption capacity. The Langmuir and Freundlich data show that adsorption is a favourable process. The Freundlich model fits the results the best. Based on the isothermal adsorption studies three activated carbons (800 °C and 10 ml H₂O of steam activation (ACBSG05), 850 °C and 15 ml H₂O of steam activation (ACBSG06), 800 °C and 10 ml H₂O of steam activation (ACBSG07)) having similar removal efficiencies as the reference carbons were selected. The adsorption capacities (Q_m 50.3 – 111.3 mg/g based on Langmuir) are a little lower than those of the reference activated carbons (Q_m 160 – 166 mg/g based on Langmuir). Nevertheless, the kinetics revealed that the produced activated carbons have higher adsorption rates than the reference ones. The kinetics are non-linear modelled with the pseudo-1st-order and pseudo-2nd-order model revealing that the adsorption follows the latter. After 5 – 6 h, 80 – 90 % of phenol is removed. The optimum range for phenol adsorption on the produced activated carbons is between 6 – 10 with a maximum of pH 8.

Finally, the potentials of the low-cost high-value activated carbons, obtained from particle board and brewer's spent grain for the removal of different pharmaceutically active compounds is investigated. Three pharmaceutical active compounds are selected as target compounds based on their medium

to high risk to the aquatic life and their frequent use and/or their long-term use over long period of time namely: i.e., Ibuprofen, Diclofenac and Sulfamethoxazole. Based on a preliminary screening assay three activated carbons are selected for further investigation in comparison with the best performing reference carbon. The equilibrium isotherms reveal high adsorption capacities of similar or higher than the reference carbon for PBUF06 and PBMUF06 (e.g., up to 190 mg/g for PBUF06 for diclofenac versus 127 mg/g for Norit GAC 1240). for ACBSG the capacities are lower for diclofenac and sulfamethoxazole Complete removal of the investigated pharmaceutically active compounds is achieved even with low carbon dosages. The kinetic investigation of the pharmaceutically active compounds in a realistic fresh water medium, indicates high uptake rates for the selected carbons in comparison with the reference carbon.

Based on the investigation (economical and chemical) it can be concluded that the selected waste materials are excellent candidates for the profitable production of activated carbon with high potential for removal of organic pollutants in polluted waters.

10 Samenvatting en algemeen besluit

Het huidige lineair economisch "take-make-consume-dispose"-model is stilaan de grenzen van haar bestaan aan het bereiken. Een snelle omschakeling naar een efficiënt gebruik van grondstoffen en een biogebaseerde circulaire economie is de sleutel tot het veilig stellen van de economische groei. Als de huidige trends doorzetten, zal de wereldbevolking naar verwachting met 30% groeien tot ongeveer 9 miljard mensen in 2050 (European Commission 2011). Zelfs uit de meest conservatieve prognose van de wereldwijde economische groei voor de komende tien jaar blijkt dat de vraag naar kolen, olie, ijzererts en andere natuurlijke hulpbronnen zal stijgen met ten minste een derde (Ellen MacArthur Foundation 2013). Een belangrijk onderdeel in de transitie naar een circulaire economie is het valoriseren van afval en bijproducten naar hoogwaardige grondstoffen en materialen.

In dit onderzoek, wordt de verwerking van industrieel afval en bijproducten onderzocht voor de productie van hoogwaardige stikstofhoudende actieve kool uit melamine formaldehyde, spaanplaat afval en bostel (brewer's spent grain, draf) een bijproduct uit de bierbrouwindustrie. Deze studie omvat een literatuurstudie omtrent de circulaire economie en actieve kool, een techno-economische analyse, de ontwikkeling van een pyrolyse/activatie reactor, karakterisatie van de geselecteerde afvalstoffen en geproduceerde actieve kolen als ook de adsorptie eigenschappen van de geproduceerde actieve kolen voor fenol en drie geselecteerde farmaceutisch actieve componenten (namelijk Ibuprofen, Sulfametoxazole en Diclofenac).

Allereerst wordt er een techno-economische analyse (hoofdstuk 4) voor het verwerken van melamine formaldehyde en spaanplaat afval voor de productie van actieve kool uitgevoerd. Het doel van deze studie is het nagaan of de uiteindelijke ontwikkelde actieve kool winstgevend kan zijn in een industriële productiefaciliteit: m.a.w. het beoordelen van het potentieel en de economische haalbaarheid van het project of idee voor er tijd en geld in de ontwikkeling wordt geïnvesteerd. Om dit doel te bereiken is er een preliminair procesdesign en economisch model ontwikkeld op basis van verschillende literatuurbronnen, voor een input-feed van 1 t/h en verschillende mengverhoudingen van twee geselecteerde afvalstoffen (namelijk: melamine formaldehyde en spaanplaat afval). De techno-economische evaluatie van het preliminair procesdesign wordt onderzocht, door het berekenen van de netto contante waarde en de internal rate of return van de kasstromen gegenereerd door een investering in de pyrolyse- en activeringsfabriek. Om risico van de verschillende aannames in het economisch model te testen is er een sensitiviteitsanalyse (Monte Carlo

simulatie) uitgevoerd. De simulaties (waarbij de waarden van de variabelen simultaan veranderen op basis van een kansverdeling) worden vervolgens gebruikt om de kans dat de netto contante waarde van de investering positief is te bepalen en om de belangrijkste factoren te identificeren die een invloed hebben op de rendabiliteit. Veelbelovende resultaten worden verkregen voor een rendabele productie van actieve kool, ondanks het feit dat de huidige veronderstellingen uitgaan van een pessimistisch scenario zoals bijvoorbeeld geen vergoeding voor de afname van melamine formaldehyde afval (die waarschijnlijk hoger zal zijn in de praktijk), geen subsidies, "first plant cost", Uit de resultaten blijkt dat de verwerkingscapaciteit een belangrijke rol speelt. Een grotere fabriek kan actieve kool produceren tegen een lagere kostprijs ondanks een hogere initiële investering. Zo zal bij een verdubbeling van de input (tot 2 t/h droge stof) de minimale verkoopprijs dalen met gemiddeld 24%. Uit de sensitiviteitsanalyse blijkt dat de rendabiliteit van de actieve kool productie zeer gevoelig is voor de investeringskosten, de productopbrengst en verkoopprijs (welk een indicatie geeft voor de kwaliteit). Op basis van de positieve resultaten verkregen uit de preliminaire techno-economische analyse, zijn screening experimenten voor de productie van actieve kool uit co-pyrolyse en stoomactivering van spaanplaat en melamine formaldehyde uitgevoerd (hoofdstuk 5). In de screening is er gestart met vijf mengsels van spaanplaat (verlijmd met melamine ureum formaldehyde) en melamine formaldehyde afval. De geproduceerde stikstofhoudende actieve kolen hebben een stikstofgehalte variërend van 2,24 tot 14 m%. Pure spaanplaat levert de hoogste opbrengst aan actieve kool op (22 m%). De kwaliteit van de geproduceerde actieve kool (stoom geactiveerd) wordt bepaald door middel van lage concentratie (100 ppm) fenol adsorptie-experimenten uit waterige oplossingen. Op basis van de verkregen resultaten en het geüpdatet economisch model (hoofdstuk 4), zijn er echt bemoedigende resultaten verkregen voor een rendabele productie van actieve kool en het opschalen ervan voor de productie van actieve kool uit spaanplaatafval.

Het tweede gedeelte van het onderzoek omvat de ontwikkeling van een pyrolyse / activatie reactor die geschikt is voor de productie van voldoende hoeveelheden actieve kool op laboratoriumschaal gelijkend op industriële installaties (hoofdstuk 3). Als eerste stap in de ontwikkeling, worden alle criteria van de nieuwe reactor opgenomen en op basis van deze een 3-D model uitgewerkt. Het model wordt geëvalueerd, verbeterd en uiteindelijk gemaakt en gebruikt.

Op basis van de screening (hoofdstuk 5) wordt een nieuwe valorisatie methode, nl. de productie van actieve kool voor spaanplaatafval ontwikkeld (hoofdstuk 6). Eerst worden de verschillende spaanplaatstalen (verlijmd met melamine ureum formaldehyde of verlijmd met ureum formaldehyde)

gekaracteriseerd met behulp van elementanalyse en thermogravimetrisch gedrag. Beide stalen bevestigen de hoge stikstofgehalten van 5,3 en 4,1 m% voor spaanplaat verlijmd met respectievelijk melamine ureum formaldehyde en ureum formaldehyde. De thermogravimetrische analyse illustreert de geschikte eigenschappen voor de productie van actieve kool. Op basis van de verkregen informatie zijn er verschillende actieve koolstalen geproduceerd met behulp van verschillende warmte- en stoomactiverings profielen in de nieuw ontwikkelde pyrolyse- en activeringsreactor. Actieve kool opbrengsten tussen 9,4 en 20 m% werden verkregen met de niet gedroogde ($\sim 7 - 7,5$ m% vocht) spaanplaatstalen. Om het adsorptievermogen van de actieve koolstalen voor fenol te evalueren is er in eerste instantie een screeningsstudie uitgevoerd. De stalen AC...03, AC...06 en AC...07 leverden de hoogste adsorptiecapaciteiten en zijn geselecteerd. Deze drie actieve koolstalen worden verder gekarakteriseerd en aan fenoladsorptie experimenten onderworpen. Stikstof adsorptie-desorptie-isothermen bij 77 K onthullen type IV-isothermen met type H4 adsorptie-desorptie hysteresislussen ingedeeld volgens IUPAC aanbevelingen. BET analyse levert uitstekende goede correlatiecoëfficiënten van meer dan 0,999 op en een groot BET oppervlak vanaf 794 en 840 m²/g voor de stalen met de laagste activeringstijd tot 1656 m²/g (hoger dan referentie actieve kolen). Op basis van de poriegrootte verdeling blijkt dat alle actieve kolen dezelfde poriedistributie vertonen. Uit de fenoladsorptie-isotherm experimenten blijkt dat alle isothermen kunnen worden gecatalogiseerd als L-type volgens de indeling van Giles. De geproduceerde actieve kolen beschikken over grote fenoladsorptiecapaciteiten rond 125 mg/g. Voor het direct meten van fenol (fenol + fenolaat) met UV-VIS spectroscopie is er een methode ontwikkeld voor het bepalen van een correctiefactor (die afhankelijk is van de pH) welke de gemeten adsorptiewaarde corrigeert naar de waarde die gemeten zou zijn bij een op voorhand gedefinieerde pH. Om meer inzicht te verkrijgen in het adsorptieproces, wordt de concentratie aan fenol, fenolaat, totale fenol en de pH continue gemonitord in functie van de tijd. Op basis van de experimenten wordt er een interessant proces ontdekt wat zich voltrekt tijdens de adsorptie-experimenten. Vanaf de actieve kool introductie, stijgt de pH onmiddellijk van 6,4 à 6,7 naar 10 – 11 met de in-situ vorming van fenolaat. Tijdens het experiment blijft de pH verder constant. De experimenten tonen een zeer snelle verwijdering van de totale fenol (fenol + fenolaat) met meer dan 50% verwijdering in de eerste 50 minuten voor de spaanplaat actieve kolen. De adsorptiecapaciteit wordt slechts licht beïnvloed door een pH-waarde onder de pH_{pZC} , hogere pH-waarden verminderen de adsorptiecapaciteit significant. Toevoeging van zout aan de oplossing heeft een klein positief effect en de adsorptiecapaciteit blijft constant over grote zoutconcentraties. Men kan hieruit besluiten dat de geproduceerde actieve kool uit spaanplaat over goede adsorptie-

eigenschappen voor de verwijdering van fenol uit waterige oplossingen beschikt in verschillende omgevingsvoorwaarden.

Vervolgens is het gebruik van bostel (hoofdstuk 7) voor de productie van actieve kool met behulp van pyrolyse en daaropvolgende stoomactivering onderzocht. Eerst is het verkregen staal met behulp van component analyse, thermogravimetrische analyse en elementanalyse gekarakteriseerd. De resultaten tonen grote hoeveelheden cellulose (20.8 m%), hemicellulose (48,8 m%) en lignine (11,3 m%) en kleinere hoeveelheden vet, ethanol extracten en as (8,17 m%, 4,7 m% en 3,2 m% respectievelijk) aan. Thermogravimetrische analyse geeft aan dat het meeste gewichtsverlies optreedt in het temperatuursinterval 200 - 500 °C. Bij 850 °C wordt er een koolstofresidue van 18 m% verkregen. Met behulp van verschillende warmte en stoomactiveringsprofielen zijn er verschillende actieve kool stalen geproduceerd met opbrengsten variërend tussen 16,1-23,6 m%. De effectiviteit van de geproduceerde actieve kool voor de verwijdering van fenol uit waterige oplossing wordt geëvalueerd door het uitvoeren van isothermadsorptiestudies (100 ppm fenol) ten opzichte van twee referentie actieve kolen (Filtrisorb F400 en Norit GAC 1240). De bereide actieve kolen vertonen hoge N-gehalten variërend van 2.1 m% tot 3.8 m% tegenover 0.7 m% voor de referentie actieve kolen. Uit de resultaten kan opgemerkt worden dat een hogere activeringstemperatuur resulteert in een hogere adsorptiecapaciteit, nochtans zijn de stalen vergelijkbaar behalve voor één actieve kool verkregen bij 800 °C en 5 ml H₂O stoomactivatie (ACBSG01). De stoomactivering heeft een sterke invloed op de adsorptiecapaciteit. Op basis van de isothermadsorptiestudies zijn er drie actieve kolen geselecteerd (800 °C en 10 ml H₂O stoomactivatie (ACBSG05), 850 °C en 15 ml H₂O stoomactivatie (ACBSG06), 800 °C en 10 ml H₂O stoomactivatie (ACBSG07)) met vergelijkbare verwijderingsefficiënties voor verdere analyse. De adsorptiecapaciteiten (Q_m 50,3 - 111,3 mg/g op basis van Langmuir model) zijn iets lager dan die van de referentie actieve kolen (Q_m 160 - 166 mg/g op basis van Langmuir model). Echter, de kinetiek van de geproduceerde actieve koolstalen vertoont hoger adsorptiesnelheden in vergelijking met de referentiestalen. De experimentele kinetiek data zijn met behulp van het pseudo-eerste-orde en pseudo-tweede-orde model niet lineair gemodelleerd. Het pseudo-tweede-orde model fit de resultaten het best. Na 5 - 6 h is 80 - 90% fenol verwijderd. Optimale fenoladsorptie wordt bereikt is bij een pH van 6 - 10 met een maximum bij een pH van 8 voor de geselecteerde stalen.

Tenslotte, is het potentieel van de geselecteerde actieve kool stalen (hoofdstuk 6 en 7) voor de verwijdering van de farmaceutisch actieve verbindingen onderzocht. Drie farmaceutisch actieve verbindingen zijn geselecteerd als doelverbindingen op basis van hun gemiddeld tot hoog risico voor het waterleven en het frequent gebruik en/of het gebruik

gedurende lange tijd namelijk: Ibuprofen, Diclofenac en Sulfamethoxazole. Op basis van een voorlopige screeningstest zijn er drie actieve koolstalen geselecteerd (ACBSG06, ACPBUF06 en ACPBMUF06) voor verder onderzoek in vergelijking met de best presterende referentie actieve kool namelijk Norit GAC 1240. Alle geselecteerde actieve koolstalen van spaanplaat hebben vergelijkbare of hogere adsorptiecapaciteiten ten opzichte van de referentie. ACPBUF06 behaalt bijvoorbeeld een adsorptiecapaciteit van 192 mg/g voor Diclofenac, terwijl Norit GAC 1240 een capaciteit haalt van 127 mg/g. Het bostel staal heeft iets lagere capaciteiten voor Diclofenac en Sulfamethoxazole. Volledige verwijdering van de onderzochte farmaceutisch werkzame verbindingen wordt zelfs bereikt bij lage actieve kool doseringen. Het kinetische onderzoek van de farmaceutisch actieve verbindingen in een realistisch zoet water medium, geeft significant hogere opname snelheden voor de geselecteerde actieve kool stalen ten opzichte van de referentie actieve kolen.

Algemeen kan geconcludeerd worden dat de onderzochte industriële afval- en bijproducten uitstekende kandidaten zijn voor het economisch produceren van hoogwaardige actieve kool met een potentieel voor het verwijderen van organische polluenten van verontreinigde wateren.

List of publications

List of publications

2015

Journal Contribution

CRESPO SARIOL, Harold; VANREPELEN, Kenny; YPERMAN, Jan; SAUVANELL, Ángel, Brito; CARLEER, Robert & NAVARRO, Campa (submitted) *A colorimetric method for the determination of the exhaustion level of granular activated carbons used in the rum production.*

VANDERHYDEN, Sara; VAN AMMEL, Raf; SOBIECH-MATURA, Katarzyna; HULT, Mikael; VANREPELEN, Kenny; SCHREURS, Sonja; SCHROEYERS, Wouter; YPERMAN, Jan & CARLEER, Robert (accepted). *Adsorption of Cs-134 on different types of activated carbon.*

In: JOURNAL OF RADIOANALYTICAL AND NUCLEAR CHEMISTRY,

Conference Material

VANDERHEYDEN, Sara; VAN AMMEL, Raf; SOBIECH-MATURA, Katarzyna; Vanreppelen, Kenny; SCHREURS, Sonja; Schroeeyers, Wouter; Yperman, Jan & Carleer, Robert (2015). *Comparison of adsorption properties of Cs on different types of activated carbon.*

In: ENVIRA2015 International Conference on Environmental Radioactivity: New Challenges with New Technologies, Thessaloniki, 21-25/09/2015. [Abstract - cat: C2]

2014

Journal Contribution

KUPPENS, Tom; VAN DAEL, Miet; VANREPELEN, Kenny; THEWYS, Theo; YPERMAN, Jan; CARLEER, Robert; SCHREURS, Sonja & VAN PASSEL, Steven (2014). *Techno-economic assessment of fast pyrolysis for the valorization of short rotation coppice cultivated for phytoextraction.*

In: JOURNAL OF CLEANER PRODUCTION, 88, p. 336-344. [Article - cat: A1]

List of publications

VANREPELEN, Kenny; VANDERHEYDEN, Sara; KUPPENS, Tom; SCHREURS, Sonja; YPERMAN, Jan & CARLEER, Robert (2014). Activated carbon from pyrolysis of brewer's spent grain: Production and adsorption properties.
In: Waste Management & Research, 32 (7), p. 634-645. [Article - cat: A1]

Proceedings Paper

KUPPENS, Tom; VAN DAEL, Miet; VANREPELEN, Kenny; CARLEER, Robert; YPERMAN, Jan; SCHREURS, Sonja & VAN PASSEL, Steven (2014). Techno-Economic Assessment of Pyrolysis Char Production and Application – A Review.
In: Ranzi, Eliseo; Kohse-Hölinghaus, Katharina (Ed.). Chemical Engineering Transactions, p. 67-72. [cat: C1]

KUPPENS, Tom; VAN DAEL, Miet; MAGGEN, Jens; VANREPELEN, Kenny; YPERMAN, Jan; CARLEER, Robert; ELEN, Henri & VAN PASSEL, Steven (2014). Techno-economic assessment of different conversion pathways for pyrolysis char from pig manure.
In: Proceedings of the 22nd European Biomass Conference & Exhibition, p. 901-911. [cat: C1]

2013

Journal Contribution

VANREPELEN, Kenny; SCHREURS, Sonja; KUPPENS, Tom; THEWYS, Theo; CARLEER, Robert & YPERMAN, Jan (2013). Activated Carbon by Co-pyrolysis and Steam Activation from Particle Board and Melamine Formaldehyde Resin: Production, Adsorption Properties and Techno Economic Evaluation.
In: JOURNAL OF SUSTAINABLE DEVELOPMENT OF ENERGY, WATER AND ENVIRONMENT SYSTEMS, 1 (1), p. 41-57. [Article - cat: A2]

Proceedings Paper

KUPPENS, Tom; VANREPELEN, Kenny; THEWYS, Theo; YPERMAN, Jan; CARLEER, Robert; SCHREURS, Sonja & VAN PASSEL, Steven (2013). Techno-economic assessment of fast pyrolysis for the valorisation of short rotation coppice cultivated for phytoextraction.
In: Proceedings of the 8th Conference on Sustainable Development of Energy, Water and Environment Systems (SDEWES 2013). [Article - cat: C1]

List of publications

VANREPELEN, Kenny; VANDERHEYDEN, Sara; KUPPENS, Tom; SCHREURS, Sonja; CARLEER, Robert & YPERMAN, Jan (2013). Activated Carbon from Pyrolysis of Brewer's Spent Grain: Production and Adsorption Properties.

In: Ban, M.; Duić, N.; Guzović, Z.; Markovska, N; Schneider, D.R.; Klemeš, J.J.; Varbanov, P.; Ababneh, A.; Østergaard, P.A.; Connolly, D.; Kafarov, V.; Krajačić, G.; Lund, H.; Mathiesen, B.V.; Mohsen, M.; Möller, B.; Perković, L.; Sikdar, S.K.; Vujanović, M. (Ed.). Proceedings of the 8th Conference on Sustainable Development of Energy, Water and Environment Systems (SDEWES 2013). [Paper - cat: C1]

Conference Material

VANREPELEN, Kenny; VANDERHEYDEN, Sara; KUPPENS, Tom; SCHREURS, Sonja; CARLEER, Robert & YPERMAN, Jan (2013). Activated Carbon from Pyrolysis of Brewer's Spent Grain: production and Adsorption Properties.

In: 8th Conference on Sustainable Development of Energy, Water and Environment Systems, Dubrovnik, 22-27/09/2013. [Presentation - cat: C2]

KUPPENS, Tom; VAN DAEL, Miet; VANREPELEN, Kenny; CARLEER, Robert; YPERMAN, Jan & VAN PASSEL, Steven (2013). Techno-economic assessment of pyrolysis char production from pig manure.

In: ManuREsource 2013 - International conference on manure management and valorization, Bruges, Belgium, 5-6/12/2013. [Presentation - cat: C2]

2012

Conference Material

Kuppens, Tom; Vanreppelen, Kenny; Yperman, Jan; Carleer, Robert & Thewys, Theo (2012). Economic trade-off between char for active coal and oil for energy from fast pyrolysis of willow cultivated for phytoremediation.

In: 14th PhD Symposium AGRICULTURAL AND NATURAL RESOURCE ECONOMICS, Brussels-Belgium, 18 April 2012. [Paper - cat: C2]

Vanreppelen, Kenny; Schreurs, Sonja; Carleer, Robert & Yperman, Jan (2012). Activated carbon by co-pyrolysis and steam activation from particle board and melamine formaldehyde resin.

In: 2nd Symposium 'Cluster Milieu', Diepenbeek, Belgium, 30

List of publications

January 2012. [Presentation - cat: C2]

Kuppens, Tom; Voets, Thomas; Vanreppelen, Kenny; Cornelissen, Tom; Schreurs, Sonja; Carleer, Robert; Yperman, Jan & Thewys, Theo (2012). *Techno-economic assessment of fast pyrolysis for the valorisation of short rotation coppice cultivated for phytoremediation in the Campine.*

In: 9th International Phytotechnology Society conference, Diepenbeek, 11-14 September 2012. [Paper - cat: C2]

2011

Journal Contribution

VANREPELEN, Kenny; KUPPENS, Tom; THEWYS, Theo; CARLEER, Robert; YPERMAN, Jan & SCHREURS, Sonja (2011). *Activated carbon from co-pyrolysis of particle board and melamine (urea) formaldehyde resin: a techno-economic evaluation.*

In: CHEMICAL ENGINEERING JOURNAL, 172(2-3). p. 835-846. [Article - cat: A1 - Validation: ecoom 2012]

Proceedings Paper

VANREPELEN, Kenny; KUPPENS, Tom; THEWYS, Theo; SCHREURS, Sonja; YPERMAN, Jan & CARLEER, Robert (2011). *Activated carbon by co-pyrolysis and steam activation from particle board and melamine formaldehyde resin: production, adsorption properties and techno economic evaluation.*

In: Guzović, Zvonimir & Ban, Marko & Matijašević, Sunčana (Ed.) The 6th Dubrovnik Conference on Sustainable Development of Energy, Water and Environment Systems: Book of Abstracts & online CD Proceedings: vol. 6. [cat: C1]

Conference Material

VANREPELEN, Kenny; KUPPENS, Tom; THEWYS, Theo; SCHREURS, Sonja; CARLEER, Robert & YPERMAN, Jan (2011). *Activated Carbon by Co-Pyrolysis and Steam Activation from Particle Board and Melamine Formaldehyde Resin: Production, Adsorption Properties and Techno Economic Evaluation.*

In: 6th Dubrovnik Conference on Sustainable Development of Energy, Water and Environmental Systems, Dubrovnik, 25-29 September. [Paper - cat: C2]

List of publications

Prices

VANREPPELEN, Kenny; **Best Paper award** 6th Dubrovnik Conference on Sustainable Development of Energy, Water and Environmental Systems, Dubrovnik, 25-29 September.

References

References

Al-Degs, Y. S., El-Barghouthi, M. I., El-Sheikh, A. H., & Walker, G. M. (2008) Effect of solution pH, ionic strength, and temperature on adsorption behavior of reactive dyes on activated carbon. *Dyes and Pigments* 77(1), 16-23

Al-Khateeb, L. A., Almotiry, S., & Salam, M. A. (2014) Adsorption of pharmaceutical pollutants onto graphene nanoplatelets. *Chemical Engineering Journal*, 191

Aliyu, S., & Bala, M. (2011) Brewer's spent grain: A review of its potentials and applications. *African Journal of Biotechnology* 10(3), 324-331

Arrigo, R., Havecker, M., Schlogl, R., & Su, D. S. (2008) Dynamic surface rearrangement and thermal stability of nitrogen functional groups on carbon nanotubes. *Chemical Communications*(40), 4891-4893

ASTM (2004). Standard Test Method for Determination of Ethanol Extractives in Biomass. United States, ASTM International. 11.06 Biological Effects and Environmental Fate; Biotechnology; Pesticides.

Baccar, R., Sarrà, M., Bouzid, J., Feki, M., & Blánquez, P. (2012) Removal of pharmaceutical compounds by activated carbon prepared from agricultural by-product. *Chemical Engineering Journal* 211-212, 310-317

Baggio, P., Baratieri, M., Gasparella, A., & Longo, G. A. (2008) Energy and environmental analysis of an innovative system based on municipal solid waste (MSW) pyrolysis and combined cycle. *Applied Thermal Engineering* 28(2-3), 136-144

Bandosz, T. J. (2009). Surface chemistry of carbon materials. *Carbon Materials for Catalysis*. P. Serp, & J. L. Figueiredo. New Jersey, John Wiley & Sons Inc: 45-92.

Bandosz, T. J., & Ania, C. O. (2006). Surface chemistry of activated carbons and its characterization. *Activated Carbon Surfaces in Environmental Remediation*. T. J. Bandosz. United Kingdom, ELSEVIER Ltd;: 571.

Bansal, R. C., & Goyal, M. (2005). *Activated carbon adsorption*. pp. 472. Taylor & Francis Group, United States of America

References

Beckham, D., & Graham, R. G. (1994). Economic assessment of a wood fast pyrolysis plant. *Advances in Thermochemical Biomass Conversion*. A. V. Bridgwater. United Kingdom, Blackie Academic and Professional: 1314-1324.

Belgostat (2010). Rentetarieven op nieuwe tarieven - Eurogebied. From (2010):
<http://ww.nbb.be/begostat/PresentationLinker,TableId=248000024&Lang=N2010>)

BFM, L. (2003). Wood waste recycling in furniture manufacturing - a good practice guide. From *The Waste and Resource Action Programme (2003)*:
<http://www.bfmenvironment.co.uk/images/wood%20waste%20recycling.pdf>
(May 4, 2003)

BFM, L. (2004). Evaluaton of the market development potential of the waste wood and wood products and reuse sector. From *The Waste & Resource Action programme (2004)*:
www.bfmenvironment.co.uk/.../Wood%20market%20development.pdf (May 5, 2004)

Biezma, M. V., & Cristóbal, J. R. S. (2006) Investment criteria for the selection of cogeneration plants—a state of the art review. *Applied Thermal Engineering* 26(5–6), 583-588

Boateng, A. A., & Barr, P. V. (1996) A thermal model for the rotary kiln including heat transfer within the bed. *International Journal of Heat and Mass Transfer* 39(10), 2131-2147

Bridgwater, A. V., Toft, A. J., & Brammer, J. G. (2002) A techno-economic comparison of power production by biomass fast pyrolysis with gasification and combustion. *Renewable & Sustainable Energy Reviews* 6(3), 181-248

Bromhead, A. (2005). Benchmarking wood waste combustion in the UK furniture manufacturing sector. From BFM Ltd (2005):
<http://www.bfmenvironment.co.uk/images/BFM%20Wood%20combustion%20benchmarking%20-%20full1.pdf> (April 5, 2005)

Brunauer, S., Emmett, P. H., & Teller, E. (1938) Adsorption of Gases in Multimolecular Layers. *Journal of the American Chemical Society* 60(2), 309-319

References

Budaeva, A. D., & Zoltoev, E. V. (2010) Porous structure and sorption properties of nitrogen-containing activated carbon. *Fuel* 89(9), 5

Busca, G., Berardinelli, S., Resini, C., & Arrighi, L. (2008) Technologies for the removal of phenol from fluid streams: A short review of recent developments. *Journal of Hazardous materials* 160(2-3), 265-288

Calisto, V., Ferreira, C. I., Oliveira, J. A., Otero, M., & Esteves, V. I. (2015) Adsorptive removal of pharmaceuticals from water by commercial and waste-based carbons. *Journal of Environmental Management* 152, 83-90

Caputo, A. C., Palumbo, M., Pelagagge, P. M., & Scacchia, F. (2005) Economics of biomass energy utilization in combustion and gasification plants: effects of logistic variables. *Biomass & Bioenergy* 28(1), 35-51

Chemical Engineering (2010). From (2010): <http://www.che.com> (20 April 2010, 2010)

Choma, J., & Jariniec, M. (2006). Characterization of nanoporous carbons by using gas adsorption isotherms. *Activated Carbon Surfaces in Environmental Remediation*. T. J. Bandosz. United Kingdom, Elsevier Ltd.

Chowdhury, Z. K., Summers, R. S., Westerhoff, G. P., Leto, B. J., Nowack, K. O., & Corwin, C. J. (2013). *Activated carbon Solution for Improving Water Quality*. pp. American Water Works Association, United States of America

Choy, K. K. H., Barford, J. P., & McKay, G. (2005) Production of activated carbon from bamboo scaffolding waste-process design, evaluation and sensitivity analysis. *Chemical Engineering Journal* 109(1-3), 147-165

Ciccarese, L., Pellegrino, P., & pettenella, D. (2014) A new principle of the European union forest policy. The cascading use of wood products. *Italian Journal of Forest and Mountain Environments* 69(5), 5

Cook, D. (2011) BREWERS' GRAINS: OPPORTUNITIES ABOUND. *Brewers' Guardian* November/december, 60 - 63

Crittenden, J. C., Trussell, R. R., Hand, D. W., Howe, K. J., & Tchobanoglous, G. (2005). *Water treatment: Principles and Design / MWH*. pp. 1947. Jhon Wiley & Sons, United States of America

References

Daian, G., & Ozarska, B. (2009) Wood waste management practices and strategies to increase sustainability standards in the Australian wooden furniture manufacturing sector. *Journal of Cleaner Production* 17(17), 1594-1602

Deconinck, D., Capon, L., Clerinx, B., & Couder, J. (2001). Indicatoren voor duurzame ontwikkeling in de Belgische Industrie. T. e. C. A. DWTC Federale Diensten voor Wetenschappelijke. Belgium, POD Wetenschapsbeleid, 74.

Delgado, L. F., Charles, P., Glucina, K., & Morlay, C. (2012) Review: The removal of endocrine disrupting compounds, pharmaceutically activated compounds and cyanobacterial toxins during drinking water preparation using activated carbon—A review. *Science of the Total Environment* 435-436, 509-525

Demirbas, A. (2011) Waste management, waste resource facilities and waste conversion processes. *Energy Conversion and Management* 52(2), 1280-1287

Devallencourt, C., Saiter, J. M., Fafet, A., & Ubrich, E. (1995) Thermogravimetry Fourier-Transform Infrared Coupling Investigations to Study the Thermal-Stability of Melamine-Formaldehyde Resin. *Thermochimica Acta* 259(1), 143-151

Diebold, J. P., & Bridgwater, A. V. (2003). Overview of fast pyrolysis of biomass for the production of liquid fuels. *Fast Pyrolysis of Biomass: A Handbook*. A. V. Bridgwater, J. Piskorz, & D. Radlein. United Kingdom, CPL Press: 14-32.

Dornburg, V., & Faaij, A. P. C. (2006) Optimising waste treatment systems - Part B: Analyses and scenarios for The Netherlands. *Resources Conservation and Recycling* 48(3), 227-248

Dornburg, V., Faaij, A. P. C., & Meuleman, B. (2006) Optimising waste treatment systems - Part A: Methodology and technological data for optimising energy production and economic performance. *Resources Conservation and Recycling* 49(1), 68-88

Drage, T. C., Arenillas, A., Smith, K. M., Pevida, C., Piippo, S., & Snape, C. E. (2007) Preparation of carbon dioxide adsorbents from the chemical

References

activation of urea-formaldehyde and melamine-formaldehyde resins. Fuel 86(1-2), 10

Dutch Association of Cost Engineers (2009). DACE-prijzenboekje. pp. Reed Bussiness BV, Netherlands

El-Naas, M. H., Al-Zuhair, S., & Abu Alhaija, M. (2010) Removal of phenol from petroleum refinery wastewater through adsorption on date-pit activated carbon. Chemical Engineering Journal 162(3), 997-1005

Ellen MacArthur Foundation (2013). Toward the circular economy. United Kingdom, Ellen MacArthur Foundation 1, 96.

Europe, F. E.-M. C. o. t. P. o. F. i. (1993). RESOLUTION H1: General Guidelines for the Sustainable Management of Forests in Europe. Second Ministerial Conference on the Protection of Forests in Europe, Ministerial Conference on the Protection of Forests in Europe

European Central Bank (2010). Statistical Data Warehouse. From (2010): <http://sdw.ecb.europa.eu/home.do?chart=t1.9> (16 July 2010, 2010)

European Commission (2011). A resource-efficient Europe - Flagship initiative under the Europe 2020 Strategy. Brussels, European Commission. 21, 16.

European Commission (2012). Innovating for Sustainable Growth: A Bioeconomy for Europe. Brussels, European Commission. Com(2012) 60, 9.

European Commission (2013). A new EU Forest Strategy: for forests and the forest-based sector Brussels, European Commission. Com(2013), 17.

European Commission (2014). Toward a circular economy: A zero waste programme for Europe. E. Commission. Brussels, European Commission. 398, 14.

Eurostat (2010). Unit labour cost - Annual data. From (2010): http://appsso.eurostat.ec.europa.eu/nui/show.do?dataset=nama_aux_ulc&lang=en (4 November 2010, 2010)

References

Eurostat (2011). Prodcom - Statistics by Product. From (2011): <http://epp.eurostat.ec.europa.eu/portal/page/portal/eurostat/home> (19 May 2013, 2011)

Faithfull, N., T. (2002). Methods in agricultural chemical analysis: a practical handbook. United Kingdom, CABI Publishing, 266.

FAOStat (2015). From FOOD AND AGRICULTURE ORGANIZATION OF THE UNITED NATIONS (2015): <http://faostat3.fao.org/> (5-02-2015, 2015)

Federation, E. P. (2011). Market information. From (2011): http://www.europanel.org/main_mi.html (April 11, 2011)

Feng, L., van Hullebusch, E. D., Rodrigo, M. A., Esposito, G., & Oturan, M. A. (2013) Review: Removal of residual anti-inflammatory and analgesic pharmaceuticals from aqueous systems by electrochemical advanced oxidation processes. A review. Chemical Engineering Journal 228, 944-964

Forest Products Laboratory (2010). Wood Handbook - Wood as an Engineering Material General Technical Report FPL-GTR-190. Madison, United States Department of Agriculture Forest Service, 508.

FPS Economy (2010). Arbeidskosten en gewerkte uren per sector (2004). From (2010): http://statbel.fgov.be/nl/statistieken/cijfers/arbeid_leven/lonen/activiteit/index.jsp (4 November 2010, 2010)

Garcia, R., & Freire, F. (2014) Carbon footprint of particleboard: a comparison between ISO/TS 14067, GHG Protocol, PAS 2050 and climate Declaration. Journal of Cleaner Production 66, 10

Gassner, M., & Marechal, F. (2009) Thermo-economic process model for thermochemical production of Synthetic Natural Gas (SNG) from lignocellulosic biomass. Biomass & Bioenergy 33(11), 1587-1604

Giles, C. H., MacEwan, T. H., Nakhwa, S. N., & Smith, D. (1960) 786. Studies in adsorption. Part XI. A system of classification of solution adsorption isotherms, and its use in diagnosis of adsorption mechanisms and in measurement of specific surface areas of solids. Journal of the Chemical Society (Resumed)(0), 3973-3993

References

Girods, P., Dufour, A., Fierro, V., Rogaume, Y., Rogaume, C., Zoulalian, A., & Celzard, A. (2009a) Activated carbons prepared from wood particleboard wastes: Characterisation and phenol adsorption capacities. *Journal of Hazardous materials* 166(1), 491-501

Girods, P., Dufour, A., Rogaume, Y., Rogaume, C., & Zoulahan, A. (2008a) Thermal removal of nitrogen species from wood waste containing urea formaldehyde and melamine formaldehyde resins. *Journal of Hazardous materials* 159(2-3), 210-221

Girods, P., Dufour, A., Rogaume, Y., Rogaume, C., & Zoulalian, A. (2009b) Comparison of gasification and pyrolysis of thermal pre-treated wood board waste. *Journal of Analytical and Applied Pyrolysis* 85(1-2), 171-183

Girods, P., Dufour, A., Rogaurne, Y., Rogaurne, C., & Zoulalian, A. (2008b) Pyrolysis of wood waste containing urea-formaldehyde and melamine-formaldehyde resins. *Journal of Analytical and Applied Pyrolysis* 81(1), 113-120

Girods, P., Rogaume, Y., Dufour, A., Rogaume, C., & Zoulalian, A. (2008c) Low-temperature pyrolysis of wood waste containing urea-formaldehyde resin. *Renewable Energy* 33(4), 648-654

Gupta, M., Abu-Ghannam, N., & Gallagher, E. (2010) Barley for Brewing: Characteristic Changes during Malting, Brewing and Applications of its By-Products. *Comprehensive reviews in food science and food safety* 9, 10

Haimes, Y. Y. (2004). *Risk Modeling, Assessment, and Management*. pp. Jhon Wiley & Sons, Hoboken, New Jersey

Hamdaoui, O., & Naffrechoux, E. (2007) Modeling of adsorption isotherms of phenol and chlorophenols onto granular activated carbon - Part I. Two-parameter models and equations allowing determination of thermodynamic parameters. *Journal of Hazardous materials* 147(1-2), 381-394

Hameed, B. H., & Rahman, A. A. (2008) Removal of phenol from aqueous solutions by adsorption onto activated carbon prepared from biomass material. *Journal of Hazardous Materials* 160(2-3), 576-581

Harwell, A. E. A. (2010). *Green Public Procurement Wall Panels technical Background report*. E. C.-D. environment. Brussels, European Commission, 44.

References

Henrich, E., Dahmen, N., & Dinjus, E. (2009) Cost estimate for biosynfuel production via biosyncrude gasification. *Biofuels Bioproducts & Biorefining-Biofpr* 3(1), 28-41

Ho, Y. S., & McKay, G. (1998) A comparison of chemisorption kinetic models applied to pollutant removal on various sorbents. *Process Safety and Environmental Protection* 76(B4), 332-340

Horngren, C. T., Bhimani, A., Dater, S. M., & Foster, G. (2003). *Management and Cost Accounting*. pp. Pearson Education limited, United Kingdom

Inagaki, M., & Tascón, J. M. D. (2006). Pore formation and control in carbon materials. *Activated carbon surfaces in environmental remediation*. T. J. Bandoz. United kingdom, ELSEVIER Ltd: 571.

Infomil (2011). Luchtemissie beperkende technieken Adsorptie actief kool/Actief kool filtratie/Koolfilter (Air emission reduction techniques Adsorption Activated carbon / Active carbon filtration / carbon filter). From Rijkswaterstaat Ministerie van Infrastructuur en Milieu (2011): <http://www.infomil.nl> (29/05/2013, 2011)

Islam, M. N., & Ani, F. N. (2000) Techno-economics of rice husk pyrolysis, conversion with catalytic treatment to produce liquid fuel. *Bioresource Technology* 73(1), 67-75

Jung, C., Park, J., Lim, K. H., Park, S., Heo, J., Her, N., Oh, J., Yun, S., & Yoon, Y. (2013a) Adsorption of selected endocrine disrupting compounds and pharmaceuticals on activated biochars. *Journal of Hazardous materials* 263, Part 2, 702-710

Jung, C., Park, J., Lim, K. H., Park, S., Heo, J., Her, N., Oh, J., Yun, S., & Yoon, Y. (2013b) Adsorption of selected endocrine disrupting compounds and pharmaceuticals on activated biochars. *J Hazard Mater* 263 Pt 2, 702-710

Kantor, M., Wajda, K., Lannoo, B., Casier, K., Verbrugge, S., Pickavet, M., Wosinska, L., Chen, J., & Mitcsenkov, A. (2010). General framework for techno-economic analysis of next generation access networks. In: Kantor, M., Wajda, K., Lannoo, B., Casier, K., Verbrugge, S., Pickavet, M., Wosinska, L., Chen, J., & Mitcsenkov, A., Eds: 2010 12th International Conference on Transparent Optical Networks, June 27 2010-July 1 2010.

References

Kasaoka, S., Sakata, Y., Tanaka, E., & Naitoh, R. (1987) Design of Molecular Sieving Carbon Studies on Adsorption of Various Dyes in Liquid Phase. *Nippon Kagaku Kaishi* 1987(12), 2260-2266

Khraisheh, M., Kim, J., Campos, L., Al-Muhtaseb, A. a. H., Al-Hawari, A., Al Ghouti, M., & Walker, G. M. (2014) Removal of pharmaceutical and personal care products (PPCPs) pollutants from water by novel TiO₂-Coconut Shell Powder (TCNSP) composite. *Journal of Industrial and Engineering Chemistry* 20, 979-987

Knauf, M. (2014) Waste hierarchy revisited – an evaluation of waste wood recycling in the context of EU energy policy and the European market. *Forest Policy and Economics*(In Press)

Ko, D. C. K., Mui, E. L. K., Lau, K. S. T., & McKay, G. (2004) Production of activated carbons from waste tire - process design and economical analysis. *Waste Management* 24(9), 875-888

Kuppens, T. (2012). Techno-economic assessment of fast pyrolysis for the valorisation of short rotation coppice cultivated for phytoextraction. *Environmental Economics*. Diepenbeek, University Hasselt. PhD, 353.

Kuppens, T., Cornelissen, T., Carleer, R., Yperman, J., Schreurs, S., Jans, M., & Thewys, T. (2010) Economic assessment of flash co-pyrolysis of short rotation coppice and biopolymer waste streams. *Journal of Environmental Management* 91(12), 2736-2747

Lazo-Cannata, J. C., Nieto-Márquez, A., Jacoby, A., Paredes-Doig, A. L., Romero, A., Sun-Kou, M. R., & Valverde, J. L. (2011) Adsorption of phenol and nitrophenols by carbon nanospheres: Effect of pH and ionic strength. *Separation and Purification Technology* 80(2), 217-224

Le Cloirec, P. (2002). Adsorption in Water and Wastewater Treatments. *Handbook of Porous Solids*. F. Schüth, K. S. W. Sing , & J. Weitkamp. germany, Wiley-VCH GmbH. 5: 57.

Legros, E. (1966). Laboratory evaluation of granular activated carbon for liquid phase applications. pp. 69. *Chemviron carbon*, n.d., Brussels

Lemmens, B., Elslander, H., Ceulemans, J., Peys, K., Van Rompaey, H., & Huybrechts, D. (2004). *Gids luchtzuiveringstechnieken*. pp. Academia Press, Belgium

References

Li, B. Z., Sun, K. Q., Guo, Y. B., Tian, J. P., Xue, Y. B., & Sun, D. K. (2013) Adsorption kinetics of phenol from water on Fe/AC. *Fuel* 110, 99-106

Li, H. (2012). Determination of Oxygen functionality on highly oriented pyrolytic graphite (HOPG). Fachbereich Biologie, Chemie, Pharmazie Berlin, Freien Universität Berlin. PhD, 116.

Lievens, C., Carleer, R., Cornelissen, T., & Yperman, J. (2009) Fast pyrolysis of heavy metal contaminated willow: Influence of the plant part. *Fuel* 88(8), 1417-1425

Lievens, C., Yperman, J., Cornelissen, T., & Carleer, R. (2008a) Study of the potential valorisation of heavy metal contaminated biomass via phytoremediation by fast pyrolysis: Part II: Characterisation of the liquid and gaseous fraction as a function of the temperature. *Fuel* 87(10-11), 1906-1916

Lievens, C., Yperman, J., Vangronsveld, J., & Carleer, R. (2008b) Study of the potential valorisation of heavy metal contaminated biomass via phytoremediation by fast pyrolysis: Part I. Influence of temperature, biomass species and solid heat carrier on the behaviour of heavy metals. *Fuel* 87(10-11), 1894-1905

Lillo-Ródenas, M. A., Cazorla-Amorós, D., & Linares-Solano, A. (2003) Understanding chemical reactions between carbons and NaOH and KOH: An insight into the chemical activation mechanism. *Carbon* 41(2), 267-275

Lima, I. M., McAloon, A., & Boateng, A. A. (2008) Activated carbon from broiler litter: Process description and cost of production. *Biomass & Bioenergy* 32(6), 568-572

Lorenc-Grabowska, E., Gryglewicz, G., & Diez, M. A. (2012) Kinetics and equilibrium study of phenol adsorption on nitrogen-enriched activated carbons. *Fuel*, 9

Lorie, J. H., & Savage, L. J. (1955) Three problems in rationing capital. *Journal of Business* 28, 10

Mantau, U. (2012). Wood flows in Europe (EU27). *Celle*, 24.

References

Marsh, H., & Rodríguez-Reinoso, F. (2006a). Activated carbon. Activated Carbon. H. M. Rodríguez-Reinoso. Oxford, Elsevier Science Ltd: 536.

Marsh, H., & Rodríguez-Reinoso, F. (2006b). Chapter 3 - Porosity in Carbons: Modeling. Activated Carbon. H. M. Rodríguez-Reinoso. Oxford, Elsevier Science Ltd: 87-142.

Menéndez-Días, J. Á., & Martín-Gullón, I. (2006). Types of carbon adsorbents and their production. Activated Carbon Surfaces in Environmental Remediation. T. J. Bandosz. United Kingdom, ELSEVIER Ltd: 48.

Mestre, A. S., Pires, R. A., Aroso, I., Fernandes, E. M., Pinto, M. L., Reis, R. L., Andrade, M. A., Pires, J., Silva, S. P., & Carvalho, A. P. (2014) Activated carbons prepared from industrial pre-treated cork: Sustainable adsorbents for pharmaceutical compounds removal. Chemical Engineering Journal 253(0), 408-417

Moreno-Castilla, C. (2004) Adsorption of organic molecules from aqueous solutions on carbon materials. Carbon 42(1), 83-94

Mussatto, S. I. (2013) Brewer's spent grain: a valuable feedstock for industrial applications. Journal of the Science of Food and Agriculture 94, 11

Mussatto, S. I., Dragone, G., & Robert, I. C. (2006) Brewers' spent grain: generation, characteristics and potential applications. Journal of Cereal Science 43(1), 14

Nabais, J. M. V., Gomes, J. A., Suhas, Carrott, P. J. M., Laginhas, C., & Roman, S. (2009) Phenol removal onto novel activated carbons made from lignocellulosic precursors: Influence of surface properties. Journal of Hazardous materials 167(1-3), 904-910

NABC (2016). Techno-Economic Analysis: Evaluating the Economic Viability and Potential of the NABC Process Strategies. From NABC (2016): <http://www.nabcprojects.org/pdfs/techno-economic-analysis-evaluating-economic-viability.pdf> (17-05-2016, 2016)

Ng, C., Marshall, W. E., Rao, R. M., Bansode, R. R., & Losso, J. N. (2003) Activated carbon from pecan shell: process description and economic analysis. Industrial Crops and Products 17(3), 209-217

References

Noh, J. S., & Schwarz, J. A. (1990) Effect of HNO₃ Treatment on the Surface-Acidity of Activated Carbons. *Carbon* 28(5), 675-682

Ochelen, S., & Putzeijs, B. (2008a). Milieubeleidskosten- begrippen en berekeningsmethoden. N. e. E. v. d. V. o. Departement Leefmilieu. Belgium.

Ochelen, S., & Putzeijs, B. (2008b). Milieubeleidskosten – begrippen en berekeningsmethoden. Brussels, Departement Leefmilieu, Natuur en energie, 1-44.

OECD Environment, H. a. S. P. S. o. T. a. A. (2001). GUIDANCE DOCUMENT ON TRANSFORMATION/DISSOLUTION OF METALS AND METAL COMPOUNDS IN AQUEOUS MEDIA. Paris, ORGANISATION FOR ECONOMIC CO-OPERATION AND DEVELOPMENT, 19.

Peacocke, G. V. C., & Bridgwater, A. V. (2004). Techno-economic assessment of power production from the Wellman Process Engineering Ltd and BTG fast pyrolysis processes. Science in Thermao and Chemical Biomass Vonversion. A. V. Bridgwater , &D. G. B. Boocock. United Kingdom, CPL Press: 1785-1802.

Pelekani, C., & Snoeyink, V. L. (2000) Competitive adsorption between atrazine and methylene blue on activated carbon: the importance of pore size distribution. *Carbon* 38(10), 1423-1436

Peters, M. S., Timmerhaus, K. D., & West, R. E. (2004). Plant design and Economics for Chemical Engineers. pp. McGraw-Hill, United States of America

Pietrzak, R. (2009) XPS study and physico-chemical properties of nitrogen-enriched microporous activated carbon from high volatile bituminous coal. *Fuel* 88(10), 1871-1877

Polagye, B. L., Hodgson, K. T., & Malte, P. C. (2007) An economic analysis of bio-energy options using thinnings from overstocked forests. *Biomass & Bioenergy* 31(2-3), 105-125

Przepiorski, J. (2006) Enhanced adsorption of phenol from water by ammonia-treated activated carbon. *Journal of Hazardous materials* 135(1-3), 453-456

References

Radovic, L. R., Bandosz, T. J., Zhu, Z. J., Rodríguez-Reinoso, F., Sepúlveda-Escribano, A., Bitter, J. H., de Jong, K. P., Figueiredo, J. L., Perreira, M. F. R., Boehm, H., Freire, C., Silva, A. R., Serp, P., Moreno-Castilla, C., De Lanthouder, K. M., Crezee, E., Kapteijn, F., Moulijn, J. A., Maillard, F., Simonov, P. A., Savinova, E. R., Faria, J. L., Wang, W., Li, J., Arunajatesan, V., Chen, B., Möbus, K., Ostgard, D. J., Tackle, T., & Wolf, D. (2009). Carbon materials for catalysis. pp. 578. John Wiley & Sons, United states of America

Raveendran, K., Ganesh, A., & Khilar, K. C. (1996) Pyrolysis characteristics of biomass and biomass components. *Fuel* 75(8), 12

Reed, T. R., & Gaur, S. (1997). The high heat of fast pyrolysis for large particles. *Developments in Thermochemical Biomass Conversion*. A. V. Bridgwater, & D. G. B. Boocock. United Kingdom, Blackie Academic and Professional: 97-103.

Rivera-Utrilla, J., Sánchez-Polo, M., Ferro-García, M. Á., Prados-Joya, G., & Ocampo-Pérez, R. (2013) Pharmaceuticals as emerging contaminants and their removal from water. A review. *Chemosphere* 93(7), 1268-1287

Rivera-Utrilla, J., Sánchez-Polo, M., Gómez-Serrano, V., Álvarez, P. M., Alvim-Ferraz, M. C. M., & Dias, J. M. (2011) Activated carbon modifications to enhance its water treatment applications. An Overview. *Journal of Hazardous materials* 187(1-3), 23

Ruthven, D. M. (1984). Principles of adsorption and adsorption processes. pp. 433. John Wiley & Sons Inc., United States of America

Sánchez-Sánchez, Á., Suárez-García, F., Martínez-Alonso, A., & Tascón, J. M. D. (2015) Synthesis, characterization and dye removal capacities of N-doped mesoporous carbons. *Journal of Colloid and Interface Science* 450(0), 91-100

Santos, M., Jiménez, J. J., Bartolomé, B., Gómez-Cordovés, C., & del Nozal, M. J. (2003) Variability of brewer's spent grain within a brewery. *Food Chemistry* 80(1), 17-21

Seredych, M., Hulicova-Jurcakova, D., Qing Lu, G., & Bandosz, T. J. (2008) Surface functional groups of carbons and the effects of their chemical character, density and accessibility to ions on electrochemical performance *Carbon* 46(11), 14

References

Seredych, M., Portet, C., Gogotsi, Y., & Bandosz, T. J. (2009) Nitrogen modified carbide-derived carbons as adsorbents of hydrogen sulfide. *J Colloid Interface Sci* 330(1), 60-66

Sing, K. S. W., Everett, D. H., Haul, R. A. W., Moscou, L., Pierotti, R. A., Rouquerol, J., & Siemieniewska, T. (1985) Reporting physisorption data for gas/solid systems with special reference to the determination of surface area and porosity (Recommendations 1984). *Pure and Applied Chemistry* 57(4), 603-619

Smets, K. (2013). Valorization of agricultural waste cake by pyrolysis: Characterization of pyrolysis products and adsorption study on produced activated carbons. *Sciences. Hasselt, Hasselt*. PhD, 289.

Smets, K., Roukaerts, A., Czech, J., Reggers, G., Schreurs, S., Carleer, R., & Yperman, J. (2013) Slow catalytic pyrolysis of rapeseed cake: Product yield and characterization of the pyrolysis liquid. *Biomass and Bioenergy* 57(0), 180-190

Smura, T., Kiiski, A., & Hämmäinen, H. (2007) Virtual operators in the mobile industry: a techno-economic analysis. *NETNOMICS: Economic Research and Electronic Networking* 8(1), 25-48

Srivastava, V. C., Swamy, M. M., Mall, I. D., Prasad, B., & Mishra, I. M. (2006) Adsorptive removal of phenol by bagasse fly ash and activated carbon: Equilibrium, kinetics and thermodynamics. *Colloids and Surfaces A: Physicochemical Engineering Aspects* 272(1-2), 15-104

Stals, M. (2011). Pyrolysis of heavy metal contaminated biomass: Characterization of obtained pyrolysis oils and study of derived activated carbon. *Science. Hasselt, Hasselt University*. PhD, 201.

Thewys, T., & Kuppens, T. (2008) Economics of willow pyrolysis after phytoextraction. *International Journal of Phytoremediation* 10(6), 22

Thoemen, H., Irle, M., & Sernek, M. (2010). *Wood-Based Panels An introduction for Specialists*. pp. 283. Brunel University Press, London

Thommes, M., Kaneko, K., Neimark Alexander, V., Olivier James, P., Rodriguez-Reinoso, F., Rouquerol, J., & Sing Kenneth, S. W. (2015). Physisorption of gases, with special reference to the evaluation of surface

References

area and pore size distribution (IUPAC Technical Report). *Pure and Applied Chemistry*. 87, 1051.

Tock, L., Gassner, M., & Maréchal, F. (2010) Thermochemical production of liquid fuels from biomass: Thermo-economic modeling, process design and process integration analysis. *Biomass and Bioenergy* 34(12), 1838-1854

Van Dael, M., Kuppens, T., Lizin, S., & Van Passel, S. (2014). *Techno-economic Assessment Methodology for Ultrasonic Production of Biofuels*, Springer.

Vandevenne, N., Vanreppelen, K., Schreurs, S., Yperman, J., & Carleer, R. (2013). Adsorptio van fenol op actieve kool geproduceerd uit spanningsplaatafval. *Industrial sciences*. Hasselt, University Hasselt. Master.

Vandewijngaarden, J., Carleer, R., Yperman, J., Stals, M., & Schreurs, S. (2010). Karakterisering en activering van pyrolysechar: inleidend onderzoek. *Industriële Wetenschappen en Technologie*. Diepenbeek, XIOS Hogeschool Limburg. Master, 109.

Vanreppelen, K., Kuppens, T., Thewys, T., Carleer, R., Yperman, J., & Schreurs, S. (2011) Activated carbon from co-pyrolysis of particle board and melamine (urea) formaldehyde resin: A techno-economic evaluation *Chemical Engineering Journal* 172(2-3), 835-846

Velghe, I., Carleer, R., Yperman, J., Schreurs, S., & D'Haen, J. (2012) Characterisation of adsorbents prepared by pyrolysis of sludge and sludge/disposal filter cake mix. *Water Research* 46(8), 2783-2794

Verlicchi, P., Al Aukidy, M., & Zambello, E. (2012) Occurrence of pharmaceutical compounds in urban wastewater: Removal, mass load and environmental risk after a secondary treatment—A review. *Science of the Total Environment* 429(0), 123-155

Vernimmen, P., Quiry, P., Le Fur, Y., Dallochio, M., & Salvi, A. (2005). *Corporate FINANCE Theory and Practice*. pp. 15-473. John Wiley & Sons Ltd., Chicester

VLAREM-II (2013). Besluit van de Vlaamse regering van 1 juni 1995 houdende algemene en sectorale bepalingen inzake milieuhygiëne (Decision of the Flemish Government of 1 June 1995 concerning General and Sectoral

References

provisions relating to Environmental Safety). 17-02-2012. From Flemish government (2013): <http://navigator.emis.vito.be/milnav-consult/2013>)

Voogt, d. P., Janex-Habibi, M. L., Sacher, F., Puijker, L., Mons, M., & Universiteit van, A. (2009). Development of a common priority list of pharmaceuticals relevant for the water cycle, 39.

Weber, W. J., & Morris, J. C. (1963) KINETICS OF ADSORPTION ON CARBON FROM SOLUTIONS. *Journal of the Sanitary Engineering Division* 89(2), 29

White, J. S., Yohannan, B. K., & Walker, G. M. (2008) Bioconversion of brewer's spent grains to bioethanol. *Fems Yeast Research* 8(7), 1175-1184

Worch, E. (2012). *Adsorption Technology in Water Treatment Fundamentals, Processes, and Modeling*. pp. 332. Walter de Gruyter GmbH & Co, Berlin

Wrap (2007). Environmental impact of higher recycled content in construction projects. B. R. Establishment. Banbury, Waste & resources Action Programme, 118.

Yassin, L., Lettieri, P., Simons, S. J. R., & Germana, A. (2009) Techno-economic performance of energy-from-waste fluidized bed combustion and gasification processes in the UK context. *Chemical Engineering Journal* 146(3), 315-327

Yousef, R. I., El-Eswed, B., & Al-Muhtaseb, A. H. (2011) Adsorption characteristics of natural zeolites as solid adsorbents for phenol removal from aqueous solutions: Kinetics, mechanism, and thermodynamics studies. *Chemical Engineering Journal* 171(3), 1143-1149

Zhou, J.-H., Sui, Z.-J., Zhu, J., Li, P., Chen, D., Dai, Y.-C., & Yuan, W.-K. (2007) Characterization of surface oxygen complexes on carbon nanofibers by TPD, XPS and FT-IR. *Carbon* 45(4), 785-796

